# TOWARDS NEW CATALYTIC SYSTEMS FOR THE FORMATION OF METHYL METHACRYLATE FROM METHYL PROPANOATE

Jacorien Coetzee

A Thesis Submitted for the Degree of PhD
at the
University of St Andrews

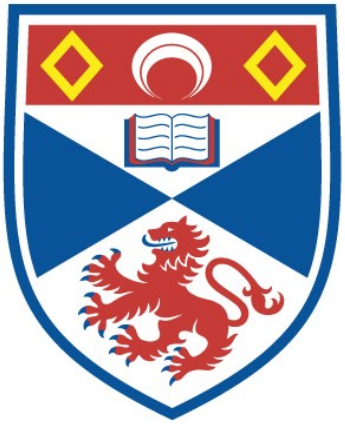

2011

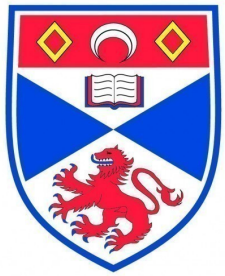


# Towards New Catalytic Systems for the Formation of Methyl Methacrylate from Methyl Propanoate

by

JACORIEN COETZEE

**THESIS**

submitted in fulfilment of the requirements

for the degree of

**DOCTOR OF PHILOSOPHY**

**UNIVERSITY OF ST. ANDREWS**

SUPERVISOR: PROF. DAVID J. COLE-HAMILTON

INDUSTRIAL SUPERVISOR: DR. GRAHAM R. EASTHAM

**MAY 2011**

# DECLARATION

***1. Candidate's declarations:***

I, Jacorien Coetzee, hereby certify that this thesis, which is approximately 69 400 words in length, has been written by me, that it is the record of work carried out by me and that it has not been submitted in any previous application for a higher degree.

I was admitted as a research student in November, 2007 and as a candidate for the degree of Doctor of Philosophy in September 2008; the higher study for which this is a record was carried out in the University of St Andrews between 2007 and 2011.

Date: signature of candidate:

***2. Supervisor's declaration:***

I hereby certify that the candidate has fulfilled the conditions of the Resolution and Regulations appropriate for the degree of Doctor of Philosophy in the University of St Andrews and that the candidate is qualified to submit this thesis in application for that degree.

Date: signature of supervisor:

***3. Permission for electronic publication:***

In submitting this thesis to the University of St Andrews I understand that I am giving permission for it to be made available for use in accordance with the regulations of the University Library for the time being in force, subject to any copyright vested in the work not being affected thereby. I also understand that the title and the abstract will be published, and that a copy of the work may be made and supplied to any bona fide library or research worker, that my thesis will be electronically accessible for personal or research use unless exempt by award of an embargo as requested below, and that the library has the right to migrate my

thesis into new electronic forms as required to ensure continued access to the thesis. I have obtained any third-party copyright permissions that may be required in order to allow such access and migration, or have requested the appropriate embargo below.

The following is an agreed request by candidate and supervisor regarding the electronic publication of this thesis:

*Embargo on both all of printed copy and electronic copy for the same fixed period of 2 years on the following ground: publication would be commercially damaging to the researcher, or to the supervisor, or the University.*

Date :

signature of candidate : signature of supervisor:

# ABSTRACT

The two stage Lucite Alpha Process for the industrial manufacturing of methyl methacrylate (MMA) represents one of the most efficient technologies currently available for the large scale production of this important chemical commodity. The second stage of this process, which involves the condensation of methyl propanoate (MeP) with formaldehyde over a heterogeneous fixed bed catalyst, however, still shows great scope for improvement. Herein the development of a novel homogeneous catalytic system that would promote the condensation of either propanoic acid or MeP with formaldehyde is explored. Since C–C bond forming reactions which proceed *via* C–H activation pathways typically display high atom efficiency, our efforts were particularly focussed on employing a functionalisation strategy that is mediated by C–H activation.

In the case of propanoic acid, the possibility of achieving regioselective $\alpha$-methylenation by linking the substrate to phosphorus was evaluated. Thus, a series of acyloxyphosphines and acylphosphites derived from either propionic acid or phenylacetic acid was prepared and, where stability allowed, fully characterised. Some of the resultant simple mixed anhydrides posed problems relating to their stability, so the stabilisation of such ligand systems by using electronic and / or steric effects was therefore explored. In addition, the coordination chemistry and in solution behaviour of Rh(I) and Ru(II) complexes containing these ligands was examined. Similar to the free ligands, complexes derived from these mixed anhydrides rearranged in solution *via* a number of decomposition pathways, with the specific pathway dependent on the nature of the auxiliary ligands. For most of these complexes, however, ligand decarbonylation was the route of preference for decomposition. Despite the instability of these complexes, a selection of Rh(I) mixed anhydride complexes were assessed for their potential as C-H activation catalysts in reactions aimed at the $\alpha$-methylenation of saturated carboxylic acids.

Furthermore, the stabilisation of Rh(I) mixed anhydride complexes with chelating auxilary ligands, such as bisphosphines or N-substituted diphosphinoamines, was explored. In particular, a series of new Rh(I) mixed anhydride complexes containing dppe, dppb and dppbz

as secondary ligands were prepared and the effects of these secondary ligands on the in solution stability of these complexes assessed.

As MeP represents the final product in the first stage of the Alpha process and not propanoic acid, the utilisation of PNP iridium pincer complexes in the regioselective $sp^3$ C–H activation of MeP and related esters was also examined. The factors that govern the regioselectivity of such reactions were of great interest to us and, in particular, the effects of water on the reactivity and regioselectivity of these reactions were explored. For MeP, preferential C–H activation of the methoxy group was found to proceed under anhydrous conditions and the catalytic functionalisation of this site with ethene using this activation approach was considered.

Formaldehyde, employed in the second stage of the Alpha process, is a difficult substance to manufacture and handle, especially on a large scale. A preliminary study on the *in situ* production of anhydrous formaldehyde *via* the catalytic dehydrogenation of methanol was therefore performed. During this study, catalytic systems based on carbonate salts and / or transition metal complexes were considered. In the hope of reducing the number of steps required in the production of MMA, a new one-pot cascade reaction for the indirect *α*-methylenation of MeP with methanol was developed. Although the production of MMA using this system only proceeded with low efficiency, the obtained results serve as an important proof of concept for future developments in this area.

Finally, the capacity of a series of simple bases to catalyse the condensation of MeP with formaldehyde was assessed as part of a fundamental study directed towards determining the factors that govern the efficiency of this reaction. In addition, the extent to which each base effects the deprotonation in the *α*-position of MeP was determined with the aid of deuterium labelling experiments. Similarly, using sodium propanoate as model base a rough estimate of the kinetics of deprotonation could be made based on the degree of deuterium incorporation over time. These studies suggested that the low efficiency of this condensation reaction is not caused by ineffective deprotonation but rather by the weak nucleophilicity of the generated carbanion. For this reason, attempts to increase the electrophilicity of formaldehyde through Mannich-type condensations reactions involving secondary amine and carboxylic acid additives were made.

*~ To my parents and loving husband ~*

# ACKNOWLEDGEMENTS

There are several people whom have meant a great deal to me during the execution of this study and have made this a very rewarding and enriching experience on so many levels. I would, however, like to thank a few people in particular:

Firstly, I would like to express my deepest gratitude to my academic supervisor Prof. David Cole-Hamilton for having granted me with such a wonderful and life changing opportunity. David, your endless enthusiasm throughout the execution of this study, as well as unwavering optimism have proved to be both essential and highly contagious! Furthermore, your continuous support, useful suggestions and great wisdom were indispensable and I am so grateful for it. Thank you for having always made time to discuss my work, regardless of how impossibly hectic your schedule was. I am also sincerely grateful to my industrial supervisors Dr. Graham Eastham and David Johnson for their interest in this study as well as many useful discussions. Also, for giving me my first taste of industrial chemistry and for allowing an insightful "behind the scenes" look at the inner workings of an industrial company.

I would also like to thank my colleagues and friends with whom I have worked alongside in the DJCH group over the last 3 and a half years: Jan Blank, Ruben Duque, Jennifer Amey, Bianca Munõz Moreno, Gregorio Barrios Guisado, Nicolas Vautravers, Simon Desset, Ine Boogaerts, Gavin Hill, Gong Zhen Xin, Tania Quintas, Lynzi Robb, Molise Mokhadinyana, Björn Loges, Juma Mmongoyo, Deborah Dodds, Patrizia Lorusso and Marc Vuerst. Thank you all for creating such a stimulating and pleasant working environment. Also, thank you for all the many useful discussions, help in and around the lab and for enduring my occasional frustration venting sessions. Peter Porgorzelec deserves special mention here for his indispensible practical expertise. Peter, thank you so much for your general friendliness, eagerness to lend a hand and for always being ready with useful technical and practical advice. It was such a pleasure to work with you. Also, many thanks to my colleagues from other research groups Marzia Nuzzolo, Peter Deuss, Arnald Grabulosa, Nelly Bonnet, Aga and Marcin Kosinski for your valuable friendships.

Many thanks to: Melanja Smith and Tomas Lebl for your excellent NMR services and kind assistance with more complicated NMR experiments; Caroline Horsburgh and the wonderful

people at Swansea EPSRC Mass spectrometry service for the collection of mass spectrometric data; Alex Slawin for all your friendly and uplifting chats as well as meticulous care in X-ray data collections and refinements and Sylvia Williamson for the collection of elemental analysis data.

In particular, I would also like to thank my amazing parents for their sustained love and support throughout my studies and life. Thank you for having supplied me with so many wonderful opportunities to develop myself as a person and for always supporting my life choices regardless of how far they may take me from the nest. Also, many thanks to my brother Johannes and sister Karolien, as well as their spouses, Natasha and Francois for all their constant love and encouragement.

A heartfelt thank you to my darling husband and pillar of strength, William. Thank you for your unconditional love, relentless support and for always reminding me of what the truly beautiful and important things in life are. Thank you for never allowing me to indulge in selfpity when things didn't quite go my way and for giving me the "kick-up-the-backside" that I sometimes so desperately required!

I am also greatly indebted to all my friends local, in South Africa and abroad for so many lasting memories, for their endless support and for providing healthy distractions at just the right times. My fellow expat South Africans and close friends Vinet Coetzee, Veronica Patterson, Leigh-Anne De Jong, Molise Mokhadinyana, Tia Jacobs, Anneke Kruger, Davina de Beer and Renee Terrell deserve special mention for bringing "home" a little closer to St. Andrews.

Lastly, but certainly not least, I would like to thank my heavenly father for all the countless ways in which he has blessed me.


For financial support, I would like to acknowledge Lucite International.

"For strange effects and extraordinary combinations we must go to life itself, which is always far more daring than any effort of the imagination."

*~ Arthur Conan Doyle ~*

"It is an old maxim of mine that when you have excluded the impossible, whatever remains, however improbable, must be the truth."

*~ Sherlock Holmes (Arthur Conan Doyle) ~*

*(...also quoted by David Cole-Hamilton on many occasions during this study....)*

# CONTENTS

## CHAPTER 3

## Rhodium and ruthenium complexes of mixed anhydrides



## CHAPTER 4

## Rhodium mixed anhydride complexes with chelated auxiliary ligands

## CHAPTER 5

## Iridium PNP complexes in the C–H activation of methyl propanoate



## CHAPTER 6

## Methanol dehydrogenation for the *in situ* production of anhydrous formaldehyde

## CHAPTER 7

## Simple base catalysed condensation of formaldehyde with propanoate derivatives



## CHAPTER 8

## Conclusions and future work



## APPENDIX 1

## Crystallographic data tables

# ABBREVIATIONS

| | |
|---|---|
| Å | Ångstrom ($10^{-10}$ m) |
| Ac | Acetyl |
| ACH | acetone cyanohydrin |
| Ar | Aryl |
| Bu | Butyl |
| $^{t}$Bu | Tertiary butyl |
| Bz | Benzyl |
| CI | Chemical ionisation |
| CIF | Crystallographic information framework |
| COE | Cyclooctene |
| COD | Cyclooctadiene |
| CsP | Cesium propanoate |
| Cy | Cyclohexyl |
| DAP | Dialkyl acylphosphonate |
| dba | *trans*,*trans*-dibenzylideneacetone |
| DBU | 1,8-diazobicyclo[5.4.0]undec-7-ene |
| DOE | Direct Oxidative Esterification |
| DP | Dialkylphosphonate |
| dppb | 1,4-bis(diphenylphosphino)butane |
| dppbz | 1,2-bis(diphenylphosphino)benzene |
| dppe | 1,2-bis(diphenylphosphino)ethane |
| DTBPMB | 1,2-bis(di-*tert*-butylphosphinomethyl)benzene |
| EI | Electron impact |
| Et | Ethyl |
| ES | Electrospray |
| FT | Fourier Transform |
| GC | Gass chromatography |
| *gem* | Geminal |
| h | Hour |
| IR | Infrared |
| ICI | Imperial Chemical Industries |
| LED | Light Emitting Diode |
| NaP | Sodium propanoate |
| nbd | 2,5-Norbornadiene |
| *m* | Meta |
| MAA | Methacrylic acid |
| MBS | Methacrylate-butadiene-styrene |
| M$^{i}$Bu | Methyl isobutyrate |
| MeP | Methyl propanoate |
| min | Minute(s) |
| MMA | Methyl methacrylate |
| Mp | Melting point |
| MS | Mass spectrometry |
| NMR | Nuclear Magnetic Resonance |
| *p* | Para |
| Ph | Phenyl |

| | | |
|---|---|---|
| | PMMA | Polymethyl methacrylate |
| | Pr | Propyl |
| | $^{i}$Pr | Isopropyl |
| | PVC | Polyvinylchlorine |
| | Py | Pyridine |
| | R | Alkyl, aryl or hydrogen group |
| | R.T. | Room temperature |
| | TBMPX | (*S,S*)-*α,α*'-Bis(*tert*-butylmethylphosphino)-*o*-xylene |
| | *tert* | Tertiary |
| | TFA | Trifluoroacetic acid |
| | thf | Tetrahydrofuran |
| | TMS | Tetramethylsilane |
| | tpdp | Tetraphenyldiphosphoxane |
| | V | Volume |
| | *vs.* | *Versus* |
| | w | Weight |
| NMR | bs | Broad singlet |
| | COSY | H–H Correlation Spectroscopy |
| | d | Doublet |
| | DEPT | Distorsionless Enhancement by Polarisation Transfer |
| | dd | Doublet of doublets |
| | ddd | Doublet of doublets of doublets |
| | dt | Doublet of triplets |
| | dvt | Doublet of virtual triplets |
| | $\delta$ | Chemical shift (ppm) |
| | HMQC | Heteronuclear Multiple Quantum Coherence |
| | HSQC | Heteronuclear Single Quantum Coherence |
| | Hz | Hertz |
| | *J* | Coupling constant (Hz) |
| | m | Multiplet |
| | MHz | Mega Hertz |
| | ppm | Parts per million |
| | q | Quartet |
| | s | Singlet |
| | t | Triplet |
| | v | Virtual |
| | vt | Virtual triplet |
| | Δ | Difference |
| MS | ES-MS | Electrospray mass spectrometry |
| | $M^{+}$ | Molecular ion |
| | *m/z* | Mass/charge ratio |
| IR | $\nu$ | Stretching vibration |
| | $\tilde{\nu}$ | Frequency |
| | st | Strong |
| | w | Weak |
| | m | Medium |

# Chapter 1

# General Introduction

– General introduction and project objectives –

*Methyl methacrylate (MMA) represents the key monomer for the production of many of the acrylic plastics that are ubiquitous in everyday life. With such a wide range of applications, the demand for MMA grows annually and with it the challenges for the large scale, cost effective and environmentally benign production thereof. This chapter highlights some of the current technologies available for the industrial manufacturing of this important chemical commodity as well as the shortcomings still associated with each individual process. In addition, this chapter emphasises the value of transition metal catalysed C–H activation as an alternative route to cleaner C–C bond forming reactions. The activation of $sp^3$ vs. $sp^2$ C–H bonds is, however, a more challenging task and the fundamental reasons for this variance are reviewed.*

## 1.1 Importance of methyl methacrylate

Methyl methacrylate (MMA) is predominantly used as monomer in the production of the transparent acrylic plastic, polymethyl methacrylate (PMMA), which is commonly known by brand names such as Plexiglas™, Perspex™ or Lucite™.[1] PMMA is a lightweight, stable, weather resistant polymer with high visible light transmittance which can be easily moulded, coloured and recycled. It is for these attractive properties that PMMA has found its use in the semiconductor and photonics industry and is often employed as a shatterproof, hardwearing substitute for glass in applications such as laptop screens, mobile phones, LED signage, car headlights, submarine viewing ports, aquaria tanks, motorcycle helmets and working surfaces, to name a few. PMMA and MMA are also compatible with the human body; a characteristic that has enabled their use in important medical artefacts such as dentures, bone cement and artificial lenses.[1] MMA can also be co-polymerised with other monomers in the productions of resins and polymers with versatile characteristics. One example of such a co-polymer is methyl methacrylate-butadiene-styrene (MBS), commonly used as a modifier for PVC.[2] With such a wide and growing range of applications, the demand for MMA rises annually and with it, the need for more efficient industrial processes for its large scale production.

## 1.2 Industrial approaches to the production of methyl methacrylate

### *1.2.1 Acetone cyanohydrin (ACH) process*

In 1933, Rohm & Haas Co. was the first to produce a methacrylic ester (ethyl methacrylate) industrially. This invention was later refined by Imperial Chemical Industries (ICI) and commercialised as the acetone cyanohydrin (ACH) process for the production of MMA. Prior to 1982, this remained the only industrial process for this purpose and even today, the ACH process still represents the most widely-used route to the large scale manufacturing of MMA.[3] The ACH process consists of three stages: 1) initial generation of a cyanohydrin followed by 2) dehydration of the alcohol group with concurrent hydration of the cyano group and finally 3) conversion of the amide salt to the methyl ester (Scheme 1.1).[4] In the first stage, cyanohydrin is generated in high yield and selectivity (92-99 %) by the nucleophilic addition of cyanide to the carbonyl carbon of acetone in a basic medium under very mild conditions (temperatures below 40 °C). Subsequent conversion of the cyanohydrin to the corresponding amide salt is

achieved by the reaction of cyanohydrin with sulphuric acid at 80–140 °C. The role of the acid during this step is twofold, governing both double bond formation *via* water elimination and transformation of the cyano group to the amide salt. Finally, treatment of this salt with methanol furnishes MMA in good selectivity (77%).[4]

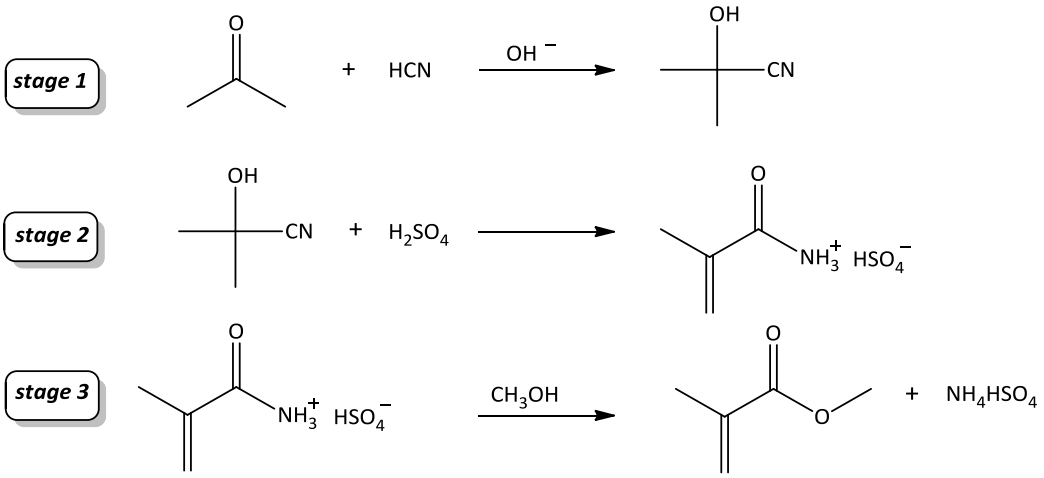


**Scheme 1.1** The three stage acetone cyanohydrin (ACH) process for the large scale production of MMA.

This process, while economically competitive, suffers from the generation of a large amount of ammonium bisulphate waste. About 1.5 tons of ammonium bisulphate is generated for every ton of MMA produced, posing a serious disposal issue, which, together with the necessity to make use of highly toxic hydrogen cyanide, represent two major drawbacks of this route. Although ammonium bisulphate is often employed in the production of fertilisers, the ammonium bisulphate generated during the ACH process is too acidic for this purpose and therefore, the only way to dispose of this byproduct is by conversion to sulphuric acid at high temperatures.[5] By this approach, however, the nitrogen component is not recycled and consequently a fresh molecule of HCN is required for each molecule of MMA produced.

To circumvent this problem, Mitsubishi Gas Chemical Company developed a new HCN recycling approach to improve the atom efficiency of the ACH process (Scheme 1.2). In their approach, the generation of ammonium salts are avoided by replacing the sulphuric acid in the second stage of the classical ACH process with a manganese dioxide slurry in a water/acetone mixture. Furthermore, by converting the amide to the methyl ester in the presence of methyl

formate, the nitrogen component can be captured in the form of formamide [$HC(O)NH_2$], from which HCN can be recycled at elevated temperatures.[5] Despite the major improvement in atom efficiency, this approach adds additional steps to the overall process which translates to an increase in the MMA production costs.

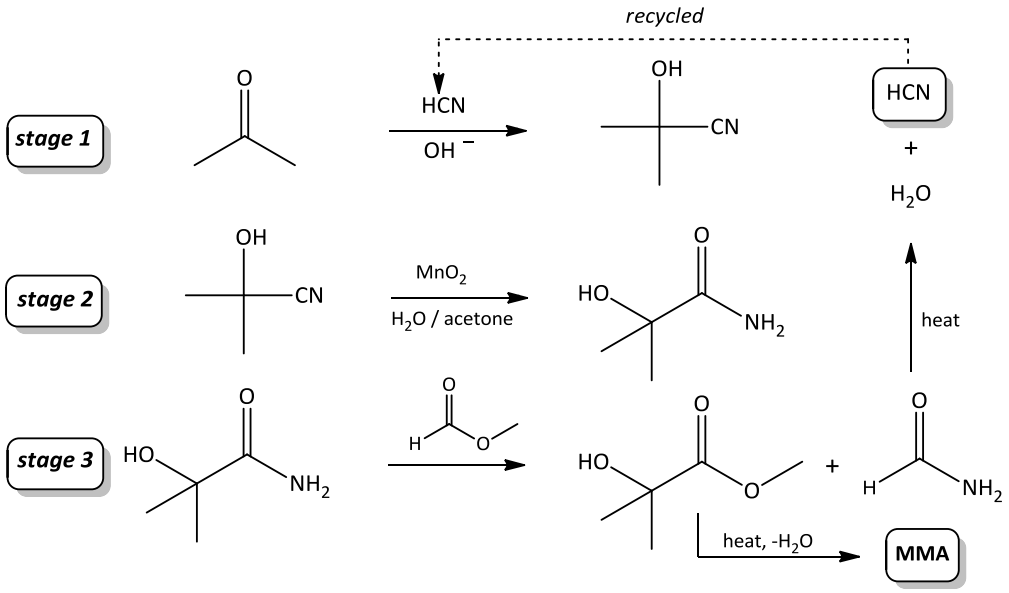


**Scheme 1.2** The more atom efficient Mitsubishi adapted ACH process for the production of MMA.

Owing to the many shortcomings associated with the ACH process, a great deal of research aimed at the development of new, cost effective and environmentally benign processes for the preparation of MMA has been conducted over the past years.[5] Many of these research efforts have led to the discovery of alternative routes which have either been commercialised already or are close to commercialisation.[3] Some of the more important developments include: (1) the ethene route developed by BASF, (2) the Shell methyl acetylene process, (3) the RTI-Eastman process, (4) the direct oxidative esterification (DOE) process established by Asahi Chemical Company and (5) the Alpha Process developed by Lucite International.[3]

### *1.2.2 BASF process*

In the BASF process, ethene is reacted with carbon monoxide and hydrogen in the first stage to generate propanal. In the second stage, propanal is converted to methacrolein by a base catalysed aldol condensation with formaldehyde. Oxidation of the methacrolein to methacrylic

acid, followed by esterification with methanol affords MMA (Scheme 1.3).[5] Although BASF reported methacrolein yields as high as 99% for the second stage, the catalyst employed for the subsequent oxidation step is in need of further improvement for this route to ever become a leading process.[3,6,7]

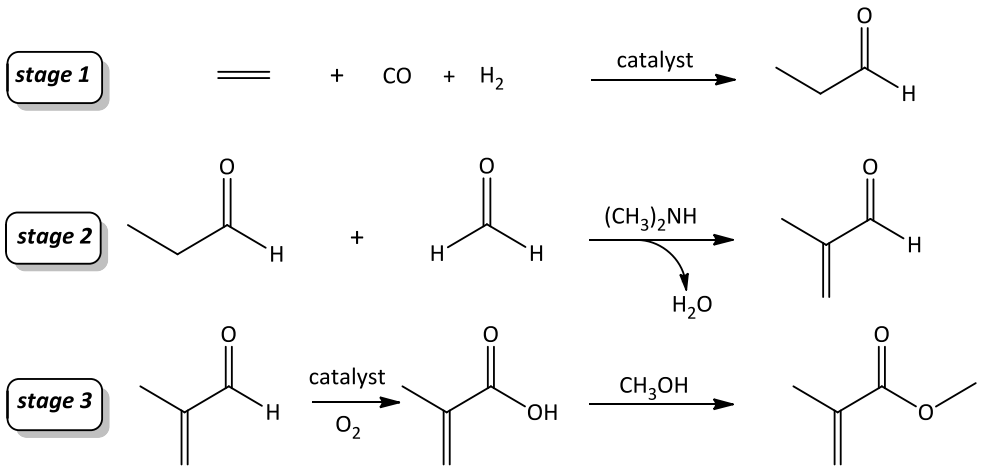


**Scheme 1.3** BASF process for the production MMA form ethylene *via* propionaldehyde, methacrolein and methacrylic acid intermediates.

### *1.2.3 Shell process*

The Shell route was based on a well-established BASF process that was developed by Reppe for the carbonylation of acetylene to acrylic acid and ester derivatives thereof. Numerous efforts by BASF to utilise their own technology for the production of MMA from methyl acetylene resulted in failure, with the Reppe nickel carbonyl catalyst proving inadequate for the large scale manufacturing of MMA.[3] Shell, however, managed to optimise this process to some extent with the discovery of a new class of highly efficient homogeneous palladium(II) catalysts. Within this class of compounds, changes in the ligand structure have a dramatic effect on the activity and specificity of the catalyst. In particular, the presence of a weakly or non-coordinating anionic ligand and a neutral phosphine ligand that contains a 2-pyridyl (py) moiety (P–N ligand) appear to be key features in the design of efficient catalytic systems. In the absence of these entities, catalytic activity and selectivity are drastically impaired. The catalytic cycle proposed by Shell is summarised in Scheme 1.4 and involves a square planar $d^8$ palladium(II) complex, **I**, containing two P—N ligand molecules. One of these is bonded in a

chelating manner *via* both the phosphorus and nitrogen atoms to create a four-membered ring structure, while the second is coordinated *via* the phosphorus atom only. Complex **I** is thought to react with methanol in the initiation step of the cycle to form the palladium-methoxy intermediate **II**. Displacement of the mono-coordinated P—$NH^+$ ligand in **II** by carbon monoxide, followed by a migratory insertion into the palladium-methoxy bond with recoordination of the P—$NH^+$ ligand yields species **IV**. In the next step, the mono-coordinated P—N ligand is displaced by methyl acetylene, which inserts into the palladium-carbomethoxy bond to give intermediate **VI**. A free protonated P—N ligand may now once again occupy the resulting vacant coordination site from where it can act as proton donor, enabling MMA formation and release by protonolysis in the final step.[8] Although MMA is produced in only one step with high catalytic and atom efficiency *via* this route, the low availability of methylacetylene limits the commercial viability of this process. Methylacetylene is only produced as a minor product during the steam cracking of petroleum fractions and supplies of this feedstock are therefore not sufficient to meet the large demand of a world-scale MMA plant.[5] An additional problem is that methylacetylene is usually contaminated with its isomer, allene, which has a very similar boiling point (-23 °C *vs.* -34 °C) so is very difficult to separate. Furthermore, allene gives stable π–allylpalladium complexes, and hence poisons the catalysis.

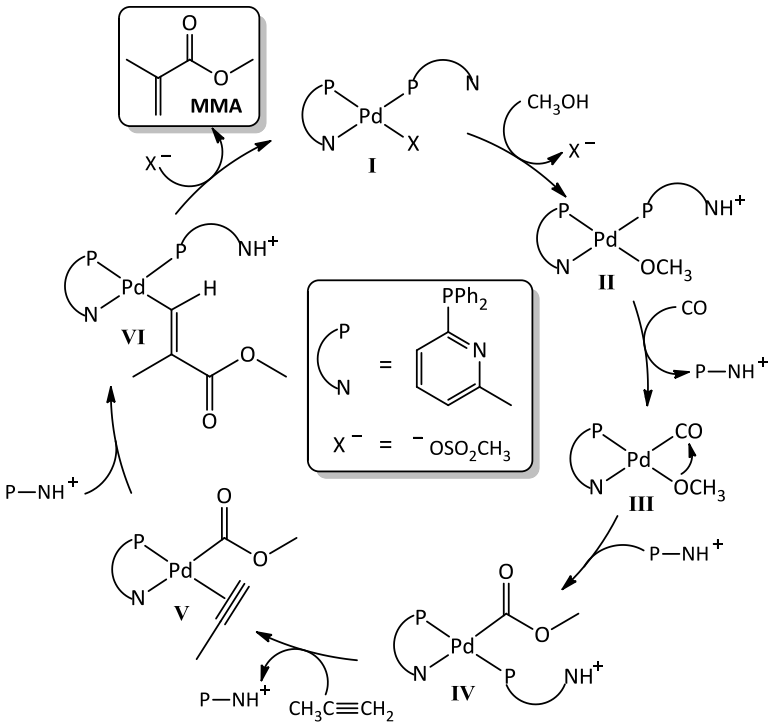


**Scheme 1.4** Proposed catalytic cycle of the Shell process for the production MMA from methyl acetylene, where P—N = 2-$PyPPh_2$ or 2-(6-$CH_3$-Py)$PPh_2$ and X = *p*-$CH_3PhSO_2OH$ or $CH_3SO_2OH$.

### 1.2.4 RTI-Eastman process

In the RTI-Eastman process, MMA is manufactured from ethene in three steps *via* a propanoic anhydride intermediate. Step 1 involves the conversion of ethene into propanoic anhydride (Scheme 1.5). Condensation of this propanoic anhydride with formaldehyde furnishes methacrylic acid in step 2, which can be converted to MMA in the final step by esterification with methanol. Although the first step is commercially practised by Eastman Chemical Company and the third step is readily achievable, the efficiency of the second condensation step poses a serious hurdle for the successful commercialisation of this process. One promising feature of this process, however, is the formation of only one mole of water for every two moles of MMA produced.[9] This represents a major advantage, since water is known to inhibit the kinetics of the condensation step and promote the hydrolysis of the ester bond present in MAA.[10]

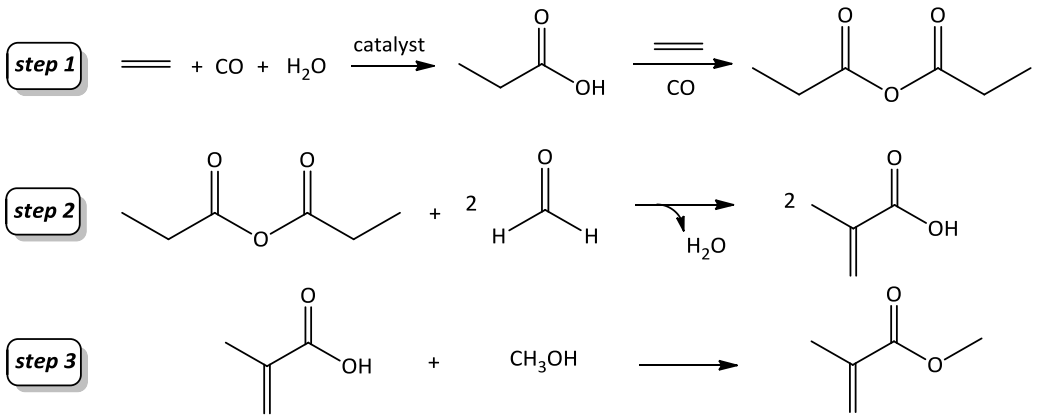


**Scheme 1.5** The three step RTI-Eastman process for the manufacturing of MMA from ethene.

### 1.2.5 Asahi Chemical Company process

In 1998, Asahi Chemical Company established a two stage process for the production of MMA from isobutene. Methacrolein, produced in the first stage by the direct vapour-phase catalytic oxidation of isobutene, is simultaneously oxidized and esterified in liquid methanol in the second stage to furnish MMA. The alumina supported palladium, lead and magnesium containing heterogeneous catalyst developed by Asahi Chemical for the second stage of the process delivers MMA in yields of up to 93%.[3,11] Several by-products such as propene,

methylformate, methacrylic acid and methylisobutyrate are, however, formed as part of the process, complicating the purification stages. However, since the invention of the original process, Asahi has further enhanced the efficiency of this process by significant fine-tuning of the catalytic system, making this a more economically competitive process.[3,5]

### *1.2.2 Lucite International Alpha process*

The most important of all the MMA technologies is arguably the Alpha process developed by Lucite International. This high yield, two-stage process not only starts from cheap, readily available chemicals (ethene, carbon monoxide and methanol), but also produces virtually no waste. In September 2008, Lucite International commissioned their first Alpha plant, based in Singapore, for the commercial production of MMA (Figure 1.1). At a cost of 230 million US dollars, this plant was 30–40 % cheaper to engineer and construct than conventional systems and in 2010 MMA production for this plant already exceeded 10 000 tonnes per month.[1]

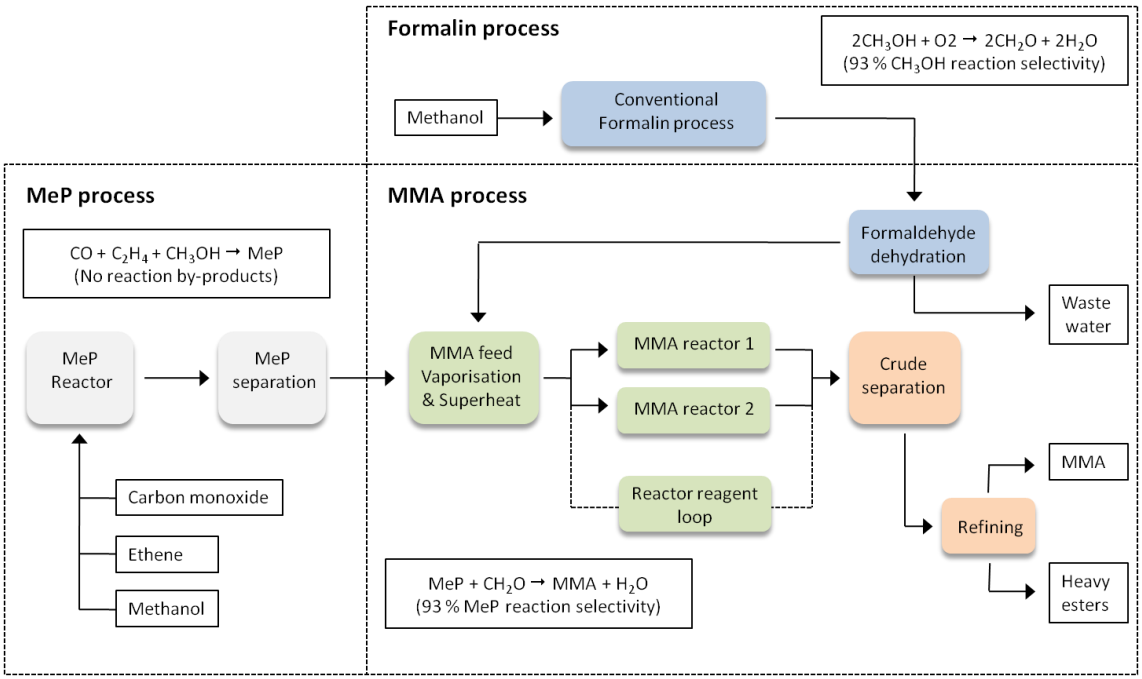


**Figure 1.1** The plant setup for the Lucite International Alpha process (reproduced from the literature).[1]

The first stage of this process involves the methoxycarbonylation of ethene to methyl propanoate (MeP), for which Lucite have developed a proprietory palladium based catalyst containing the bisphosphine 1,2-bis(di-*tert*-butylphosphinomethyl)benzene (DTBPMB) ligand

(Scheme 1.6). Addition of this ligand to $[Pd_2(dba)_3]$ (dba = *trans*,*trans*-dibenzylideneacetone) results in a zero valent complex of the formula $[Pd(dba)L_2]$ (where $L_2$ = DTBPMB) which can be transformed to the active complex by treatment with a sulfonic acid. This stage, which is done in a continuous-stirred tank reactor under moderate conditions, has been optimised and catalyst lifetimes exceed 1M turnovers with enzyme-like selectivity (>99.98%), fast reaction rates and low catalyst loading.[12]

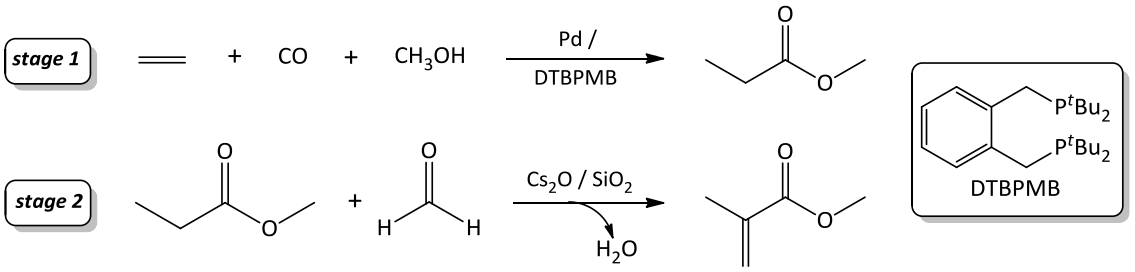


**Scheme 1.6** Two step Alpha process for the production MMA.

In the second stage, MeP is condensed with gaseous formaldehyde over a heterogeneous fixed bed catalyst with cesium oxide on silica as active component to afford MMA in 93 % selectivity (based on MeP).[1] To ensure high MMA selectivity and prevent excessive catalyst aging, the use of anhydrous formaldehyde during this stage is essential. For this reason, formaldehyde is initially produced as formalin in a separate formalin (~55 weight % formaldehyde in water) process and then dehydrated, using a Lucite patented separation process, before being introduced into the MMA feedstock (Figure 1.1). Small amounts of heavy, relatively involatile compounds are produced during this second stage. Over time, these lead to the formation of coke (solid carbonaceous material) deposits on the catalyst which reduces catalytic activity and selectivity. To circumvent this problem, two parallel MMA reactors are employed in the second stage. By this method, coke deposits are easily removed from the one reactor to restore catalytic activity and selectivity, while production is maintained through the other reactor. In the final stages, pure MMA (>99.9 %) is isolated from the crude MMA stream by a series of vacuum distillations and one proprietary reactive separation, while unreacted MeP and water are recycled *via* the formaldehyde dehydration process.[1]

Although the Alpha route is a remarkable process that offers many advantages over other MMA technologies, it still has considerable scope for improvement. Despite the high selectivity towards MMA in the second stage, a maximum yield of only 27 % is achieved per single pass and multiple passes are therefore required to meet larger MMA demands. Overcoming this problem may necessitate the development of a more efficient homogeneous catalytic system to replace the current heterogeneous one. Finding a catalyst capable of promoting C–C bond formation *via* a non-waste generating route is, however, a challenging task. Nevertheless, possible routes to explore may include catalytic C–H activation which in recent times has become more and more promising as a route to the cleaner functionalisation of otherwise inert hydrocarbons.[13-15]

## 1.3 C–H activation in the functionalisation of inert hydrocarbons

C–C bond formation is fundamental to most organic transformations and normally entails synthetic routes that consist of multiple waste generating steps. For example, it is common practise to incorporate reactive groups such as halides into precursors to promote the selective functionalisation of otherwise inert hydrocarbons. Despite the effectiveness of this approach, these precursors typically lead to the production of halide salts and other by-products. As a result the development of more efficient, atom-economical methods for the construction of elaborate molecules from simple building blocks has become the key focus of many research efforts.[15-19] The activation of unreactive C–H bonds represents a major step towards cleaner synthesis as it allows for the direct functionalisation of otherwise relatively inert alkanes and arenes. The inherent stability of C–H bonds (104 kcal/mol for methane, 106 for ethylene and 109 kcal/mol for benzene), however, makes the realisation of such direct activations a daunting task.[17]

One way of achieving C–H activation involves the insertion of a low valent transition metal into the strong C–H bond to create a weaker C–M bond, which is more susceptible to modification.[20] Functionalisation reactions of hydrocarbons with the aid of metal complexes often have the added advantage of proceeding at lower temperatures and with much greater selectivity than conventional organic routes. The ability of soluble transition metal complexes to catalyse the cleavage of unreactive C–H bonds was first recognised by Kleiman and Dubeck[21]

in 1963, when azobenzene was found to undergo *ortho* C-H bond cleavage in the presence of a nickel cyclopentadienyl complex to yield an *ortho*-nickelated species as product (Scheme 1.7). Since then, several novel synthetic systems for the catalytic transformation of alkanes, alkenes and arenes have been discovered and interest in this contemporary field of chemistry is continuously growing.

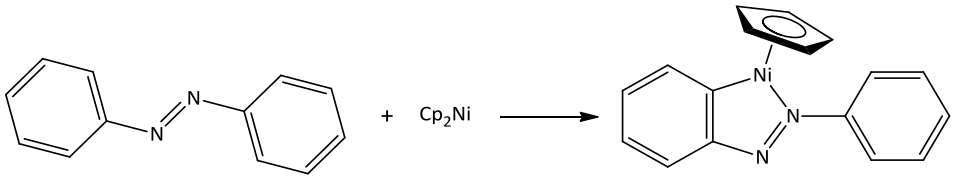


**Scheme 1.7** *Ortho*-metallation of azobenzene by a nickel cyclopentadienyl complex.

The renowned ruthenium-based Murai reaction catalyses the selective insertion of alkenes into the *ortho* C–H bonds of aromatic ketones and represents a good example of a transition metal assisted C-H activation.[22] The proposed mechanism for this reaction (Scheme 1.8) involves initial formation of a 16-electron ruthenium(0) complex (**I**) which, following addition of the acetophenone derivative, gives rise to a cyclic *ortho*-metallated intermediate (**II**). Alkene insertion into the Ru–H bond (**IV**) followed by reductive elimination, liberates the alkylated ketone with concurrent regeneration of the active species (**I**).[23] Murai and co-workers[22] found ruthenium complexes with three triphenylphosphine ligands, such as $RuH_2(CO)(PPh_3)_3$ or $Ru(CO)_2(PPh_3)_3$, to be the best catalyst precursors, promoting C–H/olefin coupling in nearly quantitive yields. Overall, this reaction is insensitive towards substitution effects, tolerating a variety of both electron-withdrawing and electron-donating substituents on the aromatic ring.[24] Furthermore, this route is not constrained to the use of aromatic C–H bonds, and also catalyses the addition of olefins to olefinic C–H bonds such as those present in acyclic enones. C–H/olefin couplings with such substrates, however, proceed less efficiently, resulting in more complex mixtures of products.[15] The ketone functionality of acetophenone can also be replaced by an ester group. In these substrates however, changes in the nature of the aromatic ring substituents do have a dramatic effect on their reactivity.[25,26] Chelation *via* coordination of the ketone functionality forms an integral part of the mechanism, by which the metal is anchored in close proximity to the reactive aromatic C–H bond.[27] Moreover, formation of the metallocycle requires the enone moiety to occupy a *cis* configuration. On account of the

need for the formation of a 5-membered ring, substrates for this reaction are restricted to the use of aromatic or olefinic ketones or esters.

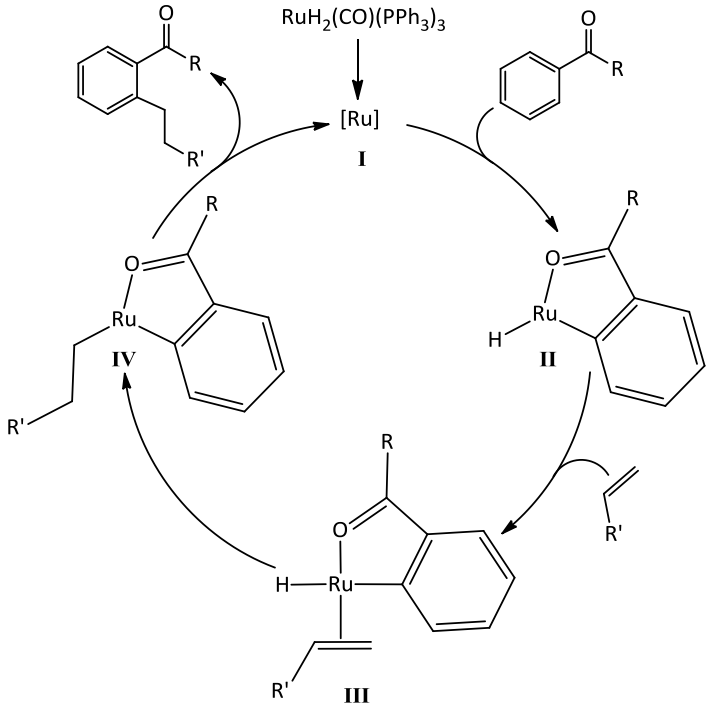


**Scheme 1.8** Proposed catalytic cycle for the Murai reaction.

In order to circumvent these limitations, Carrión and Cole-Hamilton[28] have recently developed a new catalytic process which can be viewed as an extension of the Murai reaction (Scheme 1.9). This reaction allows very similar chemistry to be performed for phenol and aniline derivatives by attaching the substrates to phosphorus. In addition, this development broadens the scope of the reaction to permit the insertion of molecules other than olefins into the *ortho* C–H bonds of phenol. These include formaldehyde which results in the formation of benzo-1,3-dioxane. Although a number of transition metal complexes can be employed as pre-catalyst to this reaction, $[RhCl(PPh_3)_3]$ (Wilkinson's catalyst) was found to give the highest overall yields under all studied reaction conditions. The proposed mechanism for the catalytic cycle involves initial coordination of the phosphinite ligand, followed by *ortho*-metallation to give a 5-membered metallocyclic intermediate (**III**). Subsequent ethene coordination and hydride migration yield intermediate **IV**, containing a coordinated ethyl group, which can undergo reductive elimination to furnish 2-ethylphenyldiphenylphosphinite. The *ortho*-alkylated

product, 2-ethylphenol, is released with concurrent introduction of substrate, *via* a transesterification reaction at phosphorus. The presence of a phosphinite ligand plays a fundamental role in this cycle as no reaction is observed in its absence. In the majority of the reactions, carried out under different conditions and catalyst loadings, diethylphenol is obtained as the major product. This is due to the fact that 2-ethylphenol itself can re-enter the catalytic cycle to result in the dialkylated product. Furthermore, diethylphenol can also result from double alkylation of the coordinated aryl prior to transesterification.

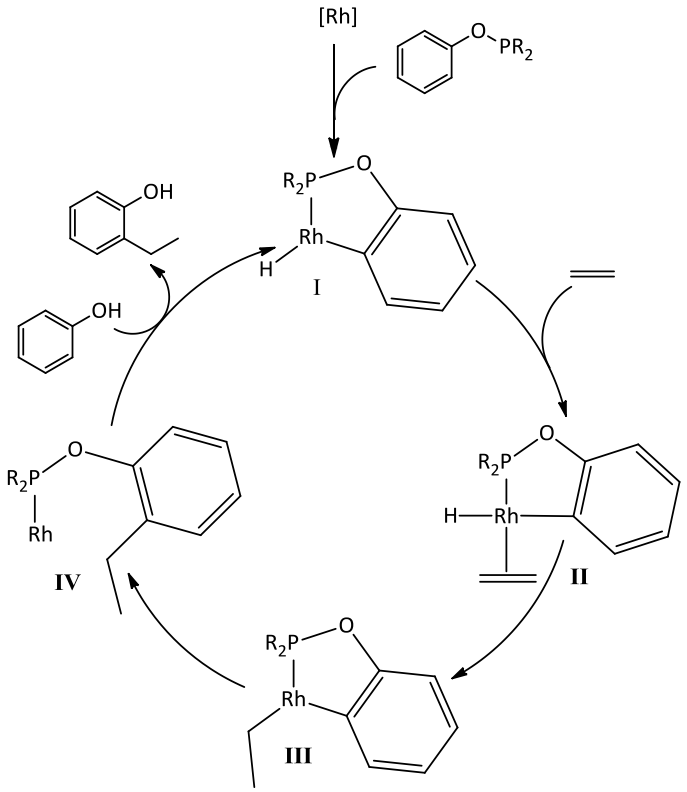


**Scheme 1.9** Possible mechanism for the ethylation of phenol by orthometallation.

Despite the greater strength of arene C–H bonds *versus* those of alkanes, arenes are much more susceptible to C–H bond cleavage than alkanes. Kinetically, arenes are also considered to be more reactive owing to interaction of the metal centre with the aromatic ring prior to C–H cleavage in conjunction with the less hindered nature of the arene C–H bond. The lack of π-electrons in alkane systems renders them less capable of interacting with empty metal orbitals.[19] These considerations are further enhanced thermodynamically by the stronger aryl

*versus* alkyl C–M bonds present in the products.[18] As a result, most transition metal mediated C–H bond activations reported prior to the 1980s, involve the participation of aromatic π-orbitals or are assisted by intramolecular reactions.[16]

The feasibility of alkane C–H activation was first demonstrated in 1969 with the aid of deuterium labelling studies. These studies revealed that platinum(II) salts induce H–D exchange between methane (or analogues thereof) and $D_2O$ at 100 $^oC$. In addition, it was established that the complex $[CoH_3(PPh_3)_3]$ possesses the ability to catalyse methane deuteration at room temperature.[29] Following these discoveries, several other examples of significant interactions between alkane C–H bonds and metal centres became known; suggesting that alkane C–H activation may proceed more readily than had first been anticipated.[30]

Shilov[19] has divided all metal promoted C–H bond splitting reactions into three classes based on their mechanisms. They can be described as: 1) "true" activation, characterised by the formation of a σ-organyl derivative; 2) activation in the absence of direct metal–C–H bond contact or 3) attack on the C–H bond by a reactive species formed *via* a metal mediated pathway. All organometallic approaches that involve σ-M–C bond formation can be classified under the term "true" activation. In these reactions alkane C–H bond cleavage usually proceeds *via* an oxidative addition pathway and is preceded by some form of direct interaction between the metal and alkane. During this interaction, the C–H proton is acidified to a large degree by ligand-to-metal charge transfer without being compensated for by back donation. In many cases, these σ-organyl complexes formed by the oxidative addition of alkanes, alkenes or arenes to a metal centre are sufficiently stable to isolate. As a rule, σ-C–H complexation in alkane metal adducts occurs at the least sterically hindered position. As a result the observed product selectivity often follows the trend primary > secondary > tertiary.[15] Rhodium carbenoids derived from methyl aryl diazoacetates represent exceptions to this rule, effectively catalysing asymmetric C–H activation in a range of alkanes and tetrahydrofuran with strong preference for insertions into C–H bonds at secondary and tertiary sites.[31] In class 2 type reactions C–H bond cleavage is usually facilitated by electron or hydrogen abstraction from an alkane to form reactive radical intermediates without the generation of a σ-C–M bond at any stage. Direct contact between the alkane and the metal centre is, however, still a prerequisite for this class of reaction. The third class involves no direct interaction between the

metal and alkane and bond cleavage follows attack on the C–H bond by some reactive species, initially generated by the metal complex.[19]

Reports of true alkane complexes (Figure 1.2, **V**), where the alkane RH bond is still intact, are scarce. Consequently, agostic complexes (**VI**) constitute the majority of known examples in this area of research. In these complexes, bonding of the alkyl group to the metal is mediated by chelation which could ultimately lead to the formation of a more stable cyclometallation product (**VII**).[18] These intramolecular C–H bond activations occur more readily than intermolecular bond cleavage and more often than not, the σ-organyl is obtained via oxidative addition.[19]

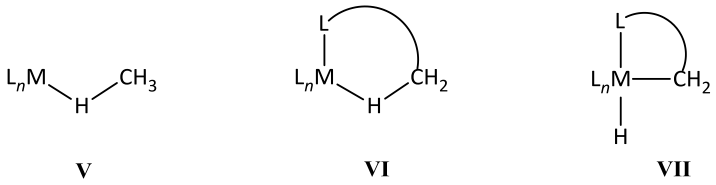


**V** **VI** **VII**

**Figure 1.2** Representation of true, agostic and cyclometallated metal alkane complexes.

An overriding criterion for the successful bonding of alkanes appears to be the presence of a low valent metal and the absence of competitive decomposition pathways. This is since low valent transition metal centres, especially those of the 2nd and 3rd row, are usually stronger π-bases capable of enhanced metal to alkane π-back donation. Increased π-back donation into the C–H σ* orbitals leads to amplified alkane-metal binding which ultimately, when strong enough, induces C–H bond cleavage to form the oxidative addition product.[32] Conversely, the σ-donation component of the M–(HC) bonding is less significant, leading only to a slight elongation of the C–H bond but no cleavage event.[33] Although low valent transition metals preferentially activate terminal C–H bonds, there have been reported cases where the opposite trend seems to hold. This suggests that the overall selectivity of alkane activation may be dependent on a number of competing factors.[34-36]

Even though recent years have been marked by major advances in the field of alkane C-H activation and several alkane metal complexes have been described, functionalisation of such systems still remains a major challenge.[37-41] One important example of such an alkane

functionalisation was reported by Sakakura and Tanaka in 1987. Through their studies they have shown that the terminal methyl group of *n*-pentane can be carbonylated regioselectively to *n*-hexanal under an atmosphere of CO in the presence of catalytic amounts of [RhCl(CO)($PMe_3$)$_2$] (Scheme 1.10). Although no formal mechanistic studies were performed, this reaction most likely involves initial photochemical $sp^3$ C–H activation of *n*-pentane to give the oxidative addition intermediate [RhCl(H)(CO){$(CH_2)_4CH_3$}($PMe_3$)$_2$]. This activation event is then followed by CO insertion and reductive elimination to liberate *n*-hexanal as product with coordination of CO in the resultant vacant site to regenerate the catalyst.[39]

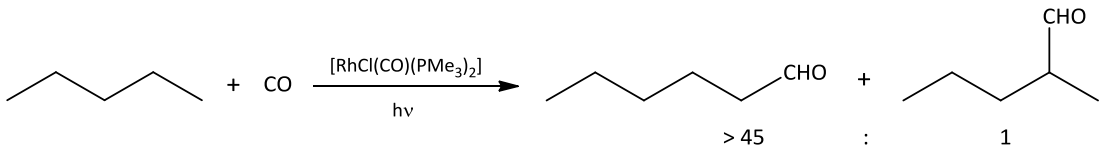


**Scheme 1.10** Regioselective Rh catalysed carbonylation of *n*-pentane *via* photochemical C–H activation.

## 1.4 Project objectives and thesis outline

### *1.4.1 Project objectives*

As was discussed in section 1.2.2, Lucite International has developed the remarkable two stage Alpha process for the large scale production of MMA. The first stage of this process has been fully optimised and proceeds with great efficiency at low catalyst loadings, affording MeP in high yield and selectivity. In contrast, the condensation of MeP with formaldehyde in the second stage only proceeds in low yield and multiple passes are therefore required. Although this stage has been optimised to a level that allows for its commercial use, it shows great scope for improvement and undoubtedly represents the Achilles heel of the Alpha process. Improving the efficiency of this condensation step would greatly reduce the overall MMA production cost and for this reason Lucite International is currently devoted to overcoming these limitations. The research presented in this account was sponsored by Lucite International and forms part of their efforts to improve this stage of the Alpha process. Thus, the objective of the larger part of this study was to explore the development of an alternative, homogeneous catalytic system capable of promoting efficient condensation of formaldehyde

with either propanoic acid or MeP. The latter was, however, preferred as substrate since MeP represents the final product in the first stage of the Alpha process.

Given the atom efficiency generally associated with C–C bond forming reactions that proceed *via* C–H activation pathways, we were particularly interested in exploring the possibility of functionalising propanoic acid or MeP selectively in the *α*-position using a C–H activation approach. Earlier results from our group have indicated that selective *ortho*-alkylation of phenol and aniline derivatives can be achieved by linking the substrate to phosphorus (Scheme 1.9).[28] In these reactions the resulting phosphinite or aminophosphino ligand serves as template for selective *ortho*-metallation, while the product is released with introduction of a fresh substrate molecule by transesterification at phosphorus.

Encouraged by these results, we envisaged the realisation of the selective *α*-alkylation of propanoic acid by a similar approach. In particular, the observation that ethene can be replaced by formaldehyde as alkylating agent in *ortho*-alkylation reactions, were of great interest within the scope of this project. In the case of phenol, insertion of formaldehyde into the *ortho* C–H bond initially gives 2-(hydroxymethyl)phenol which is trapped as the acetal, benzo-1,3-dioxane, by formaldehyde (Scheme 1.11).[42]

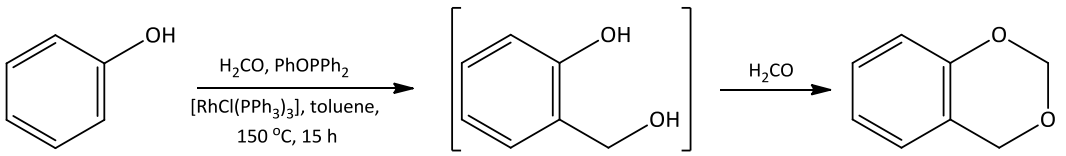


**Scheme 1.11** Catalytic alkylation of phenol with formaldehyde to give benzo-1,3-dioxane after acetal formation.

In other results from our group the selective hydrogenation of acrylic acids was shown possible using a similar approach (Scheme 1.12).[43] In these reactions the acrylic acids are linked to phosphorus by treatment with diphenylphosphinous acid in the presence of a base to form unsaturated mixed anhydride ligands. These ligands, following their coordination to a Rh(I) centre, once again direct selective hydrogenation under basic conditions by functioning as scaffolds. Similar to the earlier described *ortho*-alkylations, the hydrogenated products are released with concomitant substrate introduction and by a transesterification reaction at phosphorus.

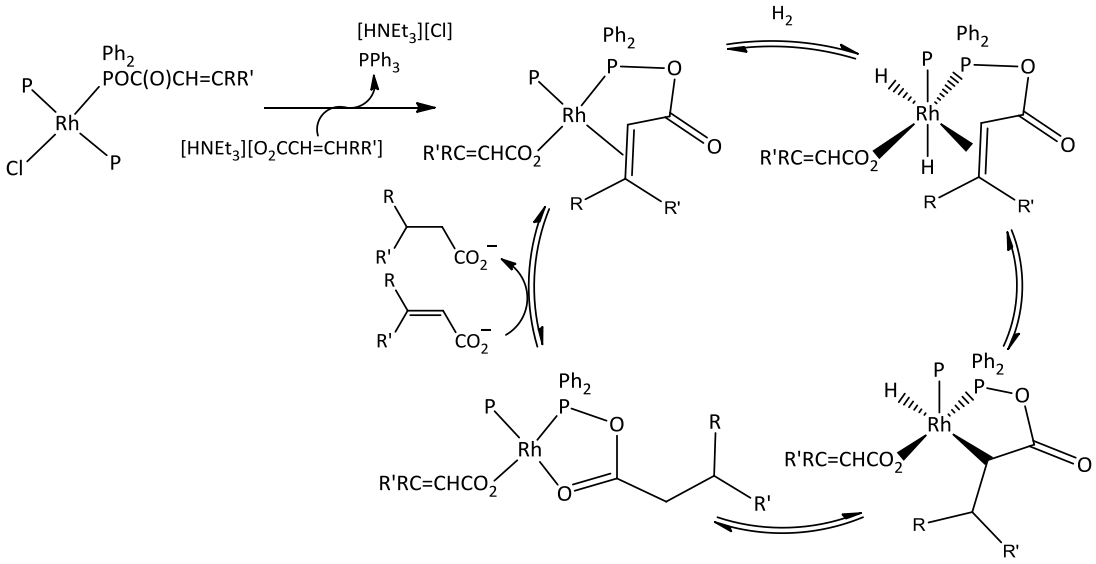

**Scheme 1.12** Mechanism for the hydrogenation of acrylic acids using Rh(I) complexes of mixed anhydrides derived from diphenylphosphorus acid and acrylic acids (where P = $PPh_3$, R = H / Me and R' = Me / -CH=CHMe ).

The initial aim of this study was to combine these two known methodologies into a catalytic cycle that would enable the *α*-methylenation of propanoic acid. The catalytic cycle proposed for this functionalisation is given in Scheme 1.13 and involves initial coordination of a mixed anhydride ligand, derived from propanoic acid and phosphinous acid, to a Rh(I) centre. Following coordination, selective C–H activation may be expected to proceed in the *α*-position of the aliphatic carbon chain since this would generate a highly favoured 5-membered ring system. This is followed by formaldehyde coordination and insertion into the activated C–H bond. Finally, following reductive elimination, the generated 3-hydroxy-2-methylpropanoic acid, is released with concurrent introduction of a fresh substrate molecule, by transesterification at phosphorus. Under the elevated reaction temperature, 3-hydroxy-2-methylpropionic acid will spontaneously eliminate water to afford methacrylic acid as the final product. Since the liberated water would lead to the rapid hydrolysis of the phosphorus ester bond, the inclusion of water scavengers would need to be explored if such an approach were to be successful.

As it would be preferable to use methyl propanoate in place of propanoic acid as substrate we further aimed to explore the functionalisation of this substrate *via* C–H activation pathways that do not necessitate covalent linkage of the substrate to phosphorus. A large number of transition metal complexes are capable of activating aliphatic C-H bonds by oxidative addition.

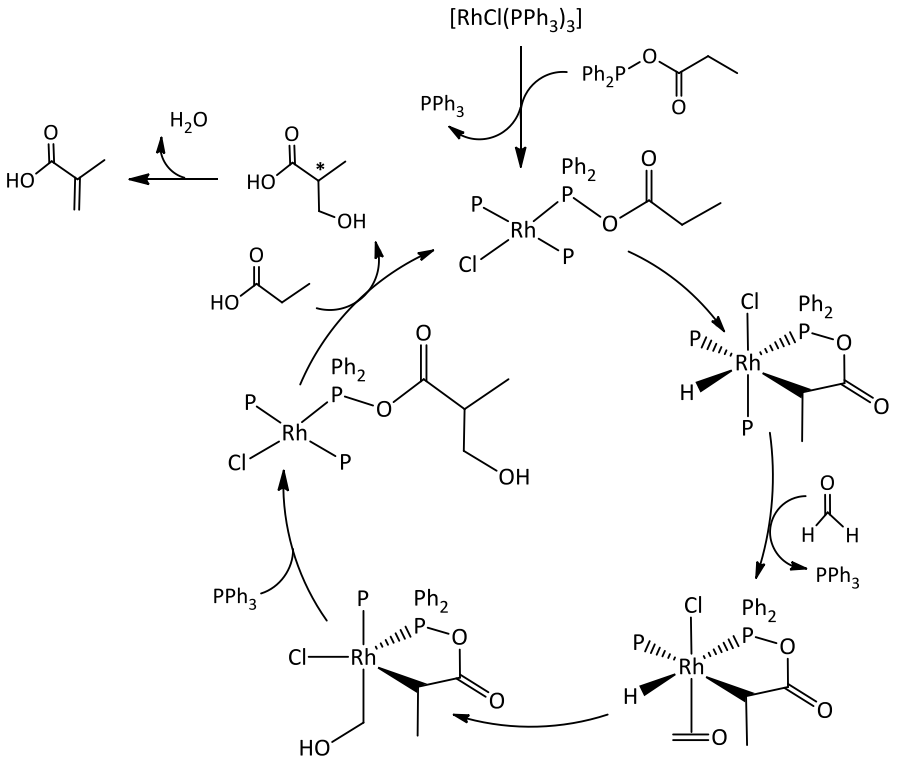


**Scheme 1.13** Proposed catalytic cycle for the functionalisation of propanoic acid *via* selective catalytic C-H activation in the α-position, followed by the insertion of formaldehyde, employing Rh(I) mixed anhydride complexes (where P = $PPh_3$).

Such reactions, however, generally work best where there is anchimeric assistance* with the formation of 5- and 6-membered metallocycles mostly favoured.[44] Recently Milstein has shown that $sp^3$ C-H activation is possible for ketones using iridium pincer complexes.[45] For these activations the regioselectivity ($\alpha$- versus $\beta$-position) can be controlled by the presence or absence of coordinating water. In this study we aimed to explore whether a similar approach could be followed to achieve regioselective C–H activation for esters such as MeP.

Although the shortcomings associated with the second stage of the Alpha process largely relate to the low efficiency of the condensation reaction between MeP and formaldehyde, the source of formaldehyde represents another area which has scope for improvement. As the use of anhydrous formaldehyde is essential for the prevention of excessive catalyst aging, dehydration of the formalin generated in the formalin process is required prior to its introduction into the MMA feed. It would therefore be of great benefit to the overall process if

* Anchimeric assistance refers to the situation where the preferential site of C–H activation is determined by a coordinating atom present in the substrate. This preference is generally determined by the size of the metallocycle generated, with 5- and 6-memebered rings typically being favoured.

this additional, costly step could be eliminated by the generation of anhydrous formaldehyde *in situ via* methanol dehydrogenation. For this reason, we further aimed to investigate the feasibility of methanol as an indirect, anhydrous alkylating agent in the second stage of the Alpha process.

Although the development of a novel, homogenous catalytic system for the second stage is highly desirable, the final part of this study was aimed at gaining a better understanding of the limitations associated with the current process in order to facilitate minor improvements in the short term. In order to achieve this, we aimed to explore the influence of fundamental factors such as the base strength, solvent system, formaldehyde source and reagent ratios on the condensation of MeP with formaldehyde. Furthermore, using deuterium labelling as a tool we further aimed to explore the efficiency of deprotonation over a range of soluble inorganic and organic bases to aid in determining the nature of the bottleneck in this condensation step.

### *1.4.2 Thesis outline*

In **Chapter 2** the preparation, characterisation and in solution behaviour of a range of mixed anhydride ligands derived from either propanoic acid or phenylacetic acid are described. The coordination chemistry, stability and catalytic potential of Rh(I) and Ru(II) complexes containing these mixed anhydrides are described in **Chapter 3** while in **Chapter 4** this series of complexes is extended to include Rh(I) mixed anhydride complexes containing chelating bisphosphines as auxiliary ligands. In **Chapter 5** the use of Ir(I) pincer complexes in the regioselective $sp^3$ C–H activation in the *α*-position of a range of esters, and in particular MeP, is explored with special focus on the effect of water on the regioselectivity of such activations. In **Chapter 6** preliminary results obtained for an investigation into the possibility of producing anhydrous formaldehyde *in situ via* the catalytic dehydrogenation of methanol in the presence of carbonate salts and / or transition metal catalysts is described. More specifically, this chapter focuses largely on the use of a one-pot setup for the catalytic, indirect *α*-methylenation of MeP with methanol as the methylene source. In **Chapter 7** the capacity of a series of simple inorganic and organic bases to catalyse the condensation of MeP with formaldehyde is assessed. In particular, the extent to which each of the bases under consideration affects deprotonation in the α-position of MeP is explored in this chapter with the aid of deuterium labelling studies. Finally, **Chapter 8** summarises the main conclusions that

could be drawn from this study and highlights a few promising initiatives to consider for future developments in this area. A number of crystal and molecular structures were determined by X-ray diffraction during the course of this study and tables summarising the crystallographic data for these structures are listed in **Appendix 1**.

## 1.5 Notes and References


(1) Harris, B. *Ingenia* **2010**, *issue 45*, 19-23.
(2) Michel, M. J. *Ger. Offen.* **1969**, DE1906747.
(3) Nagai, K. *Appl. Catal. A: Gen.* **2001**, *221*, 367-377.
(4) Wiessermel, K.; Arpe, H. J. (Ed: Lindley, C. R.) *in Industrial Organic Chemistry*, 4th edition, Wiley-VCH: New York, 2003, p46; p281-285.
(5) Green, M. M.; Wittcoff, H. A. *in Organic Chemistry principles and Industrial practice*, Wiley-VCH: Weinheim, 2003, p137-156.
(6) Merger, F.; Foerster, H. J. (BASF), *U.S. Patent* **1982**, 4408079.
(7) Duembgen, G.; Fouquet, G; Krabetz, R.; Lucas, E.; Merger, F.; Nees, F (BASF), *U.S. Patent* **1983**, 4496770.
(8) Drent, E.; Arnoldy, P.; Budzelaar, P. H. M. *J. Organomet. Chem.* **1994**, *475*, 57-63.
(9) Gogate, M. R.; Spivey, J. J.; Zoeller, J. R. *Catal. Today* **1997**, *36*, 243-254.
(10) Ai, M. *Bull. Chem. Soc. Jpn.* **1990**, *63*, 3722-3724.
(11) http://www.sriconsulting.com/PEP/Public/Reports/Phase_95/RW95-1-9/.
(12) Clegg, W.; Eastham, G. R.; Elsegood, M. R. J.; Tooze, R. P.; Wang, X. L.; Whiston, K. *Chem. Commun.* **1999**, 1877–1878.
(13) Colby, D. A.; Bergman, R. G.; Ellman, J. A. *Chem. Rev.* **2010**, *110*, 624-655.
(14) Yadav, J. S.; Antony, A.; Rao, T. S.; Reddy, B. V. S. *J. Organomet. Chem.* **2011**, *696*, 16-36.
(15) Crabtree, R. H. *J. Organomet. Chem.* **2004**, *689*, 4083-4091.
(16) Labinger, J. A.; Bercaw, J. E. *Nature* **2002**, *417*, 507-514.
(17) Jia, C.; Kitamura, T.; Fujiwara, Y. *Acc. Chem. Res.* **2001**, *34*, 633-639.
(18) Crabtree, R. H. *J. Chem. Soc., Dalton Trans.* **2001**, 2437-2450.
(19) Shilov, A. E.; Shul'pin, G. B. *Chem. Rev.* **1997**, *97*, 2879-2932.
(20) Ritleng, V.; Sirlin, C.; Pfeffer, M. *Chem. Rev.* **2002**, *102*, 1731-1769.
(21) Kleiman, J. P.; Dubeck, M. *J. Am. Chem. Soc.* **1963**, *85*, 1544-1545.
(22) Murai, S.; Kakiuchi, F.; Sekine, S.; Tanaka, Y.; Kamatani, A.; Sonoda, M.; Chatani, N. *Nature* **1993**, *366*, 529-531.
(23) Guari, Y.; Castellanos, A.; Sabo-Etienne, S.; Chaudret, B. *J. Mol. Catal. A: Chem.* **2004**, *212*, 77-82.
(24) Sonoda, M.; Kakiuchi, F.; Chatani, N.; Murai, S. *Bull. Chem. Soc. Jpn.* **1997**, *70*, 3317-3128.
(25) Kakiuchi, F.; Ohtaki, H.; Sonoda, M.; Chatani, N.; Murai, S. *Chem. Lett.* **2001**, 918-919.
(26) Sonoda, M.; Kakiuchi, F.; Kamatani, A.; Chatani, N.; Murai, S. *Chem. Lett.* **1996**, 109-110.

(27) Jazzar, R. F. R.; Varrone, M.; Burrows, A. D.; Macgregor, S. A.; Mahon, M. F.; Whittlesey, M. K. *Inorg. Chim. Acta* **2006**, *359*, 815-820.
(28) Carrion, M. C.; Cole-Hamilton, D. J. *Chem. Commun.* **2006**, 4527-4529.
(29) Gol'dshleger, N. F.; Tyabin, M. B.; Shilov, A. E.; Shteinman, A. A. *Zh. Fiz. Khim.* **1969**, 2174-2175.
(30) Arndtsen, B. A.; Bergman, R. G.; Mobley, T. A.; Peterson, T. H. *Acc. Chem. Res.* **1995**, *28*, 154-162.
(31) Davies, H. M. L.; Hansen, T.; Churchill, M. R. *J. Am. Chem. Soc.* **2000**, *122*, 3063-3070.
(32) Kubas, G. J. *Acc. Chem. Res.* **1988**, *21*, 120-128.
(33) Crabtree, R. H. *Angew. Chem. Int. Ed.* **1993**, *32*, 789-805.
(34) Jones, W. D.; Feher, F. J. *J. Am. Chem. Soc.* **1984**, *106*, 1650-1663.
(35) Janowicz, A. H.; Bergman, R. G. *J. Am. Chem. Soc.* **1983**, *105*, 3929-3939.
(36) McNamara, B. K.; Yeston, J. S.; Bergman, R. G.; Moore, C. B. *J. Am. Chem. Soc.* **1999**, *121*, 6437-6443.
(37) Zhang, S.-Y.; Tu, Y.-Q.; Fan, C.-A.; Jiang, Y.-J.; Shi, L.; Cao, K.; Zhang, E. *Chem. Eur. J* **2008**, *14*, 10201-10205.
(38) Watanabe, T.; Oishi, S.; Fuji, N.; Ohno, H. *Org. Lett.* **2008**, *10*, 1759-1762.
(39) Sakakura, T.; Tanaka, M. *J. Chem. Soc., Chem. Commun.* **1987**, 758-759.
(40) Sakakura, T.; Sodeyama, T.; Sasaki, K.; Wada, K.; Tanaka, M. *J. Am. Chem. Soc.* **1990**, *112*, 7221-7229.
(41) Sakakura, T.; Abe, F.; Tanaka, M. *Chem. Lett.* **1991**, 359-362.
(42) Carrión, M. C.; Cole-Hamilton, D. J. *Unpublished results* **2006**.
(43) Iraqi, A.; Fairfax, N. R.; Preston, S. A.; Cupertino, D. C.; Irvine, D. J.; Cole-Hamilton, D. J. *J. Chem. Soc., Dalton Trans.* **1991**, 1929-1935.
(44) Albrecht, M. *Chem. Rev.* **2010**, *110*, 576-623.
(45) Feller, M.; Karton, A.; Leitus, G.; Martin, J. M. L.; Milstein, D. *J. Am. Chem. Soc.* **2006**, *128*, 12400-12401.

# Chapter 2

## Mixed anhydride ligand systems

– Their preparation, facile rearrangement and stabilisation –

*A series of acyloxyphosphines and acylphosphites derived from either propionic acid or phenylacetic acid were prepared and, where stability allowed, fully characterised. Some of the more simple mixed anhydrides posed problems relating to their thermal lability and the stabilisation of such ligand systems by using either electronic or steric effects was explored. The acidity of the α-protons present in the acyloxy functionality is of great importance to the later application of these ligands in catalysis. The acidity of these protons could be enhanced by changing from a propionyloxy to a phenylacetyloxy group and the extent of this variance monitored by NMR spectroscopy. NMR studies also unearthed interesting coupling behaviour for some of the prepared compounds which could be correlated with their chiral nature.*

## 2.1 Introduction

(Acyloxy)diorganylphosphines or mixed anhydrides of the general form $R_2POC(O)R'$ represent an interesting class of compounds that are accessible *via* a number of synthetic routes. They can be prepared readily either by the treatment of chlorophosphines with sodium carboxylates or carboxylic anhydrides or by the reaction with carboxylic acids in the presence of a tertiary amine base.[1] However, despite some reports on the successful preparation and isolation of various mixed anhydrides, their reactive nature and indeed thermal lability have been the subjects of most discussions.[1,2,3] Their propensity to undergo spontaneous and irreversible condensation and rearrangement reactions, even at low temperatures, are known to complicate both the synthesis and in particular the purification of these compounds. In a study aimed at investigating the kinetics of such rearrangement reactions, Lindner and Wuhrmann[1] prepared a series of (perfluoracyloxy)diorganylphosphines **Ib–d** *via* different synthetic pathways and assessed their temperature dependent conversion to the (perfluoroacyl)diphenylphosphine oxides **IIb–d** (Scheme 2.1). Although compounds **Ib–d** were found to be stable at temperatures below -20 °C, they rapidly rearrange at higher temperatures to furnish **IIb–d** almost exclusively. In a separate study, the related (acyloxy)diphenylphosphine **Ia** has also been shown to rearrange to 1,1-bis(diphenylphosphinoyl)ethyl acetate **IIIa** even at temperatures as low as -10 °C. Likewise, the (acyl)diphenylphosphine oxide **IIa** is believed to act as an intermediate during the course of this dimerisation reaction.[3]

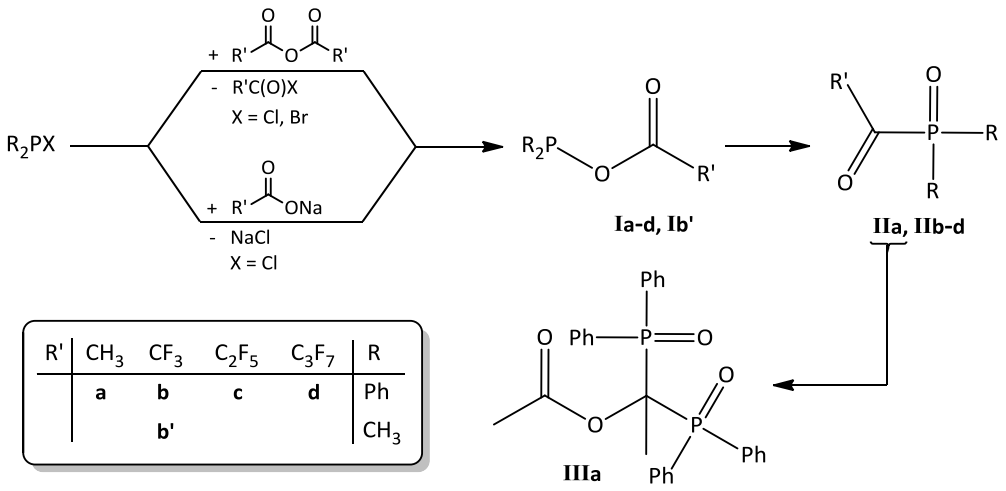


**Scheme 2.1** Two general routes for the preparation of (acyloxy)diphenylphosphines **Ia–d** and **Ib'**, with the subsequent spontaneous rearrangement of **Ia–d** to give (perfluoracyloxy)diphenylphosphines **IIa–d** (*reaction scheme adapted from literature*).[1,3]

Relying on IR-spectroscopy, Lindner and Wuhrmann[1] used changes in the characteristic ν(C=O) bands as a rough estimate for the temperature dependent rate of rearrangement. Whilst the isomerisation of **Ib–d** to **IIb–d** was found to be relatively sluggish at 20 °C, this conversion proceeds to near completion within only 60 min at 50 °C. Using a more instructive approach, the authors determined the isomerisation of **Ib** and **Ic** to be first-order, with the overall conversion **Ib** → **IIb** occurring slower than in the instance of **Ic** → **IIc**, owing to the greater activation enthalpy Δ*H** for **Ib**. Based on their findings, the mechanism of isomerisation was proposed to most likely proceed *via* an intramolecular rearrangement as outlined in Scheme 2.2.

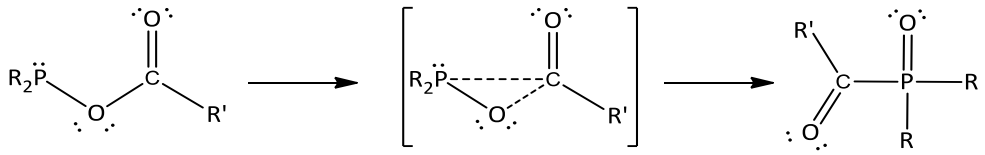

**Scheme 2.2** Mechanism, as proposed by Lindner and Wuhrmann,[1] for the intramolecular isomerisation of (acyloxy)diphenylphosphines to (perfluoracyloxy)diphenylphosphines.

Surprisingly, unsaturated mixed anhydrides derived from acrylic acids such as crotonic acid {$CH_3CH{=}CHCO_2H$}, 3-methyl crotonic acid {$(CH_3)_2CH{=}CHCO_2H$}, pyroterebic acid {$(CH_3)_2CH{=}CHCH_2CO_2H$)}, and *α*-methylcinnamic acid {$PhCH{=}C(Me)CO_2H$} prove to be remarkably stable in solution at room temperature and indefinitely stable in the solid state under an inert atmosphere.[4] On the contrary, mixed anhydrides derived from the less substituted acrylic acid {$CH_2{=}CHCO_2H$} and vinylacetic acid {$CH_2{=}CHCH_2CO_2H$}, rearrange rapidly in solution rendering their isolation unfeasible. Unlike the previously discussed (acyloxy)diorganylphosphines, these mixed anhydrides do not isomerise to the corresponding (acyl)diphenylphosphine monoxides {$Ph_2P(O)C(O)R$}, but instead rearrange to yield tetraphenyldiphosphine monoxide {$Ph_2PP(O)Ph_2$} together with carboxylic anhydrides as the major products; underlining the unpredictable nature of these compounds.[5] The stability of these compounds may therefore be a function of the steric bulk surrounding the double bond, where stable unsaturated mixed anhydrides constitute those bearing more than one substituent at the double bond.[6] Although no mechanistic studies concerning the dimerisation of these compounds have been performed, the formation of $Ph_2PP(O)Ph_2$ is unaffected by the concentrations of both $Ph_2PCl$ and $NEt_3$ and is postulated to occur *via* an intermolecular

disproportionation reaction (Scheme 2.3).[5] Although by this mechanism the diphosphoxane $Ph_2P–O–PPh_2$ forms as initial product of disproportionation, this compound is known to favour the more stable isomeric form tetraphenyldiphosphine monoxide, $Ph_2P(O)PPh_2$.[7]

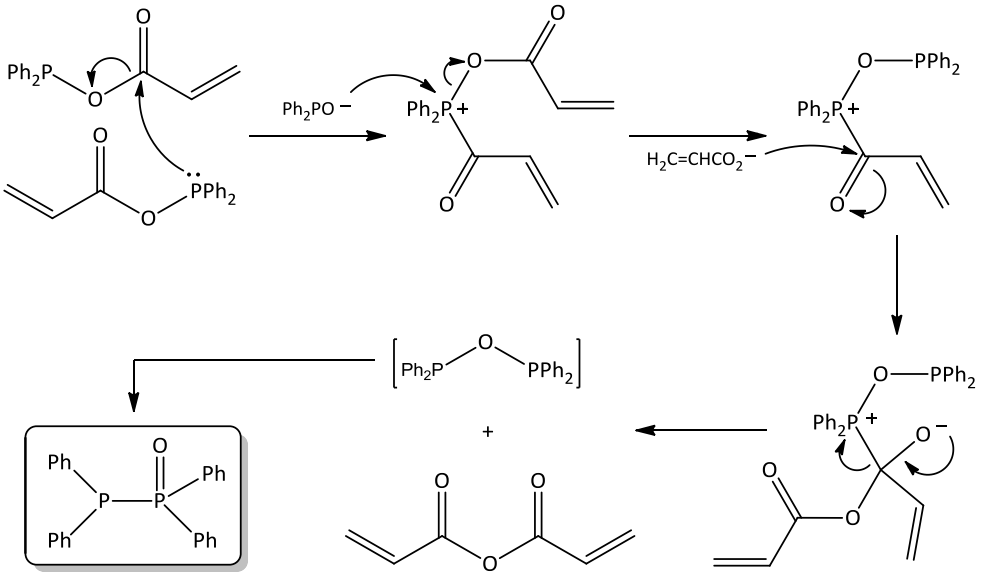


**Scheme 2.3** Proposed mechanism for the disproportionation of the mixed anhydride prepared from acrylic acid to tetraphenyldiphosphine monoxide and acrylic anhydride.[5]

In a number of more recent reports, changing from chlorophosphines to chlorophosphites as precursors during the preparation of mixed anhydrides has led to the generation of (acyl)phosphites with enhanced thermodynamic stability (Figure 2.1).[8-11] These compounds have shown promise as ligands in catalysts for both isomerisation (**IV**)[8] and asymmetric hydroformylation (**VIIa–b**)[11] as well as enantioselective hydrogenation reactions (**VIa–f**).[10] In addition, compound **V** has been employed as a precursor in the preparation of complex diaryl phosphonate esters which are of medicinal importance owing to their ability to act as irreversible dipeptidyl peptidase IV inhibitors.[9] It is noteworthy, however, that despite the general improved stability of (acyl)phosphites of this kind, within the series **VIIa–f** the formation of by-products during synthesis of compound **VIa** has been noted by Korostylev and co-workers.[10] These by-products could not be removed using standard purification techniques and were most likely the result of spontaneous rearrangement reactions, although not recognised as such by the authors. Also, in the experimental description for the preparation of **V**, Belyaev and co-workers[9] state obtaining **V** as a crude product which was used without

further purification in subsequent reactions. This could also imply the presence of minor by-products generated by unwanted rearrangement reactions.

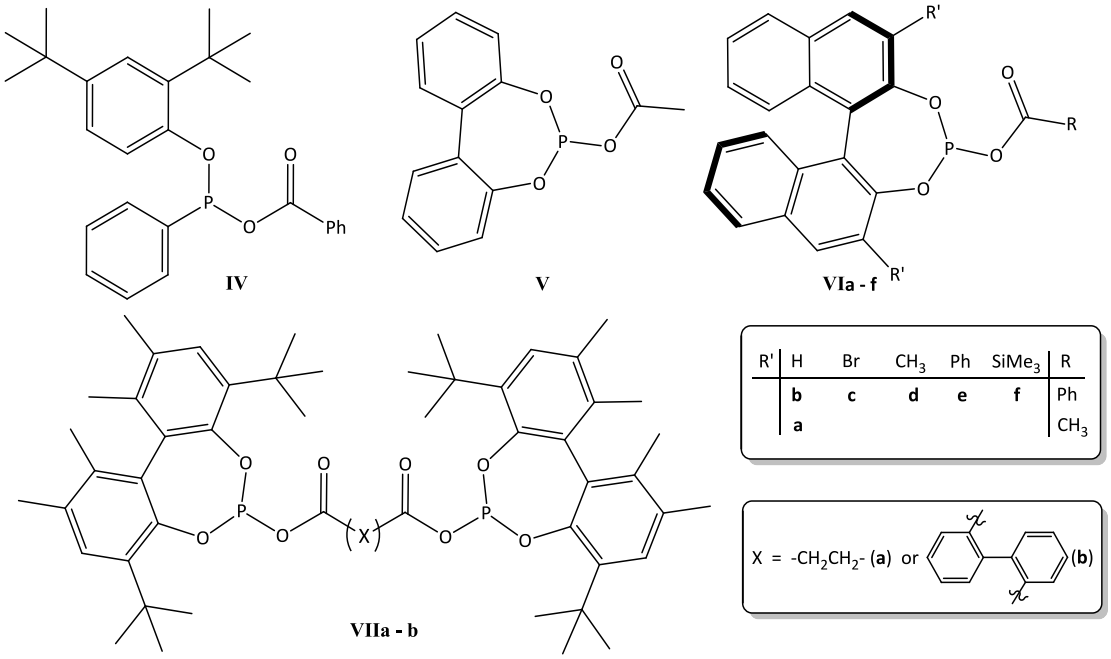


**Figure 2.1** Selected literature examples of stable (acyl)phosphite mixed anhydride ligands.

Despite the discussed challenges surrounding the preparation and isolation of mixed anhydrides, the goal of this particular part of the study was to prepare and fully characterise a number of mixed anhydrides derived from chlorophosphines or chlorophosphites and propanoic acid. These compounds, in later work, could serve as ligands for coordination to various electron rich transition metal complexes *via* their phosphorus atoms. Their function within the resultant metal complexes would be dual, serving both as substrates and as scaffolds for directing selective C–H activation in the $\alpha$-position of the propionyloxy moiety (as was explained in the overall project aims, Chapter 1). In addition, an investigation into prospective ways to stabilise ligands of this kind was launched and the outcome of this study, which allowed for additional insight into the nature and thermal lability of this class of compounds, is discussed herein. To the best of our knowledge, all mixed anhydrides presented in this chapter, bar one (as will be specified in the text), are here reported for the first time and therefore this study represents an important contribution to this somewhat ill represented class of compounds.

## 2.2 Results and Discussion

The preparation of the simple mixed anhydrides bearing a propionyloxy group and the facile rearrangements associated with these compounds are described in sections 2.2.1, whilst the outcome of an investigation into the possible ways to stabilise such compounds are discussed in section 2.2.2. Increasing the acidity of the $\alpha$-protons of the propionyloxy moiety could be achieved by minor alterations in substitution, which are described in section 2.2.3. Section 2.2.4 is devoted to interesting spectroscopic behaviour noted for all of the compounds under discussion, while section 2.2.5 deals with insights gained from molecular and crystal structure determinations.

### *2.2.1 Preparation of simple mixed anhydrides and their properties*

For any metal complex to promote C–H activation, it needs to be inherently electron rich and therefore ideally should contain highly donating ligands coordinated to a low valent transition metal centre. Taking these requirements into consideration, the first endeavour was to prepare mixed anhydride ligands which, in addition to the desired propionyloxy group, contained alkyl rather than alkoxy groups connected to the phosphorus atom. Since the propionyloxy group already represents an electron withdrawing substituent, alkyl groups were chosen over the more stable alkoxy groups in order to increase the donating abilities of the eventual ligand. With this in mind, the very simple mixed anhydride (propionyloxy)diphenyl-phosphine, **1**, was selected as point of departure. The synthesis of this compound has been reported before by Bollmacher and Sartori[12] in a study directed towards the synthesis of Cu(I) and Ag(I) complexes containing this ligand. During their studies, the desired mixed anhydride could be prepared in yields of 86-90 % by the treatment of chlorodiphenylphosphine with sodium propanoate. Following a similar approach, a suspension of sodium propanoate in tetrahydrofuran (thf) was treated with an equimolar amount of chlorodiphenylphosphine at 0 $^{o}$C for 1 h and then a further 2 h at room temperature. Subsequent removal of solid by-product (NaCl) by filtration and evaporation of all volatiles under reduced pressure afforded the product as a viscous colourless oil [Scheme 2.4 (a)]. This compound could also be prepared using an adaptation of a procedure proposed by Cupertino and Cole-Hamilton[4] by treatment of a propanoic acid solution in thf at -10 $^{o}$C with chlorodiphenylphosphine and triethylamine. Following a 10 min stirring interval, the formed [$HNEt_3$][Cl] precipitate could be removed by

filtration and the filtrate reduced to dryness to furnish **1** [Scheme 2.4 (b)]. However, although this simple mixed anhydride could be prepared in high purity using either one of the described methods, reactions were on occasions complicated by the facile rearrangement in solution to afford significant amounts of the disproportionation product, tetraphenyldiphosphine monoxide $\{Ph_2P(O)PPh_2\}$. Moreover, following successful preparation of this compound, rearrangement would generally take place during storage, even at temperatures as low as -22 $^oC$, to afford large amounts of $\{Ph_2P(O)PPh_2\}$ as a white solid. This rearrangement has also been observed by Bollmacher and Sartori[12] during attempts to purify the ligand by fractional distillation. As was mentioned in the introductory section, rearrangements of this type have also been described by Irvine and co-workers[5] for mixed anhydrides derived from chlorodiphenylphosphine and acrylic or vinylacetic acid. Compound **1**, which is highly oxygen and moisture sensitive, is soluble in most organic solvents such as hexane, dichloromethane, chloroform, thf, acetone or diethyl ether and has been fully characterised in literature.[12]

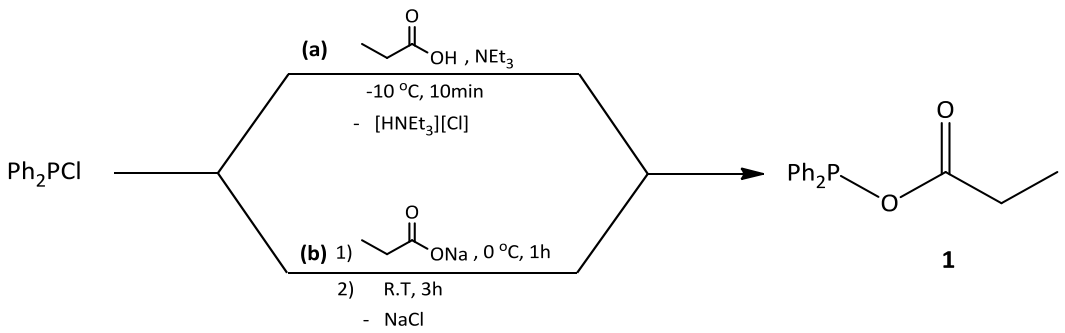


**Scheme 2.4** Reaction scheme for the preparation of (propionyloxy)diphenylphosphine (**1**) *via* (a) an adaptation of the procedure reported by Cupertino and Cole-Hamilton[4] and (b) the route reported by Bollmacher and Sartori.[12]

### *2.2.2 Stabilisation of mixed anhydride systems*

In view of the difficulties caused by the thermal lability of **1**, an investigation into potential ways to stabilise mixed anhydrides of this kind was launched. Encouraged by literature reports on more stable (acyl)phosphites (*vide supra*), we envisaged two possible approaches to achieving more stable ligands and preventing unwanted side reactions - approach **A**: by decreasing the nucleophilicity of the phosphorus atom through the incorporation of electron withdrawing heteroatoms directly bonded to phosphorus, or approach **B**: by increasing the steric requirements of the groups attached to phosphorus and thereby inhibiting close

proximity of neighbouring molecules needed for the occurrence of intermolecular disproportionation reactions (Figure 2.2).

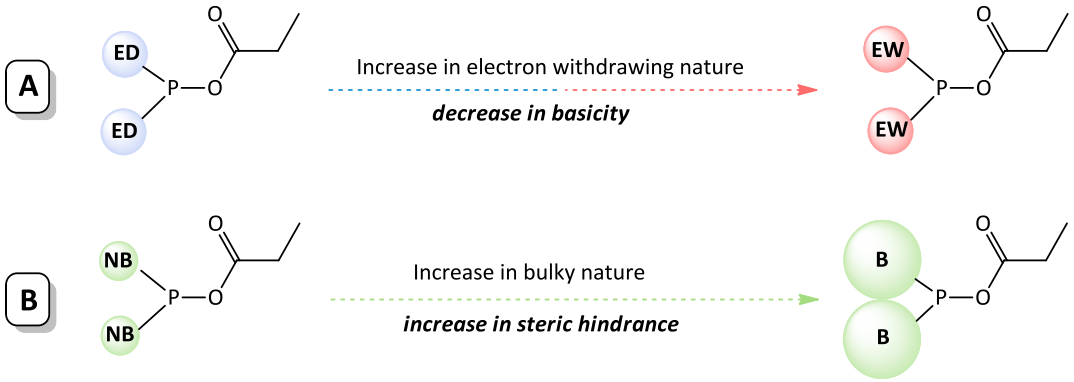


**Figure 2.2** Possible ways to stabilise mixed anhydrides derived from propanoic acid (where **ED** = electron donating, **EW** = electron withdrawing, **NB** = non bulky and **B** = bulky).

With the proposed approaches in mind, a collection of compounds was prepared and their in solution stability assessed using mainly NMR spectroscopy, especially $^{31}$P NMR spectroscopy. This collection of compounds can be divided in three series (Figure 2.3), where ***series I*** comprises of mixed anhydrides **1** and **2** which contain neither electron withdrawing groups bonded directly to phosphorus (with the exception of the propionyloxy moiety) nor bulky substituents on the phenyl rings, while ***series II*** includes mixed anhydrides **7–8** which do possess electron withdrawing atoms directly bonded to the phosphorus atom, but no bulky substituents on the rings. Finally, ***series III*** comprises of mixed anhydrides **9–10** that bear both electron withdrawing groups directly attached to phosphorus as well as bulky ring substituents. It is worth mentioning, however, that together with a gain in stability, approach **A** would also bring about a loss in the overall electron richness of the ligand, which might prove detrimental to their later application in catalysis. A fine balance will, therefore, need to be reached between ligand stability and donor abilities, for these compounds to be successful as ligands in C–H activation catalysts. For this reason, diols containing electron donating alkyl groups as ring substituents were chosen for the preparation of the chlorophosphite precursors to compounds **9–10** of ***series III*** in an attempt to counter balance the electron withdrawing effects of the oxygen atoms to some extent with inductive effects. The alkyl substituents in the

3-positions of the rings serve a dual purpose; acting both as donors of electron density and sterically demanding groups.

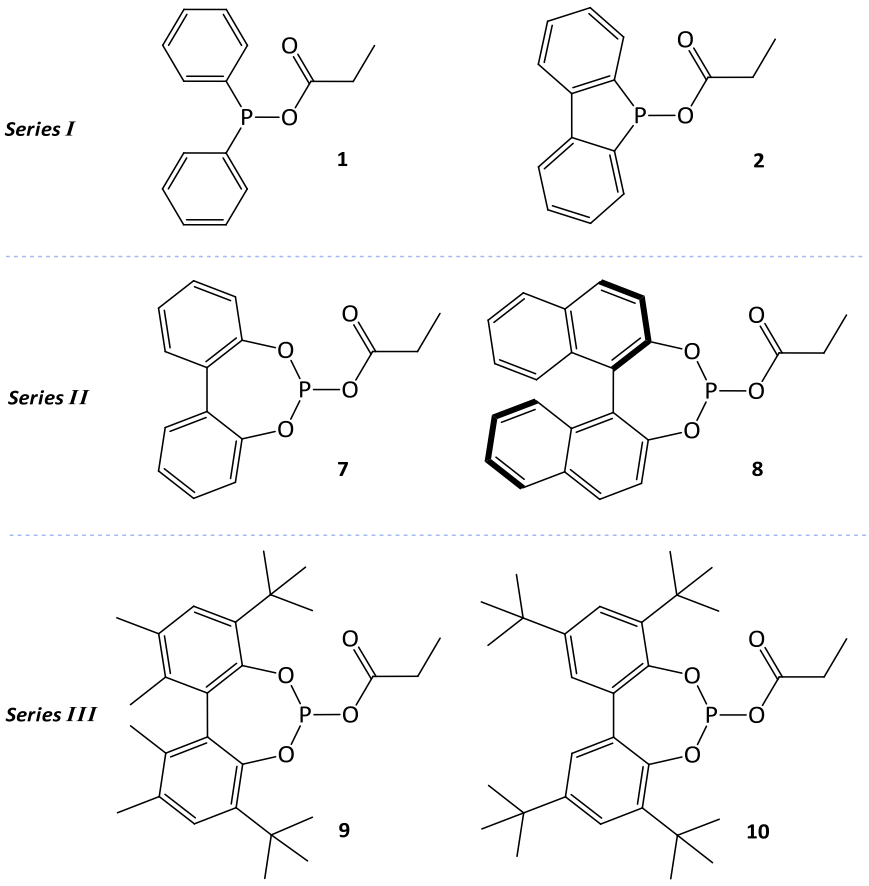


**Figure 2.3** ***Series I*** – mixed anhydrides **1–2** containing neither electron withdrawing groups bonded to the phosphorus (with the exception of the propionyloxy moiety) nor bulky substituents on the phenyl rings; ***Series II*** – mixed anhydrides **7–8** with electron withdrawing atoms bonded to the phosphorus atom, but no bulky ring substituents and ***Series III*** – mixed anhydrides **9–10** bearing both electron withdrawing groups attached to phosphorus and bulky ring substituents.

Within ***series I***, the preparation and unstable nature of (propionyloxy)diphenylphosphine, **1**, have already been described in section 2.2.2. As mentioned before, compound **1** readily rearranges to afford the disproportionation product tetraphenyldiphosphine monoxide $\{Ph_2P(O)PPh_2\}$ at a rate dependent on the temperature. To make this series more comprehensive, an attempt to prepare the related mixed anhydride 5-(propionyloxy)-dibenzophosphole, **2**, where the phosphorus atom forms part of a phosphole ring, was made. We expected this compound to be even more prone to rearrangement reactions, since the greater C–P–O angles (brought about by ring constraints) make the phosphorus atom more

accessible to neighbouring molecules. A suspension of sodium propanoate in thf was therefore treated with 5-chlorodibenzophosphole at room temperature for 2 h, after which the formed NaCl was removed by filtration and all volatiles evaporated under reduced pressure to furnish the crude product as a white solid (Scheme 2.5). However, as anticipated, this solid analysed to solely consist of rearrangement products of which the $Ph_2P(O)PPh_2$ analogue [5,5'-bibenzo[b]phosphindole]-5-oxide, constituted the major component. Although it is probable that the lifetime of **2** can be prolonged by lowering the reaction temperature, no further efforts to synthesise and isolate this compound were made.

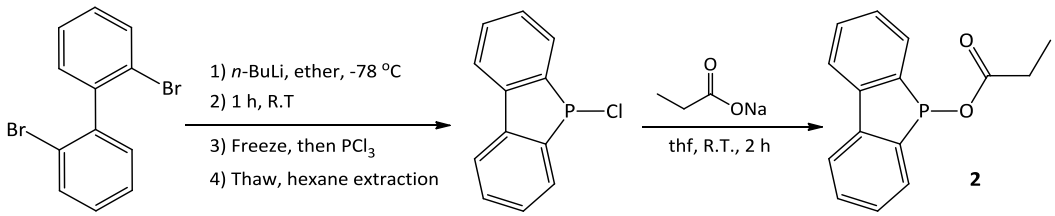


**Scheme 2.5** Preparation of compound **2** from 5-chloro-dibenzo[d,d]phosphole. The latter was prepared from 2,2'-dibromobiphenyl following a standard literature procedure.[13]

Next, the effects of electron withdrawing atoms (approach **A**) were explored by constructing ***series II***. Following a literature based procedure, chlorophosphites **3** and **4** were reacted with a suspension of sodium propanoate in thf at 45 °C for 2 h to afford (propionyl)phosphites **7**–**8**, respectively, upon work-up (Scheme 2.6).[13,10]

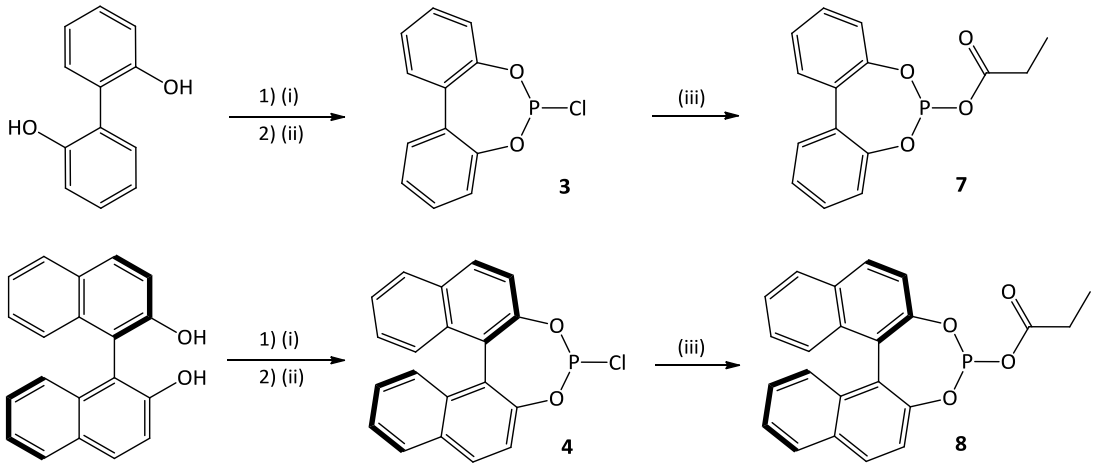


**Scheme 2.6** Reaction scheme for the preparation of chlorophosphites **3** and **4** and their corresponding mixed anhydrides **7** and **8**. Reagents: (i) $PCl_3$, thf, -10 °C; (ii) $NEt_3$, 1 h, R. T.; (iii) $CH_3CH_2CO_2Na$, 2 h, 45 °C.

Overall, **7** and **8** displayed much greater stability than the (acyloxy)phosphines and no rearrangement products of the general formula $(RO)_2P(O)P(OR)_2$ were observed for these compounds. $^{31}P$ NMR spectra, however, did reveal the presence of minor amounts of by-products $\mathbf{7}_{BP}$ and $\mathbf{8}_{BP}$ (for **7** and **8**, respectively; Scheme 2.7). These by-products most likely originated from the base catalysed reaction of dialkylphosphonates **DP** with dialkyl acylphosphonates **DAP** (Scheme 2.7), and similar reaction pathways have been reported in the literature for the preparation of tetraethyl 1-hydroxyalkylidenediphosphonates and their isomeric phosphates.[14] These reactions initially generate 1-hydroxyalkylidenediphosphonate esters as intermediates which then undergo spontaneous rearrangement to the more stable phosphates, $\mathbf{7}_{BP}$ and $\mathbf{8}_{BP}$. The dialkylphosphonate (**DP**) precursors are generated by hydrolysis of the mixed anhydrides in the presence of trace amounts of water, while the dialkyl acylphosphonates (**DAP**) are formed by the Arbuzov rearrangement of the ligands **7** and **8**. Rearrangements of this type are not uncommon for mixed anhydride ligands and similar rearrangements have been noted before by Lindner and Wuhrmann for (perfluoracyloxy)diorganylphosphines.[1] Compounds **7**–**8** are air and moisture sensitive white solids which are soluble in most aprotic organic solvents such as chloroform, dichloromethane, thf, diethyl ether, toluene, hexane and pentane (sparingly). Furthermore, compounds **7**–**8** are indefinitely stable both in solution and the solid state at room temperature, provided that a dry, base free and inert atmosphere is maintained. These findings and are in good agreement with literature reports on the general stability of (acyl)phosphites and therefore indicate that a moderate increase in stability can be achieved by the use of electron withdrawing groups on phosphorus.[10,9]

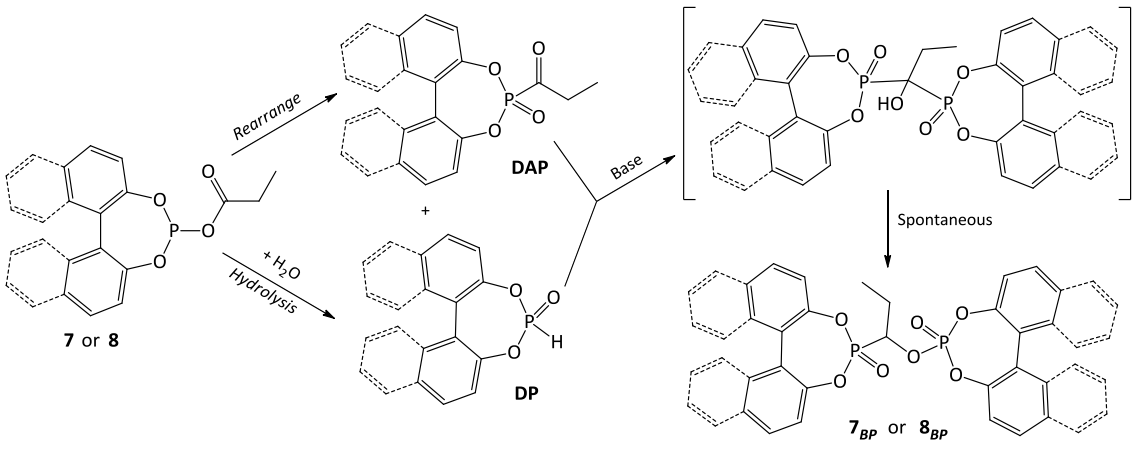


**Scheme 2.7** Formation of by-products $\mathbf{7}_{BP}$ and $\mathbf{8}_{BP}$ from ligands **7** and **8** in the presence of water.

Finally, to complete the collection, mixed anydrides **9–10** (constituting ***series III)*** were prepared from their corresponding chlorophosphites **5–6**[15] using the same methodologies described for the preparation of compounds **7** and **8** (scheme 2.8). Following approach **B**, sterically demanding *tert*-butyl groups were included as substituents in the 3-positions of both phenyl rings, shielding the phosphorus centre from neighbouring molecules. This stabilisation approach proved very successful with measured NMR spectra providing no evidence for the presence of any disproportionation products. Moreover, the analytically pure compounds **9–10** are fairly air stable white solids that proved remarkably stable towards rearrangement in solution even at temperatures as high as 60 °C. In addition, these compounds are indefinitely stable in the solid state under an inert atmosphere; emphasizing the substantial increase in stability brought about by the incorporation of steric bulk. Although **9** and **10** are incompatible with protic solvents, they are soluble in most other organic solvents such as chloroform, dichloromethane, thf, diethyl ether, toluene and even very non-polar solvents such as hexane and pentane. Owing to the superior stability of these compounds, single crystals suitable for crystal structure determination could be obtained for **9**, and the determined structure is discussed in more detail in section 2.2.5.

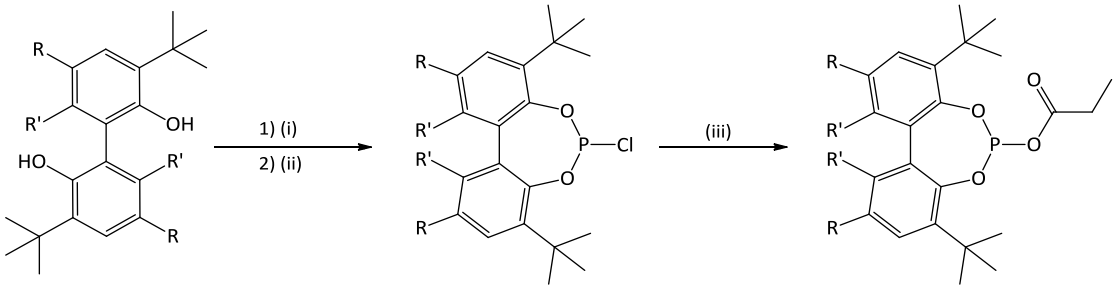


**Scheme 2.8** Reaction scheme for the preparation of **9** and **10** from chlorophosphites **5** and **6**, respectively. Chlorophosphite **5** and **6** were prepared from the appropriate diols using a modified literature approach.[15] Reagents: (i) $PCl_3$, thf, -10 °C; (ii) $NEt_3$, 1 h, R.T.; (iii) $CH_3CH_2CO_2Na$, 2 h, 45 °C.

### *2.2.3 Increasing the acidity of the α-protons in mixed anhydride ligands*

Given that C–H activation of the protons in the *α*-position of the acyl group formed an integral part of the overall study, it was also well worth exploring a few additional ligands in which the *α*-protons were slightly more acidic relative to those already discussed. The prospect that

subtle reductions in the $pK_a$ values may aid in driving these reactions captured our interest since, in principle, more acidic $\alpha$-protons should be activated more readily. In line with this, the already existing series of ligands was extended to include an additional three ligands (compounds **11–13**, Figure 2.4) in which the priopionyloxy functionality has been replaced by a phenylacetyloxy moiety.

Compounds **11–13** could be prepared by treatment of a phenylacetic acid solution in thf at –10 $^{o}$C with either chlorodiphenylphosphine (for **11**) or the chlorophosphites **5–6** (for **12** and **13**), in the presence of $NEt_3$. The stabilities of compounds **11–13** are comparable to those of their propionyl analogues with **12–13** being stable both in solution and in the solid state under an inert atmosphere, while **11** disproportionates with time at a rate dependent on the temperature. Compounds **11–13** are soluble in most aprotic organic solvents for example chloroform, dichloromethane, thf, diethyl ether and toluene, but insoluble in non-polar solvents such as hexane and pentane. Crystals suitable for X-ray crystal structure determinations could be obtained for compound **12** and **13** and both structures are discussed in the crystallographic section.

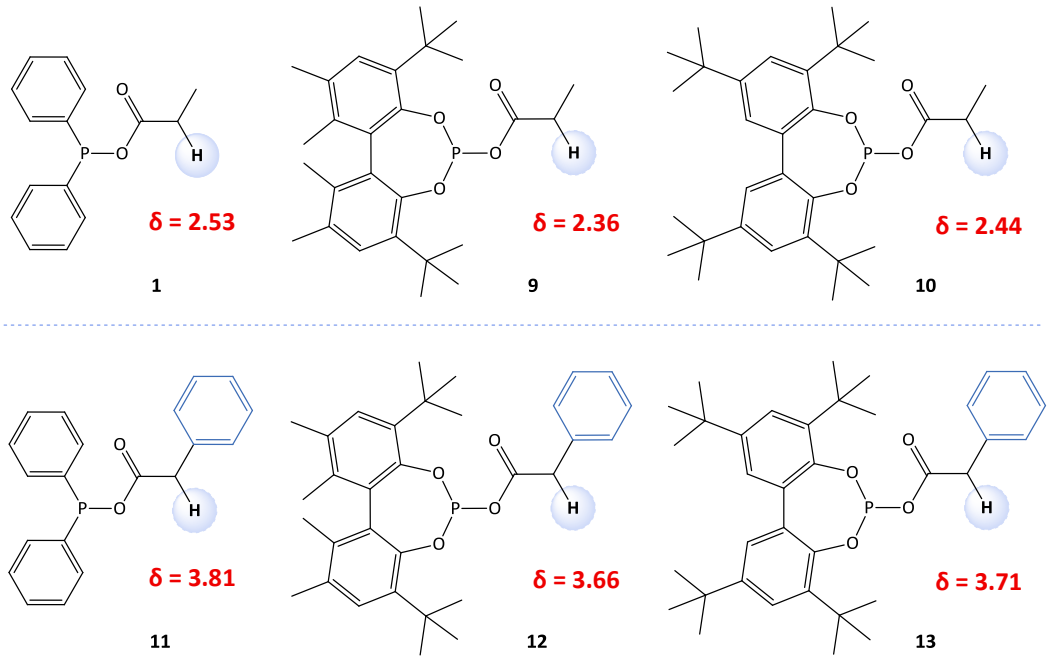


**Figure 2.4** A rough estimate of the relative acidities of $\alpha$-protons present in the propionyloxy side chain of ligands **1**, **9** and **10** *versus* those of the phenylacetyl chain of ligands **11–13**, based on differences in their respective chemical shifts (ppm) as observed in $^{1}$H NMR spectra.

As a rule in $^{1}$H NMR spectra, more acidic protons give rise to resonances with chemical shifts downfield relative to those of less acidic protons. This phenomenon can be rationalised by the fact that an increase in acidity often goes along with a decrease in the localised electron density, which in turn renders the proton more deshielded. Working on this assumption, differences in the chemical shifts between *α*-proton resonances in the measured $^{1}$H NMR spectra of compounds **1**, **9** and **10** *versus* those of **11–13** were used as a rough estimate for their relative *α*-proton acidities. From a comparison of the $^{1}$H NMR data for all the compounds in question, it was evident that changing from a propionyloxy group to a phenylacetyloxy group has a pronounced effect on chemical shifts of the *α*-protons. Chemical shifts corresponding to the *α*-protons of compounds **11–13** all appear significantly downfield (Δδ = 1.28 on average), compared to those of their propionyloxy bearing counterparts, thus confirming their enhanced *α*-proton acidity.

### *2.2.4 Spectroscopic and spectrometric analysis*

Routine FT-IR data were collected for compounds **7–13**, with all relevant absorption bands listed under the experimental section. In all cases mixed anhydrides show strong absorption bands in the region 1740–1729 cm$^{-1}$ attributable to the characteristic C=O stretching vibrations. These values are in good agreement with those reported for the literature examples (*R*)-acetyl(1,1'-binaphthyl-2,2'-diyl)phosphite (1736 cm$^{-1}$) and (propionyloxy)diphenylphosphine (**1**; 1740 cm$^{-1}$).[10,12]

Furthermore, $^{1}$H, $^{13}$C{$^{1}$H}, and $^{31}$P{$^{1}$H} NMR spectroscopic data were collected for dichloromethane-$d_2$ or chloroform-$d_1$ solutions of **1–13** and are listed in detail under the experimental section. Some of the more diagnostic resonances for compounds **1** and **7–13** are, however, summarised in Table 2.1. In the $^{31}$P{$^{1}$H} NMR spectrum of **1**, disproportionation to $Ph_2P(O)PPh_2$ is easily recognised, by the appearance of two very distinctive doublets (at δ 36.9 and δ -22.1, $^{1}J_{P\text{-}P}$ = 229.4 Hz) at the expense of **1** (singlet at δ 98.9, Figure 2.5) and are in good agreement with the literature values reported for this compound.[16] Similarly, the by-products $\mathbf{7}_{BP}$ and $\mathbf{8}_{BP}$ show very distinctive spectral profiles in the $^{31}$P NMR spectra of ligands **7** and **8**, respectively, and could be identified with the aid of standard one and two dimensional NMR techniques ($^{13}$C-DEPT, COSY, HMQC, HSQC).

**Table 2.1** $^{1}H$, $^{13}C\{^{1}H\}$ and $^{31}P\{^{1}H\}$ NMR data for the most characteristic functionalities present in ligands **1** and **7–13**.

| | $^{1}H$ NMR | | $^{13}C$ NMR | | | $^{31}P$ NMR |
|---|---|---|---|---|---|---|
| | Chemical shifts δ (ppm)† | | Chemical shifts δ (ppm)† | | | Chemical shifts δ (ppm) ‡ |
| **Compound** | δ(-C$H_3$) | δ(-C$H_2$-) | δ(-C$H_3$) | δ(-C$H_2$-) | δ(C=O) | δ(*P*) |
| **1** | 1.18 (t, $^{3}J$ = 7.5 Hz) | 2.53 (t, $^{3}J$ = 7.5 Hz) | 9.2(s) | 28.7(s) | 174.3 (s) | 98.9 (s) |
| **7** | 1.18 (t, $^{3}J$ = 7.4 Hz) | 2.46 (t, $^{3}J$ = 7.4 Hz) | 9.0 (s) | 28.9 (s) | 173.6 (d, $^{2}J_{C\text{-}P}$ = 5.1 Hz) | 124.5 (s) |
| **8** | 1.15 (t, $^{3}J$ = 7.5 Hz) | 2.40 (t, $^{3}J$ = 7.5 Hz) | 8.9 (s) | 28.9 (d, $^{3}J_{C\text{-}P}$ = 5.1 Hz) | 173.6 (d, $^{2}J_{C\text{-}P}$ = 5.1 Hz) | 141.8 (s) |
| **9** | 1.09(t, $^{3}J$ = 7.5 Hz) | 2.36 (t, $^{3}J$ = 7.5 Hz) | 8.6 (s) | 28.8 (d, $^{3}J_{C\text{-}P}$ = 2.5 Hz) | 173.5 (d, $^{2}J_{C\text{-}P}$ = 5.6 Hz) | 129.6 (s) |
| **10** | 1.13 (t, $^{3}J$ = 7.4 Hz) | 2.44 (t, $^{3}J$ = 7.4 Hz) | 8.5 (s) | 28.5 (d, $^{3}J_{C\text{-}P}$ = 2.5 Hz) | 173.3 (d, $^{2}J_{C\text{-}P}$ = 5.1 Hz) | 135.9 (s) |
| **11** | – | 3.81 (d, $^{4}J$ = 0.8 Hz) | § | § | § | 99.9 (s) |
| **12** | – | 3.66 (s) | – | 41.8 (s) | 170.5 (s) | 129.3 (s) |
| **13** | – | 3.71 (s) | – | 42.0 (d, $^{3}J_{C\text{-}P}$ = 5.1 Hz) | 170.4 (d, $^{2}J_{C\text{-}P}$ = 5.1 Hz) | 135.7 (s) |

† Chemical shifts relative to TMS ($CD_2Cl_2$ or $CDCl_3$ 25 °C) with mulitiplicity and coupling constants given in parenthesis.
‡ Chemical shifts relative to 85 % $H_3PO_4$ ($CD_2Cl_2$ or $CDCl_3$ 25 °C) with mulitiplicity given in parenthesis.
§ $^{13}C$ NMR data not determined owing to facile disproportionation over time in solution.

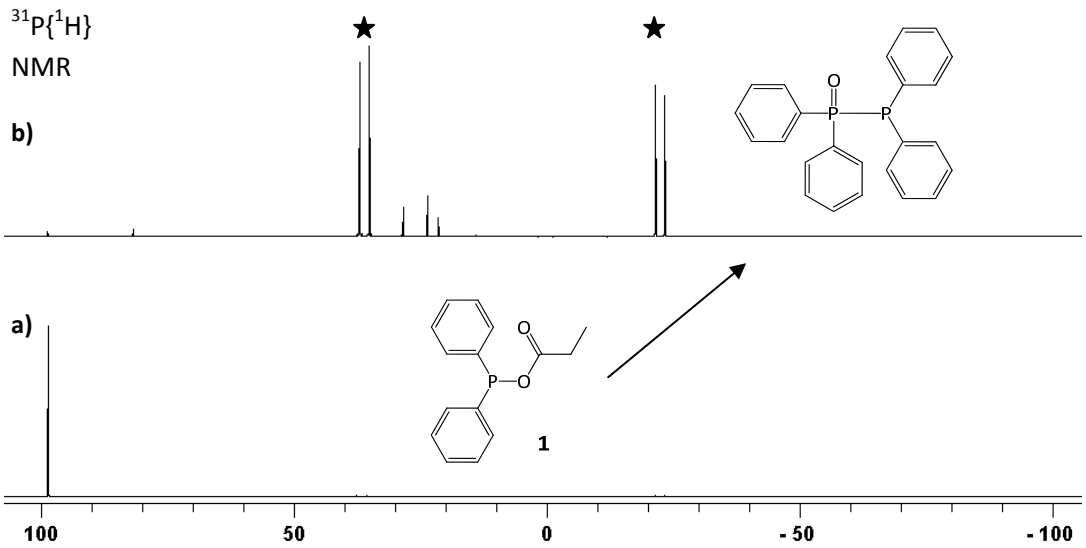


**Figure 2.5** Examples of typical $^{31}P\{^{1}H\}$ NMR spectra measured for compound **1** (a) following successful preparation and (b) after rearrangement to $Ph_2P(O)PPh_2$ has largely taken place.

In the $^{1}H$ NMR spectrum of **7**, the central –C*H*– group of the by-product $\mathbf{7}_{BP}$ gives rise to a very distinctive multiplet at δ 5.41 (Figure 2.6) as a result of coupling to phosphorus in addition to the inequivalent methene protons. Likewise, the methene protons give rise to a complex multiplet at δ 2.34, while the methyl group gives rise to a doublet of doublets observed as a broad triplet at δ 1.39. In the $^{31}P$ NMR spectrum, the two distinct P-atoms of $\mathbf{7}_{BP}$ are observed as doublets at δ 1.9 and δ 26.4 ($^{4}J_{P\text{-}P}$ = 24.1 Hz). Furthermore, in the 2D HMQC spectrum these resonances display $^{1}H$–$^{31}P$ correlations of different intensities and are therefore consistent with a structure where one of the phosphorus atoms is incorporated in a phosphate group.

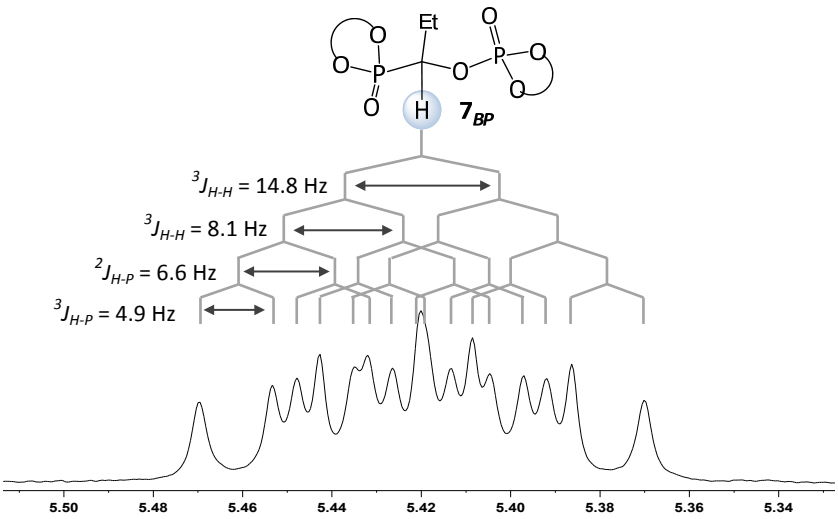


**Figure 2.6** Multiplicity and coupling constants observed for the complex $^{1}H$ NMR resonance of the central –C*H*– group in the by-product $\mathbf{7}_{BP}$.

In contrast, the by-product **8**$_{BP}$ gives rise to two sets of doublets in the $^{31}P\{^{1}H\}$ NMR spectrum with distinct $^{31}P–^{31}P$ coupling constants (Figure 2.7) owing to the planar chirality of the binol and the chirality at the central carbon atom. Since the starting diol used during the preparation of **8** was fixed as the (*R*)-isomer, only two possible diastereomers can be formed for this specific by-product; they are (*R, S, R*) and (*R ,R, R*). The two distinct diastereomers observed in the $^{31}P$ NMR spectrum of **8**$_{BP}$, display slightly different $^{31}P–^{31}P$ coupling constants of 23.3 Hz and 28.9 Hz, respectively.

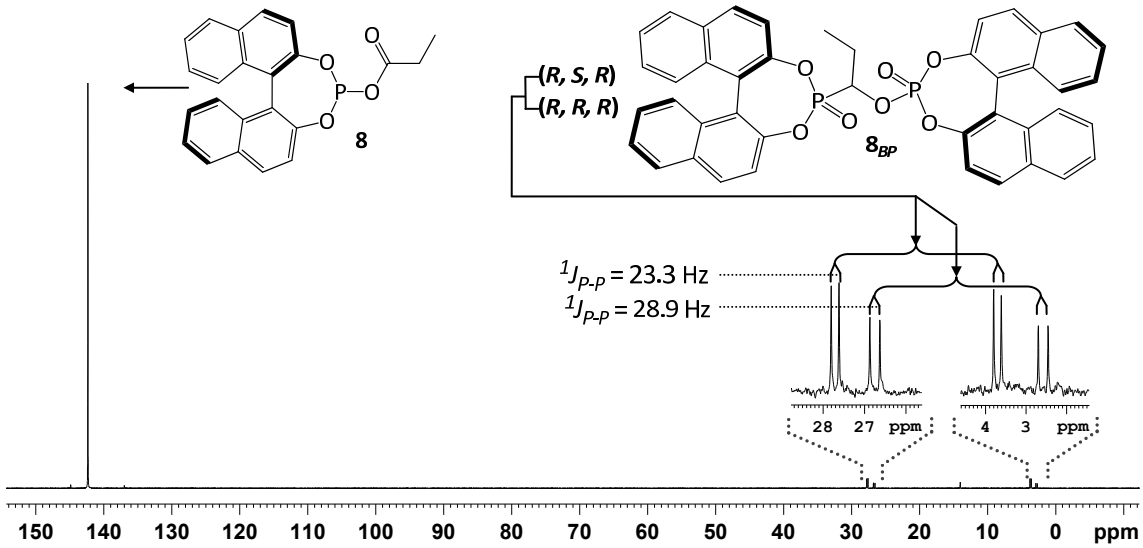


**Figure 2.7** $^{31}P\{^{1}H\}$ NMR spectrum measured for compound **8** showing the presence of minor amounts of the two diastereomers of the byproduct **8**$_{BP}$.

In the $^{13}C$ NMR spectra of **9** and **12** all carbon atoms are chemically inequivalent owing to the rotated disposition of the rings (to minimize steric interactions) as well as the chirality of these compounds. Despite this, however, like carbons in compounds **10** and **13** display accidental equivalence giving rise to single resonances in the relevant regions. Furthermore, it is worth mentioning that for **9** and **12** the constants measured for $^{13}C–^{31}P$ coupling between $C^{4}$ to P (0 Hz) and $C^{14}$ to P (4.7–5.0 Hz, see Figure 2.8 for numbering scheme) differed significantly. The values of geminal coupling constants are influenced by the angle between the coupled atoms, and variations in the P–O–C angles $\theta$ and $\beta$ (Figure 2.8) may therefore be the cause of the observed inconsistencies. Surprisingly, for

compound **10** and **13**, $C^4$ and $C^{14}$ are only observed as a single resonance signal split into a doublet by equal coupling to phosphorus [4.7 Hz (**10**) and 5.0 Hz (**13**)].

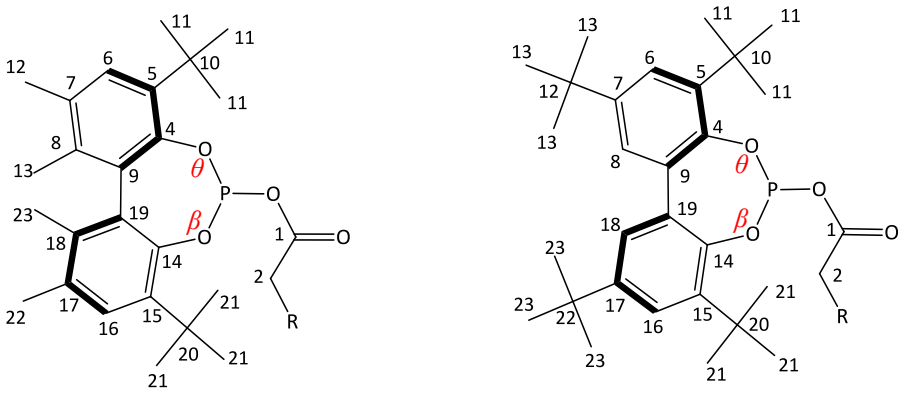

**9** : Me
**12** : Ph

**10** : Me
**13** : Ph

**Figure 2.8** Numbering scheme for NMR discussions concerning compounds **9** and **10** where $\theta$ and $\beta$ represents the $C^4$–O–P and $C^{14}$–O–P angles, respectively. Only one of the 2 possible diastereomers for each compound is shown in the diagram.

ES-MS spectrometric data were collected for compounds **7–10** and **12–13** and the relevant peaks are listed in the experimental section. Very little fragmentation was observed for these compounds with this mild ionization technique and as a result, the molecular ions $[M]^+$ and peaks originating from the loss of a either a propionyloxy group (in the case of **7–10**) or loss of a phenylacetyloxy group (for **12–13**) were the only diagnostic peaks that could be observed.

### *2.2.5 Crystal and molecular structure determinations*

The crystal and molecular structures of compounds **9**, **12** and **13** were determined by single crystal X-ray diffraction and are here, to the best of our knowledge, reported for the first time. Compound **9** crystallises from a concentrated hexane solution as colourless prisms in the orthorhombic space group *Pna*$2_1$ with Z = 4 molecules in the unit cell. Figure 2.9 depicts the molecular structure and numbering scheme of **9** and selected bond lengths and angles are summarised in Table 2.2.

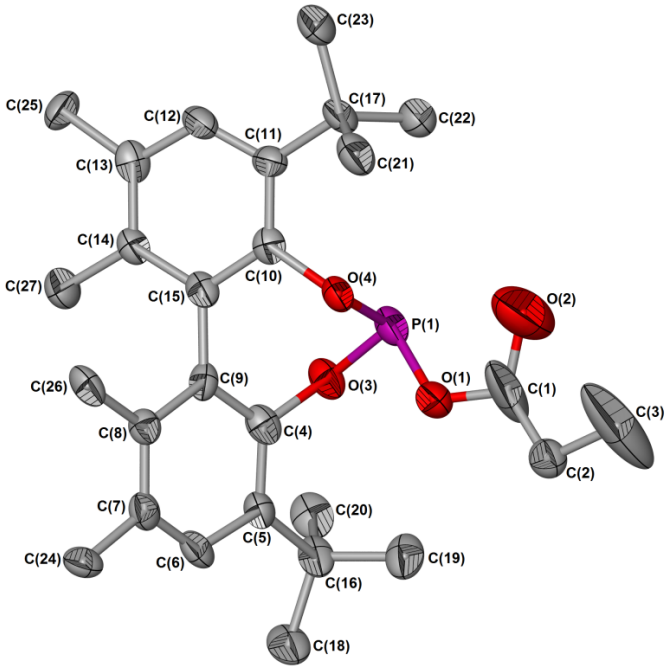


**Figure 2.9** Molecular structure of **9** showing the numbering scheme. Thermal ellipsoids set at 50% probability. Hydrogen atoms are omitted for clarity sake.

**Table 2.2** Selected bond lengths (Å) and angles (°) of **9** with estimated standard deviations in parenthesis.

| | | | |
|---|---|---|---|
| *Bond lengths (Å)* | | | |
| P(1)–O(1) | 1.654(5) | O(2)–C(1) | 1.342(14) |
| P(1)–O(3) | 1.614(5) | C(1)–C(2) | 1.452(12) |
| P(1)–O(4) | 1.645(5) | C(2)–C(3) | 1.475(12) |
| O(1)–C(1) | 1.285(10) | C(9)–C(4) | 1.407(9) |
| O(3)–C(4) | 1.415(8) | C(10)–C(15) | 1.398(9) |
| O(4)–C(10) | 1.418(8) | C(15)–C(9) | 1.509(9) |
| *Bond angles (°)* | | | |
| O(3)–P(1)–O(1) | 99.5(3) | O(2)–C(1)–C(2) | 122.0(8) |
| O(4)–P(1)–O(1) | 92.3(3) | C(1)–C(2)–C(3) | 109.2(9) |
| O(3)–P(1)–O(4) | 103.6(2) | O(3)–C(4)–C(9) | 117.6(6) |
| C(1)–O(1)–P(1) | 120.5(6) | O(3)–C(4)–C(5) | 118.9(6) |
| C(4)–O(3)–P(1) | 123.0(4) | O(4)–C(10)–C(15) | 114.6(6) |
| C(10)–O(4)–P(1) | 114.5(4) | O(4)–C(10)–C(11) | 121.4(6) |
| O(1)–C(1)–O(2) | 111.5(10) | C(4)–C(9)–C(15) | 120.5(6) |
| O(1)–C(1)–C(2) | 121.0(8) | C(10)–C(15)–C(9) | 120.0(6) |

Within the molecular structure of **9**, the two aromatic ring systems are rotated about the central carbon bond at torsion angles of 61.4(9)$^{o}$ and 60.0(9)$^{o}$ in order to minimise steric interactions between the different ring substituents. Although no crystal structures for free mixed anhydrides ligands of the general formula $(RO)_2POC(O)R'$ have been reported to date, the measured P(1)–O(1) bond length of 1.654(5) Å is in close agreement with that reported for the phosphorus ester bond in 2-(methylamino)benzoate-1,4-dihydro-1-methyl-4-oxo-2*H*-3,1,2-benzoxazaphosphorin-2-yl ester [1.6462(13) Å].[17] A very slight variation is observed between the distances for the two analogous bonds P(1)–O(3) and P(1)–O(4) [1.614(5) Å and 1.645(5) Å], and observed bonding lengths are comparable to those of the related literature example, 1,1'-biphenyl-2,2'-diyl-bis[(5,5',6,6'-tetramethyl-3,3'-di-*tert*-butyl-1,1'-biphenyl-2,2'-diyl)phosphite] [1.617(2) Å and 1.639(2)].[18]

Interestingly, the P(1)–O(3)–C(4) and P(1)–O(4)–C(10) angles of 123.0(4)$^{o}$ and 114.5(4)$^{o}$, respectively, differs significantly. This is therefore in good agreement with earlier $^{13}$C NMR spectroscopic observations concerning $^{13}$C–$^{31}$P coupling constants, where large differences observed in the coupling behaviour of C(4) to P(1) and C(10) to P(1) were tentatively ascribed to variations in the relevant P–O–C angles. However, it is noted that structural behaviour in the solid state may differ significantly from that in solution owing to crystal packing effects, and correlation of such connectivity data with other analytical data should therefore be interpreted with caution.

Compound **12** crystallises at room temperature from a hexane layered toluene solution as colourless prisms in the monoclinic space group $P2_1/n$, while **13** crystallises from chloroform also as colourless prisms in the triclinic space group $P\bar{1}$. Figures 2.10–2.11 depicts ellipsoid representations of the molecular structures of **12–13** showing the numbering schemes, with selected bond lengths and angles listed in Tables 2.3–2.4. The dihedral angles of 61.2(7)$^{o}$ and 56.7(8)$^{o}$ measured between the aryl rings of **12** are analogous to those observed for **9** and the literature example 1,1'-biphenyl-2,2'-diyl-bis[(5,5',6,6'-tetramethyl-3,3'-di-*tert*-butyl-1,1'-biphenyl-2,2'-diyl)phosphite].[18] In contrast, the corresponding torsion angles in **13** are significantly smaller [49.5 (4)$^{o}$ and 42.7(4)$^{o}$], suggesting that steric repulsions between the methyl groups in the $C^{6}$ and $C^{6'}$-positions of the rings contribute to the widening of this angle in **9** and **12**.

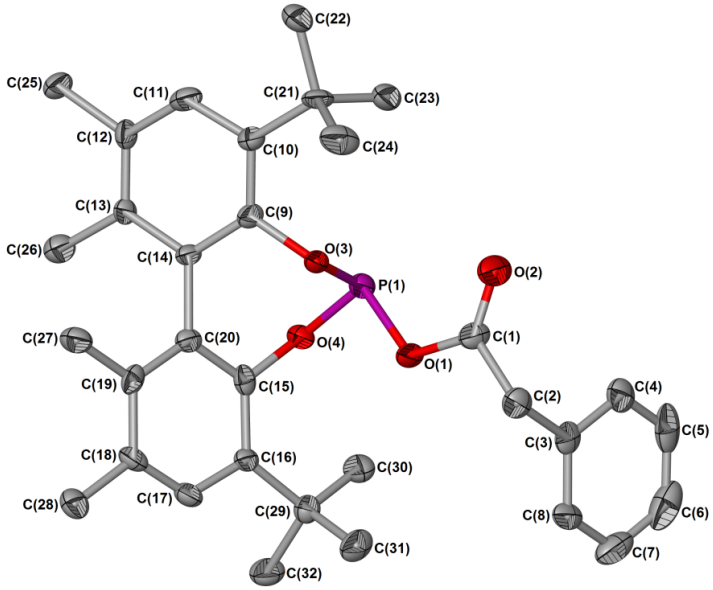


**Figure 2.10** Molecular structure of **12** showing the numbering scheme. Thermal ellipsoids set at 50% probability. Hydrogen atoms are omitted for the sake of clarity.

**Table 2.3** Selected bond lengths (Å) and angles (°) of **12** with estimated standard deviations in parenthesis.

| | | | |
|---|---|---|---|
| *Bond lengths (Å)* | | | |
| P(1)–O(1) | 1.682(4) | O(2)–C(1) | 1.203(9) |
| P(1)–O(3) | 1.629(4) | C(1)–C(2) | 1.515(8) |
| P(1)–O(4) | 1.607(5) | C(2)–C(3) | 1.504(8) |
| O(1)–C(1) | 1.345(9) | C(9)–C(14) | 1.387(9) |
| O(3)–C(9) | 1.441(7) | C(15)–C(20) | 1.404(8) |
| O(4)–C(15) | 1.406(8) | C(14)–C(20) | 1.512(9) |
| *Bond angles (°)* | | | |
| O(3)–P(1)–O(1) | 92.92(19) | O(2)–C(1)–C(2) | 125.2(7) |
| O(4)–P(1)–O(1) | 98.7(2) | C(1)–C(2)–C(3) | 110.9(5) |
| O(3)–P(1)–O(4) | 102.4(2) | O(3)–C(9)–C(10) | 119.8(6) |
| C(1)–O(1)–P(1) | 116.8(4) | O(3)–C(9)–C(14) | 115.2(5) |
| C(9)–O(3)–P(1) | 113.3(3) | O(4)–C(15)–C(20) | 117.0(6) |
| C(15)–O(4)–P(1) | 123.8(3) | O(4)–C(15)–C(16) | 120.0(5) |
| O(1)–C(1)–O(2) | 121.8(6) | C(9)–C(14)–C(20) | 119.5(5) |
| O(1)–C(1)–C(2) | 113.0(7) | C(14)–C(20)–C(15) | 119.9(6) |

From a comparison of the bond lengths and angles of **9**, **12** and **13** it is evident that variations amongst like bonds are small, nevertheless, a few observations are in order. On average, the P–O bonds lengths in **9** are somewhat longer than those in **12** and **13**, while the P(1)–O(4) bond in **12** is slightly shorter than the equivalent bond in **13**. The latter may too be the result of steric repulsions among methyl substituents on the phenyl backbone.

In line with these observations, the P(1)–O(3)–C(9) and P(1)–O(4)–C(15) angles in **13** are significantly greater than the related angles in **9** and **12**. In all cases P(1)–O(3)–C(9) and P(1)–O(4)–C(15) are significantly different and thus do not provide and explanation for the accidental equivalence of C(19) and C(15) in the $^{13}$C NMR spectra of **12** and **13**.

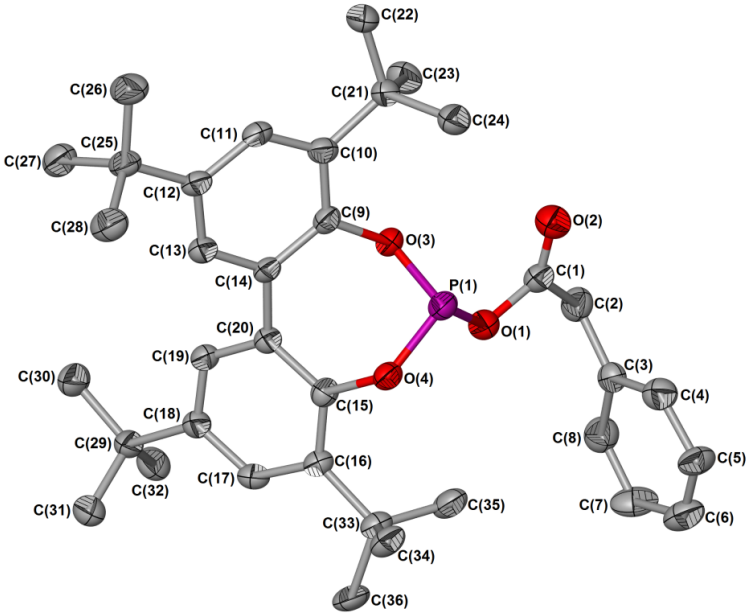


**Figure 2.11** Molecular structure of **13** showing the numbering scheme. Thermal ellipsoids set at 50% probability. Hydrogen atoms are omitted for clarity.

**Table 2.4** Selected bond lengths (Å) and angles (°) of **13** with estimated standard deviations in parenthesis.

| | | | |
|---|---|---|---|
| *Bond lengths (Å)* | | | |
| P(1)–O(1) | 1.671(2) | O(2)–C(1) | 1.203(4) |
| P(1)–O(3) | 1.635(2) | C(1)–C(2) | 1.499(5) |
| P(1)–O(4) | 1.615(2) | C(2)–C(3) | 1.473(5) |
| O(1)–C(1) | 1.370(4) | C(9)–C(14) | 1.403(4) |
| O(3)–C(9) | 1.404(3) | C(15)–C(20) | 1.396(4) |
| O(4)–C(15) | 1.421(4) | C(14)–C(20) | 1.479(4) |
| *Bond angles (°)* | | | |
| O(3)–P(1)–O(1) | 93.28(11) | O(2)–C(1)–C(2) | 125.5(3) |
| O(4)–P(1)–O(1) | 100.39(12) | C(1)–C(2)–C(3) | 114.1(3) |
| O(3)–P(1)–O(4) | 102.74(11) | O(3)–C(9)–C(10) | 121.5(2) |
| C(1)–O(1)–P(1) | 117.4(2) | O(3)–C(9)–C(14) | 115.4(3) |
| C(9)–O(3)–P(1) | 117.60(18) | O(4)–C(15)–C(20) | 117.7(3) |
| C(15)–O(4)–P(1) | 127.87(19) | O(4)–C(15)–C(16) | 118.6(3) |
| O(1)–C(1)–O(2) | 121.5(3) | C(9)–C(14)–C(20) | 123.5(2) |
| O(1)–C(1)–C(2) | 113.0(3) | C(14)–C(20)–C(15) | 124.6(3) |

## 2.3 Conclusions

The simple mixed anhydride propionyloxydiphenylphosphine could be prepared successfully from propionic acid and chlorodiphenylphosphine *via* two different routes. This compound, however, rearranges both in solution and the solid state at a rate dependent on the temperature. A moderate increase in the stability of such ligand systems could be achieved by the incorporation of electron withdrawing oxygen atoms directly bonded to the phosphorus atom. This could be achieved by changing from a chlorodiphenylphosphine to chlorophosphite precursor during the preparation of mixed anhydrides. Further stabilisation could be realised by increasing the steric bulk surrounding the phosphorus atoms, and by doing so prevent neighbouring molecules from reaching close proximity. The latter approach proved most successful, with the resultant compounds being very stable both in solution and in the solid state.

The acidity of the $\alpha$-protons in the acyloxy functionality of mixed anhydrides could be increased by changing from propionic acid to phenylacetic acid as the parent acid. This change brought about a downfield shift in the relevant proton resonances in measured $^{1}$H NMR spectra, providing a spectroscopic handle for a rough estimation of the relative acidities.

Acylphosphites derived from 5,5',6,6'-tetramethyl-3,3'-di-*tert*-butyl-1,1'-biphenyl-2,2'-diol and 3,3',5,5'-tetra-*tert*-butyl-1,1'-biphenyl-2,2'-diol represent the most stable of all the mixed anhydrides prepared during this part of the study. These compounds show interesting $^{13}$C–$^{31}$P coupling behaviour in their $^{13}$C NMR spectra, owing to their chiral nature as well as variations in the bond lengths and angles among like bonds. These variations are brought about by steric repulsions between the bulky ring substituents and were also observed in their solid state molecular structures and which could be determined by single crystal X-ray diffraction.

## 2.4 Experimental

### *2.4.1 General materials, methods and instruments*

Reactions were carried out under dinitrogen gas ($N_2$, passed through a column of dichromate adsorbed on silica) using standard Schlenk, vacuum-line and cannula techniques. All glassware was flame-dried under vacuum prior to use. Triethylamine ($NEt_3$), chlorodiphenylphosphine

($Ph_2Cl$) and phosphorus trichloride ($PCl_3$) were purchased from Aldrich and distilled under $N_2$ prior to use. Before distillation, the $NEt_3$ was dried over potassium hydroxide (KOH) pellets while $PCl_3$ was refluxed for 3 h to remove any free hydrochloric acid (HCl). 5,5'-6,6'-Tetramethyl-3,3'-di-*tert*-butyl-1,1'-biphenyl-2,2'-diol, sodium propanoate and phenylacetic acid, were purchased from Aldrich and dried azeotropically with toluene. 2,2'-Biphenyldiol (purified by sublimation), (*R*)-(*+*)-1,1'-Bi(2-naphthol) (dried azeotropically with toluene), 2,2'-dibromobiphenyl and 2,4-di-*tert*-butylphenol were purchased from Alfa Aesar and used as received unless stated otherwise. *N,N*'-tetramethyl-1,2-diaminoethane (TMEDA) and anhydrous copper(II) chloride ($CuCl_2$) were purchased from Aldrich and used as received. Propanoic acid, purchased from BDH laboratories, was dried over $Na_2CO_3$ and distilled under $N_2$ prior to use. 3,3',5,5'-Tetra-*tert*-butyl-1,1'-biphenyl-2,2'-diol was prepared using a standard literature procedure.[19] 5-Chloro-dibenzophosphole was prepared from 2,2'-dibromobiphenyl following a reported literature procedure.[13]

Toluene, thf, diethyl ether and hexane were dried using a Braun Solvent Purification System and degassed by additional freeze-pump-thaw cycles when deemed necessary. Methanol was distilled under nitrogen from magnesium. Deuterated dichloromethane and chloroform were purchased from Aldrich and dried over phosphorus pentoxide ($P_2O_5$), degassed *via* three freeze-pump-thaw cycles and trap-to-trap distilled prior to use.

NMR spectra were recorded on a Bruker Avance 300 FT or Bruker Avance II 400 MHz spectrometer ($^1H$ NMR at 300/400 MHz, $^{13}C\{^1H\}$ NMR at 75/100 MHz and $^{31}P\{^1H\}$ NMR at 121/162 MHz) with chemical shifts δ reported relative to tetramethylsilane (TMS)($^1H$, $^{13}C$) or 85 % $H_3PO_4$ ($^{31}P\{^1H\}$) as external reference. $^1H$ and $^{13}C\{^1H\}$ NMR spectra were measured internally relative to deuterated solvent resonances which were referenced relative to TMS.

Solid state IR spectra were recorded using pressed KBr pellets on a Perkin Elmer Spectrum GX IR spectrometer. Elemental analysis was performed by the University of St. Andrews microanalytical service using a Carlo Erba CHNS/O microanalyser. Melting points were determined on a Gallenkamp apparatus and are uncorrected. Mass spectra were recorded by the Mass Spectrometry Service Centre at the University of St. Andrews on either a Micromass GCT EI/CI or a Micromass LCT ES instrument.

### *2.4.2 Single crystal X-ray structure determinations*

A table containing a summary of the crystal data collection and refinement paramaters of compounds **9**, **12** and **13** can be found in Appendix 1. Data sets were collected on a Rigaku Mo MM007 (dual port) high brilliance diffractometer with graphite monochromated MoK$\alpha$ radiation ($\lambda$ = 0.71075 Å). The diffractometer is fitted with Saturn 70 and Mercury CCD detectors and two XStream LT accessories. Data reduction was carried out with standard methods using the software package Bruker SAINT,[20] SMART,[21] SHELXTL[22] and and Rigaku CrystalClear, CrystalStructure, HKL2000. All the structures were solved using direct methods and conventional difference Fourier methods. All non-hydrogen atoms were refined anisotropically by full-matrix least squares calculations on $F^2$ using SHELX-97[23] within an X-seed[24,25] environment. The hydrogen atoms were fixed in calculated positions. Figures were generated with X-seed and POV-Ray for windows with the displacement ellipsoids at 50% probability level unless stated otherwise. Further information is available on request from Prof. Alexandra Slawin at the School of Chemistry, University of St. Andrews.

### *2.4.3 Synthetic procedures*

***(Propionyloxy)diphenylphosphine, 1***

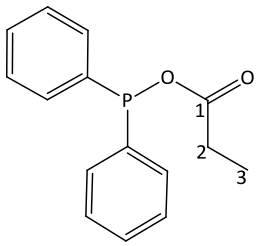


*Compound **1** was prepared following either the known procedure[12] or the adapted literature procedure[4] as described here:*

$Ph_2PCl$ (1.32 g, 6.00 mmol, 1.08 ml) was added dropwise to a solution of propanoic acid (0.44 g, 6.00 mmol, 0.48 ml) in thf (30 ml) at -10 °C with stirring. $NEt_3$ (0.61 g, 6.00 mmol, 0.84 ml) was added to the mixture, leading to the immediate formation of $[HNEt_3][Cl]$ in the form of a white precipitate. After having stirred at -10 °C for 10 min, the mixture was filtered over a plug of anhydrous $MgSO_4$ and all volatiles removed from the filtrate by evaporation under reduced pressure to furnish compound **1** as a colourless oil (yield: 1.43 g, 93 %). $^1$H NMR (300 MHz, $CD_2Cl_2$): $\delta_H$ = 1.18 (t, 3H, $^3J$ = 7.5 Hz; $H^3$), 2.53 (m, 2H, $^3J$ = 7.5 Hz; $H^2$), 7.40–7.59 (m, 10H, Ph). $^{31}P\{^1H\}$ NMR (121 MHz, $CD_2Cl_2$): $\delta_P$ = 98.9 (s). For complete characterisation see literature report.[12]

### *5-(Propionyloxy)dibenzophosphole, 2*

A solution of 5-chloro-dibenzophosphole (0.97 g, 4.45 mmol) in thf (10 ml) was added to a sodium propanoate (0.43 g, 4.45 mmol) suspension in thf (10 ml) at room temperature. The resulting mixture was allowed to stir at this temperature for 2 h, during which time the white sodium propanoate suspension cleared and sodium chloride (NaCl) precipitated from solution. After the 2 h stirring period, the formed NaCl was removed by filtration (cannula fitted with a membrane filter) and the colourless filtrate reduced to dryness *in vacuo* to yield the product as a colourless viscous oil which analysed to consist solely of disproportionation products.

### *General procedure for the preparation of bisphenoxyphosphorus chlorides, 3-6*

*These compounds were prepared according to a modified literature procedure.*[15] A solution of the appropriate diol (9.22 mmol) in thf (20 ml) was added to a solution of $PCl_3$ (1.27 g, 9.22 mmol, 0.81 ml) in thf (10 ml) at -40 °C. $NEt_3$ (1.87 g, 18.45 mmol, 2.57 ml) was then added dropwise *via* a syringe to the colourless solution. This led to the immediate precipitation of the formed $[HNEt_3][Cl]$ as a white solid. The resulting mixture was stirred at -40 °C for 1 h and then for a further 1 h at room temperature. After this period, the mixture was filtered and reduced to dryness *in vacuo* to obtain the pure products.

### *a) (1,1'-Biphenyl-2,2'-dioxy)chlorophosphine, 3*

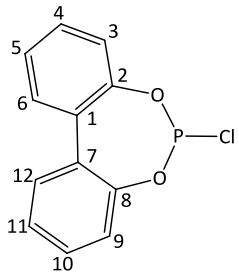


Starting diol: 2,2'-Biphenyldiol (1.72 g, 9.22 mmol). The title product was obtained as a viscous colourless oil (yield: 1.92 g, 83 %). $^{1}$H NMR (300 MHz, $CD_2Cl_2$): $\delta_H$ = 7.29 (dm, 2H, $^{3}J$ = 7.5 Hz; $H^3$ / $H^9$), 7.47 (td, 2H, $^{3}J$ = 7.5 Hz, $^{4}J$ = 2.0 Hz; $H^4$ / $H^{10}$), 7.40 (tm, 2H, $^{3}J$ = 7.5 Hz; $H^5$ / $H^{11}$), 7.56 (dd, 2H, $^{3}J$ = 7.5 Hz, $^{4}J$ = 2.0 Hz; $H^6$ / $H^{12}$). $^{13}C\{^{1}H\}$ NMR (75 MHz, $CD_2Cl_2$): $\delta_C$ = 122.6 (d, $^{3}J_{C\text{-}P}$ = 1.9 Hz; $C^3$ / $C^9$), 126.9 (s; $C^5$ /$C^{11}$), 130.0 (s, $C^4$ /$C^{10}$), 130.3 (d, $^{3}J_{C\text{-}P}$ = 3.3 Hz; $C^1$ / $C^7$), 130.7 (s; $C^6$ / $C^{12}$), 149.7 (d, $^{2}J_{C\text{-}P}$ = 5.6 Hz; $C^2$ / $C^8$). $^{31}P\{^{1}H\}$ NMR (121 MHz, $CD_2Cl_2$): $\delta_P$ = 179.7 (s).

### *b) (R)-(1,1'-binaphthalen-2,2'-dioxy)chlorophosphine, 4*

Starting diol: (*R*)-(+)-1,1'-Bi(2-naphthol) (2.64 g, 9.22 mmol). The title product was obtained as a white solid (yield: 2.23 g, 69 %). $^{1}$H NMR (300 MHz, $CD_2Cl_2$): $\delta_H$ = 7.26–7.33 (m, 2H), 7.38 (dd, 2H, $^{3}J$ = 8.1 Hz, $^{4}J$ = 3.4 Hz), 7.49–7.52 (m, 3H), 7.55 (dd, 1H, $^{3}J$ = 8.8 Hz, $^{4}J$ = 0.9 Hz), 8.0 (dd, 2H, $^{3}J$ = 8.2 Hz, $^{4}J$ = 2.8 Hz), 8.05 (dd, 2H, $^{3}J$ = 8.8 Hz, $^{4}J$ = 2.8 Hz). $^{13}C\{^{1}H\}$ NMR (75 MHz, $CD_2Cl_2$): $\delta_C$ =

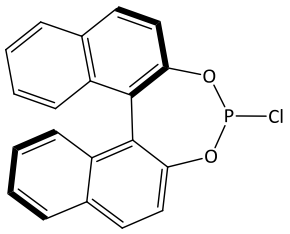

121.5 (s), 121.9 (s), 123.5 (d, $^{3}J_{C\text{-}P}$ = 2.8 Hz), 124.7 (d, $^{3}J_{C\text{-}P}$ = 5.8 Hz), 125.9 (s), 126.1 (s), 126.9 (s), 127.0 (s), 127.1 (s), 127.2 (s), 128.9 (s), 130.5 (s), 131.5 (s), 131.8 (s), 132.0 (s), 132.5 (s), 132.8 (s), 133.1 (s), 147.2 (d, $^{2}J_{C\text{-}P}$ = 3.0 Hz), 148.6 (d, $^{2}J_{C\text{-}P}$ = 4.86 Hz). $^{31}P\{^{1}H\}$ NMR (121 MHz, $CD_2Cl_2$): 178.3(s).

### *c) (5,5',6,6'-tetramethyl-3,3'-di-tert-butyl-1,1'-biphenyl-2,2'-dioxy)chlorophosphine, 5*

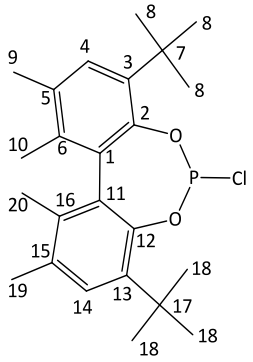

Starting diol: 5,5'-6,6'-tetramethyl-3,3'-di-*tert*-butyl-1,1'-biphenyl-2,2'-diol (3.27 g, 9.22 mmol). The title product was obtained as a white solid (yield: 3.17 g, 82 %). $^{1}H$ NMR (300 MHz, $CDCl_3$): $\delta_H$ = 1.56 (s, 18H; $H^{8}$ / $H^{18}$), 1.93 (s, 3H; $H^{9}$), 1.99 (s, 3H; $H^{19}$), 2.39 (s, 6H; $H^{10}$ / $H^{20}$), 7.32 (s, 1H; $H^{4}$), 7.33 (s, 1H; $H^{14}$). $^{13}C\{^{1}H\}$ NMR (75 MHz, $CDCl_3$): $\delta_C$ = 16.6 (s; $C^{10}$), 16.9 (s; $C^{20}$), 20.1 (s, $C^{9}$ / $C^{19}$), 31.2 (s; $C^{8}$), 32.3 (d, $^{5}J_{C\text{-}P}$ = 5.0 Hz; $C^{18}$), 34.7 (s; $C^{7}$), 35.1 (s; $C^{17}$),128.3 (s; $C^{4}$), 129.0 (s; $C^{14}$), 130.4 (d, $^{3}J_{C\text{-}P}$ = 2.8 Hz; $C^{1}$), 131.9 (d, $^{3}J_{C\text{-}P}$ = 5.7 Hz; $C^{11}$), 132.9 (s; $C^{5}$), 133.9 (s; $C^{15}$), 137.6 (d, $^{3}J_{C\text{-}P}$ = 1.8 Hz; $C^{3}$), 138.5 (d, $^{3}J_{C\text{-}P}$ = 3.5 Hz; $C^{13}$), 143.9 (d, $^{2}J_{C\text{-}P}$ = 5.7 Hz; $C^{2}$), 145.5 (s; $C^{12}$). $^{31}P\{^{1}H\}$ NMR (121 MHz, $CDCl_3$): $\delta_P$ = 164.3 (s).

### *d) (3,3',5,5'-Tetra-tert-butyl-1,1'-biphenyl-2,2'-dioxy)chlorophosphine, 6*

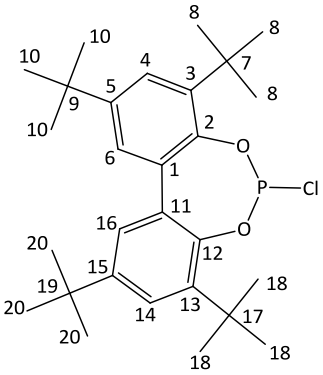

Starting diol: 3,3'-5,5'-tetra-*tert*-butyl-1,1'-biphenyl-2,2'-diol (3.79 g, 9.22 mmol). The title product was obtained as a white solid (yield: 3.24 g, 74 %). $^{1}H$ NMR (300 MHz, $CDCl_3$): $\delta_H$ = 1.39 (s, 18H; $H^{8}$ / $H^{18}$), 1.51 (s, 18H; $H^{10}$ / $H^{20}$), 7.21 (d, 2H, $^{4}J$ = 2.5 Hz; $H^{4}$ / $H^{14}$), 7.50 (d, 2H, $^{4}J$ = 2.5 Hz; $H^{6}$ / $H^{16}$). $^{13}C\{^{1}H\}$ NMR (75 MHz, $CDCl_3$): $\delta_C$ = 31.5 (s; $C^{8}$ / $C^{18}$), 31.5 (s; $C^{10}$ / $C^{20}$), 34.8 (s; $C^{9}$ / $C^{19}$), 35.6 (s; $C^{7}$ / $C^{17}$), 124.9 (s, $C^{4}$ / $C^{14}$), 126.8 (s; $C^{6}$ / $C^{16}$), 132.7 (d, $^{3}J_{C\text{-}P}$ = 4.2 Hz; $C^{1}$ / $C^{11}$), 140.5 (d, $^{3}J_{C\text{-}P}$ = 2.2 Hz; $C^{3}$ / $C^{13}$), 145.6 (d, $^{2}J_{C\text{-}P}$ = 6.2 Hz; $C^{2}$ / $C^{12}$). $^{31}P\{^{1}H\}$ NMR (121 MHz, $CDCl_3$): $\delta_P$ = 171.6 (s).

### *Propionyl-(1,1'-biphenyl-2,2'-diyl)phosphite, 7*

*This procedure was adapted from a literature procedure for the preparation of (R)-acetyl-(1,1'-binaphthyl-2,2'-diyl)phosphite.*[10] A solution of **3** (1.45 g, 5.80 mmol) in thf (20 ml) was added to a sodium propanoate (0.56 g, 5.80 mmol) suspension in thf (15 ml) at 45 $^{o}$C. The resulting

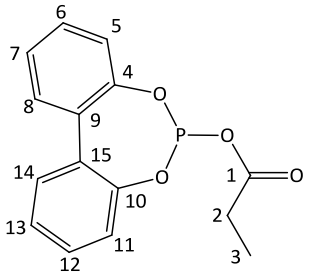

mixture was allowed to stir at this temperature for 2 h, during which time the white sodium propanoate suspension cleared and sodium chloride (NaCl) precipitated from solution. After the 2 h stirring period, the formed sodium chloride was removed by filtration (either over a $MgSO_4$ plug or by using a cannula fitted with a membrane filter) and the colourless filtrate reduced to dryness *in vacuo* to yield the product as a colourless viscous oil contaminated with *c.a.* 8 % (based on NMR integration) of the by-product **7*BP*** (crude yield: 1.54 g, 93 %). This impurity could not be separated from the title compound, using standard purification techniques. $^{1}$H NMR (300 MHz, $CD_2Cl_2$): $\delta_H$ = 1.18 (t, 3H, $^{3}J$ = 7.4 Hz; $H^3$), 2.46 (q, 2H, $^{3}J$ = 7.4 Hz; $H^2$), 7.27 (dd, 2H, $^{3}J$ = 7.6 Hz, $^{4}J$ = 1.2 Hz; $H^5$ / $H^{11}$), 7.37 (td, 2H, $^{3}J$ = 7.6 Hz, $^{4}J$ = 1.2 Hz; $H^7$ / $H^{13}$), 7.45 (td, 2H, $^{3}J$ = 7.6 Hz, $^{4}J$ = 2.0 Hz; $H^6$ / $H^{12}$), 7.54 (dd, 2H, $^{3}J$ = 7.6 Hz, $^{4}J$ = 2.0 Hz; $H^8$ / $H^{14}$). $^{13}C\{^{1}H\}$ NMR (75 MHz, $CD_2Cl_2$): $\delta_C$ = 9.0 (s; $C^3$), 28.9 (s; $C^2$), 122.4 (s; $C^5$ / $C^{11}$), 126.3 (s; $C^7$ / $C^{13}$), 129.9 (s; $C^6$ / $C^{12}$), 130.6 (s; $C^8$ / $C^{14}$), 131.5 (d, $^{3}J_{C\text{-}P}$ = 3.4 Hz; $C^9$ / $C^{15}$), 149.3 (d, $^{2}J_{C\text{-}P}$ = 4.9 Hz; $C^4$ / $C^{10}$), 173.6 (d; $^{2}J_{C\text{-}P}$ = 5.1 Hz; $C^1$). $^{31}P\{^{1}H\}$ NMR (121 MHz, $CD_2Cl_2$): $\delta_P$ = 142.5 (s). IR (solution in $CH_2Cl_2$): $\tilde{\nu}$ = 3066 [w, $sp^2$ $\nu$(C–H)], 2970–2877 [w, $sp^3$ $\nu$(C–H)], 1740 [st, $\nu$(C=O)], 1499–1436 [st, Ar $\nu$(C=C)], 769 [st, $\nu$(P–O)]. ES-MS: *m/z* (%) = 289 (8) $[M]^+$, 215 (100) $[M - OC(O)CH_2CH_3]^+$. For by-product **7*BP***: $^{1}$H NMR (300 MHz, $CDCl_3$): $\delta_H$ = 1.39 (dd, 3H, $^{3}J$ = 7.5 Hz; $H^3$), 2.34 (m, 2H; $H^2$), 5.41 (m, 1H, $^{3}J_{H\text{-}H}$ = 14.8 Hz, $^{3}J_{H\text{-}H}$ = 8.1 Hz, $^{2}J_{H\text{-}P}$ = 6.6 Hz, $^{2}J_{H\text{-}P}$ = 4.9 Hz; $H^1$), 7.20–7.54 (m, 16H; Ph). $^{13}C\{^{1}H\}$ NMR (75 MHz, $CDCl_3$): $\delta_C$ = 8.5 (s; $C^3$), 25.7 (s; $C^2$), 74.4 (d, $^{2}J_{C\text{-}P}$ = 7.5 Hz; $C^1$). $^{31}P\{^{1}H\}$ NMR (121 MHz, $CDCl_3$): $\delta_P$ = 1.9 (d, $^{3}J_{PA\text{-}PB}$ = 24.1 Hz; $P_A$), 26.4 (d, $^{3}J_{PB\text{-}PA}$ = 24.1 Hz; $P_B$).

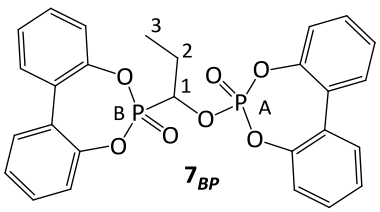

**7*BP***

### *(R)-Propionyl-(1,1'-binaphthyl-2,2'-diyl)phosphite, 8*

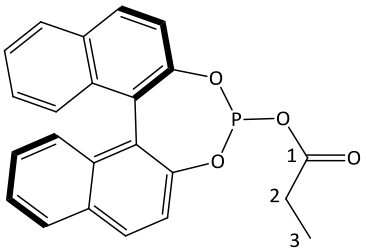

Ligand **8** was prepared using the same method as was described for **7**, by treating a solution of **4** (1.28 g, 3.64 mmol) in thf (15 ml) with a sodium propanoate (0.35 g, 3.64 mmol) suspension in thf (20 ml) at 45 °C for 2 h. The title product was obtained as a white solid contaminated by small amounts of by-product **8*BP*** (8 %, based on NMR integrals), which could not be separated from **8** using standard purification techniques. $^{1}$H NMR (300 MHz, $CD_2Cl_2$): $\delta_H$ = 1.15 (t, 3H, $^{3}J$ = 7.5 Hz; $H^3$), 2.40 (qd, 2H, $^{3}J$ = 7.5 Hz, $^{4}J_{H\text{-}P}$ = 0.8 Hz; $H^2$), 7.26–7.33 (m, 2H), 7.38 (m, 2H), 7.45–7.52 (m, 3H),

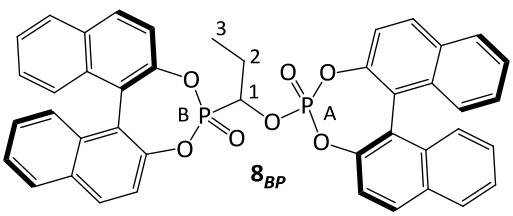


**8*BP***

7.58 (dd, 1H, $^{3}J$ = 8.8 Hz, $^{4}J$ = 0.9 Hz), 8.0 (d, 2H, $^{3}J$ = 8.2 Hz), 8.05 (m, 2H). $^{13}C\{^{1}H\}$ NMR (75 MHz, $CD_2Cl_2$): $\delta_C$ = 8.9 (s; $C^3$), 28.9 (d, $^{3}J_{C\text{-}P}$ = 2.2 Hz; $C^2$), 121.6 (s), 121.9 (s), 123.3 (d, $^{3}J_{C\text{-}P}$ = 2.5 Hz), 124.7 (d, $^{3}J_{C\text{-}P}$ = 5.6 Hz), 125.7 (s), 125.9 (s), 126.9 (s), 127.0 (s), 127.1 (s), 127.2 (s), 128.8 (s), 128.9 (s), 130.5 (s), 131.2 (s), 131.8 (s), 132.3 (s), 132.8 (s), 133.1 (s), 147.1 (d, $^{2}J_{C\text{-}P}$ = 2.2 Hz), 147.9 (d, $^{2}J_{C\text{-}P}$ = 4.1 Hz), 173.6 (d, $^{2}J_{C\text{-}P}$ = 5.0 Hz; $C^1$). $^{31}P\{^{1}H\}$ NMR (121 MHz, $CD_2Cl_2$): $\delta_P$ = 141.8 (s). IR (KBr): $\tilde{\nu}$ = 3059 [w, $sp^2$ $\nu$(C–H)], 2980–2940 [w, $sp^3$ $\nu$(C–H)], 1739 [st, $\nu$(C=O)], 1508–1407 [m, Ar $\nu$(C=C)], 746 [st, $\nu$(P–O)]. For by-product **8*BP***: *Diastereomer 1*: $^{1}H$ NMR (300 MHz, $CDCl_3$): $\delta_H$ = 1.23 (dd, 3H, $^{3}J$ = 7.5 Hz; $H^3$), 2.18 (m, 2H; $H^2$), 5.26 (m, 1H; $H^1$), 7.25–8.10 (m, 24H; Ph). $^{31}P\{^{1}H\}$ NMR (121 MHz, $CDCl_3$): $\delta_P$ = 3.57 (d, $^{3}J_{PA\text{-}PB}$ = 23.3 Hz; $P_A$), 27.6 (d, $^{3}J_{PB\text{-}PA}$ = 23.3 Hz; $P_B$). *Diastereomer 2*: $^{1}H$ NMR (300 MHz, $CDCl_3$): $\delta_H$ = 1.43 (dd, 3H, $^{3}J$ = 7.5 Hz; $H^3$), 2.35 (m, 2H; $H^2$), 5.27 (m, 1H; $H^1$), 7.25–8.10 (m, 24H; Ph). $^{31}P\{^{1}H\}$ NMR (121 MHz, $CDCl_3$): $\delta_P$ = 2.67 (d, $^{3}J_{PA\text{-}PB}$ = 28.9 Hz; $P_A$), 26.6 (d, $^{3}J_{PB\text{-}PA}$ = 28.9 Hz; $P_B$).

### *Propionyl-(5,5',6,6'-tetramethyl-3,3'-di-tert-butyl-1,1'-biphenyl-2,2'-diyl)phosphite, 9*

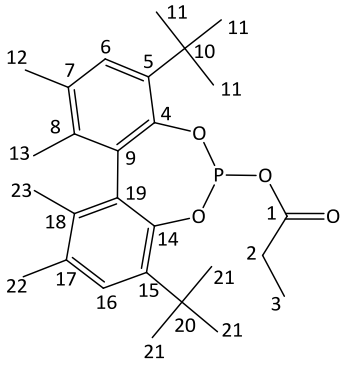


Compound **9** was prepared using a similar methodology to that described for the preparation of **7**. A solution of **5** (1.17 g, 2.79 mmol) in thf (10 ml) was added to a suspension of sodium propanoate (0.26 g, 2.79 mmol) in thf (10 ml) at 45 $^{o}$C. After a 2 h stirring period, the formed NaCl was removed by filtration (cannula fitted with a membrane filter) and the colourless filtrate reduced to dryness *in vacuo*. The resulting white residue was extracted with hexane (40 ml), filtered and subsequently stripped of solvent under reduced pressure to furnish the analytically pure product as a white solid (yield: 1.20 g, 94 %). Crystals (colourless prisms) suitable for single crystal X-ray diffraction determination could be obtained by slow cooling of a saturated solution of **9** in warm hexane (40 $^{o}$C) to -22 $^{o}$C. Mp 151-153 $^{o}$C. *Anal.* Calculated (%) for $C_{27}H_{37}O_4P$: C 71.03, H 8.17; Found C 71.07, H 8.59. $^{1}H$ NMR (300 MHz, $CD_2Cl_2$): $\delta_H$ = 1.09 (t, 3H, $^{3}J$ = 7.5 Hz; $H^3$), 1.45 (s, 9H; $H^{11}$), 1.49 (s, 9H; $H^{21}$), 1.83 (s, 3H; $H^{12}$), 1.86 (s, 3H; $H^{22}$), 2.29 (s, 6H; $H^{13}$ / $H^{23}$), 2.36 (q, 2H, $^{3}J$ = 7.5 Hz; $H^2$), 7.23 (s, 1H; $H^6$), 7.24 (s, 1H, $H^{16}$). $^{13}C\{^{1}H\}$ NMR (75 MHz, $CD_2Cl_2$): $\delta_C$ = 8.6 (s; $C^3$), 16.6 (s; $C^{13}$), 16.8 (s; $C^{23}$), 20.5 (s; $C^{12}$ / $C^{22}$), 28.8 (d, $^{3}J_{C\text{-}P}$ = 2.5 Hz; $C^2$), 31.1 (d, $^{5}J_{C\text{-}P}$ = 4.6 Hz; $C^{11}$), 31.7 (s; $C^{21}$), 34.9 (s; $C^{10}$), 35.1 (s; $C^{20}$), 128.5 (s; $C^6$), 128.8 (s; $C^{16}$), 130.7 (d, $^{3}J_{C\text{-}P}$ = 2.9 Hz; $C^9$), 132.2 (d, $^{3}J_{C\text{-}P}$ = 5.5 Hz; $C^{19}$), 132.8 (s;

$C^7$), 133.9 (s; $C^{17}$), 134.7 (s; $C^8$), 135.6 (s; $C^{18}$), 137.7 (s; $C^5$), 139.1 (d, $^3J_{C\text{-}P}$ = 3.2 Hz; $C^{15}$), 144.2 (s; $C^4$), 144.9 (d, $^2J_{C\text{-}P}$ = 5.0 Hz; $C^{4'}$), 173.5 (d, $^2J_{C\text{-}P}$ = 5.6 Hz; $C^1$). $^{31}P\{^1H\}$ NMR (121 MHz, $CD_2Cl_2$): $\delta_P$ = 129.6 (s). IR (KBr): $\tilde{\nu}$ = 3036 [w, $sp^2$ $\nu$(C–H)], 2952–2868 [st, $sp^3$ $\nu$(C–H)], 1740 [st, $\nu$(C=O)], 1480–1393 [m, Ar $\nu$(C=C)], 738 [m, $\nu$(P–O)]. ES-MS: *m/z* (%) = 456 (20) $[M]^+$, 383 (100) $[M - OC(O)CH_2CH_3]^+$.

### *Propionyl-(3,3',5,5'-tetra-tert-butyl-1,1'-biphenyl-2,2'-diyl)phosphite, 10*

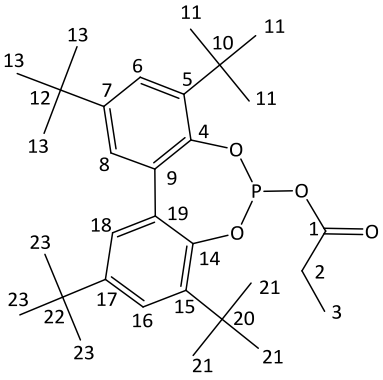

Employing a similar procedure to that followed during the preparation of compound **7**, a solution of **6** (2.34 g, 4.93 mmol) in thf (20 ml) was reacted with a sodium propanoate (0.47 g, 4.93 mmol) suspension in thf (15 ml) at 45 °C for 2 h. After work-up (as described for **7**), the product was extracted with hexane, filtered and reduced to dryness *in vacuo* to yield the analytically pure product as a white solid (yield: 2.34 g, 92 %). Mp 139-143 °C. *Anal.* Calculated (%) for $C_{31}H_{45}O_4P$: C 72.63, H 8.85; Found C 72.77, H 9.31. $^1H$ NMR (300 MHz, $CD_2Cl_2$): $\delta_H$ = 1.13 (t, 3H, $^3J$ = 7.4 Hz; $H^3$), 1.38 (s, 18H; $H^{11}$ / $H^{21}$), 1.50 (s, 18H; $H^{13}$ / $H^{23}$), 2.44 (m, 2H, $^3J$ = 7.4 Hz; $H^2$), 7.23 (d, 2H, $^4J$ = 2.5 Hz; $H^6$ / $H^{16}$), 7.51 (d, 2H, $^4J$ = 2.5 Hz; $H^8$ / $H^{18}$). $^{13}C\{^1H\}$ NMR (75 MHz, $CD_2Cl_2$): $\delta_C$ = 8.5 (s; $C^3$), 28.5 (d, $^3J_{C\text{-}P}$ = 2.5 Hz; $C^2$), 31.1 (d, $^5J_{C\text{-}P}$ = 1.9 Hz; $C^{11}$ / $C^{21}$), 31.6 (s; $C^{13}$ / $C^{23}$), 35.5 (s; $C^{12}$ / $C^{22}$), 34.7 (s; $C^{10}$ / $C^{20}$), 124.6 (s; $C^6$ / $C^{16}$), 126.6 (s; $C^8$ / $C^{18}$), 132.7 (s; $C^9$ / $C^{19}$), 140.5 (s; $C^5$ / $C^{15}$), 145.0 (d, $^2J_{C\text{-}P}$ = 4.7 Hz; $C^4$ / $C^{14}$), 147.1 (s; $C^7$ / $C^{17}$), 173.3 (d, $^2J_{C\text{-}P}$ = 5.1 Hz; $C^1$). $^{31}P\{^1H\}$ NMR (121 MHz, $CD_2Cl_2$): $\delta_P$ = 135.9 (s). IR (KBr): $\tilde{\nu}$ = 3054 [w, $sp^2$ $\nu$(C–H)], 2962–2871 [st, $sp^3$ $\nu$(C–H)], 1743 [st, $\nu$(C=O)], 1459–1397 [m, Ar $\nu$(C=C)], 748 [m, $\nu$(P–O)]. ES-MS: *m/z* (%) = 512 (31) $[M]^+$, 493 (100) $[M - OC(O)CH_2CH_3]^+$.

### *(Phenylacetyloxy)diphenylphosphine, 11*

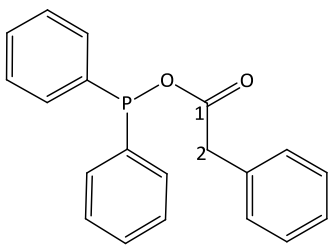

A solution of 2-phenylacetic acid (1.36 g, 10.00 mmol) at -10 °C was treated with $NEt_3$ (0.607 g, 0.836 ml, 6.00 mmol). $Ph_2PCl$ (0.817 g, 6.00 mmol) was then added dropwise *via* a syringe leading to the immediate precipitation of $[HNEt_3][Cl]$. The resulting mixture was allowed to stir for 10 min at -10 °C and subsequently filtered into a separate flask using a cannula fitted with a membrane filter. The filtrate was subsequently reduced to dryness to furnish the product as a white microcrystalline

solid (yield: 1.37 g, 72 %). Mp 22–24 °C. $^{1}$H NMR (300 MHz, $CD_2Cl_2$): $\delta_H$ = 3.91 (d, 2H, $^{4}J$ = 1.0 Hz; $H^{2}$), 7.42–7.65 (m, 15H, Ph). $^{13}C\{^{1}H\}$ NMR (75 MHz, $CD_2Cl_2$): $\delta_C$ = 42.6 (d, $^{3}J_{C\text{-}P}$ = 2.1 Hz; $C^{2}$), 127.6 (s; Ph–$C^{para}$), 128.9 (d, $^{4}J_{C\text{-}P}$ = 7.03 Hz; PPh–$C^{meta}$), 129.0 (s; PPh–$C^{para}$), 129.8 (s; Ph–$C^{meta}$), 130.5 (s; Ph–$C^{ortho}$), 131.2 (d, $^{2}J_{C\text{-}P}$ = 23.8 Hz, PPh-$C^{ortho}$), 134.2 (s; P–$C^{ipso}$), 139.4 (d, $^{1}J_{C\text{-}P}$ = 19.4 Hz; PPh–$C^{ipso}$). $^{31}P\{^{1}H\}$ NMR (121 MHz, $CD_2Cl_2$): $\delta_P$ = 100.2 (s). IR (KBr): $\tilde{\nu}$ = 3058 [w, $sp^2$ $\nu$(C–H)], 3027–2860 [w, $sp^3$ $\nu$(C–H)], 1720 [st, $\nu$(C=O)], 1497–1439 [st, Ar $\nu$(C=C)], 738 [st, $\nu$(P–O)].

### *Phenylacetyl-(5,5',6,6'-tetramethyl-3,3'-di-tert-butyl-1,1'-biphenyl-2,2'-diyl)phosphite, 12*

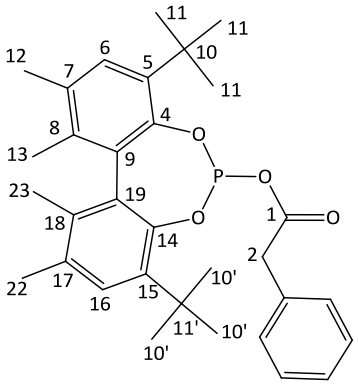


Phenylacetic acid (0.53 g, 3.86 mmol) was dissolved in thf (15 ml) and cooled to -10 °C. $NEt_3$ (0.39 g, 0.54 ml, 3.86 mmol) was added dropwise *via* syringe to this solution and the resulting mixture was allowed to stir for 5 min. A solution of **5** (1.62 g, 3.86 mmol) in thf (20 ml) was then cannulated into the mixture, while maintaining the external temperature at -10 °C. The reaction solution was allowed to stir for 20 min at this temperature and then for another 20 min at room temperature. The formed $[HNEt_3][Cl]$ was subsequently removed by filtration (cannula fitted with a membrane filter) and the colourless filtrate stripped of all volatiles under reduced pressure to obtain the crude product as a white foam. This foam was washed with copious amounts of hexane (3 × 30 ml) and dried *in vacuo* to yield the analytically pure product as a white solid (1.84 g, 92%). Colourless prisms suitable for single crystal X-ray analysis could be obtained by slow diffusion of a hexane into a solution of **12** in toluene at room temperature. Mp 164-166 °C. *Anal.* Calculated (%) for $C_{32}H_{39}O_4P$: C 74.11, H 7.58; Found C 73.27, H 7.58. $^{1}$H NMR (300 MHz, $CDCl_3$): $\delta_H$ = 1.44 (s, 9H; $H^{11}$), 1.45 (s, 9H; $H^{21}$), 1.82 (s, 3H; $H^{12}$), 1.86 (s, 3H; $H^{22}$), 2.28 (s, 3H; $H^{13}$), 2.30 (s, 3H; $H^{23}$), 3.66 (s, 2H; $H^{2}$), 7.23 (s, 1H; $H^{6}$), 7.24 (s, 1H; $H^{16}$), 7.18–7.34 (m, 5H, Ph). $^{13}C\{^{1}H\}$ NMR (75 MHz, $CDCl_3$): $\delta_C$ = 16.6 (s; $C^{13}$), 16.9 (s; $C^{23}$), 20.5 (s; $C^{12}$ / $C^{22}$), 31.0 (d, $^{5}J_{C\text{-}P}$ = 4.5 Hz; $C^{11}$), 31.5 (s; $C^{21}$), 34.7 (s; $C^{10}$), 34.9 (s; $C^{20}$), 41.8 (s; $C^{2}$), 127.3 (s; Ph–$C^{para}$), 128.1 (s; Ph–$C^{meta}$), 128.3 (s; Ph–$C^{ortho}$), 129.5 (s; $C^{6}$), 130.2 (s; $C^{16}$), 130.2 (s; $C^{9}$), 132.0 (s; Ph–$C^{ipso}$), 132.8 (s; $C^{19}$), 132.4 (s; $C^{7}$), 133.4 (s; $C^{17}$), 134.4 (s; $C^{8}$), 135.2 (s; $C^{18}$), 137.2 (s; $C^{5}$), 138.9 (s, $C^{15}$), 143.9 (s; $C^{4}$), 144.6 (d, $^{2}J_{C\text{-}P}$ = 4.7 Hz; $C^{14}$), 170.5 (d, $^{2}J_{C\text{-}P}$ = 5.3 Hz; $C^{1}$). $^{31}P\{^{1}H\}$ NMR (121 MHz, $CD_2Cl_2$): $\delta_P$ = 129.3 (s). IR (KBr): $\tilde{\nu}$ = 3042 [w, $sp^2$ $\nu$(C–H)], 2952–2863 [st, $sp^3$ $\nu$(C–H)], 1729

[st, $\nu$(C=O)], 1493–1359 [m, Ar $\nu$(C=C)], 735 [st, $\nu$(P–O)]. ES-MS: *m/z* (%) = 518 (48) $[M]^+$, 383 (100) $[M - OC(O)CH_2(C_6H_5)]^+$.

***Phenylacetyl(3,3',5,5'-tetra-tert-butyl-1,1'-biphenyl-2,2'-diyl)phosphite, 13***

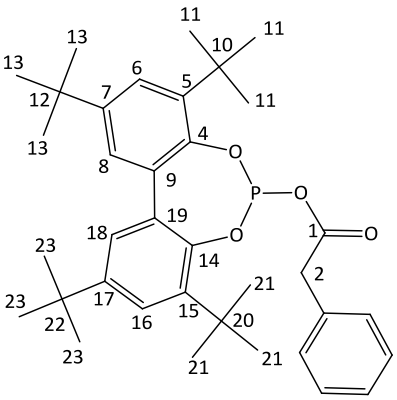


Compound **13** was prepared according to the procedure described for **12**, employing phenylacetic acid (0.82 g, 6.04 mmol), $NEt_3$ (0.61 g, 0.84 ml, 6.04 mmol) and **6** (2.87 g, 6.04 mmol). The analytically pure product was obtained as a white solid (yield: 3.12 g, 95 %) and colourless prisms suitable for analysis by single crystal X-ray diffraction could be obtained by slow evaporation of a dichloromethane solution of **13** at room temperature. Mp 165-167 °C. *Anal.* Calculated (%) for $C_{36}H_{47}O_4P$: C 75.23, H 8.24; Found C 75.11, H 8.50. $^1$H NMR (300 MHz, $CD_2Cl_2$): $\delta_H$ = 1.37 (s, 18H; $H^{11}$ / $H^{21}$), 1.46 (s, 18H; $H^{13}$ / $H^{23}$), 3.71 (s, 2H; $H^2$), 7.19 (d, 2H, $^4J$ = 2.5 Hz; $H^6$ / $H^{16}$), 7.20–7.35 (m, 5H, Ph), 7.46 (d, 2H, $^4J$ = 2.5 Hz; $H^8$ / $H^{18}$). $^{13}C\{^1H\}$ NMR (75 MHz, $CD_2Cl_2$): $\delta_C$ = 31.0 (s; $C^{13}$), 31.1 (s; $C^{23}$), 31.6 (s; $C^{11}$ / $C^{21}$), 35.5 (s; $C^{12}$ / $C^{22}$), 34.8 (s; $C^{10}$ / $C^{20}$), 42.0 (d, $^3J_{C\text{-}P}$ = 2.6 Hz; $C^2$), 124.6 (s; $C^6$ / $C^{16}$), 126.6 (s; $C^8$ / $C^{18}$), 127.3 (s; Ph–$C^{para}$), 128.6 (s; Ph–$C^{meta}$), 129.5 (s; Ph–$C^{ortho}$), 132.7 (d, $^3J_{C\text{-}P}$ = 3.7 Hz; $C^9$ / $C^{19}$), 132.8 (s; Ph–$C^{ipso}$), 140.5 (s; $C^5$ / $C^{15}$), 145.0 (d, $^2J_{C\text{-}P}$ = 5.0 Hz; $C^4$ / $C^{14}$), 147.2 (s; $C^7$ / $C^{17}$), 170.4 (d, $^2J_{C\text{-}P}$ = 5.0 Hz; $C^1$). $^{31}P\{^1H\}$ NMR (121 MHz, $CD_2Cl_2$): $\delta_P$ = 135.7 (s). IR (KBr): $\tilde{\nu}$ = 3044 [w, $sp^2$ $\nu$(C–H)], 2955–2865 [st, $sp^3$ $\nu$(C–H)], 1730 [st, $\nu$(C=O)], 1474–1394 [m, Ar $\nu$(C=C)], 733 [m, $\nu$(P–O)]. ES-MS: *m/z* (%) = 574 (9) $[M]^+$, 439 (100) $[M - OC(O)CH_2(C_6H_5)]^+$.

## 2.5 Notes and References


(1) Lindner, E.; Wuhrmann, J. C. *Chem. Ber.* **1981**, *114*, 2272-2286.
(2) Sartori, P.; Thomzik, M. *Z. Anorg. Allg. Chem.* **1972**, *394*, 157-170.
(3) Miller, J. A.; Stewart, D. *J. Chem. Soc., Perkin Trans. I* **1977**, 1898-1901.
(4) Cupertino, D. C.; Cole-Hamilton, D. J. *J. Chem. Soc., Dalton Trans.* **1987**, *49*, 443-449.
(5) Irvine, D. J.; Glidewell, C.; Cole-Hamilton, D. J.; Barnes, J. C.; Howie, A. *J. Chem. Soc., Dalton Trans.* **1991**, 1765-1772.
(6) Irvine, D. J., *PhD thesis*, University of St. Andrews (St. Andrews) **1990**, Chapter 3, pp 116-121.
(7) Hoge, B.; Kurscheid, B. *Angew. Chem. Int. Ed.* **2008**, *47*, 6814-6816.
(8) Selent, D.; Wiese, K.; Boerner, A. *Chemical Industries* **2005**, *104*, 459-469.

(9) Belyaev, A.; Zhang, X.; Augustyns, K.; Lambeir, A.; De Meester, I.; Vedernikova, I.; Sharpé, S.; Haemers, A. *J. Med. Chem.* **1999**, 1041-1052.
(10) Korostylev, A.; Monsees, A.; Fischer, C.; Börner, A. *Tetrahedron: Asymmetry* **2004**, *15*, 1001-1005.
(11) Whiteker, G. T.; Klosin, J.; Gardner, K. J. (The Dow Chemical Company), *U.S. Pat. Appl. Publ.* **2004**, 2004199023, 20 pp.
(12) Bollmacher, H.; Sartori, P. *Chemiker Zeitung* **1982**, *106*, 391-395.
(13) Teunissen, H. T.; Hansen, C. B.; Bickelhaupt, F. *Phosphorus, Sulfur and Silicon* **1996**, *118*, 309-312.
(14) Fitch, S. J.; Moedritzer, K. *J. Am. Chem. Soc.* **1962**, *84*, 1876-1879.
(15) Scherer, J.; Huttner, G.; Büchner, M. *Chem. Ber.* **1996**, *129*, 697-713.
(16) Abraham, K. M; van Wazer, J. R *J. Organomet. Chem* **1975**, *85*, 41-46.
(17) Neda, I.; Fischer, A.; Kaukorat, T.; Jones, P. G.; Schmutzler, R. *Chem. Ber.* **1994**, *127*, 1579-1586.
(18) Cobley, C. J.; Gardner, K.; Klosin, J.; Praquin, C.; Catherine Hill; Whiteker, G. T.; Zanotti-Gerosa, A.; Petersen, J. L.; Abboud, K. A. *J. Org. Chem.* **2004**, *69*, 4031-4040.
(19) Buisman, G. J. H.; Kamer, P. C. J.; Leeuwen, P. W. N. M. v. *Tetrahedron: Asymmetry* **1993**, *4*, 1625-1634.
(20) *SAINT Data Reduction Software (version 6.45)*, Bruker AXS Inc. (Madison), WI, USA, **2003**.
(21) *SMART Data Collection Software (version 5.629)*, Bruker AXS Inc. (Madison), WI, USA, **2003**.
(22) *SHELXL program package (version 5.1)*, Bruker APX Inc. (Madison), WI, USA.
(23) Sheldrick, G. M. *SHELX-97 Program for Crystal Structure Analysis*, University of Göttingen (Göttingen), Germany, **1997**.
(24) Barbour, L. J. *J. Supramol. Chem.* **2003**, *1*, 189-191.
(25) Atwood, J. L.; Barbour, L. J. *Cryst. Growth Des.* **2003**, *3*, 3-8.

# Chapter 3

# Rhodium and ruthenium complexes of mixed anhydrides

– Their preparation, lability and potential as C–H activation catalysts –

*The coordination chemistry and in solution behaviour of Rh(I) and Ru(II) complexes derived from mixed anhydride ligands* ***1*** *and* ***7–13****, were explored. Similar to the free ligands, mixed anhydride complexes rearranged in solution* via *a number of pathways. Plausible mechanisms could be proposed for some of these routes and by-product formation followed with the aid of NMR spectroscopy. Where stability allowed, new complexes were fully characterised, including solid state structures for four of the unrearranged mixed anhydride complexes and two of the interesting rearrangement products. Despite their instability, a selection of Rh(I) mixed anhydride complexes were also assessed for their potential as C-H activation catalysts in reactions aimed at the functionalisation of the* α*-C–H bonds in saturated carboxylic acids.*

## 3.1 Introduction

The coordination chemistry of mixed anhydrides of the general formula [$R_2POC(O)R'$] and their application in catalysis remain a rather uncharted area of chemistry with only a small number of reports in the literature relating to this topic. Furthermore, amongst reporters, Cole-Hamilton and co-workers[1-9] have been most prominent as the developers of such chemistry. Through their initial work, Cupertino and Cole-Hamilton[1,3] demonstrated that mixed anhydride ligands derived from diphenylphosphinous acid and acrylic acids react readily with [{RhCl(cyclooctene)$_2$}$_2$] to form complexes of the general formula [{RhCl($Ph_2PO_2CCR=CR'R''$}$_2$], containing the allylic-mixed anhydride bound in a chelating manner *via* the phosphorus atom and the C=C double bond. In a later study directed toward regioselective alkene hydrogenation, this series was extended to include complexes of these ligands derived from Wilkinson's catalyst. Although these complexes proved inferior to [$RhCl(PPh_3)_3$] in the catalytic hydrogenation of alkenes such as hex-1-ene, they were superior as catalysts for the hydrogenation of acrylic acids under basic conditions. Within these catalytic systems the substrate is initially fixed to the catalyst by a phosphorus ester bond and then released again, following hydrogenation, together with the introduction of a fresh substrate molecule by a base catalysed transesterification reaction at phosphorus (Scheme 3.1).[7] The precatalyst [$RhCl(PPh_3)_2(Ph_2OP(O)CCH=CMe_2)$], in particular, was found to be very efficient in the hydrogenation of a variety of highly substituted alkenes.

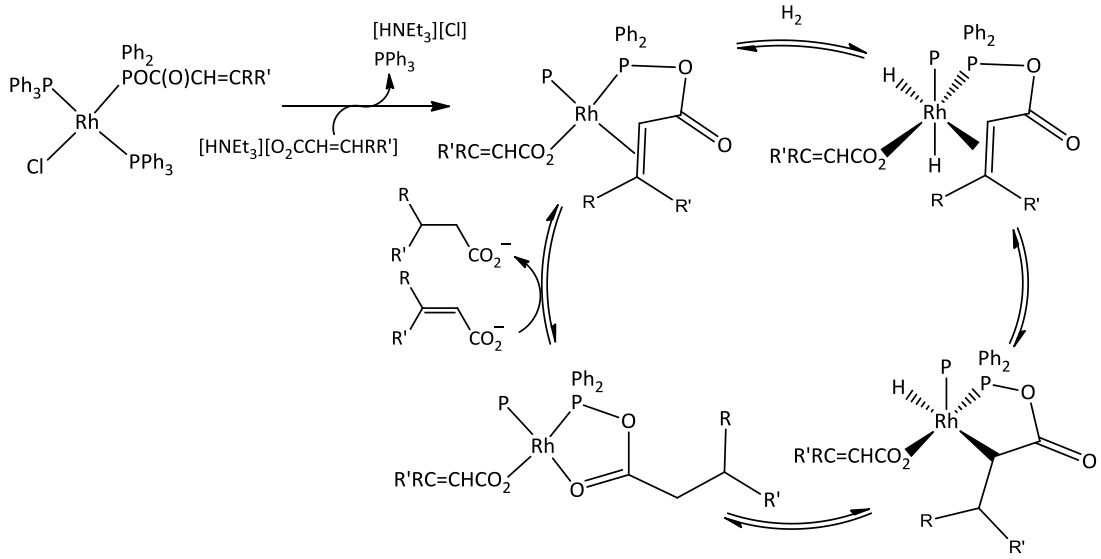


**Scheme 3.1** Mechanism for the hydrogenation of acrylic acids using Rh(I) complexes of mixed anhydrides derived from diphenylphosphorus acid and acrylic acids (where P = $PPh_3$, R = H / Me and R' = Me / -CH=CHMe ).

Although in $[RhCl(PPh_3)_2(Ph_2OP(O)CCH{=}CMe_2)]$ the mixed anhydride only binds *via* phosphorus, double bond assisted chelation does form an integral part of the catalytic mechanism, not only enhancing the rate of double bond hydrogenation but also promoting selective hydrogenation of only one double bond within a conjugated system.[2,7] In addition to the two modes of bonding already mentioned, a third, namely chelated bonding through the phosphorus atom and the carbonyl oxygen, has also been observed for complexes of mixed anhydride ligands.[4,6] In all cases, the preferred mode of bonding seems to be governed by steric factors together with the electronic nature of the metal centre, with even small changes therein leading to variations in the manner of bonding. Whilst mixed anhydride ligands of acrylic acids with three substituents (including the carboxylate group) on the double bond demonstrate preferential binding through only the phosphorus atom, chelation through P and the double bond is prevalent in mixed anhydrides with less substituted double bonds. Treatment of any of these complexes with $TlPF_6$ or $AgSbF_6$ results in the loss of a chloride ligand which affects binding *via* the third mode (P and O as in $[Rh(PPh_3)_2(Ph_2PO_2CCH{=}CMe_2)][SbF_6]$). Relief of steric congestion around the metal centre together with an increased hardness in character have been proposed as driving forces for this conversion.[6]

As mentioned in Chapter 2,[10] the chemistry associated with mixed anhydrides derived from acrylic $\{CH_2{=}CHCO_2H\}$ and vinylacetic $\{CH_2{=}CHCH_2CO_2H\}$ acids, differs significantly from that of their more substituted analogues. These ligands are thermally labile in the uncoordinated state and readily undergo spontaneous disproportionation reactions to furnish $Ph_2PP(O)Ph_2$ as one of the major by-products.[8] In addition, complexes of the form $[RhCl(PPh_3)_2L]$ (where L = $Ph_2PO_2CCH{=}CH_2$ or $Ph_2PO_2CCH_2CH{=}CH_2$), when left in solution, revert back to $[RhCl(PPh_3)_3]$ with simultaneous formation of the ligand disproportionation product $Ph_2PP(O)Ph_2$ and the zwitterion $Ph_3P^+CH_2CH_2CO_2^-$ [Scheme 3.2 (i)–(iii)]. Once again, steric factors determine the stability and stereochemistry of these complexes, with *trans* phosphine ligands favoured in the absence of steric congestion. Furthermore, reactions of $[RhCl(PPh_3)_3]$ with an excess of $Ph_2PO_2CCH{=}CH_2$ or $Ph_2PO_2CCH_2CH{=}CH_2$ result in the formation of the chelated rearrangement product, $[RhCl(PPh_3)(Ph_2POPPh_2)]$ [Scheme 3.2 (iv)]. Although the direct reactions of $Ph_2P(O)PPh_2$ with $[M(CO)_6]$ complexes (M = Cr, Mo or W) in refluxing dyglyme are known to produce [*cis*-$M(CO)_4(Ph_2POPPh_2)$] complexes,[11,12] the formation of $[RhCl(PPh_3)(Ph_2POPPh_2)]$ in this instance is believed to be metal promoted, since direct reactions between $[RhCl(PPh_3)_3]$

and $Ph_2PP(O)Ph_2$ failed to produce $[RhCl(PPh_3)(Ph_2POPPh_2)]$. Furthermore, $[RhCl(PPh_3)L]$ (where L represents the unrearranged mixed anhydride) has been detected as an intermediate during *in situ* NMR studies.[4,8]

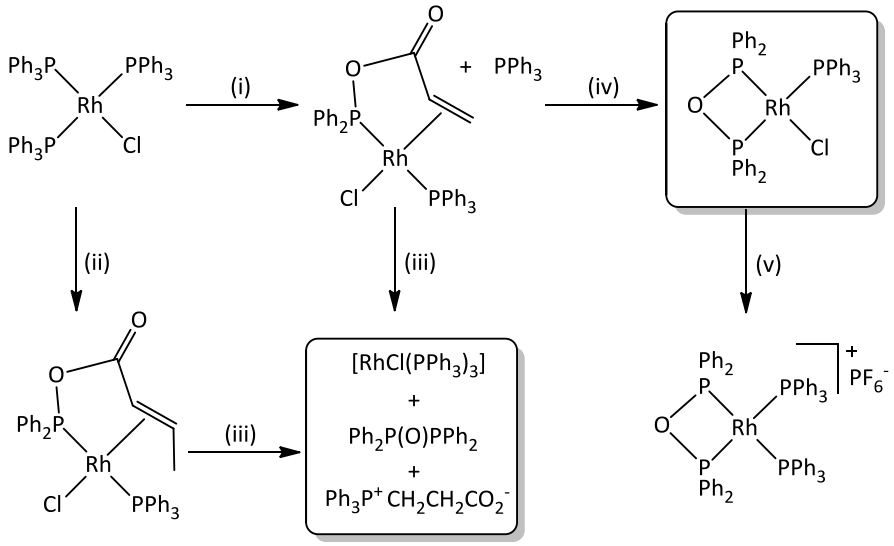


**Scheme 3.2** Reactions of $[RhCl(PPh_3)_3]$ with $Ph_2PO_2CCH{=}CH_2$ (L) or $Ph_2PO_2CCH_2CH{=}CHMe$ (L'). (i) L (1 eq.), 0 °C, thf, 10 min.; (ii) L' (1 eq.), 0 °C, thf, 10 min.; (iii) thf, 0 °C, several hours; (iv) standing in solution for several hours or in the presence of excess ligand; (v) $TlPF_6$, 0 °C, thf, 1 h in the presence of $PPh_3$.

In contrast to the rhodium(I) mixed anhydride complexes, where chelate binding *via* the P- and carbonyl O-atoms are generally only observed for cationic species, the analogous ruthenium(II) complexes display a strong preference for this mode of bonding. Thus, $[RuCl_2(PPh_3)_4]$ reacts with 2 mole equivalents of $Ph_2PO_2CCR{=}CR'R''$ (R = H, R' = R'' = Me or R = Me, R' = H, R'' = Ph) to give $[RuCl_2(Ph_2O_2CCR{=}CR'R'')_2]$ (**Ia–b**) or 1 equivalent of $Ph_2PO_2CCH{=}CMe_2$ to give $[RuCl_2(PPh_3)_2(Ph_2PO_2CCR{=}CR'R'')_2]$ (**II**) [Scheme 3.3 (i)–(ii)], where the mixed anhydride ligands are bound through both the P- and carbonyl O-atom. Similar to their Rh(I) counterparts, Ru(II) complexes of the less substituted mixed anhydrides $Ph_2PO_2CCH{=}CHR$ (R = H or Me), lead to the formation of rearrangement products. When $Ph_2PO_2CCH{=}CH_2$ is reacted with $[RuCl_2(PPh_3)_4]$ in a 2:1 ratio, the rearrangement product $[RuCl_2(PPh_3)(Ph_2POPh_2)$-$(Ph_2PO_2CCH{=}CH_2)]$ (**III**) is obtained, containing a chelating POP ligand [Scheme 3.3 (iii)]. However, when less substituted ligands $Ph_2PO_2CCH{=}CHR$ are reacted in a 1:1 ratio, a different rearrangement occurs with the final product mixture containing, in addition to the desired complexes $[RuCl_2(PPh_3)_2(Ph_2PO_2CCH{=}CHR)]$ (**IVa–b**), the interesting rearrangement product

[RuCl{$(Ph_2PO)_2H$}$(PPh_3)(O_2CCH_2CHRPPh_2)$] (**Va–b**) [Scheme 3.3 (iv)]. Coordination through the double bond can be forced by employing an excess of an unsaturated phosphinite such as $Ph_2POCH_2CH{=}CMe_2$ where bonding through oxygen is not possible. With this approach a six-coordinate complex, $[RuCl_2(PPh_3)_2(Ph_2POCH_2CH{=}CMe_2)]$ (**VI**), is obtained as major product [Scheme 3.3 (v)].[9]

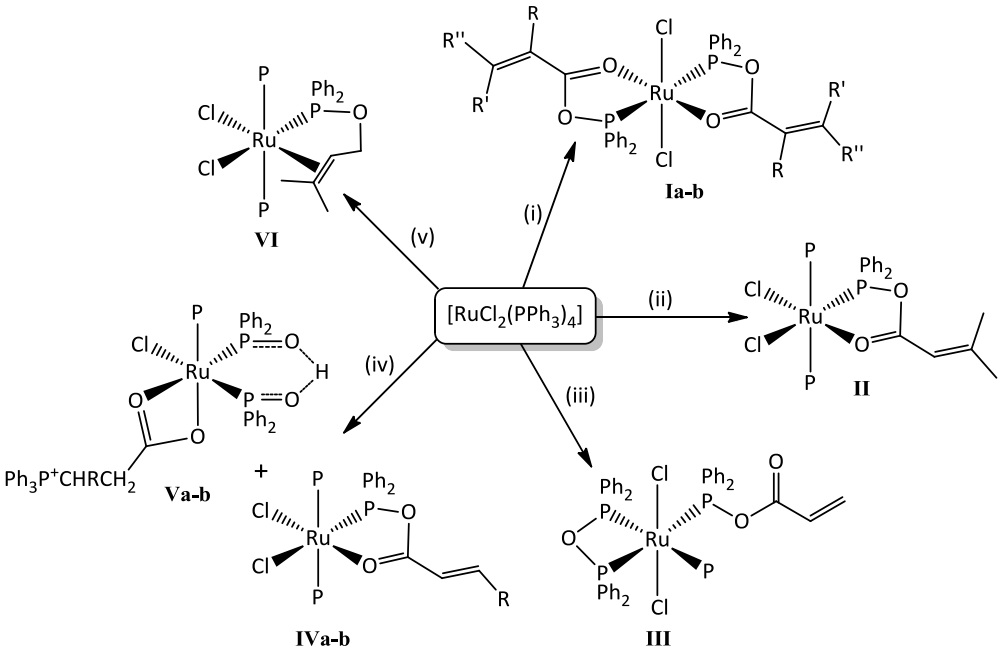


**Scheme 3.3** Reactions of $[RuCl_2(PPh_3)_4]$ with (i) $Ph_2PO_2CCR{=}CR'R''$ where for **a** R = H, R' = R'' = Me and **b** R = Me, R' = H, R'' = Ph (1:2); (ii) $Ph_2PO_2CCH{=}CMe_2$ (1:1); (iii) $Ph_2PO_2CCH{=}CH_2$ (1:2); (iv) $Ph_2PO_2CCH{=}CHR$ where for R = Me or H; (v) $Ph_2POCH_2CH{=}CMe_2$. P = $PPh_3$.

In view of the success of mixed anhydride Rh(I) complexes in hydrogenation catalysis, we aimed to further explore the potential of such complexes as regioselective C–H activation catalysts in this part of the study. During our investigations, however, saturated mixed anhydrides derived from either propanoic or phenylacetic acid (ligands **1** and **7**-**13**, Chapter 2) were employed as ligands with the saturated $sp^3$ $\alpha$-C-H bonds present in the parent carboxylic acids being conceived as targets for catalytic C-H activation. Since linking the substrate to phosphorus has proved highly beneficial in achieving regioselective hydrogenation in dienes, we deemed it possible that such an approach may have the same favourable outcome when employed in systems for catalytic C-H activation. Within these systems, the formation of a highly favoured 5-membered metallocycle would act as the driving force for the selective C–H activation in the $\alpha$-position of the substrates (Scheme 3.4). If successful, this position of the

activated substrates can be functionalised in subsequent steps with formaldehyde to furnish methacrylic acid (MAA). In contrast to the hydrogenation cycle, release of the functionalised product with concomitant introduction of fresh substrate would be facilitated by an acid driven transesterification reaction at phosphorus rather than a base catalysed transesterification. As a chiral centre (*, Scheme 3.4) will be generated during the reductive elimination step, this catalytic cycle would also have scope for asymmetric catalysis.

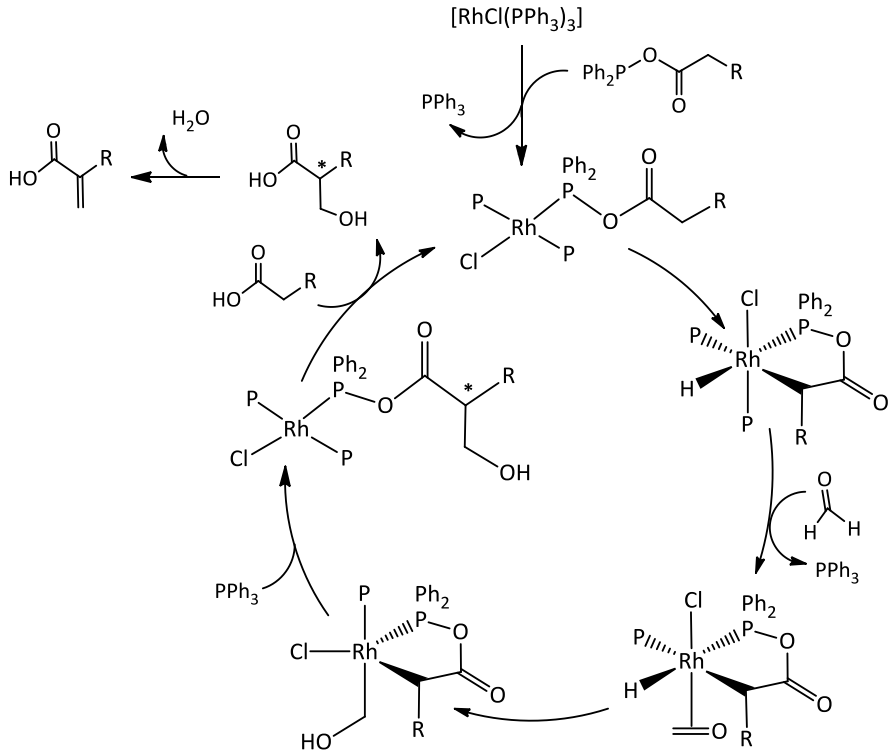


**Scheme 3.4** Proposed catalytic cycle for the functionalisation of saturated carboxylic acid *via* selective catalytic C–H activation in the *α*-position, followed by reaction with formaldehyde, employing Rh(I) mixed anhydride complexes (where R = H or Ph, P = $PPh_3$ and * indicates a chiral centre).

In addition to catalytic investigations, the coordination chemistry associated with Rh(I) and Ru(II) complexes of mixed anhydride ligands **1** and **7–13** is also explored, with special focus placed on their stability in solution, solid state behaviour and various pathways of rearrangement. The nature of these compounds is known to be unpredictable, and knowledge gained from the study reported herein serves as further testimony to this. Relying on standard analytical tools (NMR, IR, ES-MS and single crystal X-ray diffraction), all mixed anhydride complexes under investigation could be characterised to varied degrees (depending on their stability) and are to the best of our knowledge reported here for the first time.

## 3.2 Results and Discussion

All preliminary work was focussed on the coordination of the thermally labile mixed anhydrides, (propionyloxy)diphenylphosphine (**1**) and (phenylacetyloxy)diphenylphosphine (**11**), to Rh(I) (section 3.2.1) and Ru(II) (section 3.2.2) centres. In subsequent work, the coordination of stabilised ligands **7–10** and **12–13** to Rh(I) centres was explored and the outcome of this study is discussed in section 3.2.3. Spectroscopic analysis, and in particular NMR, proved crucial for gaining a better understanding of the pathways of decomposition observed for these compounds as well as the characterisation of reaction intermediates and is discussed in greater detail in section 3.2.3. The crystal and molecular structures for four of the new complexes as well as four of the observed rearrangement products were determined and are reported in section 3.2.4. Lastly, section 3.2.5 is devoted to preliminary assessments of the catalytic potential of selected complexes.

### *3.2.1 Rhodium(I) complexes of (propionyloxy)diphenylphosphine (**1**)*

#### ***3.2.1.1 Metal promoted rearrangements of propionyloxydiphenylphosphine***

Although earlier studies with mixed anhydrides derived from acrylic acid and vinylacetic acid have indicated metal complexes of sterically undemanding mixed anhydrides to be prone to rearrangement,[8,9] the simple mixed anhydrides **1** and **11** were still considered as ligands in Rh(I) precatalyst complexes. Given that electron richness is an overriding criterion for the success of a C–H activation catalyst, the more basic acyloxyphosphine ligands **1** and **11** were considered as better suited for this purpose compared to their less basic acylphosphite equivalents (**7–10** and **11–13**). Thus **1** was reacted in a 1:1 ratio with a solution of $[RhCl(PPh_3)_3]$ in thf at -10 $^oC$ for 80 min. This afforded an orange solid upon work-up. Not surprisingly, NMR analysis of this solid indicated, in addition to Wilkinson's catalyst, the presence of a significant amount of the rearrangement product $[RhCl(PPh_3)(Ph_2POPPh_2)]$ (**14**), while none of the unrearranged complex, $[RhCl(PPh_3)_2(Ph_2POC(O)CH_2CH_3)]$ (**15**), could be observed [Scheme 3.5 (i)]. As mentioned in the introductory section, this compound also represented the major by-product in reactions involving $[RhCl(PPh_3)_3]$ and mixed anhydrides of vinylacetic or acrylic acid. Moreover, the formation thereof was suggested to be metal promoted with disruption of the ligand succeeding coordination to the metal centre.[4,8] Considering that rearrangements of this kind might be time dependent, the reaction was repeated, reducing the reaction time to 40

min, while preserving all other reaction conditions. This unfortunately did not result in a more favourable outcome with recorded NMR spectra comparable to those previously obtained. As the nature of the solvent system may play a determining role in the rate of the observed side reactions, the procedure was repeated using dichloromethane as solvent instead of thf. Work-up of the reaction after 30 min at -10 $^{o}$C furnished an orange solid, which in appearance closely resembled those obtained during previous attempts. However, $^{31}P\{^{1}H\}$ NMR analysis of this solid revealed the presence of resonances attributable to a new species which, even though only present in minor amounts, corresponded well with those expected for the desired complex *trans*-[RhCl($PPh_3$)$_2${$Ph_2POC(O)CH_2CH_3$}] (**15**) [Scheme 3.5 (iii)].

Reacting [RhCl($PPh_3$)$_3$] with an excess of **1** (in either a 1:2 or 1:6 mole ratio) led to the isolation of a mixture that comprised of an array of rearrangement products. Species detected in the $^{31}P\{1H\}$ NMR spectra included a considerable amount of the free ligand disproportionation product, $Ph_2PP(O)Ph_2$, together with [RhCl($PPh_3$)($Ph_2POPPh_2$)] (**14**). Furthermore, strong evidence for the presence of an additional new complex [RhCl{$Ph_2POC(O)CH_2CH_3$}-($Ph_2POPPh_2$)] (**16**), bearing intact **1**, was also obtained [ratio of 14 : 16 – 1 : 1.4 Scheme 3.5 (iv)].

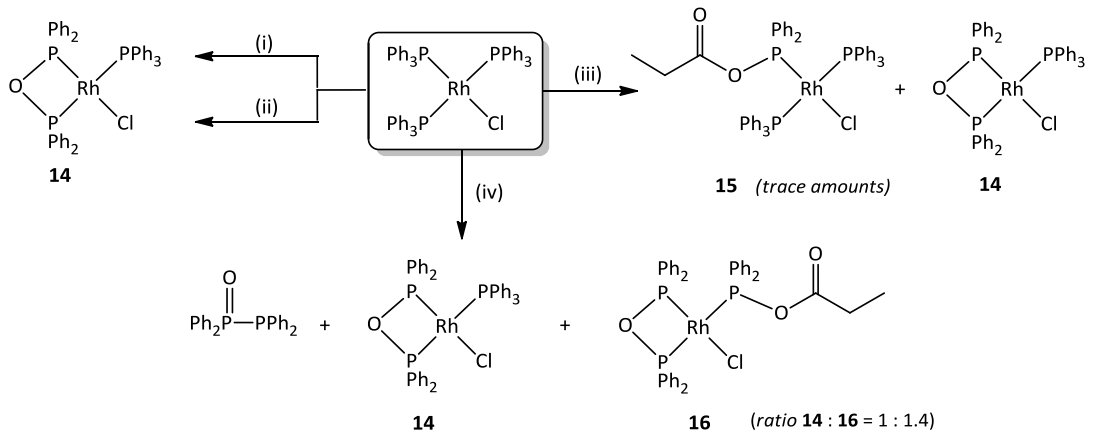


**Scheme 3.5** Reaction conditions: (i) **1** (1:1 ratio), thf, -10 $^{o}$C, 80 min.; (ii) **1** (1:1 ratio), thf, -10 $^{o}$C, 40 min.; (iii) **1** (1:1 ratio), $CH_2Cl_2$, -10 $^{o}$C, 30 min.; (iv) **1** in excess (1:2 or 1:6 mole ratio), $CH_2Cl_2$, -10 $^{o}$C, 1 h.

In order to determine whether [RhCl($PPh_3$)$_2${$Ph_2OC(O)CH_2CH_3$}] (**15**) perhaps forms as the major product during the early stages of the reaction and then rapidly decays to form a mixture of [RhCl($PPh_3$)$_3$] and [RhCl($PPh_3$)($Ph_2POPPh_2$)], some low temperature *in-situ* NMR studies were carried out. A solution of **1** in deuterated chloroform was added immediately after dissolution

to neat [$RhCl(PPh_3)_3$] at -30 °C. Without delay, a small volume of the resulting solution was transferred to an NMR tube and subjected to low temperature (-10 °C) $^{31}P\{^1H\}$ NMR analysis at regular intervals (approximately every 5 minutes for 50 minutes). Although the recorded spectra were very different to those recorded for earlier attempts, surprisingly little variation was observed between different spectra within the recorded series. Despite the presence of $Ph_2PP(O)Ph_2$, significant amounts of the desired *trans*-[$RhCl(PPh_3)_2\{PPh_2OC(O)CH_2CH_3\}$] (**15a**), together with the related *cis*-isomer (**15b**), were also observed. In addition, a set of resonances corresponding to yet another new species could be tentatively assigned to the ionic complex, [$Rh(PPh_3)_2(Ph_2POPPh_2)$][X], (**17**) where $X^-$ represents an unknown anion, most likely chloride. Although more substantial proof is required to verify this speculation, the measured data is in very good agreement with literature values reported for the related complex [$Rh(PPh_3)_2(Ph_2POPPh_2)$][$PF_6$] [Scheme 3.6 (i)].[8]

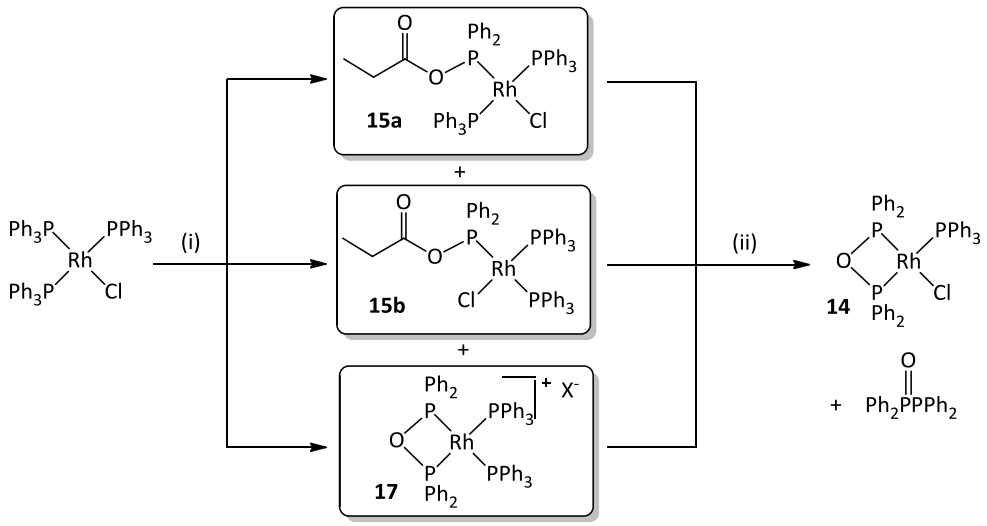


**Scheme 3.6** Species observed in the $^{31}P\{^1H\}$ NMR spectra recorded (i) during *in situ* NMR experiments, **1** (1:1.2 mole ratio),$CDCl_3$, -10 °C; (ii) for a sample taken from the same solution after a 2 h standing interval at -10 °C.

In view of the fact that no major product decay was observed during the execution of the *in situ* NMR experiment, the original reaction mixture was allowed to stand for a further 70 min at -10 °C, whereafter the solution was again analysed by means of $^{31}P$ NMR spectroscopy. The spectrum obtained for this sample differed significantly from spectra recorded during the *in situ* experiment, with both isomers of **15** as well as compound **17** completely absent, while new signals present could be assigned to the familiar rearrangement product

[$RhCl(PPh_3)(Ph_2POPPh_2)$] (**14**) [Scheme 3.6 (ii)]. The absence of any product decay during the measurement period suggests that such rearrangements may be heavily dependent on reaction times, concentrations and temperatures. Moreover, the detection of **15a** and **15b** as intermediates prior to the formation of **14** supports the notion that this rearrangement is metal promoted and not the result of a direct reaction between $Ph_2PP(O)Ph_2$ and [$RhCl(PPh_3)_3$].

### *3.2.1.2 Preparation of (propionyloxy)diphenylphosphine (1) on the metal centre*

Bedford and co-workers[13] have recently reported an elegant route towards the preparation of rhodium-chlorophosphine pre-catalysts for the *ortho*-arylation of phenols. These chloro-phosphine adducts could be converted *in situ* into catalytic systems containing phosphinite ligands (Scheme 3.7).

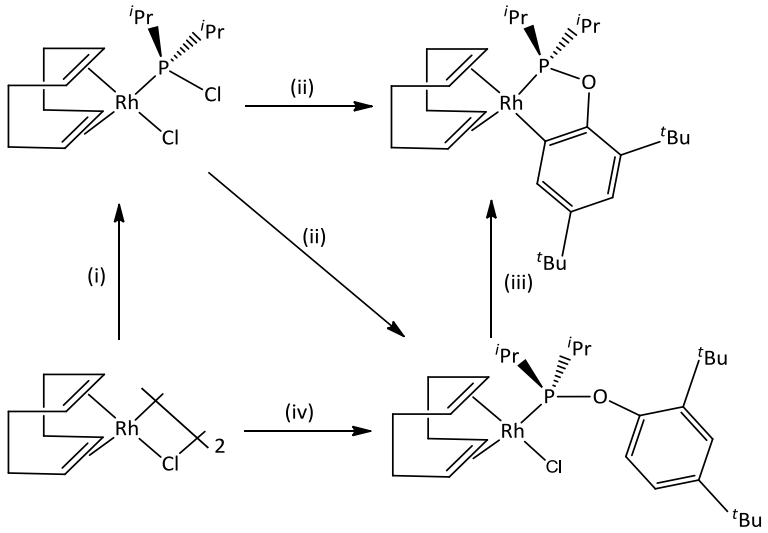


**Scheme 3.7** *In situ* preparation of rhodium phosphinite systems. Conditions: (i) $^{i}Pr_2PCl$, $CH_2Cl_2$, rt, 2 h; (ii) $HOC_6H_3$-2,4-$^{t}Bu_2$, $NaO^{t}Bu$, toluene, 80 °C, 1 h; (iii) $NaO^{t}Bu$, toluene, 80 °C, 1 h; (iv) $^{i}Pr_2P(OC_6H_3$-2,4-$^{t}Bu_2)$, $CH_2Cl_2$, rt, 1 h.[13]

In the present study, this methodology was utilised in the exploration of more attractive routes to the preparation of complex **15**. This strategy seemed like a promising alternative to earlier methods, since formation of the ligand directly on the rhodium centre would prevent the formation of unwanted disproportionation products often associated with the free ligand in solution. Moreover, this method would also provide an additional means of testing whether

formation of [RhCl(PPh$_3$)(Ph$_2$POPPh$_2$)] (**14**) indeed takes place *via* a metal mediated mechanism, as was previously proposed by Irvine and co-workers.[4,8] The precursor complex, [RhCl(PPh$_3$)$_2$(Ph$_2$PCl)] (**18**), was therefore successfully prepared and isolated using a similar methodology to that described by Bedford and co-workers[13] for the synthesis of [RhCl(COD)($^i$Pr$_2$PCl)]. Due to the thermal lability of **1**, elevated temperatures were avoided in all preliminary experiments aimed at converting complex **18** into [RhCl(PPh$_3$)$_2$(Ph$_2$POC(O)CH$_2$CH$_3$)] (**15**). Thus a solution of **18** in dichloromethane was cooled to –10 $^o$C and treated with propanoic acid and triethylamine (Scheme 3.8). NMR analysis of the crude orange product obtained upon work-up, however, failed to deliver any recognisable products other than large amounts of triphenylphosphine oxide. To ensure that product oxidation did not occur as a result of experimental error, the reaction was repeated following the same reaction and work-up protocol. However, despite meticulous maintenance of an inert atmosphere throughout the procedure, the isolated product mixture again contained significant amounts of P(O)Ph$_3$. Another attempt performed at room temperature also had the same unfavourable outcome. The reaction was subsequently also carried out using the same reaction conditions reported for the literature example. Treatment of complex **18** with propanoic acid and NaO$^t$Bu in toluene at 80 $^o$C, however, still did not lead to the formation of **15** with recorded NMR spectra comparable to those of earlier attempts.

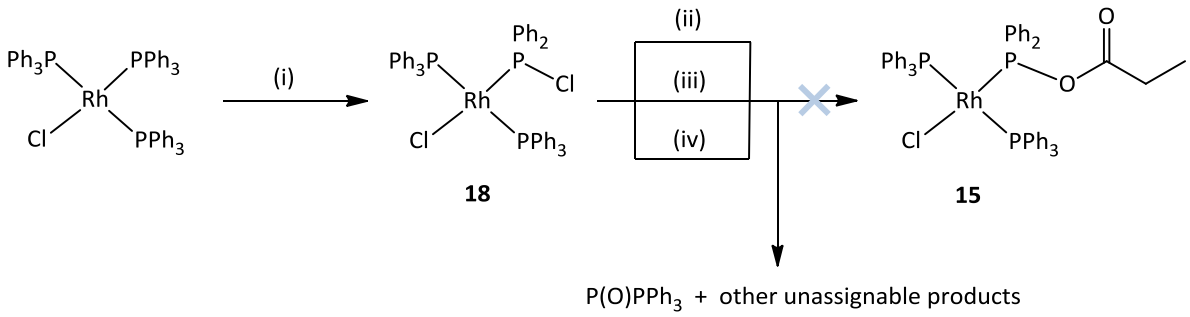


**Scheme 3.8** Attempts to prepare **1** onto a Rh(I) centre: (i) Ph$_2$PCl, CH$_2$Cl$_2$, R.T., 2 h; (ii) NaO$_2$CCH$_2$CH$_3$, CH$_2$Cl$_2$, -10 $^o$C; (iii) NaO$_2$CCH$_2$CH$_3$, CH$_2$Cl$_2$, R.T.; (iv) HO$_2$CCH$_2$CH$_3$, NaO$^t$Bu, toluene, 80 $^o$C, 1 h.

### *3.2.1.3 Rhodium(I) complexes of 1 devoid of any phosphine auxillary ligands*

In light of the difficulties experienced with the metal promoted rearrangement of **1**, the possibility that the presence of PPh$_3$ may facilitate such rearrangements was considered.

Attention was therefore directed towards the use of Rh(I) precursors devoid of any $PPh_3$ ligands. Consequently, the chloro-bridged rhodium dimer $[\{RhCl(COE)_2\}_2]$ (where COE = cyclooctene) was chosen as precursor, since this complex had proved highly successful in the preparation of Rh(I) complexes of higher substituted mixed anhydrides.[3] Treatment of a solution of $[\{RhCl(COE)_2\}_2]$ in dichloromethane at -10 $^oC$ with four equivalents of **1** for 30 min [Scheme 3.9] did indeed result in a slightly more favourable outcome with the final product mixture, after work-up, containing small amounts (~ 7 %) of the desired unrearranged dimer $[\{RhCl(Ph_2PO_2CCH_2CH_3)_2\}_2]$ (**19**). This was a significant improvement on earlier attempts, since the $PPh_3$ Rh(I) complex **15** could not be isolated and was only observed *in situ*. Furthermore, analysis of the product mixture also produced evidence for the presence of significant (~ 71 %) amounts a monomeric complex, $[RhCl(Ph_2PO_2CCH_2CH_3)_2]$ (**20**), where one of the (propionyloxy)diphenylphosphine (**1**) ligands was coordinated in a chelating fashion *via* both the phosphorus atom and the carbonyl oxygen, while the second was only coordinated *via* phosphorus. As mentioned before, this mode of bonding, although not favoured in the presence of superior donors, is not uncommon for such complexes and has been reported for the cationic complex $[Rh(PPh_3)_2(Ph_2PO_2CCH{=}CMe_2)][SbF_6]$.

Despite the apparent greater stability of these complexes in the absence of $PPh_3$, complexes **19** and **20** still underwent rearrangement in solution to afford the POP dimer $[\{RhCl(Ph_2POPh_2)\}_2]$ (**21,** ~11 %) and more interestingly, the diphenylphosphinito dimer $[\{RhCl\{(Ph_2PO)_2H\}(C(O)CH_2CH_3)\}_2]$ (**22**, ~11 %) containing propionyl moieties directly coordinated to the Rh(III) centres [Scheme 3.9].

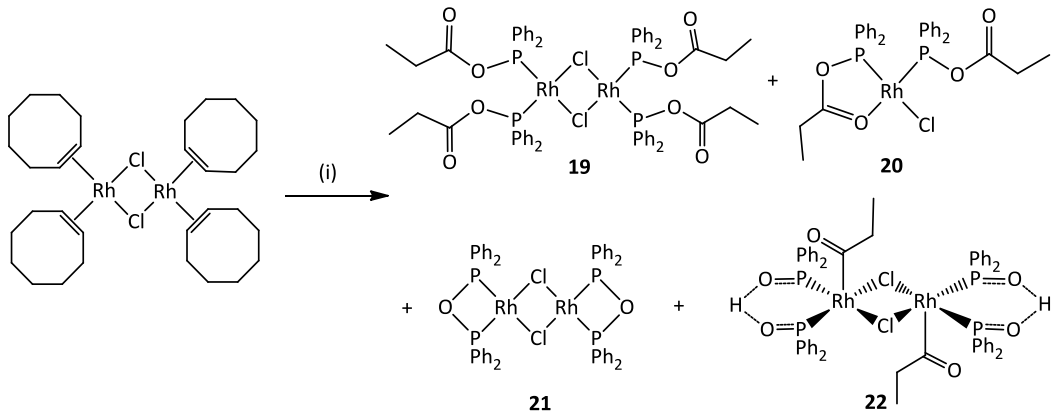


**Scheme 3.9** Product mixture obtained for reactions of $[\{RhCl(COE)_2\}_2]$ with **1**. Conditions: (i) **1** (4 mole equivalents), $CH_2Cl_2$, -10 $^oC$, 30 min.

Although **21** could only be assigned tentatively, the identity of **22** could be verified by X-ray structure determinations performed on crystals of **22** isolated from a chloroform solution of **19**. Numerous reports on transition metal complexes containing hydrogen bonded [{$Ph_2PO$}$_2$H] ligands, similar to **22**, exist in the literature with several routes to their preparation described.[14-18] In the majority of cases, however, complexes have been prepared either by the reaction of metal complex precursors with diphenylphosphinous acid or by the hydrolysis of metal complexes of chlorodiphenylphosphine or diphenylphosphinite. More recently, Irvine[19] has also showed that the related complex [$RuCl_2(Ph_2POPPh_2)(Ph_2POH)_2$] can be prepared by refluxing [$RuCl_2(PPh_3)_4$] in thf with 1 mole equivalent of $Ph_2PP(O)Ph_2$.

Although no formal mechanistic studies have been performed, Scheme 3.10 represents a plausible mechanism for the rearrangement of **19** to **21** in the absence of water or alcohol, and to **22** in the presence of water or alcohol. It is noteworthy that, even though all reactions were performed under dry and inert conditions, a water / 2-propanol mixture was used as reaction solvent during the preparation of the [{$RhCl(COE)_2$}$_2$] precursor and that the latter may therefore be the source of such trace contaminants. In both mechanisms, the initial step involves nucleophilic attack of a neighbouring Rh(I) centre on the electrophilic carbonyl carbon of ligand **1**.

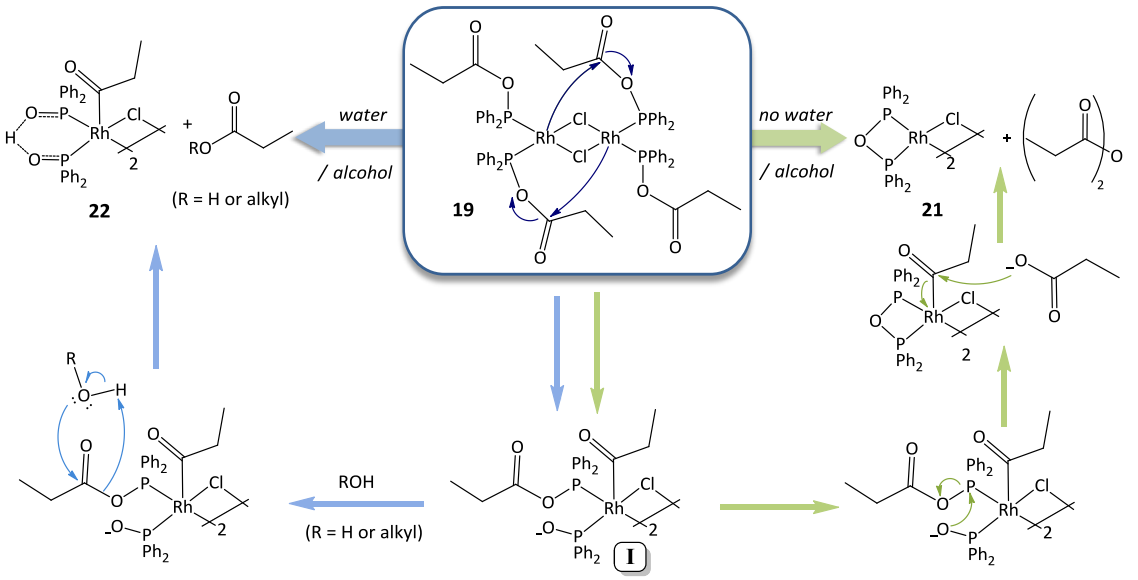


**Scheme 3.10** Proposed mechanism for the formation of rearrangement product **21** in the absence of water or alcohol ( ■ mechanism) and **22** in the presence of water or alcohol ( ■ mechanism).

This results in a dimeric Rh(III) intermediate (**I**) containing, in addition to two diphenylphosphinito ligands, two propionyl groups directly coordinated to the Rh(III) centres. Intermediate **I** can then participate in further reactions, with the particular route of rearrangement dependent on the availability of water or alcohol. In the presence of water or alcohol, **I** undergoes hydrolysis or alcoholysis to form the observed dimer **22**. However, in the absence of water or alcohol this route is inaccessible and the diphenylphosphinito ligands present in **I** proceed with an intramolecular nucleophilic attack on the carbonyl carbons of the two remaining (propionyloxy)diphenylphosphino ligands instead. This gives rise to the observed chelating POP ligands together with the liberation of propanoate species which, in the final step, aids in the reductive elimination of the coordinated propionyl groups to form the POP dimer **21** together with propanoic anhydride.

#### *3.2.1.4 Spectroscopic characterisation of Rh(I) complexes 14–22*

All species observed in reactions involving **1** could be identified with the aid of $^{31}P\{^{1}H\}$ NMR spectroscopy. Data collected for compounds **14–22** are summarised in Table 3.1, with any additional data listed under the experimental section. In all cases where [RhCl($PPh_3$)($Ph_2POPPh_2$)] (**14**) is formed as the product of rearrangement, three sets of doublet of doublet of doublets at $\delta$ 106.1, $\delta$ 80.9 and $\delta$ 24.7, respectively, are observed in measured $^{31}P\{^{1}H\}$ NMR spectra. This spectral profile is in very good agreement with the literature values reported for **14**.[8]

Resonance signals at $\delta$ 121.3 (dt), $\delta$ 107.6 (ddd) and $\delta$ 82.8 (dt) could be assigned tentatively to [RhCl($Ph_2PO_2CCH_2CH_3$)($Ph_2POPPh_2$)], (**16**), in which the $PPh_3$ ligand present in **14** has been replaced by ligand **1**. Figure 3.1 depicts the $^{31}P\{^{1}H\}$ NMR spectral profile of this compound, where resonances corresponding to the chelated POP ligand are overlapped with those of the rearrangement product, [RhCl($PPh_3$)($Ph_2POPPh_2$)] (**14**). A doublet of triplets rather than a doublet of doublets of doublets is observed at $\delta$ 82.8 for $P_B$ and has been ascribed to equal coupling of $P_B$ to both rhodium and $P_C$ (see Table 3.1 for symbol assignments). Furthermore, resonances associated with $P_B$ and $P_C$ are shifted slightly downfield with respect to those of complex **14** ($\Delta\delta$ 1.9 and 1.5 for $P_B$ and $P_C$ respectively) and enhanced coupling between the mutually *trans* phosphorus atoms $P_A$ and $P_B$ ($\Delta J_{PA\text{-}PB}$ = 70 Hz) is observed.

**Table 3.1** $^{31}P\{^{1}H\}$ NMR spectral data for rhodium complexes **14–22**.

| | | Chemical shifts δ (ppm)† | | | Coupling constants *J* (Hz) | | | | | |
|---|---|---|---|---|---|---|---|---|---|---|
| **Compound*** | | **$P_A$** | **$P_B$** | **$P_C$** | **Rh-$P_A$** | **Rh-$P_B$** | **Rh-$P_C$** | **$P_A$-$P_B$** | **$P_A$-$P_C$** | **$P_B$-$P_C$** |
| **14** | $[RhCl(P_APh_3)(Ph_2P_BOP_CPh_2)]$ | 24.7 (ddd) | 80.9 (ddd) | 106.1 (ddd) | 132.2 | 127.0 | 167.8 | 380.9 | 121.8 | 29.7 |
| **15a** | *trans*-$[RhCl(P_APh_3)_2\{Ph_2P_COC(O)CH_2CH_3\}]$ | 32.6 (dd) | — | 138.2 (dt) | 128.7 | — | 213.4 | — | 37.5 | — |
| **15b** | *cis*-$[RhCl(P_{A\backslash B}Ph_3)_2\{Ph_2P_COC(O)CH_2CH_3\}]$ | 31.1 (ddd) | § | 129.7 (ddd) | 133.2 | § | 175.9 | 40.9 | 383.6 | 17.3 |
| **16** | $[RhCl(Ph_2P_BOP_CPh_2)\{Ph_2P_AOC(O)CH_2CH_3\}]$ | 121.3 (ddd) | 82.8 (dt) | 107.6 (ddd) | 158.9 | 124.7 | 163.3 | 450.0 | 28.9 | 124.7 |
| **17** | $[RhCl(P_{A\backslash B}Ph_3)_2(Ph_2P_COP_DPh_2)][X]$ ($X^-$ unknown) | Accurate values can only be determined by simulation, see literature example for accurate assignments.[8] | | | | | | | | |
| **18** | $[RhCl(P_APh_3)_2(Ph_2P_BCl)]$ | 32.4 (dd) | 113.7 (dt) | — | 138.0 | 230.1 | — | 40.1 | — | — |
| **19** | $[\{RhCl(Ph_2P_AOC(O)CH_2CH_3)\}_2]$ (dimer) | 135.1 | — | — | 228.1 | — | — | — | — | — |
| **20** | $[RhCl(Ph_2P_{A\backslash B}OC(O)CH_2CH_3)_2]$ (O coordinated)‡ | 139.5 (bm) | 177.5 (bm) | — | Fluxional – not determined owing to substantial line broadening. | | | | | |
| **21** | $[\{RhCl(Ph_2P_AOP_APh_2)\}_2]$ | 87.1 (d) | — | — | 161.3 | — | — | — | — | — |
| **22** | $[\{RhCl\{(Ph_2P_AO)_2H\}(C(O)CH_2CH_3)\}_2]$ | 83.7 (d) | — | — | 160.5 | — | — | — | — | — |

* Note: Identical labels given to different phosphorus atoms present within the same complex indicate magnetic equivalence.
† Chemical shifts relative to 85 % $H_3PO_4$ ($CD_2Cl_2$, 25 °C) with mulitiplicity given in parenthesis.
§ Could not be measured owing to extensive overlap of resonances in the relevant region.
‡ Significant line broadening observed as a result of an unresolved dynamic process.

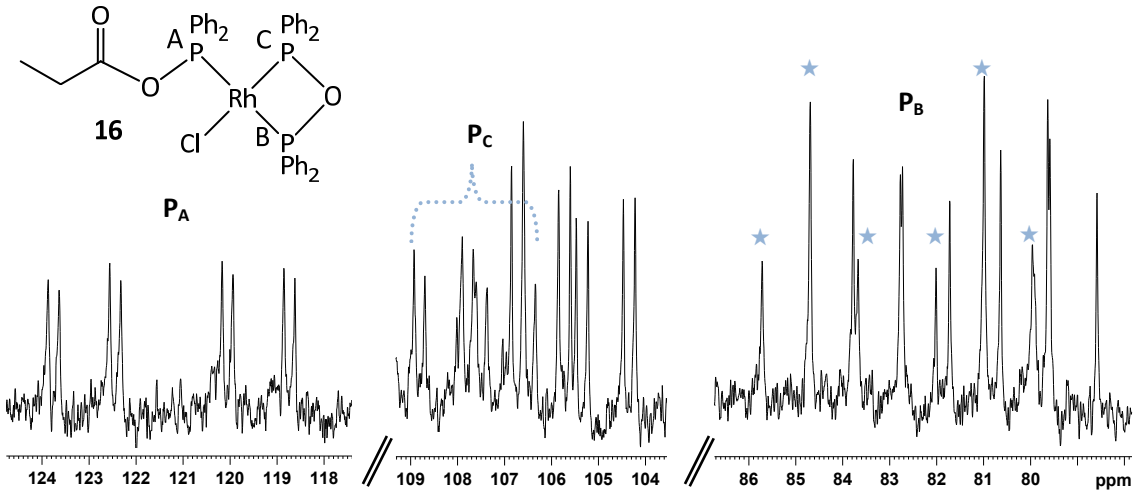


**Figure 3.1** Resonance signals detected in the $^{31}P$ NMR attributable to complex **16**. Resonances corresponding to $P^B$ and $P^C$ overlap with the corresponding resonances of complex **14** and are therefore indicated by ····· and ★.

In the desired *trans*-[$RhCl(PPh_3)_2(Ph_2PO_2CCH_2CH_3)$] (**15a**) complex, coordinated **1** gives rise to a doublet of triplets at δ 138.2 ($J_{P\text{-}Rh}$ = 213.4 Hz and $J_{P\text{-}P}$ = 37.5 Hz), consistent with coordination only through phosphorus [Figure 3.2 (a)] , while the magnetically equivalent $PPh_3$ ligands give rise to a doublet of doublets at δ 32.6 (Figure 3.3). These values are comparable to values reported for the related complex [$RhCl(PPh_3)_2(PO_2CCH_2CH_2CH_3)$] [δ 131.0 (dt) and δ 33.0 (dd)].[7] In the *cis*-isomer **15b**, coordinated **1** gives rise to a doublet of doublets of doublets at δ 129.7 ($J_{P\text{-}Rh}$ = 175.9 Hz, $J_{P\text{-}Ptrans}$ = 383.6 Hz and $J_{P\text{-}Pcis}$ = 40.9 Hz), slightly upfield from the corresponding signals of **15a** [Figure 3.2 (b)]. Owing to the presence of several $PPh_3$ containing products within the same $^{31}P\{^1H\}$ NMR spectrum, extensive overlap of resonances within the region δ 24–δ 35 is observed. As a result, resonances corresponding to the $PPh_3$ *cis* to ligand **1** in **15b** could not be assigned unambiguously.

For the same reason discussed above, the $PPh_3$ resonances of [$Rh(PPh_3)_2(Ph_2POPPh_2)$][X] (**17**) could also not be assigned without some degree of uncertainty. The chemically equivalent, but magnetically inequivalent phosphorus atoms the POP and $PPh_3$ ligands present in [$Rh(PPh_3)_2(Ph_2POPPh_2)$][X] (**17**), represent an AA'XX' spin system giving rise to second-order spectral effects. Complex resonances at δ 98.0 [Figure 3.2 (c)] could be assigned to phosphorus atoms present in the POP ligand while signals at δ 26.4 corresponds to the $PPh_3$ ligands (Figure 3.3). Unfortunately, the signal to noise ratios in all spectra recorded during "*in situ*" NMR experiments were too low to allow for a better interpretation of these signals. However, as

mentioned before, the same cation has been reported for the analogous compound $[Rh(PPh_3)_2(Ph_2POPPh_2)][PF_6]$ and has very similar spectral parameters.[8]

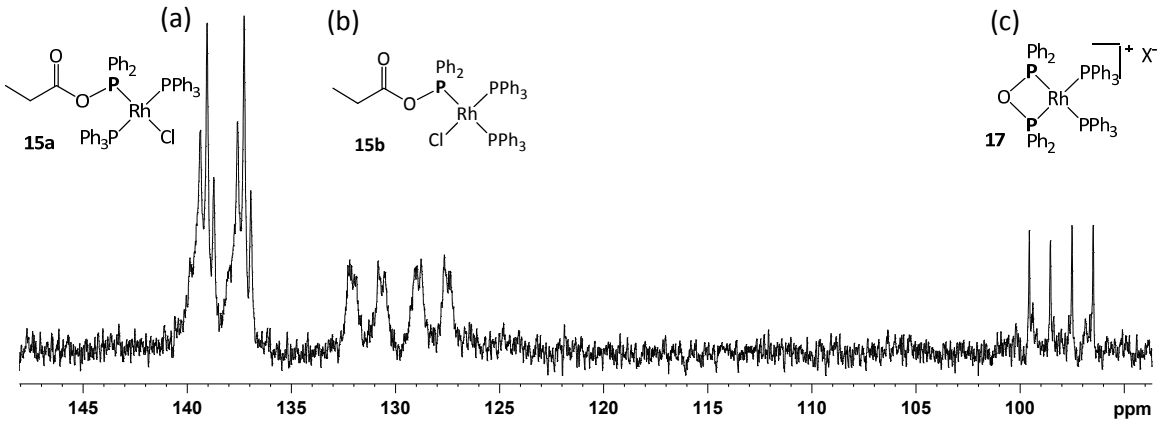


**Figure 3.2** $^{31}P$ NMR resonance signals attributable to $P_C$ (in bold) in complex: (a) **15a**; (b) **15b** and (c) **17**.

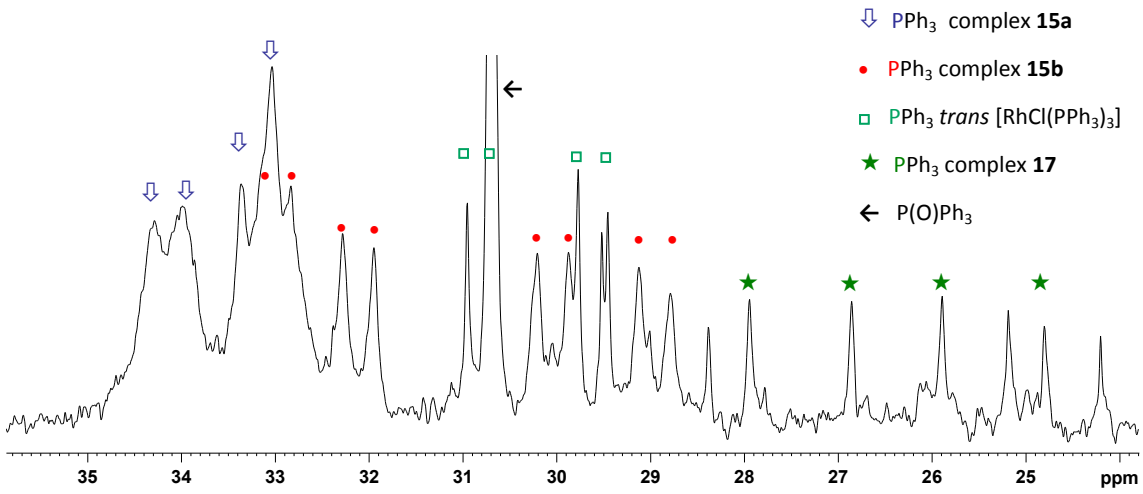


**Figure 3.3** Region in the $^{31}P$ NMR spectrum, recorded during the *in situ* experiment, displaying the overlapping $PPh_3$ resonance signals of unreacted $[RhCl(PPh_3)_3]$, **15a**, **15b** and **17**.

Figure 3.4 depicts the $^{31}P\{^1H\}$ NMR spectrum recorded for the product mixture obtained from the reaction of $[\{RhCl(COE)_2\}_2]$ with **1**. Doublets at δ 135.1 and δ 87.1 could be assigned tentatively to compounds **19** and **21**, respectively, while compound **22** gives rise to a doublet at δ 83.7. The assignment of the latter could also be verified by NMR analysis of an analytically pure crystalline sample of **22** together with X-ray structure determination. The unambiguous

assignment of **20**, as well as the determination of the relevant $J_{Rh-P}$ and $J_{P-P}$ values, was complicated by substantial line broadening as a consequence of an unresolved dynamic process involving the free and coordinated carbonyl oxygens of ligands **1**. However, the high field chemical shift of the broad multiplet observed at δ 177.5 is consistent with the incorporation of **1** in a five membered metallocycle by bonding through both phosphorus and oxygen.[20] Likewise, the chemical shift observed for the broad multiplet at δ 139.5 is consistent with coordination of **1** to a Rh(I) only *via* phosphorus.

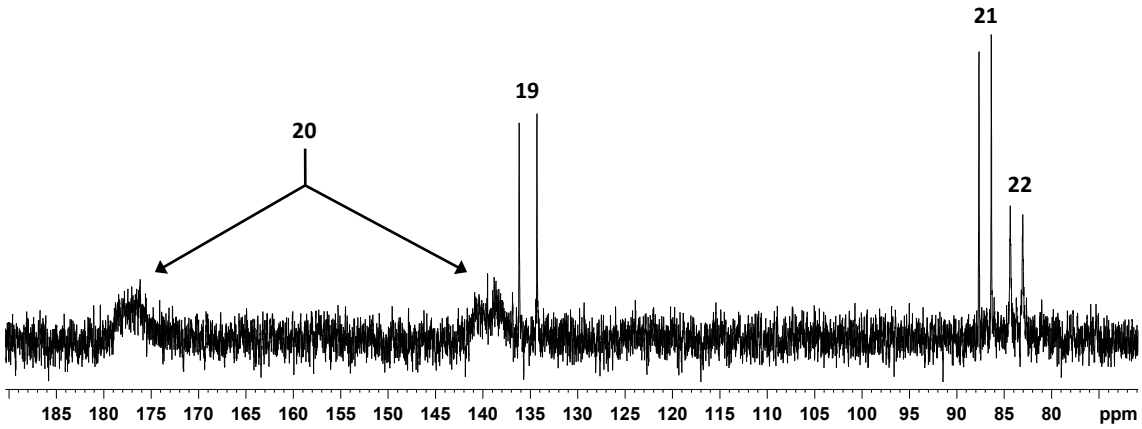


**Figure 3.4** $^{31}P\{^{1}H\}$ NMR spectrum recorded for the product mixture obtained for the reaction of $[\{RhCl(COE)_2\}_2]$ with **1** showing resonance signals assigned to complexes **19–22**.

## *3.2.2 Ruthenium(II) complexes of (propionyloxy)diphenylphosphine*

### *3.2.2.1 Preparation, in solution behaviour and spectroscopic characterisation*

Reactions of either $[RuCl_2(PPh_3)_3]$ or $[RuCl_2(PPh_3)_4]$ with **1** in a 1:2 ratio resulted in bright orange solids which analysed as $[RuCl_2(PPh_2O_2CCH_2CH_3)_2]$ (**23**), in which **1** is coordinated in a chelating fashion *via* both the phosphorus and carbonyl oxygen atoms (Scheme 3.11). As mentioned before, this has been shown to represent the preferential mode of bonding for mixed anhydride Ru(II) complexes of the general form $[RuCl_2(Ph_2PO_2CCH{=}RR')_2]$.[9] In contrast to the mentioned literature examples where phosphorus atoms are in positions mutually *trans*, spectroscopic evidence suggest the phosphorus atoms in **23** to occupy positions *cis* with respect to one another. X-ray structure determination of crystals obtained for **23** confirmed this suggestion, although it is noted that single crystals may not always be representative of the bulk.

In contrast to the Rh(I) complexes of **1**, compound **23** could be obtained in high purity and yield without the interference of unwanted side-reactions. Furthermore, **23** could also be stored in the solid state for prolonged periods of time, provided that an inert atmosphere is maintained. The greater stability of **23** compared to the Rh(I) analogues comes as no surprise, since one can expect the relatively more electron poor Ru(II) centre to be less likely to participate in any rearrangements that necessitate oxidation of the metal centre or nucleophilic attack on the carbonyl carbon of **1** by the metal as part of their mechanism.

Despite the enhanced stability, **23** does rearrange within hours when left standing in solution to afford the chloro-bridged Ru(II) dimer **24**, where one of the two mixed anhydrides per Ru(II) centre have been converted to diphenylphosphinous acid (Scheme 3.11). During all initial attempts to crystallise **23** by slow diffusion of pentane into dichloromethane or chloroform solutions of **23**, orange prisms of **24** crystallised from solution allowing for structure determination by X-ray crystallography (discussed in Section 3.2.4).

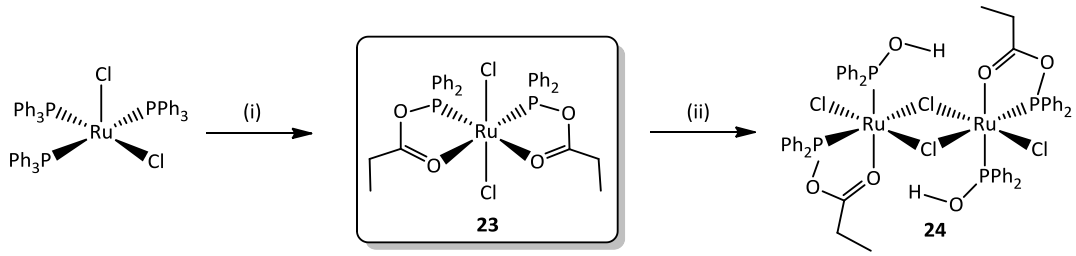


**Scheme 3.11** Preparation of **23** and subsequent rearrangement thereof to form **24**. Conditions: (i) **1** (2 mole equivalents), $CH_2Cl_2$, R.T., 2 h; (ii) standing in solution overnight.

In the $^{31}P\{^{1}H\}$ NMR spectrum of **23** the magnetically equivalent phosphorus atoms give rise to a sharp singlet at δ 188.6, very high field in comparison to the values observed for coordinated but unchelated **1** in the discussed Rh(I) complexes [Figure 3.5 (a)]. This serves as further confirmation for binding through both phosphorus and the carbonyl oxygen, since the resultant five membered metallocycle would lead to high field shift in the phosphorus resonances. Furthermore, in the IR-spectrum of **23** the C=O bonds vibrate at a much lower frequency [single band at 1649 $cm^{-1}$ $\nu$(C=O)], than typically observed for such bonds [~1700 $cm^{-1}$],[6,21] consistent with reduced double bond character as a result of coordination to a metal centre. Although no significant change in the chemical shift of resonances attributable to **1** is

observed in the $^{31}P\{^{1}H\}$ NMR spectrum of **24**, relative to that of **23**, P-P coupling to coordinated $Ph_2POH$ results in the detection of this signal as a doublet at 188.3 ppm. Similarly, the $Ph_2POH$ ligands give rise to a doublet at $\delta$ 132.5 with a mutual coupling constant of 44.2 Hz [Figure 3.5 (b)].

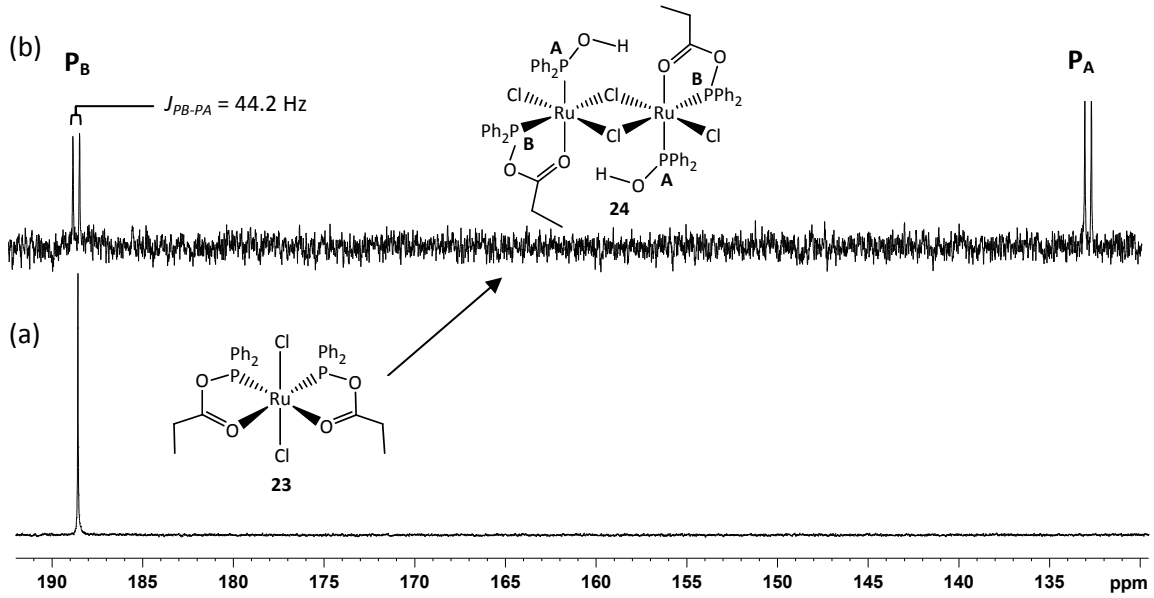


**Figure 3.5** $^{31}P\{^{1}H\}$ NMR spectra recorded for (a) **23** before rearrangement and (b) the rearranged product **24** that crystallised from a chloroform solution of **23** after standing overnight.

## *3.2.3 Rhodium(I) complexes with stabilised (acyl)phosphite ligands*

### *3.2.3.1 Their preparation and metal promoted rearrangement*

As discussed in Chapter 2, mixed anhydrides derived from propanoic acid, sodium propanoate or phenylacetic acid could be stabilised by changing from chlorodiphenylphosphine as precursor to chlorophosphites. By this approach, a series of (acyl)phosphites could be prepared that can be divided into two categories, namely (i) those devoid of any sterically demanding groups in the vicinity of phosphorus (ligands **7** and **8**) and (ii) those bearing nearby *tert*-butyl groups which shelter the phosphorus from neighbouring molecules (ligands **9**, **10**, **12** and **13**); with ligands belonging to the second category superior in terms of stability. In reactions of the first type with $[RhCl(PPh_3)_3]$, the desired *trans*-$[RhCl(PPh_3)_2(L)]$ complexes **25** (L = **7**) and **27** (L = **8**) were obtained as the major products. However, similar to Rh(I) complexes

of **1**, complexes **25** and **27** were prone to rearrangement and as a result product mixtures were heavily contaminated with the POP containing rearrangement products **26** and **28** (Scheme 3.12). In contrast to the previously observed complex [RhCl($PPh_3$)($Ph_2POPPh_2$)] (**14**), the POP ligands in complexes **26** and **28** are coordinated in a bridging rather than chelating manner between two neighbouring Rh(I) centres. The more rigid bond angles of the phosphorus atoms, which are already constrained in a ring system, together with the increased steric demands of the biphenyl and binaphthyl containing alkoxy groups may be the cause of this observed preference. Furthermore, the concentrations of **26** and **28** are found to increase over time at the expense of **25** and **27** when product mixtures are left in solution, suggesting once again that these rearrangements are metal mediated.

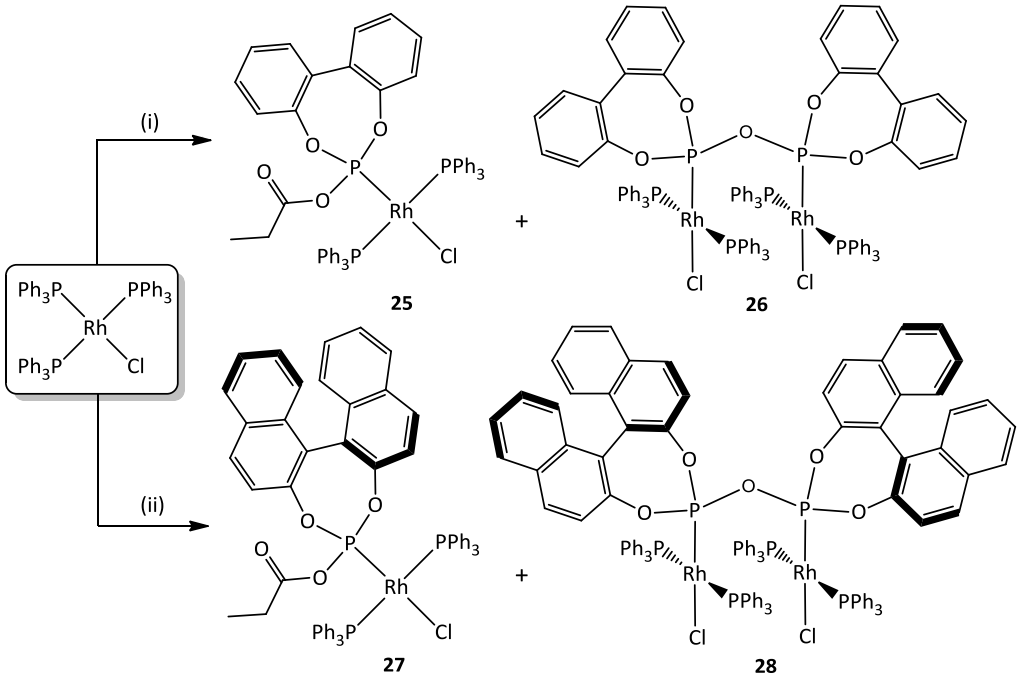


**Scheme 3.12** Reaction products observed for reactions of [RhCl($PPh_3$)$_3$] with the (propionyl)phosphite ligands **7** and **8**. Conditions: (i) **7** (1:1), $CH_2Cl_2$, R.T., 30 min.; (ii) **8** (1:1), $CH_2Cl_2$, R.T., 1 h.

For Rh(I) complexes of the more stable (propionyl)phosphites **9–10**, and (phenylacetyl)phosphites **12–13** (which have sterically demanding *tert*-butyl groups in the vicinity of their phosphorus atoms) rearrangements of this type were not observed with no POP complexes detected in any of the reaction products. The *trans*-[RhCl($PPh_3$)$_2$(L)]complexes **29–32** could be prepared in high yield by reacting solutions of ligands **9**, **10**, **12** or **13** in dichloromethane with [RhCl($PPh_3$)$_3$] at room temperature for 1 h. In most cases, crude

products could be successfully purified by washing with copious amounts of hexane [Scheme 3.13 (i) and (ii)]. In addition, these complexes could be further purified by recrystallisation and single crystals suitable for X-ray structure determinations could be obtained for complexes **29** and **31** by cooling concentrated dichloromethane solutions of the complexes to -22 $^{o}$C, while **30** could be crystallised by slow diffusion of hexane into a solution of **30** in toluene. Complexes **29**–**32** are soluble in aprotic organic solvents such as dichloromethane, thf and toluene and indefinitely stable in the solid state if kept under a dry and inert atmosphere. In solution, however, these complexes undergo complete rearrangement within 1 to 2 days *via* a mechanism different from those previously observed. Instead of POP complexes, a variety of highly symmetrical rearrangement products are obtained with the known carbonyl complex *trans*-[RhCl(CO)($PPh_3$)$_2$] (**33**) representing the major product of rearrangement.[22] Large quantities of the latter crystallised, as either yellow prisms or yellow needles from solutions of **29** – **30** when left standing for a period of 1 to 2 days. The structure of **33** could also be confirmed by X-ray crystallography, with the two different types of crystals representing two polymorphic structures, one of which is always ordered (needles) whilst the other contains CO/ Cl disorder over an inversion centre (prisms). In addition to **33**, the dimer [{RhCl($PPh_3$)$_2$}$_2$] (**34**) is also observed as a product of decay and often crystallises as burgundy prisms from solutions of **29**–**30** following their time dependant rearrangement [Scheme 3.13 (iii)].

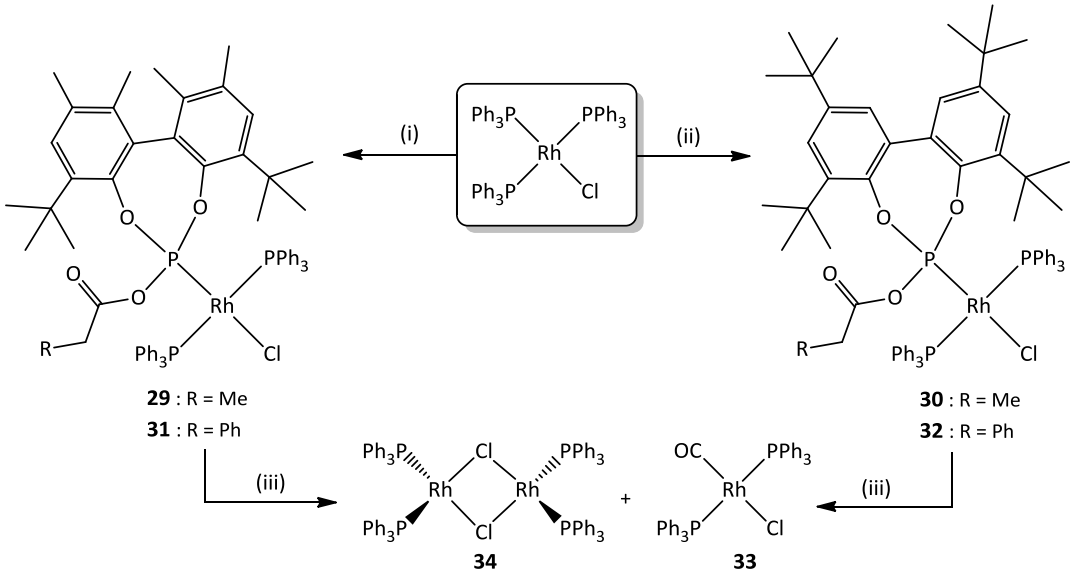


**Scheme 3.13** Reaction scheme for the preparation of complexes **29**–**32** and their subsequent rearrangement to complexes **33** and **34**. Conditions: (i) **9** or **12**, $CH_2Cl_2$, R.T., 1 h.; (ii) **10** or **13**, $CH_2Cl_2$, R.T., 1 h; (iii) standing in solution at R.T. for 1–2 days.

Although no formal mechanistic studies were conducted, it is plausible that the formation of **33** involves decarbonylation of coordinated ligands **9–10** and **12–13** *via* a dimeric metal acyl intermediate. Scheme 3.14 depicts the proposed mechanism of rearrangement for (propionyl)phosphite complexes **29** and **30** only. It is, however, possible that a similar mechanism applies for complexes **31–32**. In the initial stages of the rearrangement, complexes **29–30** dimerise to form mixtures of $[\{RhCl(PPh_3)_2\}_2]$ and $[\{RhCl(PPh_3)(L)\}_2]$ (where L = **9–10**). While the former is very insoluble and as a consequence crystallise from solution, the latter (**I**) can undergo further rearrangement to generate the Rh(III) acyl phosphito intermediate **II** *via* nucleophilic attack of neighbouring Rh(I) centres on the electrophilic carbonyl carbons of (acyl)phosphites in complex **I**. The coordinated acyl groups can then undergo ethyl migration, cleaving the chloro-bridged dimer, to give the monomeric Rh(III) CO complex **III**. $\beta$-Hydrogen abstraction from the coordinated ethyl moiety gives **IV** from which ethene can be eliminated. Reduction of the Rh(III) centre, together with protonation of the phosphito ligand, gives **V** which can be converted to the observed $[RhCl(CO)(PPh_3)_2]$ complex by exchange of the formed phosphite ligand with free $PPh_3$ present in solution. The released phosphite $(RO)_2POH$ would co-exist with the more stable phosphonate $(OR)_2P(O)H$ form in a tautomeric equilibrium shifted towards the phosphonate.

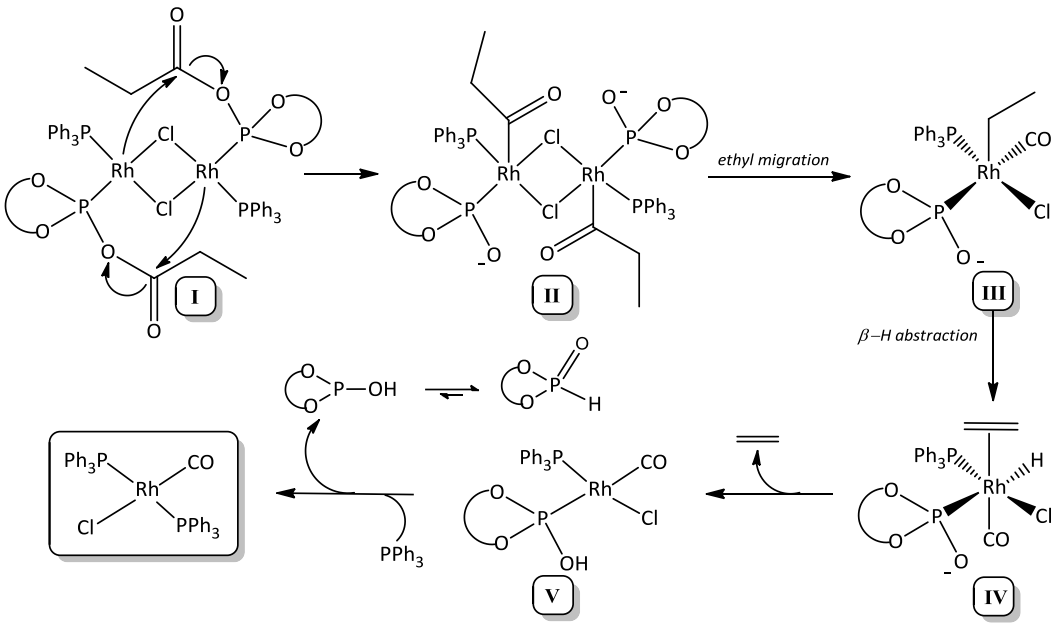


**Scheme 3.14** Proposed mechanism for the formation of Rh(I) CO complexes by the decarbonylation of (propionyl)phosphite ligands **9–10**.

Migratory deinsertion of CO is not uncommon and similar decarbonylation pathways to the one postulated above have been described in the literature for complexes obtained from the reaction of $[RhCl(PPh_3)_3]$ with phenylacetylchloride [Scheme 3.15 (a)] as well as for the five-coordinate acyl hydride Rh(III) complex $[Rh(dpephos)H(Me_SCH_2CH_2CO)][CB_{11}H_6Cl_6]$ [Scheme 3.15 (b)].[23,24] An analogous migratory deinsertion has also been described by Milstein and co-workers[25] for the (hydroxyacetyl)rhodium(III) complex $[RhCl(H)(PMe_3)_3(OCCH_2OH)]$. For this compound, phosphine dissociation was found to be the rate-determining step with higher $PMe_3$ concentrations resulting in retarded reaction rates.

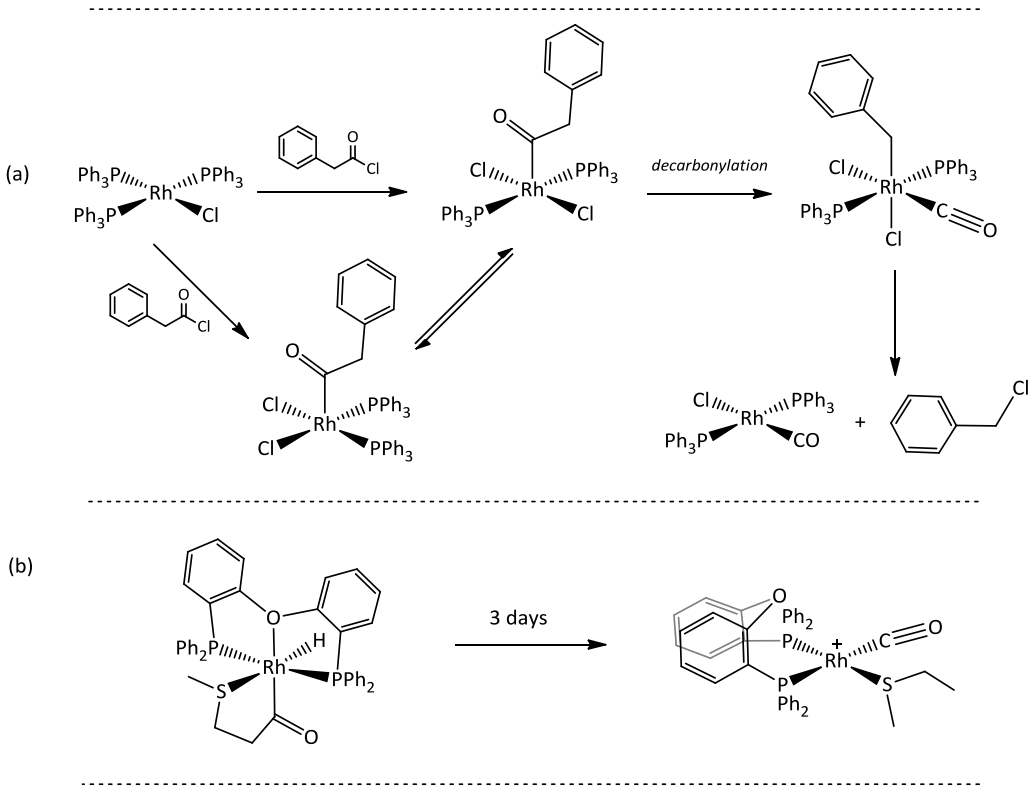


**Scheme 3.15** Literature examples for the formation of Rh(I) CO complexes *via* spontaneous decarbonylation of (a) coordinated phenylacetyl or (b) $MeSCH_2CH_2CO$.[23,24]

### *3.2.3.2 Spectroscopic characterisation of complexes 25-26*

Routine spectroscopic data were collected for complexes **25**–**32** and are listed in more detail under the experimental section, $^{31}P\{^1H\}$ NMR data for complexes **25**–**34** are, however, summarised in Table 3.2 to aid in discussions relating to their in solution behaviour. In the FT-IR spectra of complexes **25**, **27** and **29**–**31** the presence of an uncoordinated acyl group is evident from the characteristic $\nu$(C=O) bands observed in the region 1751–1780 $cm^{-1}$.

**Table 3.2** $^{31}P\{^{1}H\}$ NMR spectral data for rhodium complexes **25**–**34**.

| | | Chemical shifts δ (ppm)† | | | Coupling constants *J* (Hz) | | | | | |
|---|---|---|---|---|---|---|---|---|---|---|
| **Compound*** | | $P_A$ | $P_B$ | $P_C$ | Rh-$P_A$ | Rh-$P_B$ | Rh-$P_C$ | $P_A$-$P_B$ | $P_A$-$P_C$ | $P_B$-$P_C$ |
| **25** | $[RhCl(P_APh_3)_2(\mathbf{7})]$ ‡ | 36.1 (dd) | — | 134.5 (dt) | 132.7 | — | 321.8 | — | 46.6 | — |
| **26** | $[\{RhCl(P_APh_3)_2(P_COP_C)\}_2]$ § | 21.7 (dd) | — | 79.9 (dt) | 113.0 | — | 260.5 | — | 19.0 | — |
| **27** | $[RhCl(P_APh_3)_2(\mathbf{8})]$ ‡ | 35.2 (dd) | — | 133.9 (dt) | 132.9 | — | 322.5 | — | 46.2 | — |
| **28** | $[\{RhCl(P_{A\backslash B}Ph_3)_2(P_COP_C)\}_2]$ ¤ | 20.6 (ddd) | 20.5 (ddd) | 84.7 (ddd) | 113.3 | 111.3 | 261.1 | 370.5 | 17.2 | 21.2 |
| **29** | $[RhCl(P_{A\backslash B}Ph_3)_2(\mathbf{9})]$ ‡ | 34.4 (ddd) | 37.2 (ddd) | 129.3 (ddd) | 138.2 | 138.2 | 331.3 | 349.5 | 44.3 | 44.3 |
| **30** | $[RhCl(P_{A\backslash B}Ph_3)_2(\mathbf{10})]$ ‡ | 33.8 (ddd) | 38.2 (ddd) | 124.9 (ddd) | 135.3 | 135.3 | 331.8 | 347.9 | 48.3 | 48.3 |
| **31** | $[RhCl(P_{A\backslash B}Ph_3)_2(\mathbf{12})]$ ‡ | 34.9 (ddd) | 37.8 (ddd) | 131.1 (ddd) | 134.9 | 134.9 | 332.7 | 344.3 | 46.3 | 46.3 |
| **32** | $[RhCl(P_{A\backslash B}Ph_3)_2(\mathbf{13})]$ ‡ | 33.8 (ddd) | 38.7 (ddd) | 127.0 (ddd) | 134.9 | 134.9 | 334.0 | 346.9 | 46.3 | 46.3 |
| **33** | $[\{RhCl(P_APh_3)_2\}_2]$ | 52.7 (d) | — | — | 198.7 | — | — | — | — | — |
| **34** | $[RhCl(CO)(P_APh_3)_2]$ | 29.0 (d) | — | — | 127.6 | — | — | — | — | — |

* Note: Identical labels given to different phosphorus atoms present within the same complex indicate magnetic equivalence.
† Chemical shifts relative to 85 % $H_3PO_4$ ($CD_2Cl_2$, 25 °C) with mulitiplicity given in parenthesis.
‡ Phosphorus present in coordinated (acyl)phosphites listed as $P_C$.
§ POP represents 4,4'-oxydidinaphtho[2,1-*d*:1',2'-*f*][1,3,2]dioxaphosphepine.
¤ POP represents 6,6'-oxydidibenzo[*d,f*][1,3,2]dioxaphosphepine.

As can be expected, the $\nu$(C=O) bands are observed at frequencies slightly higher than those reported for analogous Rh(I) complexes of unsaturated mixed anhdyrides derived from acrylic acids in which the carbonyl functionalities form part of a conjugated system.[6]

In the $^{31}P\{^{1}H\}$ NMR spectrum of complex **25** coordinated **7** gives rise to a doublet of triplets at δ 134.5, owing to coupling to rhodium and the magnetically equivalent $PPh_3$ ligands ($J_{P\text{-}Rh}$ = 321.8 Hz, $J_{P\text{-}P}$ = 46.2 Hz). The latter resonates as a doublet of doublets at δ 36.1. The observed coupling pattern confirms the identity of **25** as the *trans*-complex, while the chemical shift of coordinated **7** is consistent with bonding only through phosphorus. Likewise, a doublet of triplets at δ 133.9 and a broad doublet of doublets δ 35.2 are detected for complex **27** and are in good agreement with literature values reported for the complex [Rh(COD){(R)-acetyl-(1,1'-binaphthyl-2,2'-diyl)phosphite}][$BF_4$].[26]

In the $^{31}P\{^{1}H\}$ NMR spectrum of partially rearranged **25**, the bridging POP ligand of the rearrangement product, **26**, resonates as a doublet of triplets at δ 79.9 ($J_{P\text{-}Rh}$ = 260.5 Hz, $J_{P\text{-}P}$ = 19.0 Hz), while the magnetically equivalent $PPh_3$ ligands are detected as a doublet of doublets at δ 21.7 ($J_{P\text{-}Rh}$ = 113.0 Hz, $J_{P\text{-}P}$ = 19.0 Hz). In contrast, the $PPh_3$ ligands of the rearrangement product **28** (present in the product mixture of **27**) are magnetically inequivalent, owing to the chirality of the bridging POP ligand. The chemical shifts of the $PPh_3$ are, however, very similar and **28** therefore represents an ABMX spin system (A and B = *P*$Ph_3$, M = *POP* and X = *Rh*) which gives rise to the more complex second order spectrum depicted in Figure 3.6. For both **26** and **28**, the observed chemical shifts, coupling patterns and coupling constants are consistent with the assigned structures, where a POP ligand is coordinated in a bridging fashion between two *trans*-[RhCl($PPh_3$)$_2$] entities.

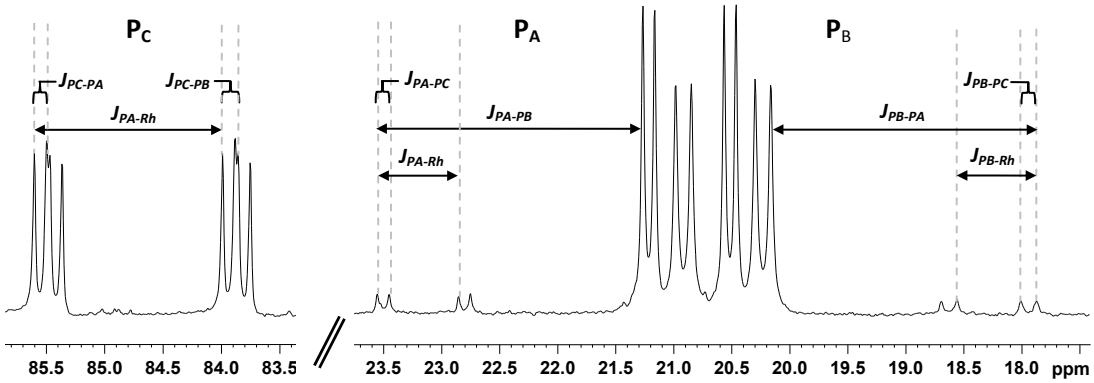


**Figure 3.6** Resonances corresponding to **28** in the $^{31}P\{^{1}H\}$ NMR spectrum of partially rearranged **27**. In **28** mutually *trans* $PPh_3$ ligands are chemically and magnetically inequivalent (indicated as $P_A$ and $P_B$) resulting in the observed second order spectral effects, while the P-atoms in the POP ligand are equivalent (represented by $P_C$).

Complexes **29**–**31** all display very similar behaviour in solution and $^{31}P\{^{1}H\}$ NMR spectra recorded for these compounds are almost identical with very little variation among the complexes in terms of their chemical shifts and coupling constants. Similar to complex **28**, the $PPh_3$ ligands in complexes **29**–**31** are chemically inequivalent with chemical shifts very close in value, once again leading to second order spectral effects. Figure 3.7 represents the $^{31}P\{^{1}H\}$ NMR spectrum of **31**; an example of the typical spectral profile associated with these complexes. Coupling constants for coupling between the coordinated (acyl)phosphite and the $PPh_3$ ligands are equal in magnitude and the phosphorus resonance from the (acyl)phosphite ligand ($P_c$) is observed as a doublet of doublets of doublets at δ 124.9 ($J_{P\text{-}Rh}$ = 331.3 Hz, $J_{PC\text{-}PA}$ = $J_{PC\text{-}PB}$ = 48.3 Hz). The $PPh_3$ ligands give rise to an AB pattern of doublets of doublets of doublets at δ 33.8 and δ 38.2, respectively. In addition to mutual *trans* coupling ($J_{PA\text{-}PB}$ = 347.9 Hz), these ligands display equal coupling to both Rh ($J_{PA\text{-}Rh}$ = $J_{PB\text{-}Rh}$ = 135.3 Hz) and $P_c$ ($J_{PA\text{-}PC}$ = $J_{PB\text{-}PC}$ = 48.3 Hz) and as a result the observed coupling pattern is highly symmetrical with the close proximity of their chemical shifts resulting in the pattern depicted in Figure 3.7.

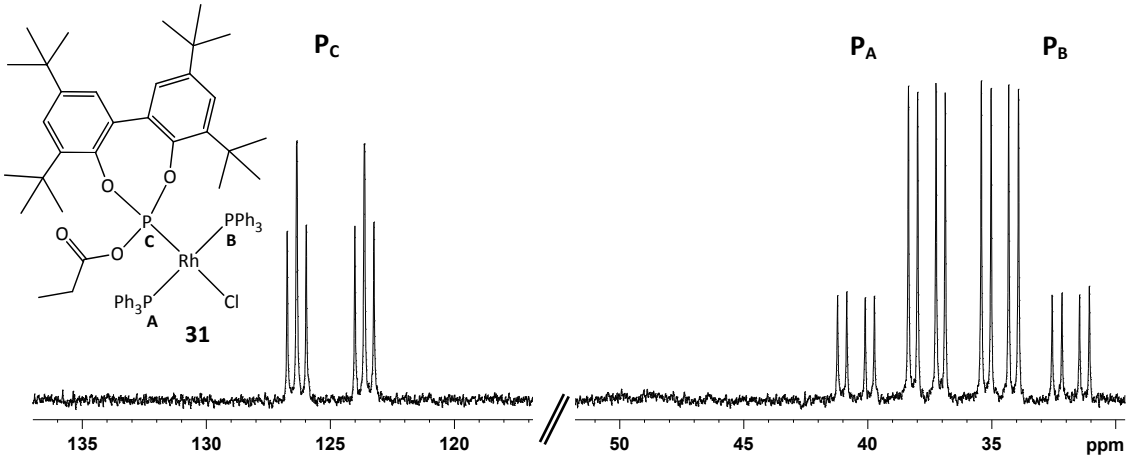


**Figure 3.7** $^{31}P\{^{1}H\}$ NMR spectrum of complex **31**, representing an example of the typical spectral profile observed for complexes of the form $[RhCl(PPh_3)_2(L)]$ where L denotes **9**, **10**, **12** or **13**.

The gradual rearrangement of **31** in solution to $[RhCl(CO)(PPh_3)_2]$ (**33**) and various other symmetrical rearrangement products could be followed using NMR spectroscopy over a period of 4 days by subjecting a solution of **31** in dichloromethane-$d_2$ to $^{31}P\{^{1}H\}$ NMR analysis at room temperature at different time intervals. Figure 3.8 depicts a comparison of the collected spectra at times = 0, 22 h, 44 h and 4 days. From this comparison it is evident that very little rearrangement occurs at room temperature during the first 22 h in solution. However, over

the next 22 h **31** begins to undergo gradual conversion so that the $^{31}P\{^{1}H\}$ NMR spectrum recorded after t = 44 h displays the presence of a large variety of intermediates. Many of these intermediates still contain high field resonances in the region δ 130–140 which cannot be assigned unambiguously. Although it is possible that these resonances may correspond to coordinated hydrogen phosphite ligands [$(RO)_2POH$] (see proposed mechanism Scheme 3.14), they are more likely to correspond to intermediates that still contain **10** with the propionyl group intact. This assumption is based on literature reports for related Rh(I) phosphinato complexes, where coordinated phosphinato ligands typically display resonances within the range δ 116–119.

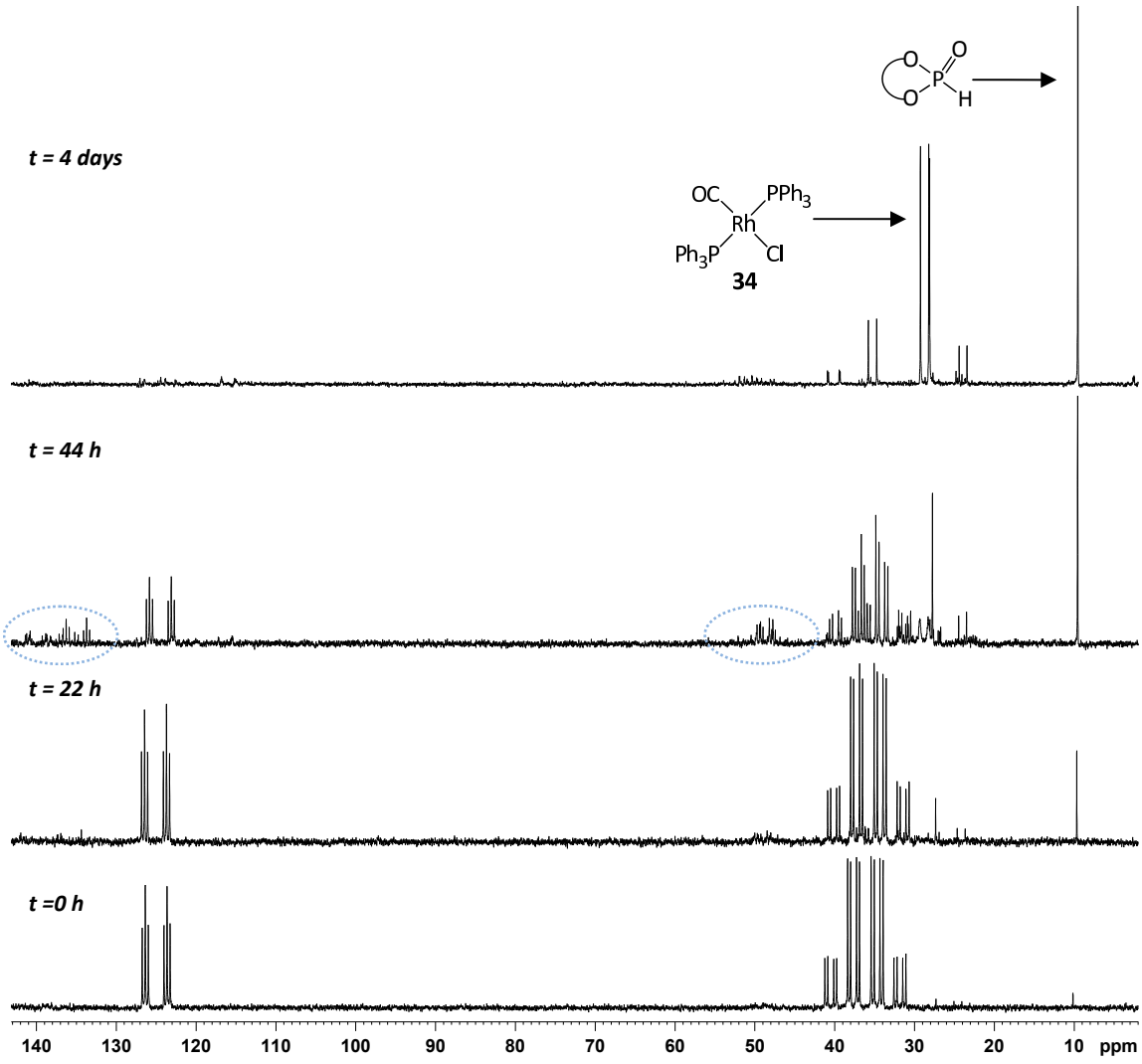


**Figure 3.8** Time dependant rearrangement of **31** in solution to [$RhCl(CO)(PPh_3)_2$] and other products, followed by $^{31}P\{^{1}H\}$ NMR spectroscopy over a period of 4 days. The dotted ovals at time = 22 h highlights the formation of a large variety of intermediates, which could not be assigned unambiguously.

In addition to the various new metal complexes detected, the formation of $[RhCl(CO)(PPh_3)_2]$ and significant amounts of phosphonate $[(RO)_2P(O)H]$ is observed in the form of a doublet at δ 29.0 ($J_{P\text{-}Rh}$ = 127.6 Hz) and a singlet at δ 10.0, respectively. These observations are consistent with the mechanism earlier proposed in Scheme 3.14.

After a period of four days, conversion of complex **31**, together with most of the observed intermediates, had gone to completion, with the recorded $^{31}P\{^1H\}$ NMR spectrum only revealing resonances corresponding to $[RhCl(CO)(PPh_3)_2]$, $[(RO)_2P(O)H]$ and three more unassigned, highly symmetrical complexes. Although the mechanism proposed in Scheme 3.14 represents one plausible decomposition pathway, it is possible that more than one route exists. Based on the relative quantities of the final rearrangement products, however, decarbonylation appears to be the decomposition pathways of preference. More mechanistic investigations are, however, required to warrant a more conclusive answer.

### *3.2.4 Crystal and molecular structure determinations*

The crystal and molecular structures of the new complexes **22–24** and **29–31** were determined by single crystal X-ray-diffraction and are here, to the best of our knowledge, reported for the first time. The crystal and molecular structures of the known Rh(I) dimer $[\{RhCl(PPh_3)_2\}_2]$ (**34**) and $[RhCl(CO)(PPh_3)_2]$ (**33**) were also determined and are included in this section, although not discussed in detail.

The interesting acyl Rh(III) dimer **22** crystallises, together with one molecule of disordered toluene per asymmetric unit, as yellow prisms in the monoclinic space group *C*2/*c* from a chloroform solution of the product mixture obtained from **19**. Figure 3.9 depicts the molecular structure of **22**, showing the numbering scheme, while principle bond lengths and angles together with their standard deviations in parenthesis are summarised in Table 3.3. The geometry about each Rh(III) centre is best described as square pyramidal with the propionyl groups occupying apical positions while the Rh(III) centres share two bridging chloride atoms in the basal plane. A similar geometry has been reported in the literature for the molecular structure of monomeric *cis*-$[RhCl_2(PPh_3)_2(OCEt)]$.[27] The Rh-C(propionyl) bonding distance of 1.991(3) Å is comparable to those reported for other rhodium(III)-acyl complexes such as *cis*-$[RhCl_2(PPh_3)_2(OCEt)]$ [1.953(10) Å] and $[Rh_2Cl_3(PMe_2Ph)_4(OCCH_3)_2]$ [2.010(5) Å and 1.995 (5) Å].[27,28]

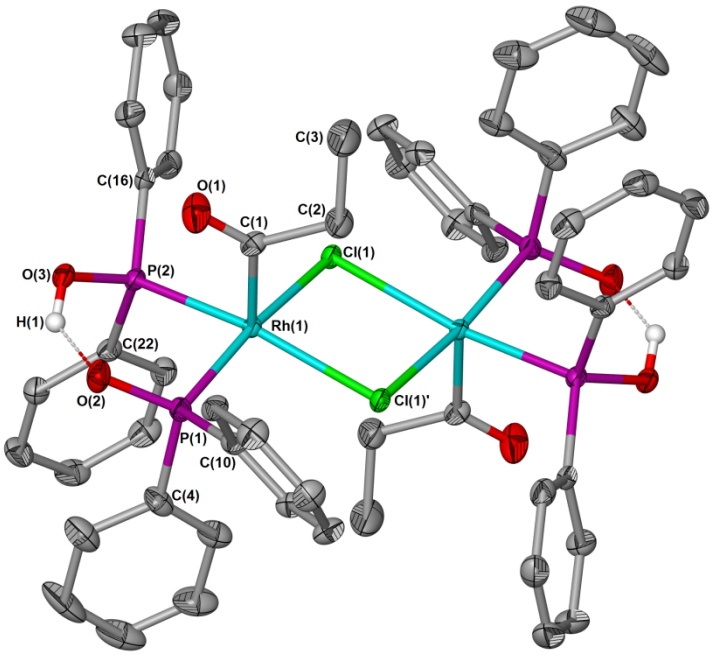


**Figure 3.9** Molecular structure of the rearrangement product **22** showing the numbering scheme. Thermal ellipsoids set at 50 % probability. Hydrogen atoms (with the exception of O–H hydrogens) and the included solvent molecule are omitted for clarity. Only half of the shown structure forms part of the asymmetric unit with the other half being symmetry generated.

**Table 3.3** Selected bond lengths (Å) and angles (°) of **22** with estimated standard deviations in parenthesis.

*Bond lengths (Å)*

| | | | |
|---|---|---|---|
| Rh(1)–C(1) | 1.991(3) | P(1)–O(2) | 1.5580(19) |
| Rh(1)–Cl(1) | 2.4524(11) | P(2)–C(16) | 1.817(3) |
| Rh(1)–P(1) | 2.2517(10) | P(2)–C(22) | 1.821(3) |
| Rh(1)–P(2) | 2.2511(8) | P(2)–O(3) | 1.5345(18) |
| O(1)–C(1) | 1.188(3) | C(1)–C(2) | 1.522(4) |
| P(1)–C(4) | 1.833(3) | C(2)–C(3) | 1.506(5) |
| P(1)–C(10) | 1.815(3) | | |

*Bond angles (°)*

| | | | |
|---|---|---|---|
| Rh(1)–C(1)–O(1) | 125.9(2) | C(1)–Rh(1)–Cl(1) | 99.23(8) |
| Rh(1)–C(1)–C(2) | 112.07(18) | O(1)–C(1)–C(2) | 122.0(2) |
| P(1)–Rh(1)–P(2) | 88.23(3) | C(1)–C(2)–C(3) | 112.1(3) |
| Cl(1)–Rh(1)–Cl(1)' | 83.25(2) | Rh(1)–P(1)–O(2) | 116.62(8) |
| P(2)–Rh(1)–Cl(1) | 92.86(2) | Rh(1)–P(2)–O(3) | 117.01(7) |
| P(1)–Rh(1)–Cl(1)' | 93.55(3) | Rh(1)–P(1)–C(10) | 114.70(9) |
| P(1)–Rh(1)–Cl(1) | 170.74(2) | Rh(1)–P(1)–C(4) | 107.32(9) |
| C(1)–Rh(1)–P(1) | 89.93(8) | Rh(1)–P(2)–C(16) | 112.53(8) |
| C(1)–Rh(1)–P(2) | 91.53(8) | Rh(1)–P(2)–C(22) | 103.91(9) |

As can be expected, the Rh(1)–Cl(1) distance of 2.4524(11) Å is comparable to those in the dinuclear complex $[Rh_2Cl_3(PMe_2Ph)_4(OCCH_3)_2]$ [2.431(2) Å to 2.485(1) Å], but significantly longer than those reported for the monomeric complex *cis*-$[RhCl_2(PPh_3)_2(OCEt)]$ [2.370(3) Å and 2.379(3) Å] where the chloride ligands are not bridging. While the P–Rh–Cl and P–Rh–C angles are all perpendicular, measured P–Rh–P, Cl–Rh–Cl and Cl–Rh–C angles deviate slightly from the ideal value of 90°. The measured values are, however, once again comparable to those reported for the mentioned literature examples.

The (propionyloxy)diphenylphosphine Ru(II) complex **23** crystallises as orange platelets in the monoclinic space group $P2_1/c$ from a solution of **23** in toluene layered with diethyl ether. The asymmetric unit contains one molecule of the *cis*-isomer of **23** co-crystallised with two disordered toluene molecules. Figure 3.10 depicts the molecular structure of **23** giving the numbering scheme, while selected bond lengths and angles are listed in Table 3.4. In agreement with previously discussed NMR- and IR-results, the molecular structure of **23** contains two (propionyloxy)diphenylphosphine ligands, coordinated *cis* to one another in a chelated manner *via* both their phosphorus and carbonyl oxygen atoms. The immediate coordination sphere around the central Ru(II) atom is best described as distorted octahedral with measured P–Ru–P and O–Ru–O angles greater than 90° [105.91(8)° and 92.66(19)°] and P–Ru–O angles smaller than 90° [80.36(14)° and 81.04(15)°] owing to ring constraints.

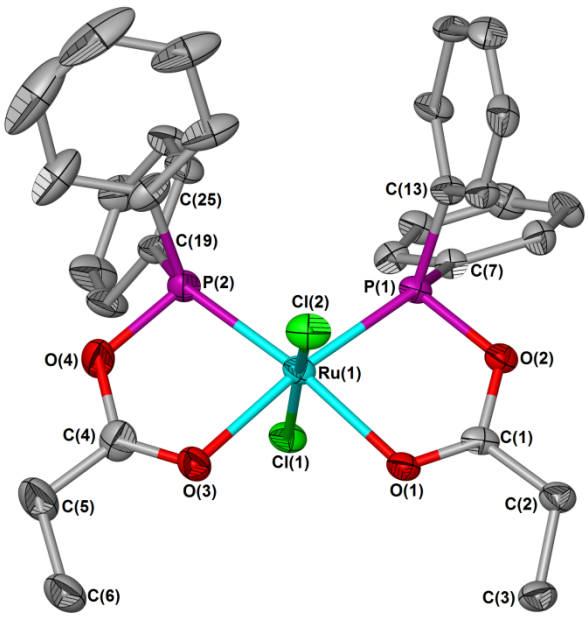


**Figure 3.10** Molecular structure of **23** showing the numbering scheme. Thermal ellipsoids set at 35 % probability. Hydrogen atoms and solvent molecules are omitted for clarity.

Measured Ru–O and Ru–P bonding distances are comparable to those reported for the literature example [Ru(OAc){(binaphthyl)$PR_2$}($R_2PO_2CCH_3$)] (R = cyclohexyl) where the $R_2PO_2CCH_3$ ligand are also chelated [2.164(3) Å and 2.187(1) Å].[29] Furthermore, the P(1)–Ru(1)–O(1) and P(2)–Ru(1)–O(3) angles [80.36(14)$^o$ and 81.04(15)$^o$, respectively] are also similar to that of the mentioned literature example [80.54(8)$^o$]. In order to minimise steric repulsions, axial chlorides are slightly bent towards the equatorial plane in the direction of the carbonyl oxygen atoms, and as a result the Cl(1)–Ru(1)–Cl(2) angle deviates from the ideal linearity [168.76(7)$^o$].

**Table 3.4** Selected bond lengths (Å) and angles (°) of **23** with estimated standard deviations in parenthesis.

| | | | |
|---|---|---|---|
| *Bond lengths (Å)* | | | |
| Ru(1)–Cl(1) | 2.379(2) | P(2)–C(19) | 1.819(7) |
| Ru(1)–Cl(2) | 2.389(2) | P(2)–C(25) | 1.794(9) |
| Ru(1)–P(1) | 2.181(2) | O(2)–C(1) | 1.328(8) |
| Ru(1)–P(2) | 2.181(2) | O(1)–C(1) | 1.216(8) |
| Ru(1)–O(1) | 2.170(5) | O(4)–C(4) | 1.353(10) |
| Ru(1)–O(3) | 2.174(5) | O(3)–C(4) | 1.218(9) |
| P(1)–O(2) | 1.716(5) | C(1)–C(2) | 1.473(10) |
| P(2)–O(4) | 1.707(6) | C(2)–C(3) | 1.508(10) |
| P(1)–C(7) | 1.797(7) | C(4)–C(5) | 1.488(12) |
| P(1)–C(13) | 1.804(7) | C(5)–C(6) | 1.533(12) |
| *Bond angles (°)* | | | |
| Ru(1)–O(1)–C(1) | 117.6(4) | Cl(1)–Ru(1)–P(1) | 95.16(7) |
| Ru(1)–O(3)–C(4) | 117.1(5) | Cl(1)–Ru(1)–P(2) | 91.15(9) |
| Ru(1)–P(1)–O(2) | 101.93(17) | Cl(2)–Ru(1)–P(1) | 92.27(7) |
| Ru(1)–P(2)–O(4) | 101.9(2) | Cl(2)–Ru(1)–P(2) | 94.92(9) |
| P(1)–Ru(1)–O(3) | 172.96(15) | P(1)–O(2)–C(1) | 117.1(4) |
| P(2)–Ru(1)–O(1) | 173.58(13) | P(2)–O(4)–C(4) | 117.6(5) |
| P(1)–Ru(1)–O(1) | 80.36(14) | O(1)–C(1)–O(2) | 122.4(6) |
| P(2)–Ru(1)–O(3) | 81.04(15) | O(3)–C(4)–O(4) | 122.0(8) |
| P(1)–Ru(1)–P(2) | 105.91(8) | O(2)–C(1)–C(2) | 114.0(6) |
| O(1)–Ru(1)–O(3) | 92.66(19) | O(4)–C(4)–C(5) | 113.4(7) |
| Cl(1)–Ru(1)–Cl(2) | 168.76(7) | O(1)–C(1)–C(2) | 123.6(6) |
| Cl(1)–Ru(1)–O(1) | 86.84(14) | O(3)–C(4)–C(5) | 124.6(8) |
| Cl(1)–Ru(1)–O(3) | 83.46(15) | C(1)–C(2)–C(3) | 114.8(6) |
| Cl(2)–Ru(1)–O(1) | 86.09(14) | C(4)–C(5)–C(6) | 111.3(8) |
| Cl(2)–Ru(1)–O(3) | 88.14(15) | | |

Complex **24**, crystallises from a pentane layered solution of rearranged **23** in chloroform as orange platelets in the triclinic space group $P\bar{1}$. A centre of inversion exists for **24**, and as a result the asymmetric unit contains only half of one molecule of **24** together with one chloroform molecule. Figure 3.11 depicts the molecular structure of **24** showing the

numbering scheme and selected bond lengths and angles are listed in Table 3.5. Within the molecular structure of **24**, the Ru(II) centres, chloride atoms and mixed anhydride phosphorus atoms all lie roughly within the same plane, while the $Ph_2POH$ and propionyl moieties are situated above and below the plane. Geometries about the Ru(II) centres are best described as distorted octahedral with chloride ligands bound to the Ru(II) in a meridional orientation. Not surprisingly the non-bridged Ru(1)–Cl(1) and bridged Ru(1)–Cl(2) bond lengths [2.325(5) Å and 2.423(6) Å] differ significantly and are shorter and longer, respectively, than the average separation observed for the Ru–Cl bonds in complex **23**. This observed shorter Ru(1)–Cl(1) separation is attributable to the reduced *trans*-influence of a bridged relative a non-bridged chloride ligand. Furthermore, the sharing of electron density between two Ru(II) centres result in the weaker and hence longer Ru(1)–C(2) bond. Similarly, the measured Ru(1)–P(1) bond length [2.149(6) Å] is slightly shorter than the corresponding bond in **23** [2.181(2) Å] owing to the weaker *trans*-influence of the bridging chloride ligand in **24** relative to the carbonyl oxygen *trans*-influence in **23**. A Ru(1)–P(2) bond length of 2.155(6) Å is observed, and is significantly shorter than that reported for the literature example $[RuCl(PPh_3)\{(Ph_2PO)_2H\}(O_2CCH_2CH_2PPh_3)]$.[9] There are no noteworthy differences between the P(1)–Ru(1)–O(2) angle in **24** and the related angles in complex **23.**

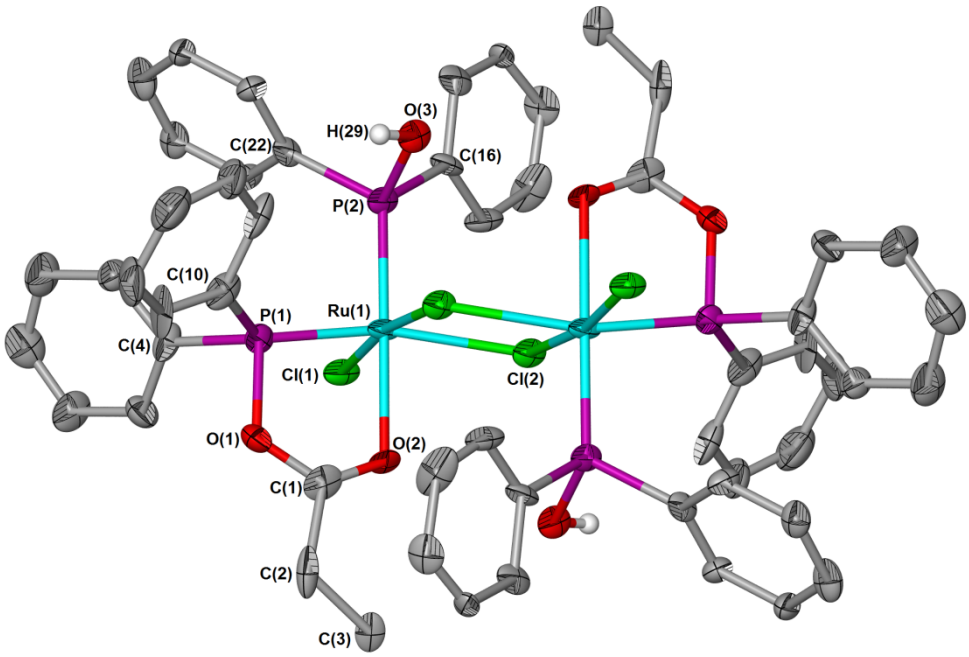


**Figure 3.11** Molecular structure of the rearrangement product **24** showing the numbering scheme. Thermal ellipsoids set at 35 % probability. Hydrogen atoms (with the exception of O–H hydrogens) and solvent molecules are omitted for clarity. Only half of the shown structure forms part of the asymmetric unit with the other half being symmetry generated.

**Table 3.5** Selected bond lengths (Å) and angles (°) of **24** with estimated standard deviations in parenthesis.

| | | | |
|---|---|---|---|
| *Bond lengths (Å)* | | | |
| Ru(1)–Cl(1) | 2.325(5) | P(2)–O(3) | 1.602(14) |
| Ru(1)–Cl(2) | 2.423(6) | P(1)–C(4) | 1.74(2) |
| Ru(1)–P(1) | 2.149(6) | P(1)–C(10) | 1.82(2) |
| Ru(1)–P(2) | 2.155(6) | P(2)–C(16) | 1.83(2) |
| Ru(1)–O(2) | 2.210(13) | P(2)–C(22) | 1.787(19) |
| P(1)–O(1) | 1.689(16) | C(1)–C(2) | 1.53(4) |
| O(1)–C(1) | 1.31(3) | C(2)–C(3) | 1.50(3) |
| O(2)–C(1) | 1.17(3) | | |
| *Bond angles (°)* | | | |
| Ru(1)–O(2)–C(1) | 113.5(14) | O(1)–C(1)–O(2) | 126(2) |
| Ru(1)–P(1)–O(1) | 101.9(5) | O(1)–C(1)–C(2) | 110(2) |
| Ru(1)–P(2)–O(3) | 115.3(6) | O(2)–C(1)–C(2) | 124(2) |
| Ru(1)–Cl(2)–Ru(1)' | 97.7(2) | C(1)–C(2)–C(3) | 111.9(19) |
| P(1)–Ru(1)–O(2) | 80.9(4) | P(1)–O(1)–C(1) | 117.1(16) |
| P(1)–Ru(1)–P(2) | 98.9(2) | C(4)–P(1)–C(10) | 100.3(10) |
| P(1)–Ru(1)–Cl(1) | 91.7(2) | C(16)–P(2)–C(22) | 99.2(9) |
| P(1)–Ru(1)–Cl(2) | 164.7(2) | C(4)–P(1)–O(1) | 96.5(10) |
| P(2)–Ru(1)–O(2) | 179.8(4) | C(10)–P(1)–O(1) | 96.5(11) |
| P(2)–Ru(1)–Cl(1) | 91.77(19) | C(16)–P(2)–O(3) | 98.4(9) |
| P(2)–Ru(1)–Cl(2) | 95.8(2) | C(22)–P(2)–O(3) | 98.9(8) |
| Cl(1)–Ru(1)–Cl(2) | 92.3(2) | | |

Compound **29** crystallise as yellow platelets from a concentrated dichloromethane solution of **29** at -22 °C in the orthorhombic space group $Pna2_1$, while **30** crystallises from a concentrated solution in toluene layered with hexane at room temperature as yellow needles in the monoclinic space group $P2_1/n$. The molecular structures determined for **29** and **30** together with the labelling schemes are shown in Figures 3.12–3.13 with selected bond lengths and angles summarised in Tables 3.6–3.7. In the asymmetric unit of **29**, two molecules of **29** are co-crystallised with at least eight dichloromethane molecules, and as a result, the determined structure is heavily disordered. The poor quality of this data set did not allow for anisotropic refinement and all atoms in Figure 3.12 are, therefore, drawn as spheres rather than the more accurate ellipsoid representation. Measured bond lengths and angles for **29** and **30** are comparable, however, devoid of any disorder, the structure determined for **30** is of superior quality and measured bond lengths and angles are thus more reliable for use in any comparative discussions involving literature examples. In both structures, the four-coordinate Rh(I) centres are in distorted square planar environments with $PPh_3$ ligands coordinated in mutually *trans*-positions.

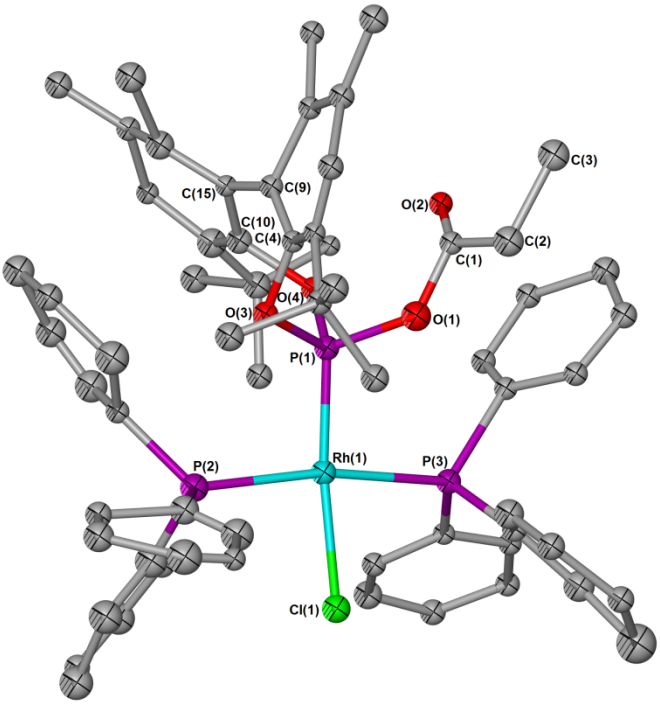


**Figure 3.12** Molecular structure of one of the two molecules of **29** present in the asymmetric unit showing the numbering scheme. Owing to the extent of disorder, this structure could not be refined anisotropically. Hydrogen atoms and solvent molecules are omitted for clarity.

**Table 3.6** Selected bond lengths (Å) and angles (°) of **29** with estimated standard deviations in parenthesis.

*Bond lengths (Å)*

| | | | |
|---|---|---|---|
| Rh(1)–P(1) | 2.115(6) | O(1)–C(1) | 1.36(3) |
| Rh(1)–P(2) | 2.348(8) | C(1)–O(2) | 1.15(3) |
| Rh(1)–P(3) | 2.345(7) | C(1)–C(2) | 1.56(3) |
| Rh(1)–Cl(1) | 2.349(6) | C(2)–C(3) | 1.42(4) |
| P(1)–O(1) | 1.69(2) | O(3)–C(4) | 1.41(3) |
| P(1)–O(3) | 1.635(18) | O(4)–C(10) | 1.48(3) |
| P(1)–O(4) | 1.624(15) | | |

*Bond angles (°)*

| | | | |
|---|---|---|---|
| P(1)–Rh(1)–P(2) | 95.1(3) | O(1)–P(1)–O(3) | 102.0(10) |
| P(1)–Rh(1)–P(3) | 95.3(2) | O(1)–P(1)–O(4) | 98.6(9) |
| P(1)–Rh(1)–Cl(1) | 167.7(3) | O(3)–P(1)–O(4) | 100.1(8) |
| P(2)–Rh(1)–Cl(1) | 87.4(2) | P(1)–O(1)–C(1) | 126.4(17) |
| P(3)–Rh(1)–Cl(1) | 83.4(2) | O(3)–C(4)–C(9) | 107.9(18) |
| P(2)–Rh(1)–P(3) | 168.6(2) | O(4)–C(10)–C(15) | 106.4(19) |
| Rh(1)–P(1)–O(1) | 111.4(8) | O(1)–C(1)–O(2) | 128(2) |
| Rh(1)–P(1)–O(3) | 115.9(6) | O(2)–C(1)–C(2) | 120.0(18) |
| Rh(1)–P(1)–O(4) | 125.4(6) | O(1)–C(1)–C(2) | 109.3(18) |

Suprisingly, coordination of ligands **9** or **10** to a Rh(I) centre does not lead to any noteworthy changes in the P–O bonding distances or dihedral angles measure between the biphenyl rings compared to those observed for the related free ligand structures (see chapter 2). Likewise, no appreciable differences exist between the Rh(1)–P(1) bond lengths observed for **29** and **30** [2.115(6) Å and 2.140(3) Å], suggesting that ligands **9** and **10**, upon coordination, lead to Rh(1)-P(1) bonds of comparable strength. In contrast, the observed Rh(1)–P(1) bonds are shorter than that reported for the literature example [$RhCl(PPh_3)(Ph_2PO_2CCH{=}CHCH_3)$] [2.171(3) Å].[6] In the latter, however, ring strain as a result of chelated bonding of the mixed anhydride *via* both the phosphorus atom and double bond may cause slight elongation of the Rh–P bond. The coordination angles in **29** and **30** all vary from the ideal 90°, with the steric requirements of the bulky (propionyl)phosphite ligands resulting in widening of the measured P(1)–Rh(1)–P(2) and P(1)–Rh(1)–P(3) angles [95–98° on average] with consequential contraction of the Cl(1)–Rh(1)–P(2) and Cl(1)–Rh(1)–P(3) angles [84–87° on average].

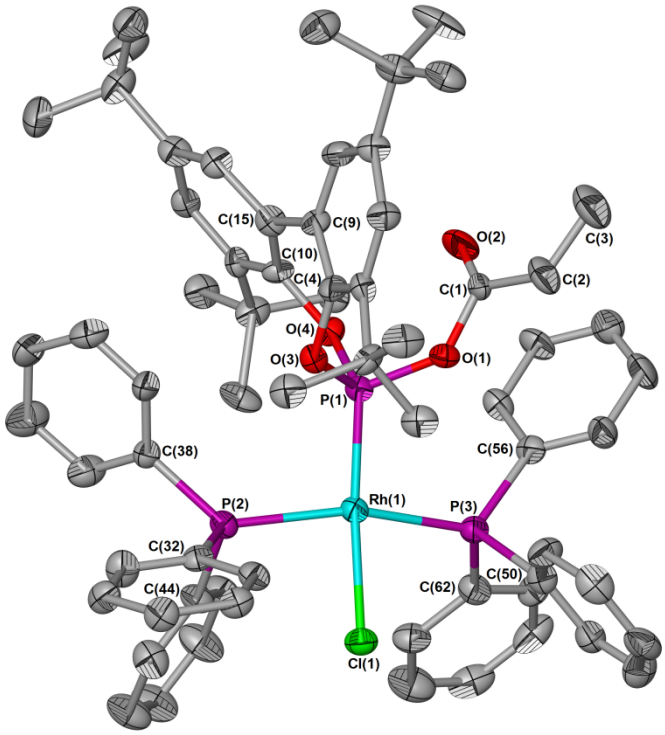


**Figure 3.13** Molecular structure of **30** showing the numbering scheme. Thermal ellipsoids set at 50 % probability. Hydrogen atoms are omitted for clarity.

**Table 3.7** Selected bond lengths (Å) and angles (°) of **30** with estimated standard deviations in parenthesis.

| | | | |
|---|---|---|---|
| *Bond lengths (Å)* | | | |
| Rh(1)–P(1) | 2.140(2) | O(1)–C(1) | 1.383(10) |
| Rh(1)–P(2) | 2.338(2) | C(1)–O(2) | 1.184(10) |
| Rh(1)–P(3) | 2.310(2) | C(1)–C(2) | 1.502(13) |
| Rh(1)–Cl(1) | 2.384(2) | C(2)–C(3) | 1.503(14) |
| P(1)–O(1) | 1.643(6) | O(3)–C(4) | 1.398(10) |
| P(1)–O(3) | 1.637(6) | O(4)–C(10) | 1.412(9) |
| P(1)–O(4) | 1.597(6) | | |
| *Bond angles (°)* | | | |
| P(1)–Rh(1)–P(2) | 97.71(8) | O(1)–P(1)–O(3) | 99.4(3) |
| P(1)–Rh(1)–P(3) | 98.41(8) | O(1)–P(1)–O(4) | 102.1(3) |
| P(1)–Rh(1)–Cl(1) | 161.18(9) | O(3)–P(1)–O(4) | 102.7(3) |
| P(2)–Rh(1)–Cl(1) | 84.46(8) | P(1)–O(1)–C(1) | 133.0(5) |
| P(3)–Rh(1)–Cl(1) | 84.13(8) | O(3)–C(4)–C(9) | 118.6(7) |
| P(2)–Rh(1)–P(3) | 159.96(9) | O(4)–C(10)–C(15) | 123.2(7) |
| Rh(1)–P(1)–O(1) | 113.8(2) | O(1)–C(1)–O(2) | 123.0(8) |
| Rh(1)–P(1)–O(3) | 111.7(2) | O(2)–C(1)–C(2) | 127.1(8) |
| Rh(1)–P(1)–O(4) | 123.9(2) | O(1)–C(1)–C(2) | 109.9(7) |

The (phenylacetyl)phosphite complex **31** crystallises as yellow prisms from a concentrated dichloromethane solution of **31** at -22 $^{o}$C in the triclinic space group *P*$\bar{1}$ with one molecule of **31** and four molecules of dichloromethane included in the asymmetric unit. An ellipsoid representation of the molecular structure of **31** is given in Figure 3.14 with selected bond lengths and angles collected in Table 3.8. Similar to the analogous complexes **29** and **30**, the geometry about the Rh(I) centre is best described as distorted square planar with angles deviating from the ideal 90$^{o}$ for the same reasons mentioned before. Consistent with NMR observations, it is evident that the orientation of the acylphosphite ligand backbone in the structures of complexes **29**–**31** causes the $PPh_3$ ligands to occupy chemically distinct environments. For **31** the Rh(1)–P(1) bonding distance of 2.1414(14) Å is in good agreement with those observed for complexes **29**–**30**, suggesting once again that ligands **9**, **10** and **12** form Rh(I)–P bonds of comparable strength upon coordination. Furthermore, the *trans*-influence of ligand **12** appears to be in the same order of magnitude as for ligands **9** and **10**, with no appreciable difference observed between the measured Rh(1)–Cl(1) separation [2.3902(14) Å] and those of compounds **29** [2.349(6) Å] and **30** [2.384(2) Å]. As before, coordination of **12** to a $[RhCl(PPh_3)_2]$ entity does not bring about any noteworthy changes in the dihedral angles between the phenyl rings [60.6(8)$^{o}$ and 58.5(8)$^{o}$], with measured angles similar to those of the free ligand structure [61.2(7)$^{o}$ and 56.7(8)$^{o}$].

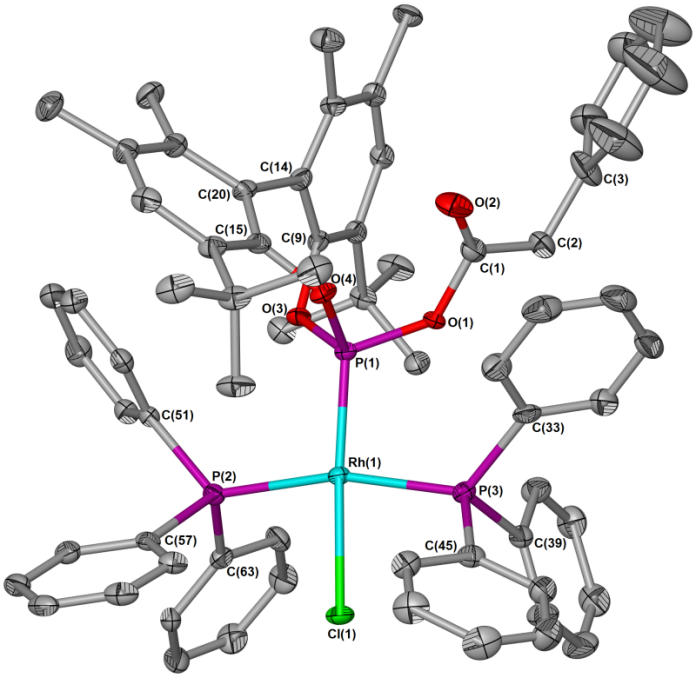


**Figure 3.14** Molecular structure of **31** showing the numbering scheme. Thermal ellipsoids set at 50 % probability. Hydrogen atoms and solvent molecules are omitted for clarity.

**Table 3.8** Selected bond lengths (Å) and angles (°) of **31** with estimated standard deviations in parenthesis.

*Bond lengths (Å)*

| | | | |
|---|---|---|---|
| Rh(1)–P(1) | 2.1414(14) | O(1)–C(1) | 1.405(7) |
| Rh(1)–P(2) | 2.3270(15) | C(1)–O(2) | 1.191(8) |
| Rh(1)–P(3) | 2.3045(15) | C(1)–C(2) | 1.501(9) |
| Rh(1)–Cl(1) | 2.3902(14) | C(2)–C(3) | 1.515(9) |
| P(1)–O(1) | 1.643(4) | O(3)–C(9) | 1.408(7) |
| P(1)–O(3) | 1.620(4) | O(4)–C(15) | 1.399(7) |
| P(1)–O(4) | 1.614(4) | | |

*Bond angles (°)*

| | | | |
|---|---|---|---|
| P(1)–Rh(1)–P(2) | 98.61(5) | O(1)–P(1)–O(3) | 100.7(2) |
| P(1)–Rh(1)–P(3) | 96.27(5) | O(1)–P(1)–O(4) | 99.4(2) |
| P(1)–Rh(1)–Cl(1) | 173.84(5) | O(3)–P(1)–O(4) | 104.1(2) |
| P(2)–Rh(1)–Cl(1) | 82.63(5) | P(1)–O(1)–C(1) | 133.1(4) |
| P(3)–Rh(1)–Cl(1) | 82.30(5) | O(3)–C(9)–C(14) | 117.4(5) |
| P(2)–Rh(1)–P(3) | 164.89(5) | O(4)–C(15)–C(20) | 119.1(5) |
| Rh(1)–P(1)–O(1) | 113.15(14) | O(1)–C(1)–O(2) | 123.9(6) |
| Rh(1)–P(1)–O(3) | 114.93(15) | O(2)–C(1)–C(2) | 128.3(6) |
| Rh(1)–P(1)–O(4) | 121.55(15) | O(1)–C(1)–C(2) | 107.8(5) |

The rearrangement complex [RhCl(CO)($PPh_3$)$_2$] (**33**) crystallises from dichloromethane either as yellow prisms in the monoclinic space group $P2_1/n$ or as yellow needles in the orthorhombic space group *Pbca*. While the determined orthorhombic structures always display disordered *trans* CO and Cl groups, no such disorder was observed for the monoclinic structures. To the best of our knowledge all previously reported structures of **33** suffered from CO/Cl disorder, and for this reason the ordered structure determined during this study is included in this discussion. Figure 3.15 depicts the molecular structure of **33**, while selected bond lengths and angles are given in Table 3.9. All measured bond lengths and angles are in good agreement with literature values reported for structures of this compound.[22]

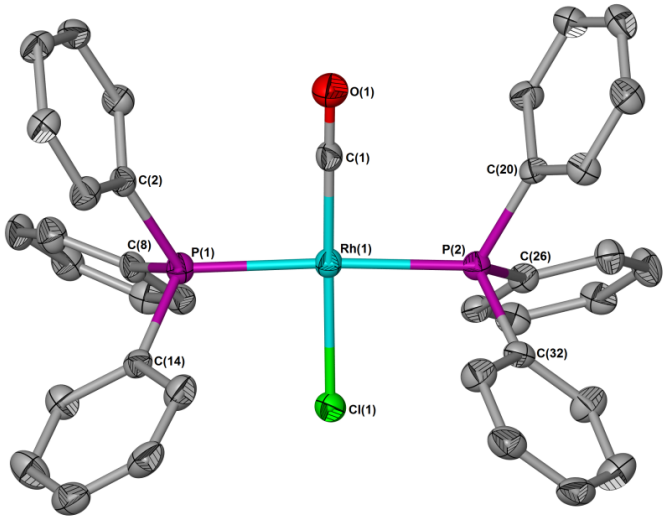


**Figure 3.15** Molecular structure of the rhodium(I) carbonyl rearrangement complex, **33,** showing the numbering scheme. Thermal ellipsoids set at 50 % probability. Hydrogen atoms are omitted for clarity.

**Table 3.9** Selected bond lengths (Å) and angles (°) of **33** with estimated standard deviations in parenthesis.

| | | | |
|---|---|---|---|
| *Bond lengths (Å)* | | | |
| Rh(1)–P(1) | 2.3197(14) | P(1)–C(8) | 1.829(5) |
| Rh(1)–P(2) | 2.3180(13) | P(1)–C(14) | 1.837(4) |
| Rh(1)–Cl(1) | 2.3730(13) | P(2)–C(20) | 1.831(4) |
| Rh(1)–C(1) | 1.818(5) | P(2)–C(26) | 1.839(4) |
| C(1)–O(1) | 1.141(5) | P(2)–C(32) | 1.821(5) |
| *Bond angles (°)* | | | |
| P(1)–Rh(1)–P(2) | 176.12(5) | P(2)–Rh(1)–C(1) | 91.91(14) |
| P(1)–Rh(1)–C(1) | 91.86(14) | P(2)–Rh(1)–Cl(1) | 87.26(4) |
| P(1)–Rh(1)–Cl(1) | 89.06(4) | C(1)–Rh(1)–Cl(1) | 174.72(15) |

Complex **34** crystallises from dichloromethane as burgundy prisms in the triclinic space group $P\bar{1}$. The molecular structure is given in Figure 3.16 with selected bond lengths and angles listed in Table 3.10. All measured bond lengths and angles are in good agreement with literature values for this compound.[30]

.

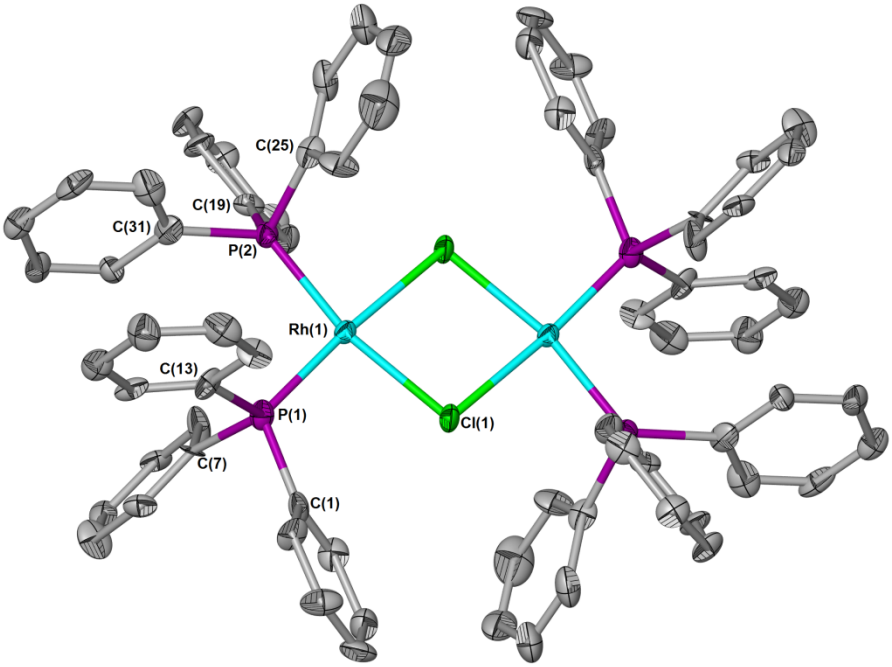


**Figure 3.16** Molecular structure of the chloro bridged rhodium dimer, **34,** showing the numbering scheme. Thermal ellipsoids set at 50 % probability. Hydrogen and atoms and solvent molecules are omitted for clarity.

**Table 3.10** Selected bond lengths (Å) and angles (°) of **34** with estimated standard deviations in parenthesis.

| | | | |
|---|---|---|---|
| *Bond lengths (Å)* | | | |
| Rh(1)–P(1) | 2.205(5) | P(1)–C(13) | 1.87(2) |
| Rh(1)–P(2) | 2.221(5) | P(2)–C(19) | 1.873(18) |
| Rh(1)–Cl(1) | 2.404(4) | P(2)–C(25) | 1.837(19) |
| P(1)–C(1) | 1.854(19) | P(2)–C(31) | 1.855(18) |
| P(1)–C(7) | 1.845(18) | | |
| *Bond angles (°)* | | | |
| P(1)–Rh(1)–P(2) | 97.13(18) | Cl(1)–Rh(1)–Cl(1)' | 81.60(16) |
| P(1)–Rh(1)–Cl(1) | 94.03(16) | P(1)–Rh(1)–Cl(1)' | 175.40(18) |
| P(2)–Rh(1)–Cl(1) | 168.41(16) | | |

### *3.2.5 Attempts at catalytic C–H activation using the described complexes*

As mentioned in the introductory section, the ultimate aim of this part of the study was to explore the potential of mixed anhydride complexes as regioselective C–H activation catalysts. Based on findings by Carrión and Cole-Hamilton[31] with phosphinite Rh(I) systems as C–H activation catalysts, together with the earlier discussed success of mixed anhydride Rh(I) complexes as hydrogenation catalysts,[7] we envisaged that the mixed anhydride complexes presented in this study may also be functional as C–H activation catalysts for the selective functionalisation of saturated acids. The proposed catalytic cycle for this reaction is given in Scheme 3.4 (see Section 3.1) where the substrate is initially linked to phosphorus and selective C–H activation in the *α*-position is driven by the formation of a highly favoured 5-membered metallocycle. In the final stages of the proposed cycle, product release with concurrent introduction of a fresh substrate molecule is facilitated by a transesterification reaction at phosphorus.

Rh(I) complexes of ligand **1**, **8**, **10**, **12** and **13** were therefore, despite the facile rearrangements associated with these systems, tested for their potential as C–H activation catalysts. $[RhCl(PPh_3)_3]$ was used as pre-catalyst in all cases and converted *in situ* into the active catalysts by treatment with equimolar amounts of ligands **1**, **8**, **10**, **12** or **13**. Propanoic acid was used as substrate in all reactions involving **1**, **8** and **10** as ligands, while phenylacetic acid served as substrate in reactions with ligands **12** and **13**. Since the real product of interest was methyl methacrylate, formaldehyde was used as functionalisation agent in reactions involving propanoic acid as substrate. In successful reactions, propanoic acid would be converted to 3-hydroxy-2-methylpropanoic acid which would, under the employed reaction conditions (100–130 $^{o}$C), spontaneously eliminate water to yield 2-methylacrylic acid as product. This product can then be converted to MMA, in a separate step, by esterification with methanol.

Since the presence of water would lead to the hydrolysis of the mixed anhydride phosphorus ester bond, a dry source of formaldehyde was essential and for this reason paraformaldehyde was employed. Paraformaldehyde, however, has limited solubility in most reaction solvents and to ensure that catalysis is not hindered by this limitation, test reactions using ethene gas as functionalisation agent were also performed. Scheme 3.16 summarises preliminary reactions performed and the specific reaction conditions used. All reaction ratios and conditions were based on the literature procedure for the catalytic *ortho*-alkylation of phenol using $[RhCl(PPh_3)_2(Ph_2P(OPh)]$ as C-H activation catalyst.[31,32]

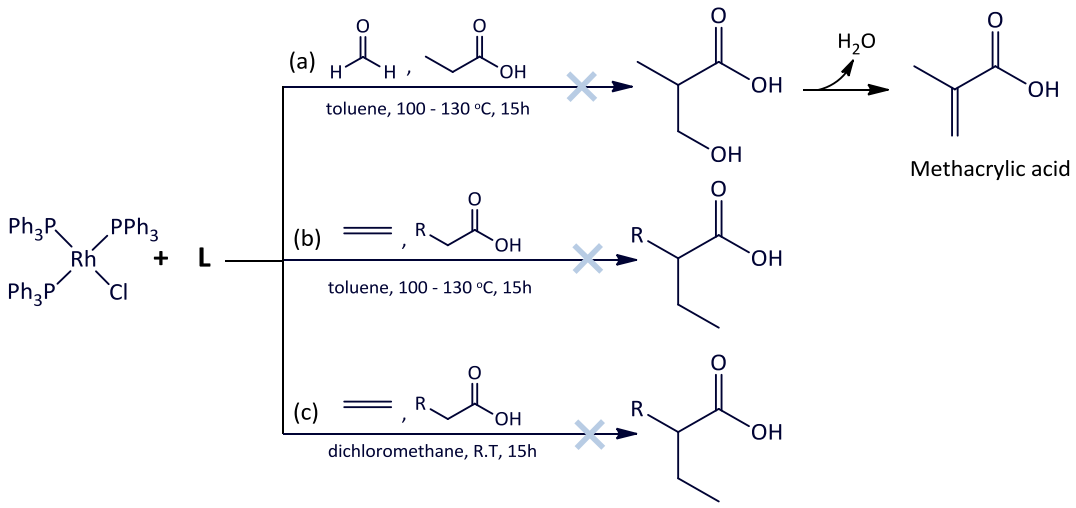


**Scheme 3.16** Attempts to functionalise catalytically saturated acids *via* selective C-H activation in their α-position, employing Rh(I) mixed anhydride complexes. Conditions: (a) L = ligands **1** or **10**; (b) L = ligands **1** or **10** (where R = $CH_3$) or **12–13** (where R = Ph), ethene 30 bar; (c) L = ligand **8**, ethene 30 bar. Ligand: $[RhCl(PPh_3)_3]$ : acid ratio in all cases 1 : 1 : 20 and where applicable ligand : paraformaldehyde ratio 1 : 300.

In reactions with mixed anhydrides **1** or **10** as ligands, propanoic acid as substrate, toluene as solvent and formaldehyde as functionalisation agent, bi-phasic product mixtures consisting of a pale yellow liquid phase and a pale yellow solid phase were obtained. GS-MS and NMR spectroscopic analysis of the liquid phase revealed propanoic acid unaltered with no traces of 3-hydroxy-2-methylpropanoic acid or methacrylic acid. Not surprisingly, in the case of **10** the solid phase contained, in addition to unreacted paraformaldehyde, significant amounts of the previously observed rearrangement product $[RhCl(CO)(PPh_3)_3]$ (**33**). In the case of **1**, however, the solid phase did not contain the rearrangement product $[RhCl(PPh_3)(Ph_2POPPh_2)]$ (**14**) typically associated with the thermal decomposition of $[RhCl(PPh_3)_3(Ph_2PO_2CCH_2CH_3)]$ (**15**). Instead, the rearrangement product $[RhCl(CO)(PPh_3)_3]$ (**33**), was again observed as the major component of the solid phase together with unreacted paraformaldehyde.

Reactions employing mixed anhydrides **1**, **10**, **12** or **13** as ligands, propanoic acid as substrate, toluene as solvent and ethene as functionalisation agent all had the same outcome as reactions involving paraformaldehyde with the final product mixtures consisting of bright yellow liquid phases while yellow crystals analysing as $[RhCl(CO)(PPh_3)_2]$ (**33**) lined the inner walls of the autoclave. GC-MS and NMR spectroscopic analysis of the obtained liquid phases revealed the parent acids unaltered and the absence of any desired reaction products.

Given that elevated temperatures increase the rate of rearrangement of mixed anhydride complexes, and additional reaction using **8** as ligand, ethene as trapping agent and dichloromethane as solvent was performed at room temperature. This too, however, did not bring about the catalytic conversion of propanoic acid to 2-methylbutanoic acid.

## 3.3 Conclusions

Herein the coordination chemistry of a series of Rh(I) and Ru(II) complexes derived from mixed anhydrides **1** and **7-13** was described. The present work has shown that these complexes spontaneously rearrange in solution *via* a number of pathways, with the pathway of choice dependent on the mixed anhydride employed, the auxiliary ligands present as well as the nature of the metal centre. Where very unstable (acyloxy)diphenylphosphines were reacted with $[RhCl(PPh_3)_3]$, the resultant complexes could only be observed *in situ* with isolation thereof unfeasible. These complexes were found to favour rearrangements that led to the formation of stable $[RhCl(PPh_3)_3(Ph_2POPPh_2)]$ in which the POP type ligand is coordinated in a chelating fashion.

The reaction of **1** with $[\{RhCl(COE)_2\}_2]$, devoid of $PPh_3$ ligands, afforded the mixed anhydride complex $[\{RhCl(Ph_2PO_2CCH_2CH_3)_2\}_2]$ which displayed increased stability. However, despite this increase in stability, the latter also rearranged in solution over time to form the POP dimer $[\{RhCl(Ph_2POPPh_2)\}_2]$ and $[\{RhCl\{(Ph2PO)_2H\}(OCCH_2CH_3)\}_2]$ as the major products. Plausible mechanisms for the formation of these products could be proposed, although more advanced mechanistic studies are required to have a more conclusive answer.

By changing to $[RuCl_2(PPh_3)_3]$ as metal precursor in reactions with **1**, the octahedral complex *cis*-$[RhCl_2(Ph_2PO_2CCH_2CH_3)_2]$ containing two chloride ligands in axial positions and two molecules of **1** coordinated in a chelating fashion *via* phosphorus and the carbonyl oxygen in the equatorial plane were obtained. This structure could also be confirmed by X-ray crystallography. The mentioned complex is indefinitely stable in the solid state and could be obtained analytically pure and in very high yield. In solution, however, this complex rearranged to furnish the Ru(II) chloro-bridged dimer $[\{RuCl_2(Ph_2POH)(Ph_2PO_2CCH_2CH_3)\}_2]$.

$[RhCl(PPh_3)_2(L)]$ complexes of (propionyl)phosphite ligands **7**–**8**, underwent spontaneous rearrangements in solution, similar to those observed for reactions with **1**, to afford complexes containing POP ligands coordinated in a bridging rather than chelating fashion. In contrast, $[RhCl(PPh_3)_2(L)]$ complexes derived from the much more stable (acyl)phosphite ligands **9**,**10**, **12** and **13**, could be obtained in high yield and purity and did not rearrange to POP complexes. Instead, the mixed anhydride ligands present in these complexes underwent decarbonylation when left in solution for a period of 1-2 days to give $[RhCl(CO)(PPh_3)_3]$, $[\{RhCl(PPh_3)_2\}_2]$ and $(RO)_2P(O)H$ as the major products of decay.

Owing to their thermal lability, $[RhCl(PPh_3)_2(L)]$ complexes (where L = **1**, **8**, **9**–**13**) did not show any potential as C–H activation catalysts. All attempts to employ these complexes as catalysts in the catalytic functionalisation of the $\alpha$-C–H bonds in saturated carboxylic acids were hindered by their facile rearrangement at elevated temperatures. In all cases, employed mixed anhydride complexes were converted to the inactive CO complex, $[RhCl(CO)(PPh_3)_2]$, thus preventing the occurrence of catalytic conversion.

## 3.4 Experimental

### *3.4.1 General materials, methods and instruments*

Reactions were carried out under dinitrogen gas ($N_2$, passed through a column of dichromate adsorbed on silica) using standard Schlenk, vacuum-line and cannula techniques. All glassware was flame-dried under vacuum. Triethylamine ($NEt_3$) and chlorodiphenylphosphine ($Ph_2Cl$) were purchased from Aldrich and distilled under $N_2$ prior to use. Before distilling, the $NEt_3$ was dried over potassium hydroxide (KOH) pellets. Sodium propanoate were also purchased from Aldrich and dried azeotropically with toluene before use. Cyclooctene, triphenylphosphine, paraformaldehyde, sodium tertiarybutoxide and isopropanol were purchased from Aldrich and used as received. Propanoic acid, purchased from BDH laboratories, was dried over $Na_2CO_3$ and distilled under $N_2$ prior to use. All gases were purchased from BOC gases. $[RhCl(PPh_3)_3]$ was prepared from $[RhCl_3{\cdot}3H_2O]$ and $PPh_3$, while $[RuCl_2(PPh_3)_4]$ and $[RuCl_2(PPh_3)_3]$ were prepared from $[RuCl_3{\cdot}3H_2O]$ and $PPh_3$, using standard literature procedures.[33,34] $[RhCl_3{\cdot}3H_2O]$ was purchased from either Engelhard or Alfa Aesar and $[RuCl_3{\cdot}3H_2O]$ from Strem Chemicals.

$[\{RhCl(COE)_2\}_2]$ (where COE = cyclooctene) was prepared from $[RhCl_3 \cdot 3H_2O]$ and cyclooctene using a literature procedure.[35]

Toluene, thf, diethyl ether and hexane were dried using a Braun Solvent Purification System and degassed by additional freeze-pump-thaw cycles when deemed necessary. Methanol and ethanol was distilled under nitrogen from magnesium. Deuterated dichloromethane and chloroform were purchased from Aldrich and dried over phosphorus pentoxide ($P_2O_5$), degassed *via* three freeze-pump-thaw cycles and trap-to-trap distilled prior to use.

NMR spectra were recorded on a Bruker Avance 300 FT or Bruker Avance II 400 MHz spectrometer ($^1H$ NMR at 300/400 MHz, $^{13}C\{^1H\}$ NMR at 75/100 MHz and $^{31}P\{^1H\}$ NMR at 121/162 MHz) with chemical shifts δ reported relative to tetramethylsilane (TMS)($^1H$, $^{13}C\{^1H\}$) or 85 % $H_3PO_4$ ($^{31}P\{^1H\}$) as external reference. $^1H$ and $^{13}C\{^1H\}$ NMR spectra were referenced internally to deuterated solvent resonances which were referenced relative to TMS.

Solid state IR spectra were recorded using pressed KBr pellets on a Perkin Elmer Spectrum GX IR spectrometer. Elemental analysis was performed by the University of St. Andrews microanalytical service using a Carlo Erba CHNS/O microanalyser. Melting points were determined on a Gallenkamp apparatus and are uncorrected. Mass spectra were recorded either by the EPSRC National Mass Spectrometry Service Centre, Swansea on a Thermofisher LTQ Orbitrap XL high resolution instrument coupled to an Advion TriVersa NanoMate electrospray infusion system or by the Mass Spectrometry Service Centre at the University of St. Andrews using either of a Micromass GCT EI/CI or a Micromass LCT ES instrument.

GC-MS chromatograms were recorded on a Hewlett Packard 6890 series GC system equipped with an Agilent J&W HP-1 general purpose column (fused silica capillary) and an HP 5973 Mass selective detector for both qualitative and quantitative analysis. Method: flow rate 1 ml $min^{-1}$ (He carrier gas), split ratio 100:1, starting temperature 50 $^{\circ}C$ (4 min) ramp rate 20 $^{\circ}C$ $min^{-1}$ to 130 $^{\circ}C$ (2 min), ramp rate 20 $^{\circ}C$ $min^{-1}$ to 220 $^{\circ}C$ (15.5 min).

### *3.4.2 Single crystal X-ray structure determinations*

A table containing a summary of the crystal data collection and refinement paramaters of compounds **22**–**24**, **29**–**31**, **33** and **34** can be found in Appendix 1. Data sets were collected on a Rigaku Mo MM007 (dual port) high brilliance diffractometer with graphite monochromated

MoK$\alpha$ radiation ($\lambda$ = 0.71075 Å). The diffractometer is fitted with Saturn 70 and Mercury CCD detectors and two XStream LT accessories. Data reduction was carried out with standard methods using the software package Bruker SAINT,[36] SMART,[37] SHELXTL[38] and and Rigaku CrystalClear, CrystalStructure, HKL2000. All the structures were solved using direct methods and conventional difference Fourier methods. All non-hydrogen atoms were refined anisotropically by full-matrix least squares calculations on $F^2$ using SHELX-97[39] within an X-seed[40,41] environment. The hydrogen atoms were fixed in calculated positions. Figures were generated with X-seed and POV Ray for Windows, with the displacement ellipsoids at 50 % probability level unless stated otherwise. Further information is available on request from Prof. Alexandra Slawin at the School of Chemistry, University of St. Andrews.

### *3.4.3 Synthetic procedures*

***Attempts to prepare [RhCl(PPh$_3$)$_2$(Ph$_2$PO$_2$CCH$_2$CH$_3$)], 15***

***Method 1:*** A solution of **1** (0.05 g, 0.19 mmol) in thf (4 ml) was added dropwise with a syringe to a solution of [RhCl(PPh$_3$)$_3$] (0.18 g, 0.19 mmol) in thf (30 ml) at -10 $^o$C under an inert atmosphere of dinitrogen. This reaction mixture was allowed to stir for 1 h 20 min at -10 $^o$C. During this time the deep red coloured solution underwent a colour change to yield an orange solution. The reaction mixture was filtered over anhydrous MgSO$_4$ while keeping the filtrate temperature below 0 $^o$C. The filtrate was subsequently evaporated to dryness under reduced pressure. The resulting orange solid was washed with diethyl ether (2 × 10 ml) and hexane (3 × 10 ml) and dried *in vacuo* to yield an orange solid. NMR analysis of the solid indicated the composition thereof to be a mixture of rearrangement products and Wilkinson's catalyst.

***Method 2:*** The procedure for method 2 is exactly the same as described for method 1, with the only difference being a reduction in the reaction time from 1 h 20 min. to only 40 min. The work-up of the reaction was carried out in the exact same manner as described for method 2 to yield a light orange solid. NMR spectra obtained for this solid agreed closely with those of the product obtained with method 1.

***Method 3:*** A solution of **1** (0.06 g, 0.23 mmol) in dichloromethane (5 ml) was added to a solution of [RhCl(PPh$_3$)$_3$] (0.22 g, 0.23 mmol) in dichloromethane (25 ml) at -10 $^o$C under an

inert atmosphere of dinitrogen. Upon addition of the phosphinite ligand, the deep-red colour of the solution lightened to result in an orange solution. The reaction mixture was stirred for 30 min at -10 °C. The reaction mixture was filtered over anhydrous $MgSO_4$ while maintaining the filtrate temperature below 0 °C. The filtrate was subsequently evaporated to dryness under reduced pressure to yield an oily orange solid. The crude product washed with diethyl ether (2 × 20 ml) and hexane (4 × 10 ml) and dried *in vacuo* to yield an orange solid. NMR analysis of the solid indicated the composition thereof to be a mixture of rearrangement products, Wilkinson catalyst and a small amount of the desired product.

***Method 4:*** A solution of **1** (0.33 g, 1.28 mmol) in dichloromethane (5 ml) was added, without delay after solvation, to a solution of $[RhCl(PPh_3)_3]$ (0.19 g, 0.20 mmol) in dichloromethane (15 ml) at -10 °C. The reaction mixture was allowed to stir for 1 h during which time the original deep burgundy colour of the solution lightened to yield an orange solution. After the 1 h stirring period, the mixture was evaporated to dryness under vacuum and the resulting residue extracted with diethyl ether (3 × 20 ml). The ether soluble fraction was separated from the insoluble light orange precipitate and the ether removed under reduced pressure. Both residues were analysed by means of NMR spectroscopy.

### *In situ NMR experiment for monitoring the formation and rearrangement of $[RhCl(PPh_3)_2(Ph_2PO_2CCH_2CH_3)]$, 15*

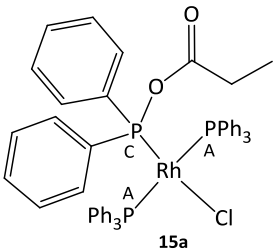

**15a**

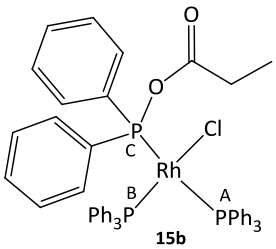

**15b**

A solution of **1** (0.06 g, 0.08 mmol) in chloroform-$d_1$ (10 ml) was added, directly after solvation, to $[RhCl(PPh_3)_3]$ (0.06, 0.07 mmol) at approximately -10 °C. A small volume of the mixture was immediately transferred to an NMR tube and subjected to $^{31}P$ NMR analysis at -10 °C. Several spectra, at regular intervals of approximately 5 min., were recorded at this temperature. The reaction mixture was allowed to stand for 2 h at approximately -10 °C, after which time another sample was taken and analysed by means of NMR spectroscopy. $^{31}P\{^1H\}$ NMR (121 MHz, $CDCl_3$): **15a** $\delta_P$ = 32.6 (dd, $^1J_{PA\text{-}Rh}$ = 128.7 Hz, $^2J_{PA\text{-}PC}$ = 37.5 Hz; $P_A$), 138.2 (dt, $^1J_{PC\text{-}Rh}$ = 213.4 Hz, $^2J_{PC\text{-}PA}$ = 37.5 Hz; $P_C$). **15b** $\delta_P$ = 31.1 (ddd, $^1J_{PA\text{-}Rh}$ = 133.2 Hz, $^2J_{PA\text{-}PB}$ = 40.9 Hz, $^2J_{PA\text{-}PC}$ = 383.6 Hz; $P_A$), 129.7 (ddd, $^1J_{PC\text{-}Rh}$ = 175.9 Hz, $^2J_{PC\text{-}PA}$ = 383.6 Hz, $^2J_{PC\text{-}PB}$ = 17.3 Hz ; $P_C$). $P_B$ could not be measured owing to extensive overlap of resonances in the relevant region.

### *[RhCl(PPh$_3$)$_2$(Ph$_2$PCl)], 18*

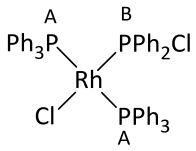


*Procedure adapted from literature procedure.*[13] $Ph_2PCl$ (0.14 g, 0.12 ml, 0.65 mmol) was added dropwise to a solution of [$RhCl(PPh_3)_3$] (0.61 g, 0.66 mmol) in dichloromethane (10 ml) at room temperature. The reaction mixture was allowed to stir for 2 h after which the mixture was reduced to dryness under vacuum. The crude oily orange product was washed with ether (3 × 30 ml) and dried *in vacuo* to yield the product as a bright orange solid (yield: 0.56 g, 96 %).$^1$H NMR (300 MHz, $CDCl_3$): $\delta_H$ = 6.87–7.87 (m, 40H; Ph). $^{31}P\{^1H\}$ NMR (121 MHz, $CDCl_3$): $\delta_P$ = 32.4 (dd, $^1J_{PA\text{-}Rh}$ = 138.0 Hz, $^2J_{PA\text{-}PB}$ = 40.1 Hz; $P_A$), 113.7 (dt, $^1J_{PB\text{-}Rh}$ = 230.1 Hz, $^2J_{PB\text{-}PA}$ = 40.1 Hz; $P_B$).

### *Attempts to prepare 15 from [RhCl(PPh$_3$)$_2$(Ph$_2$PCl)] (18)*

***Method 1 (at low temperature):*** [$RhCl(PPh_3)_2(Ph_2PCl)$] (0.25 g, 0.28 mmol) was dissolved in dichloromethane (20 ml) and cooled to -10 $^o$C. To this solution, propanoic acid (0.03 ml, 0.43 mmol) and $NEt_3$ (0.06 ml, 0.43 mmol) were added *via* syringe under an inert atmosphere of dinitrogen. After a 15 min stirring period, a small volume of the reaction mixture was transferred to an NMR tube and subjected to NMR analysis. The remainder of the reaction mixture was allowed to stir for a further 10 min before removal of the solvent at -10 $^o$C under reduced pressure. The resulting orange solid was washed with ether (2 × 20 ml) and both the ether extract and the remaining solid were dried *in vacuo*. The ether extract, after removal of the solvent, yielded a dark orange oily residue while the solid that proved insoluble in ether was isolated as a light orange solid. Both products were analysed by means of NMR spectroscopy.

***Method 2 (at higher temperatures):*** *trans*-[$RhCl(PPh_3)_2(Ph_2PCl)$] (0.20 g, 0.23 mmol) was suspended in toluene (10 ml). Propanoic acid (0.02 ml, 17 mg, 0.23 mmol) was added to this suspension *via* syringe. To this, a suspension of $NaO^tBu$ (0.05 g, 0.48 mmol) in toluene (10 ml) was added and the reaction mixture was subsequently heated at 80 $^o$C for 1 h. During this period of time the colour of the solution lightened somewhat, but not significantly. After the 1 h stirring period, the solution was cooled to room temperature and the toluene removed under reduced pressure. The remaining residue was taken up into ether and filtered over celite under an inert atmosphere of $N_2$. The collected filtrate was reduced to dryness under vacuum and the resulting dark orange solid was analysed by means of NMR spectroscopic techniques.

***Method 3 (with sodium propanoate):*** A solution of sodium propanoate (0.13 g, 0.14 mmol) in dichloromethane (5 ml) was added to a solution of $[RhCl(PPh_3)_2(Ph_2PCl)]$ (0.12 g, 0.14 mmol) in dichloromethane (15 ml) at room temperature. The reaction mixture was allowed to stir for 1 h during which time the original deep burgundy colour of the solution lightened slightly to yield an orange solution. After the 1h stirring period, the mixture was reduced to dryness under vacuum and the resulting residue extracted with diethyl ether (3 × 20 ml). The ether soluble fraction was separated from the insoluble light orange precipitate and the ether removed under reduced pressure.

### *$[\{RhCl(Ph_2PO_2CCH_2CH_3)_2\}_2]$, 19*

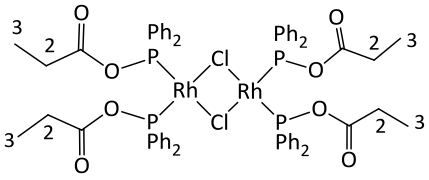

A solution of **1** (0.09 g, 0.35 mmol) in dichloromethane (5 ml) was added to a solution of $[\{RhCl(COE)_2\}_2]$ (0.06 g, 0.088 mmol) in dichloromethane (10 ml) at -10 °C. Upon addition, the reaction colour changed from orange to light yellow. The mixture was stirred for 30 min at -10 °C, after which the solution was concentrated and the product precipitated with hexane (20 ml). The resulting orange solid was isolated, washed with hexane (2 × 20ml) and dried *in vacuo*. Although the isolated product contained the title product, the final product was contaminated with significant amounts of by-products generated by spontaneous rearrangement reactions. These by-products could not be separated from the title product without bringing about further rearrangement (yield: 14% based on $^{31}P$ NMR integrals). $^{1}H$ NMR (300 MHz, $CD_2Cl_2$): $\delta_H$ = 0.74 (t, 3H, $^{3}J$ = 7.2 Hz; $H^3$), 3.22 (q, 2H, $^{3}J$ = 7.2 Hz; $H^2$), 7.02–7.77 (m, 40H, Ph). $^{31}P\{^{1}H\}$ NMR (121 MHz, $CD_2Cl_2$): $\delta_P$ = 135.1 (d, $^{1}J_{P\text{-}Rh}$ = 228.1 Hz; P).

### *$[\{RhCl(C(O)CH_2CH_3)\{(Ph_2PO)_2H\}\}_2]$, 22*

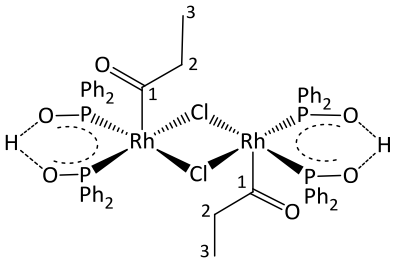

The rearrangement product, **22**, crystallised as yellow prisms at room temperature from a chloroform-$d_1$ solution of the product mixture obtained for **19**. These crystals were isolated and analysed by X-ray diffraction and NMR spectroscopy. $^{1}H$ NMR (300 MHz, $CD_2Cl_2$): $\delta_H$ = 0.47 (t, 3H, $^{3}J$ = 7.2 Hz; $H^3$), 3.05 (q, 2H, $^{3}J$ = 7.2 Hz; $H^2$), 6.99–7.78 (m, 40H, Ph). $^{31}P\{^{1}H\}$ NMR (121 MHz, $CD_2Cl_2$): $\delta_P$ = 83.7 (d, $^{1}J_{P\text{-}Rh}$ = 160.5 Hz; P).

### *[RuCl$_2$(Ph$_2$PO$_2$CCH$_2$CH$_3$)$_2$], 23*

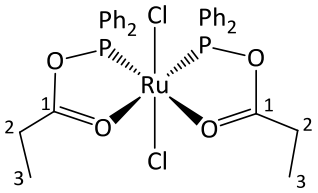

A solution of **1** (0.21 g, 0.80 mmol) in dichloromethane (5 ml) was added to a solution of [RuCl$_2$(PPh$_3$)$_3$] (0.34 g, 0.35 mmol) or [RuCl$_2$(PPh$_3$)$_4$] (0.43 g, 0.35 mmol) in dichloromethane (10 ml) at room temperature. Upon addition the reaction mixture colour immediately became lighter until finally a bright orange solution was observed. The reaction mixture was allowed to stir at room temperature for 2 h after which the mixture was concentrated and the product precipitated by the addition of hexane (20 ml). The resulting light orange precipitate was then isolated, washed with hexane (2 × 20 ml) and dried *in vacuo* to yield the analytically pure product as a bright light orange solid (yield: 0.21 g, 87 %). Single crystals in the form of orange platelets suitable for analysis by single crystal X-ray diffraction could be obtained by slow diffusion of diethyl ether into a toluene solution of **23** at room temperature. *Anal.* Calculated (%) for $C_{30}H_{30}Cl_2O_4P_2Ru$: C 52.34, H 4.39; Found C 51.87, H 3.95. $^1$H NMR (400 MHz, $CDCl_3$): $\delta_H$ = 1.44 (t, 3H, $^3J$ = 7.4 Hz; H$^3$), 2.98 (q, 2H, $^3J$ = 7.4 Hz; H$^2$), 7.20–7.42 (m, 20H; Ph). $^{13}$C{$^1$H} NMR (100 MHz, $CDCl_3$): $\delta_C$ = 9.6 (s; C$^3$), 28.7 (s; C$^2$), 127.8 (m, $J_{C\text{-}P}$ = 5.7 Hz; PPh–C$^{meta}$), 131.7 (s; PPh–C$^{para}$), 133.0 (m, $J_{C\text{-}P}$ = 5.7 Hz; PPh-C$^{ortho}$), 134.8 (d, $^1J_{C\text{-}P}$ = 56.0 Hz; PPh–C$^{ipso}$), 179.4 (s; C$^1$). $^{31}$P{$^1$H} NMR (161 MHz, $CDCl_3$): $\delta_P$ = 188.6 (s; P). IR (KBr): $\tilde{\nu}$ = 3054 [w, sp$^2$ $\nu$(C–H)], 2940 [w, sp$^3$ $\nu$(C–H)], 1649 [st, $\nu$(C=O)], 1434–1364 [st, Ar $\nu$(C=C)], 694 [m, $\nu$(P–O)]. ES-MS: *m/z* (%) = 653 (100) [M – Cl]$^+$.

### *[{RuCl$_2$(Ph$_2$PO$_2$CCH$_2$CH$_3$)(Ph$_2$POH}$_2$], 24*

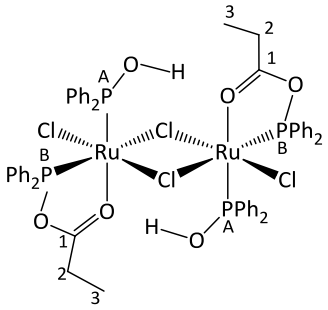

Compound **23** although stable in the solid state, rearranges to the chloro-bridged Ru(II) dimer **24** when left standing in solution. Single crystals of **24** suitable for X-ray analysis were obtained as orange prisms during initial attempts to crystallise **23** by vapour diffusion of pentane into a chloroform-$d_1$ solution of the **23** at room temperature. $^1$H NMR (300 MHz, $CDCl_3$): $\delta_H$ = 1.18 (t, 3H, $^3J$ = 7.5 Hz; H$^3$), 2.43 (qd, 2H, $^3J$ = 7.5 Hz, $^4J_{H\text{-}P}$ = 1.6 Hz; H$^2$), 6.51–8.09 (m, 40H; Ph). $^{31}$P{$^1$H} NMR (161 MHz, $CDCl_3$): $\delta_P$ = 132.5 (d, $^2J_{PA\text{-}PB}$ = 44.2; P$_A$), 188.3 (d, $^2J_{PB\text{-}PA}$ = 44.2; P$_B$).

### *[RhCl(PPh$_3$)$_2$(propionyl-(1,1'-biphenyl-2,2'-diyl)phosphite)], 25*

A solution of ligand **7** (0.08 g, 0.27 mmol) in dichloromethane (15 ml) was added to a solution of [RhCl(PPh$_3$)$_3$] (0.25 g, 0.27 mmol) in dichloromethane (10 ml) at room temperature. Upon

addition the reaction mixture colour changed from burgundy to light yellow. Following a 30 minute stirring period, the reaction mixture was reduced to dryness, the residue washed with hexane (4 × 20 ml) and then dried *in vacuo* to furnish the product as a yellow solid. This major product was, however, contaminated with the ligand disproportionation product as well as the rearrangement product **26**. The title product could not be separated from these by-products using standard separation techniques. For complex **25** - $^{1}$H NMR (300 MHz, $CD_2Cl_2$): $\delta_H$ = 0.87 (t, 3H, $^{3}J$ = 7.5 Hz; $H^3$), 1.54 (q, 2H, $^{3}J$ = 7.5 Hz; $H^2$), 6.60–7.7 (m, 2H; Ph). $^{13}C\{^{1}H\}$ NMR (75 MHz, $CD_2Cl_2$): $\delta_C$ = 8.8 (s; $C^3$), 28.5 (s; $C^2$), 122.3 (s; $C^5$ / $C^{11}$), 125.7 (s; $C^7$ / $C^{13}$), 127.8 (d, $^{3}J_{C\text{-}P}$ = 4.7 Hz; PPh-$C^{meta}$), 129.7 (s; PPh-$C^{para}$), 130.0 (s; $C^6$ / $C^{12}$), 131.0 (s; $C^8$ / $C^{14}$), 135.5 (d, $^{2}J_{C\text{-}P}$ = 6.0 Hz; PPh-$C^{ortho}$), 135.9 (s; $C^9$ / $C^{15}$), 137.7 (d, $^{1}J_{C\text{-}P}$ = 11.5 Hz; PPh-$C^{ipso}$), 149.5 (d, $^{2}J_{C\text{-}P}$ = 10.6 Hz; $C^4$ / $C^{10}$), 170.2 (d; $^{2}J_{C\text{-}P}$ = 3.4 Hz; $C^1$). $^{31}P\{^{1}H\}$ NMR (121 MHz, $CD_2Cl_2$): $\delta_P$ = 36.1 (dd, $^{1}J_{PA\text{-}Rh}$ = 132.7 Hz, $^{2}J_{PA\text{-}PB}$ = 46.6 Hz; $P_A$), 134.5 (dt, $^{1}J_{PB\text{-}Rh}$ = 321.8 Hz, $^{2}J_{PB\text{-}PA}$ = 46.6 Hz; $P_B$). IR (KBr): $\tilde{\nu}$ = 3054 [w, $sp^2$ $\nu$(C–H)], 3009 [w, $sp^3$ $\nu$(C–H)], 1761 [w, $\nu$(C=O)], 1498–1434 [st, Ar $\nu$(C=C)], 694 [st, $\nu$(P–O)]. For complex **26** - $^{31}P\{^{1}H\}$ NMR (121 MHz, $CD_2Cl_2$): $\delta_P$ = 21.7 (dd, $^{1}J_{PA\text{-}Rh}$ = 113.0 Hz, $^{2}J_{PA\text{-}PC}$ = 19.0 Hz; $P_A$), 79.9 (dt, $^{1}J_{PC\text{-}Rh}$ = 260.5 Hz, $^{2}J_{PB\text{-}PA}$ = 19.0 Hz; $P_C$).

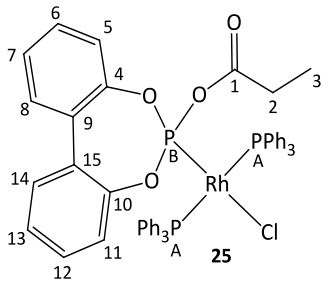

**25**

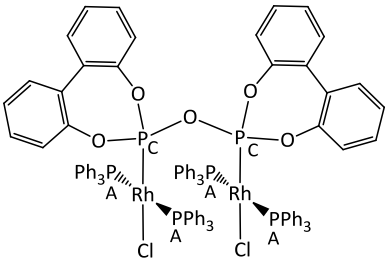

**26**

### *[RhCl(PPh$_3$)$_2${(R)-Propionyl-(1,1'-binaphthyl-2,2'-diyl)phosphite}], 27*

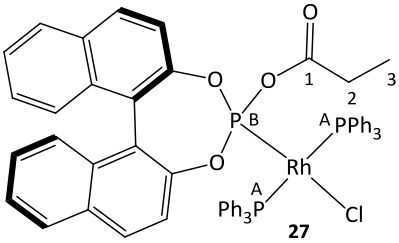

**27**

Compound **27** was prepared using a similar method to that described for **25**, by treating a solution of $[RhCl(PPh_3)_3]$ (0.22 g, 0.24 mmol) in dichloromethane (10 ml) with a solution of **8** (0.09 g, 0.24 mmol) in dichloromethane (15 ml) at room temperature for 1 h. The title product was obtained as an orange solid which, despite representing the major product, was contaminated by the rearrangement product **28**. These products could not be separated from **27,** using standard purification techniques, without effecting further rearrangement. For complex **27** - $^{1}$H NMR (300 MHz, $CD_2Cl_2$): $\delta_H$ = 0.91 (t, 3H, $^{3}J$ = 6.6 Hz; $H^3$), 1.40 (m, 1H; $H^2$), 1.61 (m, 1H; $H^2$), 7.16–8.11 (m, 42H). $^{13}C\{^{1}H\}$ NMR (75 MHz, $CD_2Cl_2$): $\delta_C$ = 8.8 (s; $C^3$), 28.4 (s; $C^2$), 120.7 (s), 122.5 (s), 123.3 (s),123.9 (s), 125.4 (s), 125.8 (s), 126.6 (s), 127.1 (s), 127.5 (s), 127.7 (d, $^{3}J_{C\text{-}P}$ = 4.8 Hz; PPh-$C^{meta}$), 128.8 (s), 129.1 (s), 129.6 (s; PPh-$C^{para}$), 129.8

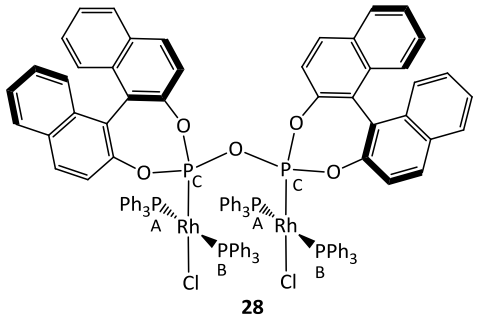

**28**

(s), 130.4 (s), 131.4 (s), 132.5 (s), 133.1 (s), (d, $^{2}J_{C\text{-}P}$ = 5.7 Hz; PPh-C$^{ortho}$), 135.8 (d, $^{1}J_{C\text{-}P}$ = 22.7 Hz; PPh-C$^{ipso}$), 147.6 (d, $^{2}J_{C\text{-}P}$ = 5.5 Hz), 148.7 (d, $^{2}J_{C\text{-}P}$ = 12.9 Hz), 170.2 (d, $^{2}J_{C\text{-}P}$ = 3.0 Hz; C$^{1}$). $^{31}$P{$^{1}$H} NMR (121 MHz, $CD_2Cl_2$): $\delta_P$ = 35.2 (bdd, $^{1}J_{PA\text{-}Rh}$ = 132.9 Hz, $^{2}J_{PA\text{-}PB}$ = 46.2 Hz; $P_A$), 133.9 (dt, $^{1}J_{PB\text{-}Rh}$ = 322.5 Hz, $^{2}J_{PB\text{-}PA}$ = 46.2 Hz; $P_B$). IR (KBr): $\tilde{\nu}$ = 3049 [m, sp$^2$ $\nu$(C–H)], 3000–2960 [w, sp$^3$ $\nu$(C–H)], 1751 [w, $\nu$(C=O)], 1505–1432 [m, Ar $\nu$(C=C)], 692 [st, $\nu$(P–O)]. For complex **28** (ABMX spin system) – $^{31}$P{$^{1}$H} NMR (121 MHz, $CD_2Cl_2$): $\delta_P$ = 20.6 (ddd, $^{1}J_{PA\text{-}Rh}$ = 113.3 Hz, $^{2}J_{PA\text{-}PB}$ = 370.5 Hz, $^{2}J_{PA\text{-}PC}$ = 17.2 Hz; $P_A$), 20.5 (ddd, $^{1}J_{PB\text{-}Rh}$ = 111.3 Hz, $^{2}J_{PB\text{-}PA}$ = 370.5 Hz, $^{2}J_{PB\text{-}PC}$ = 21.2 Hz; $P_B$), 84.7 (ddd, $^{1}J_{PC\text{-}Rh}$ = 261.1 Hz, $^{2}J_{PC\text{-}PA}$ = 17.2 Hz, $^{2}J_{PC\text{-}PB}$ = 21.2 Hz; $P_C$).

### *[RhCl(PPh$_3$)$_2${propionyl-(5,5',6,6'-tetramethyl-3,3'-di-tert-butyl-1,1'-biphenyl-2,2'-diyl)phosphite}], 29*

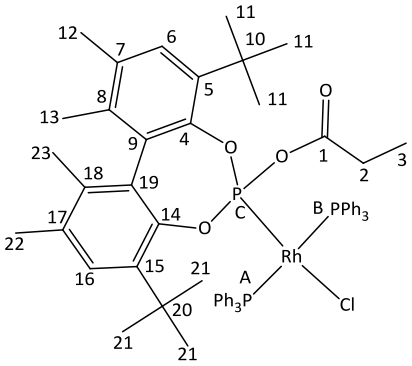

Compound **29** was prepared using a similar methodology to that which was described for the preparation of **25**. A solution of **9** (0.09 g, 0.20 mmol) in dichloromethane (15 ml) was added to a solution of [RhCl(PPh$_3$)$_3$] (0.19 g, 0.20 mmol) at room temperature. The reaction mixture was stirred at this temperature for 1 h during which time the solution colour changed from burgundy to light yellow. The mixture was subsequently stripped of all volatiles under reduced pressure and the resulting residue washed with hexane (3 × 10 ml) to yield the product as a bright yellow solid (yield: 0.17 g, 77 %). Crystals suitable for structure determination by X-ray diffraction were obtained as yellow platelets by cooling a concentrated solution of **29** in dichloromethane to -22 ºC. $^{1}$H NMR (300 MHz, $CD_2Cl_2$): $\delta_H$ = 0.20 (t, 3H, $^{3}J$ = 7.0 Hz; H$^{3}$), 0.84 (q, 2H, $^{3}J$ = 7.5 Hz; H$^{2}$), 1.37 (s, 9H; H$^{11}$), 1.50 (s, 3H; H$^{12}$), 1.55 (s, 3H; H$^{22}$), 1.74 (s, 9H; H$^{21}$), 2.09 (s, 3H; H$^{13}$), 2.26 (s, 3H; H$^{23}$), 6.91–8.31 (m, 32H; Ph). $^{13}$C{$^{1}$H} NMR (75 MHz, $CD_2Cl_2$): $\delta_C$ = 7.6 (s; C$^{3}$), 16.3 (s; C$^{13}$), 16.9 (s; C$^{23}$), 20.1 (s; C$^{12}$), 20.5 (s; C$^{22}$), 27.6 (s; C$^{2}$), 31.6 (s; C$^{11}$), 31.9 (s; C$^{21}$), 34.9 (s; C$^{10}$), 35.1 (s; C$^{20}$), 127.3 (d, $^{3}J_{C\text{-}P}$ = 8.1 Hz; PPh-C$^{meta}$), 128.0 (d, $^{3}J_{C\text{-}P}$ = 9.8 Hz; PPh-C$^{meta}$), 129.1 (s; PPh-C$^{para}$), 129.3 (s; PPh-C$^{para}$), 131.5 (s; C$^{7}$ / C$^{17}$), 132.2 (s; C$^{6}$), 132.4 (s; C$^{16}$), 132.6 (s; C$^{9}$ / C$^{19}$), 135.0 (d, $^{2}J_{C\text{-}P}$ = 8.9 Hz; PPh-C$^{ortho}$), 135.7 (d, $^{2}J_{C\text{-}P}$ = 8.9 Hz; PPh-C$^{ortho}$), 136.2 (s; C$^{8}$ / C$^{18}$), 136.6 (s; C$^{5}$ / C$^{15}$), 136.8 (d, $^{1}J_{C\text{-}P}$ = 51 Hz; PPh-C$^{ipso}$), 148.1 (s; C$^{4}$), 149.4 (s; C$^{14}$).

$^{31}P\{^{1}H\}$ NMR (121 MHz, $CD_2Cl_2$): $\delta_P$ = 34.4 (AB pattern, ddd, $^{1}J_{PA\text{-}Rh}$ = 138.2 Hz, $^{2}J_{PA\text{-}PC}$ = 44.3 Hz, $^{2}J_{PA\text{-}PB}$ = 349.5 Hz; $P_A$), 37.2 (AB pattern, ddd, $^{1}J_{PB\text{-}Rh}$ = 138.2 Hz, $^{2}J_{PB\text{-}PC}$ = 44.3 Hz, $^{2}J_{PB\text{-}PA}$ = 349.5 Hz; $P_B$), 129.3 (dt, $^{1}J_{PC\text{-}Rh}$ = 331.3 Hz, $^{2}J_{PC\text{-}PA}$ = $^{2}J_{PC\text{-}PB}$ = 44.3 Hz; $P_C$). IR (KBr): $\tilde{\nu}$ = 3054 [w, $sp^2$ $\nu$(C–H)], 2958–2866 [m, $sp^3$ $\nu$(C–H)], 1780 [m, $\nu$(C=O)], 1481–1393 [m, Ar $\nu$(C=C)], 695 [m, $\nu$(P–O)]. ES-MS: *m/z* (%) = 1083 (80) $[M - Cl]^+$, 821 (100) $[M - Cl - PPh_3]^+$, 627 (5) $[Rh(PPh_3)_2]^+$.

## *[RhCl(PPh$_3$)$_2${propionyl-(3,3',5,5'-tetra-tert-butyl-1,1'-biphenyl-2,2'-diyl)phosphite}], 30*

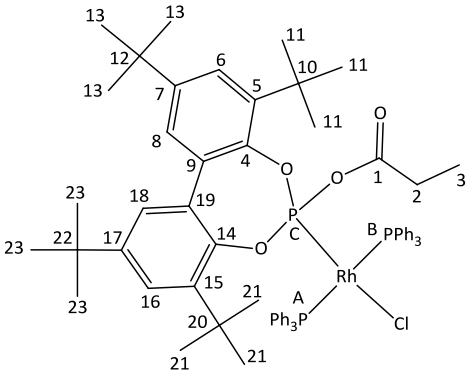


Using the same procedure as was described for the preparation of **25**, $[RhCl(PPh_3)_3]$ (0.44 g, 0.48 mmol) was reacted with an excess of ligand **10** (0.39 g, 0.76 mmol) at room temperature for 1 h. After the removal of all volatiles, the orange residue was washed with copious amounts of hexane (3 × 30 ml) to furnish the analytically pure title product as a bright yellow solid (yield: 0.52 g, 92 %). Crystals in the form of yellow needles suitable for analysis by X-ray diffraction were grown by slow diffusion of hexane into a concentrated solution of **30** in toluene at room temperature. Mp 220–222 °C (decomposed). *Anal.* Calculated (%) for $C_{67}H_{75}ClO_4P_3Rh$: C 68.45, H 6.43; Found C 68.45, H 6.64. $^{1}H$ NMR (300 MHz, $CD_2Cl_2$): $\delta_H$ = 0.21 (t, 3H, $^{3}J$ = 7.4 Hz; $H^3$), 0.88 (q, 2H, $^{3}J$ = 7.4 Hz; $H^2$), 1.32 (s, 18H; $H^{11}$ / $H^{21}$), 1.53 (s, 18H; $H^{13}$ / $H^{23}$), 6.96 (d, 2H, $^{4}J$ = 2.1 Hz; $H^6$ / $H^{16}$), 7.10 (m, 6H), 7.21 (m, 3H), 7.33 (m, 11H), 7.63 (m, 6H), 7.81 (bt, $J$ = 8.2 Hz, 6H). $^{13}C\{^{1}H\}$ NMR (75 MHz, $CD_2Cl_2$): $\delta_C$ = 7.7 (s; $C^3$), 27.1 (s; $C^2$), 31.6 (s; $C^{11}$ / $C^{21}$), 31.6 (s; $C^{13}$ / $C^{23}$), 34.8 (s; $C^{10}$ / $C^{20}$), 35.8 (s; $C^{12}$ / $C^{22}$), 124.4 (s; $C^6$ / $C^{16}$), 127.5 (d, $^{3}J_{C\text{-}P}$ = 8.8 Hz; PPh-$C^{meta}$), 128.1 (d, $^{3}J_{C\text{-}P}$ = 9.2 Hz; PPh-$C^{meta}$), 128.4 (s; $C^8$ / $C^{18}$), 129.4 (s; PPh-$C^{para}$), 134.9 (d, $^{2}J_{C\text{-}P}$ = 10.0 Hz; PPh-$C^{ortho}$), 136.4 (d, $^{2}J_{C\text{-}P}$ = 9.2 Hz; PPh-$C^{ortho}$), 136.4 (d, $^{1}J_{C\text{-}P}$ = 41.2 Hz; PPh-$C^{ipso}$), 139.2 (s; $C^5$ / $C^{15}$), 146.7 (s; $C^4$ / $C^{14}$), 145.7 (s; $C^7$ / $C^{17}$). $^{31}P\{^{1}H\}$ NMR (121 MHz, $CD_2Cl_2$): $\delta_P$ = 33.8 (AB pattern, ddd, $^{1}J_{PA\text{-}Rh}$ = 135.3 Hz, $^{2}J_{PA\text{-}PC}$ = 48.3 Hz, $^{2}J_{PA\text{-}PB}$ = 347.9 Hz; $P_A$), 38.2 (AB pattern, ddd, $^{1}J_{PB\text{-}Rh}$ = 135.3 Hz, $^{2}J_{PB\text{-}PC}$ = 48.3 Hz, $^{2}J_{PB\text{-}PA}$ = 347.9 Hz; $P_B$), 124.9 (dt, $^{1}J_{PC\text{-}Rh}$ = 331.8 Hz, $^{2}J_{PC\text{-}PA}$ = $^{2}J_{PC\text{-}PB}$ = 48.3 Hz; $P_C$). IR (KBr): $\tilde{\nu}$ = 3052 [m, $sp^2$ $\nu$(C–H)], 2956–2869 [st, $sp^3$ $\nu$(C–H)], 1775 [st, $\nu$(C=O)], 1477–1395 [m, Ar $\nu$(C=C)], 694 [m, $\nu$(P–O)]. ES-MS: *m/z* (%) = 1139 (100) $[M - Cl]^+$, 877 (35) $[M - Cl - PPh_3]^+$.

### *[RhCl(PPh$_3$)$_2${phenylacetyl-(5,5',6,6'-tetramethyl-3,3'-di-tert-butyl-1,1'-biphenyl-2,2'-diyl)phosphite}], 31*

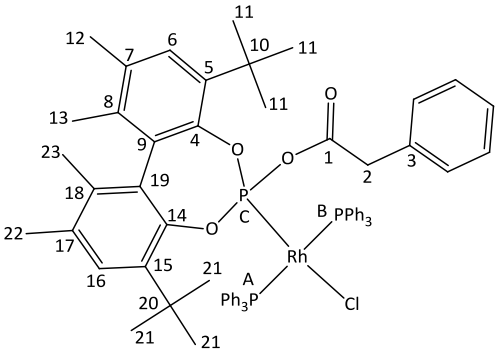

Compound **31** was prepared using the same procedure described for the preparation of **25**. A solution of **12** (0.18 g, 0.35 mmol) in dichloromethane (20 ml) was added to a solution of [RhCl(PPh$_3$)$_3$] (0.32 g, 0.35 mmol) in dichloromethane (20 ml) at room temperature. The reaction mixture was stirred at this temperature for 1 h. Removal of all volatiles under reduced pressure gave the crude product as an orange solid which could be purified by washing with hexane (3 × 20ml) (yield: 0.32 g, 78 %). Crystals suitable for X-ray structure determination were grown as yellow prisms by slowly cooling a concentrated solution of **31** in dichloromethane to -22 °C. Mp 199–204 °C (decomposed). $^1$H NMR (300 MHz, $CDCl_3$): $\delta_H$ = 1.38 (s, 9H; H$^{11}$), 1,76 (s, 9H; H$^{21}$), 1.49 (bs, 6H; H$^{12}$ / H$^{22}$), 2.04 (s, 3H; H$^{13}$), 2.22 (s, 3H; H$^{23}$), 2.33 (d, 1H, $^2J$ = 19.0 Hz; H$^2$), 2.61 (d, 1H, $^2J$ = 19 Hz; H$^2$), 6.52–7.84 (m, 37H, Ph). $^{13}$C{$^1$H} NMR (75 MHz, $CDCl_3$): $\delta_C$ = 16.5 (s; C$^{13}$), 17.1 (s; C$^{23}$), 20.4 (s; C$^{12}$), 20.5 (s; C$^{22}$), 31.7 (s; C$^{11}$), 32.0 (s; C$^{21}$), 35.0 (s; C$^{10}$ / C$^{20}$), 40.2 (s; C$^2$), 127.3 (d, $^3J_{C\text{-}P}$ = 8.8 Hz; PPh-C$^{meta}$), 127.9 (s; Ph–C$^{para}$), 128.1 (s; PPh-C$^{para}$), 128.3 (s; PPh-C$^{para}$), 128.8 (s; Ph–C$^{meta}$), 129.5 (s; Ph–C$^{ortho}$), 130.0 (s; C$^6$ / C$^{16}$), 131.5 (s; C$^9$), 132.0 (s; Ph–C$^{ipso}$), 132.4 (s; C$^{19}$), 132.8 (s; C$^7$), 133.4 (s; C$^{17}$), 134.8 (d, $^2J_{C\text{-}P}$ = 9.4 Hz; PPh-C$^{ortho}$), 135.9 (d, $^2J_{C\text{-}P}$ = 8.2 Hz; PPh-C$^{ortho}$), 136.4 (d, $^1J_{C\text{-}P}$ = 28.9 Hz; PPh-C$^{ipso}$), not observed due to overlap (C$^8$ / C$^{18}$), 137.2 (s; C$^5$ / C$^{15}$), 147.4 (s; C$^4$ / C$^{14}$). $^{31}$P{$^1$H} NMR (121 MHz, $CD_2Cl_2$): $\delta_P$ = 34.9 (AB pattern, ddd, $^1J_{PA\text{-}Rh}$ = 134.9 Hz, $^2J_{PA\text{-}PC}$ = 46.3 Hz, $^2J_{PA\text{-}PB}$ = 344.3 Hz; P$_A$), 37.8 (AB pattern, ddd, $^1J_{PB\text{-}Rh}$ = 134.9 Hz, $^2J_{PB\text{-}PC}$ = 46.3 Hz, $^2J_{PB\text{-}PA}$ = 344.3 Hz; P$_B$), 131.1 (dt, $^1J_{PC\text{-}Rh}$ = 332.7 Hz, $^2J_{PC\text{-}PA}$ = $^2J_{PC\text{-}PB}$ = 46.3 Hz; P$_C$). IR (KBr): $\tilde{\nu}$ = 3051 [m, sp$^2$ $\nu$(C–H)], 2955–2867 [m, sp$^3$ $\nu$(C–H)], 1764 [m, $\nu$(C=O)], 1482–1392 [st, Ar $\nu$(C=C)], 695 [m, $\nu$(P–O)]. ES-MS: *m/z* (%) = 1145 (100) [M – Cl]$^+$, 883 (43) [M – Cl – PPh$_3$]$^+$, 627 (8) [Rh(PPh$_3$)$_2$]$^+$.

### *[RhCl(PPh$_3$)$_2${phenylacetyl-(3,3',5,5'-tetra-tert-butyl-1,1'-biphenyl-2,2'-diyl)phosphite}], 32*

Using the same procedure as was described for the preparation of **25**–**31**, [RhCl(PPh$_3$)$_3$] (0.35 g, 0.38 mmol) was reacted with ligand **13** (0.22 g, 0.38 mmol) at room temperature for 1 h. After the removal of all volatiles, the product was extracted from the orange residue with hexane (30 ml). The hexane extract was reduced to dryness *in vacuo* to furnish the product as a bright

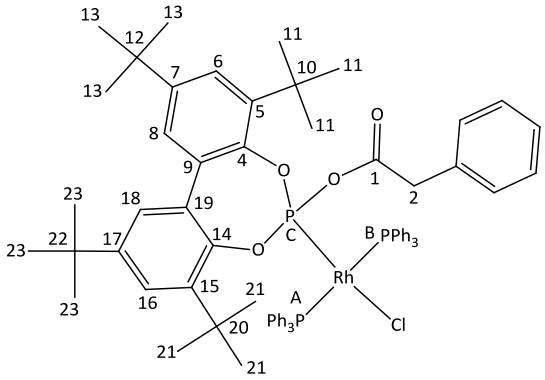


yellow solid (yield: 0.33 g, 70 %). $^{1}$H NMR (300 MHz, $CD_2Cl_2$): $\delta_H$ = 1.29 (s, 18H; $H^{11}$ / $H^{21}$), 1.54 (s, 18H; $H^{13}$ / $H^{23}$), 2.24 (s, 2H; $H^{2}$), 7.00 (d, 2H, $^{4}J$ = 2.7 Hz; $H^{6}$ / $H^{16}$), 7.10 (d, 2H, $^{4}J$ = 2.7 Hz; $H^{8}$ / $H^{18}$), 6.51–7.88 (m, 35H, Ph). $^{13}$C{$^{1}$H} NMR (75 MHz, $CD_2Cl_2$): $\delta_C$ = 31.1 (s; $C^{13}$ / $C^{23}$), 31.7 (s; $C^{11}$ / $C^{21}$), 34.9 (s; $C^{12}$ / $C^{22}$), 35.9 (s; $C^{10}$ / $C^{20}$), 40.0 (s; $C^{2}$), 124.5 (s; $C^{6}$ / $C^{16}$), 127.1 (s; $C^{8}$ / $C^{18}$), 128.2 (d, $^{3}J_{C\text{-}P}$ = 9.3 Hz; Ph-$C^{meta}$), 128.6 (s; Ph-$C^{para}$), 128.9 (d, $^{3}J_{C\text{-}P}$ = 7.5 Hz; Ph–$C^{meta}$), 129.1 (s; Ph–$C^{para}$), 129.4 (d, $^{3}J_{C\text{-}P}$ = 6.4 Hz; Ph-$C^{meta}$), 130.0 (s; Ph-$C^{para}$), 132.4 (d; $^{2}J_{C\text{-}P}$ = 10.0 Hz; Ph-$C^{ortho}$), 132.8 (s; Ph–$C^{ipso}$), 134.8 (d, $^{2}J_{C\text{-}P}$ = 10.4 Hz; Ph-$C^{ortho}$), 135.9 (d, $^{2}J_{C\text{-}P}$ = 9.8 Hz; Ph-$C^{ortho}$), 136.3 (d, $^{1}J_{C\text{-}P}$ = 38.2 Hz; PPh-$C^{ipso}$), 137.7 (s; $C^{9}$), 137.8 (s; $C^{19}$), 132.8 (s; Ph–$C^{ipso}$), 139.6 (s; $C^{5}$), 139.7 (s; $C^{15}$), 146.7 (s; $C^{4}$ / $C^{14}$), 147.9 (s; $C^{7}$), 148.1 (s; $C^{17}$), 164.4 (d, $^{2}J_{C\text{-}P}$ = 19.7 Hz; $C^{1}$). $^{31}$P{$^{1}$H} NMR (121 MHz, $CD_2Cl_2$): $\delta_P$ = 33.8 (AB pattern, ddd, $^{1}J_{PA\text{-}Rh}$ = 134.9 Hz, $^{2}J_{PA\text{-}PC}$ = 46.3 Hz, $^{2}J_{PA\text{-}PB}$ = 346.9 Hz; $P_A$), 38.7 (AB pattern, ddd, $^{1}J_{PB\text{-}Rh}$ = 134.9 Hz, $^{2}J_{PB\text{-}PC}$ = 46.3 Hz, $^{2}J_{PB\text{-}PC}$ = 346.9 Hz; $P_B$), 127.0 (dt, $^{1}J_{PC\text{-}Rh}$ = 334.0 Hz, $^{2}J_{PC\text{-}PA}$ = $^{2}J_{PC\text{-}PB}$ = 46.3 Hz; $P_C$). IR (KBr): $\tilde{\nu}$ = 3054 [m, $sp^2$ $\nu$(C–H)], 2960–2867 [st, $sp^3$ $\nu$(C–H)], 1776 [m, $\nu$(C=O)], 1496–1398 [st, Ar $\nu$(C=C)], 694 [m, $\nu$(P–O)]. ES-MS: *m/z* (%) = 1201 (100) $[M - Cl]^+$, 939 (22) $[M - Cl - PPh_3]^+$.

### *General procedure for the catalytic functionalisation of unsaturated acids with formaldehyde*

*This procedure was based on a literature procedure*.[32] A stainless steel autoclave fitted with a stirrer bar and glass liner was charged with $[RhCl(PPh_3)_3]$ (0.28 g, 0.30 mmol), paraformaldehyde (2.70 g, 90 mmol) and either one of ligands **1** or **10** (0.30 mmol) in a glovebox. The autoclave was sealed tightly and purged with three vacuum-$N_2$ cycles. A solution of propionic acid (0.44 g, 6.0 mmol, 0.48 ml) in toluene (10 ml) was added to the autoclave *via* the injection port under a flow of $N_2$. The autoclave was then sealed and heated to 100-130 $^{o}$C with stirring for 15 h. After this time the autoclave was cooled to room temperature, vented to the atmosphere and the obtained product mixtures subjected to GC-MS and NMR spectroscopic analysis.

***General procedure for the catalytic functionalisation of unsaturated acids with ethene***

*This procedure was based on a literature procedure*.[32] A stainless steel autoclave fitted with a stirring bar and glass liner was charged with [$RhCl(PPh_3)_3$] (0.28 g, 0.30 mmol) and either one of ligands **1**, **8**, **10**, **12** or **13** (0.30 mmol) in a glovebox. The autoclave was sealed tightly and purged with three vacuum-dinitrogen cycles. The autoclave was then pressure tested for leaks with ethene gas (30 bar). A solution of propionic acid (0.48 ml, 0.44 g, 6.0 mmol) (for ligands **1**, **8** and **10**) or phenylacetic acid (0.82 g, 6.0 mmol) (for ligands **12** and **13**) in toluene (10 ml) was subsequently added to the autoclave *via* the injection port under a flow of dinitrogen. The autoclave was then sealed again, pressurised to 30 bar with ethene gas and heated to 100–130 $^{o}$C with stirring for 15 h. After 15 h the autoclave was cooled to room temperature, vented to the atmosphere and the obtained product mixtures subjected to GC-MS and NMR spectroscopic analysis.

## 3.5 Notes and References


(1) Cupertino, D. C.; Harding, M. M.; Cole-Hamilton, D. J. *J. Organomet. Chem.* **1985**, *294*, C29-C32.

(2) Preston, S. A.; Cupertino, D. C.; Palma-Ramirez, P.; Cole-Hamilton, D. J. *J. Chem. Soc., Chem. Commun.* **1986**, 977-978.

(3) Cupertino, D. C.; Cole-Hamilton, D. J. *J. Chem. Soc., Dalton Trans.* **1987**, *49*, 443-449.

(4) Irvine, D. J.; Cole-Hamilton, D. J.; Barnes, J. C.; Hodgson, P. K. G. *Polyhedron* **1989**, *8*, 1575-1577.

(5) Irvine, D. J.; Borowski, A. F.; Cole-Hamilton, D. J. *J. Chem. Soc., Dalton Trans.* **1990**, 3549-3550.

(6) Borowski, A. F.; Iraqi, A.; Cupertino, D. C.; Irvine, D. J.; Cole-Hamilton, D. J. *J. Chem. Soc., Dalton Trans.* **1990**, 29-34.

(7) Iraqi, A.; Fairfax, N. R.; Preston, S. A.; Cupertino, D. C.; Irvine, D. J.; Cole-Hamilton, D. J. *J. Chem. Soc., Dalton Trans.* **1991**, 1929-1935.

(8) Irvine, D. J.; Glidewell, C.; Cole-Hamilton, D. J.; Barnes, J. C.; Howie, A. *J. Chem. Soc., Dalton Trans.* **1991**, 1765-1772.

(9) Irvine, D. J.; Preston, S. A.; Cole-Hamilton, D. J.; Barnes, J. C. *J. Chem. Soc., Dalton Trans.* **1991**, 2413-2418.

(10) *See* Introduction, section 2.1, *Chapter 2*, p3.

(11) Wong, E. H.; Ravenelle, R. M.; Gabe, E. J.; Lee, F. L.; Prasad, L. *J. Organomet. Chem.* **1982**, *233*, 321-331.

(12) Wong, E. H.; Prasad, L.; Gabe, E. J.; Bradley, F. C. *J. Organomet. Chem.* **1982**, *236*, 321-331.

(13) Bedford, R. B.; Betham, M.; Caffyn, A. J. M.; Charmant, J. P. H.; Lewis-Alleyne, L. C.; Long, P. D.; Polo-Cerón, D.; Prashar, S. *Chem. Commun.* **2008**, 990-992.
(14) Roundhill, D. M.; Sperline, R. P.; Beaulieu, W. B. *Coord. Chem. Rev.* **1978**, *26*, 263-279.
(15) Naik, D. V.; Palenik, G. J.; Jacobson, S.; Carty, A. J. *J. Am. Chem. Soc.* **1974**, *96*, 2286-2288.
(16) Gould, R. O.; Jones, C. L.; Sirne, W. J.; Stephenson, T. A. *J. Chem. Soc., Dalton Trans.* **1977**, 669-672.
(17) Robertson, I. W.; Stephenson, T. A. *Inorg. Chim. Acta* **1980**, *45*, L215-L216.
(18) Duncan, J. A. S.; Hedden, D.; Roundhill, D. M.; Stephenson, T. A.; Walkinshaw, M. D. *Angew. Chem.* **1982**, *94*, 463-464.
(19) Irvine, D. J. *PhD thesis*, University of St. Andrews (St. Andrews) **1990**, Chapter 6, pp 234-238.
(20) Garrou, P. E. *Chem. Rev.* **1981**, *81*, 229-266.
(21) Pavia, D. L.; Lampman, G. M.; Kriz, G. S. *in Introduction to spectroscopy*; Brooks/Cole: USA, 2001, pp 15-101.
(22) Dunbar, K. R.; Haefner, S. C. *Inorg. Chem.* **1992**, *31*, 3676-3679.
(23) Kampmeier, J. A.; Liu, T.-Z. *Inorg. Chem.* **1989**, *28*, 2228-2231.
(24) Moxham, G. L.; Randell-Sly, H. E.; Brayshaw, S. K.; Woodward, R. L.; Weller, A. S.; Willis, M. C. *Angew. Chem. Int. Ed.* **2006**, *45*, 7618-7622.
(25) Milstein, D.; Fultz, W. C.; Calabrese, J. C. *J. Am. Chem. Soc.* **1986**, *108*, 1336-1338.
(26) Korostylev, A.; Monsees, A.; Fischer, C.; Börner, A. *Tetrahedron: Asymmetry* **2004**, *15*, 1001-1005.
(27) Shie, J.-Y.; Lin, Y.-C.; Wang, Y. *J. Organomet. Chem.* **1989**, *371*, 383-392.
(28) Bennett, M. A.; Jeffery, J. C.; Robertson, B. B. *Inorg. Chem.* **1981**, *20*, 330-335.
(29) Geldbach, T. J.; Pregosin, P. S. *Organometallics* **2003**, *22*, 1443-1451.
(30) Curtis, M. D.; Butler, W. M.; Greene, J. *Inorg. Chem.* **1978**, *17*, 2928-2931.
(31) Carrión, M. C.; Cole-Hamilton, D. J. *Chem. Commun.* **2006**, 4527-4529.
(32) Jarvis, A. *MChem research project report*, University of St. Andrews (St. Andrews), **2007**, 15-20.
(33) Osborn, J. A.; Jardine, F. H.; Young, J. F.; Wilkinson, G. *Inorg. Phys. Theor. (J. Chem. Soc. A)* **1966**, 1711-1732.
(34) Stephenson, T. A.; Wilkinson, G. *J. Inorg. Nucl. Chem.* **1966**, *28*, 945-956.
(35) van der Ent, A.; Onderdelinden, A. L. *Inorg. Synth.* **1990**,*28*, 90-92.
(36) *SAINT Data Reduction Software (version 6.45)*, Bruker AXS Inc. (Madison), WI, USA, **2003**.
(37) *SMART Data Collection Software (version 5.629)*, Bruker AXS Inc. (Madison), WI, USA, **2003**.
(38) *SHELXL program package (version 5.1)*, Bruker APX Inc. (Madison), WI, USA.
(39) Sheldrick, G. M. *SHELX-97 Program for Crystal Structure Analysis*, University of Göttingen (Göttingen), Germany, **1997**.
(40) Barbour, L. J. *J. Supramol. Chem.* **2003**, *1*, 189-191.
(41) Atwood, J. L.; Barbour, L. J. *Cryst. Growth Des.* **2003**, *3*, 3-8.

# Chapter 4

# Rhodium mixed anhydride complexes with chelated auxiliary ligands.

– The influence of chelated auxiliary ligands on complex stability –

*In the ongoing quest to achieve Rh(I) mixed anhydride complexes with sufficient stability to be viable as C–H activation catalyst, chelating ligands, such as diphosphines and N-substituted diphosphinoamines, were explored as possible stabilising auxiliary ligands. This study then extends the existing body of Rh(I) mixed anhydride complexes described in Chapter 3, to include a series of new Rh(I) mixed anhydride complexes containing dppe, dppb and dppbz as secondary ligands. The effects of these secondary ligands on the in solution stability of the complexes within this series were once again assessed and all findings reported herein. In addition, the solid state structure of one of the new complexes could be determined by single crystal X-ray diffraction, giving further insight into the influence of chelated secondary ligands.*

## 4.1 Introduction

As was described in Chapter 3, owing to the occurrence of spontaneous metal promoted rearrangement and ligand decarbonylation reactions, Rh(I) complexes of mixed anhydride ligands **1** and **7**–**13** with $PPh_3$ auxiliary ligands in mutually *trans* positions were not viable as catalysts for the functionalisation of unsaturated carboxylic acids *via* C–H activation. In particular, the complex $[RhCl(PPh_3)_2(Ph_2PO_2CH_2CH_3)]$ (**15**) bearing ligand **1** still intact proved too unstable to isolate and could only be observed *in situ*. All attempts to isolate this complex led to the formation of large amounts of the stable rearrangement product $[RhCl(PPh_3)(Ph_2POPh_2P)]$ (**14**).

One mechanism proposed for the rearrangement of mixed anhydride complexes containing unidentate secondary ligands such as $PPh_3$, involves the attack by one rhodium on a mixed anhydride attached to another rhodium atom in a binuclear complex (see Scheme 3.1, p 57). This mechanism has been supported by the isolation of various reaction intermediates. Since the formation of the binuclear complex involves initial dissociation of one of the spectator unidentate ligands, it seems logical to investigate the use of bidentate ligands which cannot readily dissociate. This approach should remove such bimolecular decomposition pathways. In partial support of this suggestion, we noted that in the presence of an excess of **1**, rearrangement product **14** was converted partially to $[RhCl(Ph_2POPPh_2)(Ph_2PO_2CH_2CH_3)]$ [**16**, Figure 4.1 (a)], containing **1** still intact. Furthermore, **16** displayed increased stability when compared to the $PPh_3$ counterpart **15** and formed part of the final isolated product mixtures, possibly because it does contain a bidentate rather than unidentate ligands. Consistent with these findings, very similar reaction products have been reported in the literature for reactions of either $[RuCl_2(PPh_3)_4]$ [Figure 4.1 (b)] or $[\{RhCl(COE)_2\}_2]$ [Figure 4.1 (c)] with an excess of the unstable mixed anhydride $Ph_2PO_2CCH{=}CH_2$.[1,2]

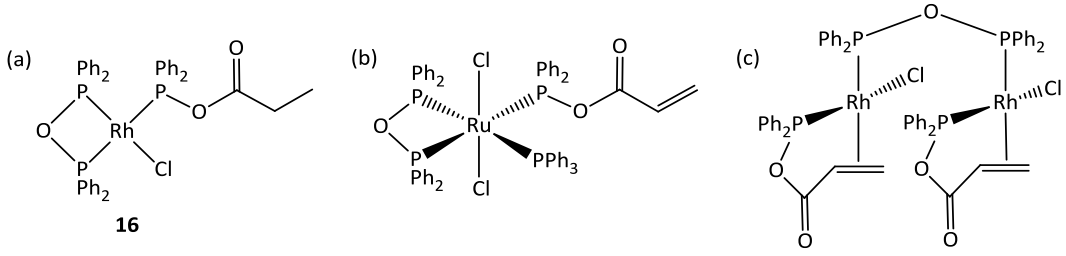


**Figure 4.1** (a) POP Complex **16**, the only example of a Rh(I) phosphine complex bearing **1** still intact.[3] (b) and (c) Literature examples of similar POP stabilised complexes.[1,2]

Inspired by the enhanced stability brought about by the chelated POP auxiliary in these complexes, this part of the study was focussed on evaluating the effects that other more electron rich bipodal diphosphine ligands may have on the stability of mixed anhydride Rh(I) complexes. Also, complexes with such ligands were anticipated to be less susceptible to metal mediated ligand decarbonylation reactions since the formation of chloride bridged Rh(I) dimers are less likely to proceed for diphosphine complexes. As described earlier in Chapter 3, the formation of chloride bridged dimers is believed to be an integral part of the proposed decarbonylation mechanism for complexes of the general formula $[RhCl(PPh)_2(L)]$ (where L = mixed anhydride ligands **9**, **10**, **12** or **13**; see Scheme 3.14). To facilitate our investigation into the stability of diphosphine mixed anhydride complexes, a series of new Rh(I) mixed anhydride complexes with either 1,2-(diphenylphosphino)ethane (dppe), 1,4-(diphenylphosphino)butane (dppb) or 1,2-(diphenylphosphino)benzene (dpppbz) as auxiliary ligands were prepared and their stability assessed.

In addition, since complexes with potential as C–H activation catalysts should ideally possess highly electron rich metal centres, the electron rich diphosphine 1,2-bis(di-*tert*-butylphosphinomethyl)benzene (DTBPMB) was also considered as a possible chelating ligand. This ligand and the related (*S,S*)-*α,α*'-Bis(*tert*-butylmethylphosphino)-*o*-xylene (TBMPX) have been employed before in Rh(I) complexes such as [RhX(CO)(DTBPMB)] (x = $Cl^-$ or $I^-$) [Figure 4.2 (a)] and Rh(TBMPX)(nbd)][$BF_4$] (nbd = 2,5-norbornadiene) [Figure 4.2 (b)].[4,5] However, DTBPMB and its analogues are more often utilized as ligands in palladium catalysts for the methoxycarbonylation of alkenes.[6,7] Of these, the palladium zero complex [Pd(DTBPMB)(dba)] (dba = *trans,trans*-dibenzylideneacetone) [Figure 4.2 (c)] is most prominent, owing to its application as the catalyst in the Lucite International founded Alpha process for the large scale production of methyl propanoate (MeP) *via* the methoxycarbonylation of ethene.[8,9]

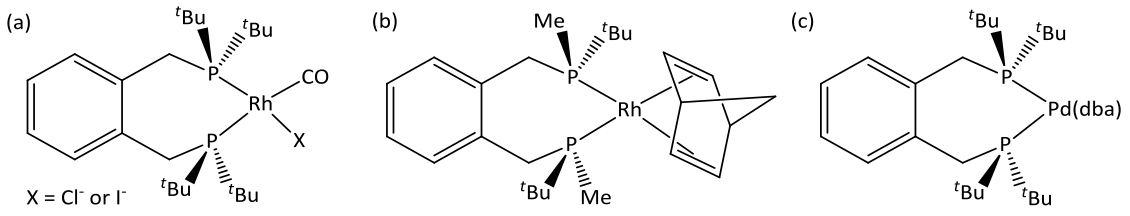


**Figure 4.2** (a)–(b) Literature examples of Rh(I) complexes with 1,2-bis(dialkylphosphinomethyl)benzene type ligands; (c) the Pd based catalyst used for the production of MeP in the Alpha process.

Bidentate *N*-substituted diphosphazanes (PNP) of the general form $RN(PR'_2)_2$ are more closely related to the stable POP ligands, since both of these ligand systems contain heteroatoms as part of their backbone. In contrast to the POP systems, however, PNP ligands are less rigid and their bonding properties and basicity can be fine tuned readily by varying the electronic and steric contributions of the R and R' substituents.[10,11] For these reasons, PNP ligands have found their use in a variety of catalytic reactions ranging from the co-polymerisation of ethene with CO[12] or styrene,[13] the tri-[14-16] tetra-[10,17,18] and polymerisation of ethene[19] and the asymmetric hydrogenation of alkenes.[20] As part of our continuing efforts to stabilise Rh(I) mixed anhydride complexes, these versatile PNP systems were also explored as possible stabilising secondary ligands and the outcome of this study is reported herein.

## 4.2 Results and Discussion

In this chapter the series of new Rh(I) mixed anhydride complexes is extended to include Rh(I) complexes with bipodal diphosphine auxiliary ligands rather than monodentate $PPh_3$ ligands. The preparation and in solution stability of such Rh(I) mixed anhydride complexes containing 1,2-(diphenylphosphino)ethane (dppe), 1,1-(diphenylphosphino)butane (dppb) and 1,2-(diphenylphosphino)benzene (dppbz) as auxiliaries are described in Section 4.2.1. Attempts to prepare related complexes bearing the electron rich 1,2-bis(di-*tert*-butylphosphinomethyl)benzene coordinated in a chelated manner were made and are discussed in section 4.2.2. In addition, PNP Rh(I) complexes, similar to the POP type complexes, were prepared. Their potential as precursors in the preparation of stable PNP Rh(I) mixed anhydride complexes were assessed and are the subject of Section 4.2.3. Finally, the crystal and molecular structure for a new Rh(I) mixed anhydride complex containing dppbz as auxiliary ligand was determined by X-ray crystallography and is discussed in Section 4.2.4.

### *4.2.1 Rh(I) mixed anhydride complexes with dppe, dppb and dppbz ligands*

#### *4.2.1.1 Preparation and in solution stability towards metal promoted rearrangements*

It is well established that $[\{RhCl(diphosphine)\}_2]$ complexes can be prepared by reacting $[\{RhCl(CH_2{=}CH_2)_2\}_2]$, $[\{RhCl(COE)_2\}_2]$ (COE = cyclooctene) or $[\{RhCl(COD)\}_2]$ (COD = cyclooctadiene) with the relevant diphosphines.[21-23] Using this methodology, the Rh(I)

diphosphine precursors [{RhCl(dppe)}$_2$], [{RhCl(dppb)}$_2$] and [{RhCl(dppbz)}$_2$] could be prepared by treating [{RhCl($CH_2$=$CH_2$)$_2$}$_2$] in toluene with dppe, dppb or dppbz at room temperature for 21 h. Reactions of these precursors with mixed anhydrides **1**, **8**, **9** and **10** proceeded with varied success. The reaction of 2 equivalents of **1** with [{RhCl(dppe)}$_2$] in thf at room temperature for 2 h afforded the desired complex [RhCl(dppe)($Ph_2PO_2CCH_2CH_3$)] (**35**) as the major product [Scheme 4.1]. This product was, however, contaminated with various by-products of which the cationic complex [Rh(dppe)($Ph_2POPPh_2$)][Cl] (**37**) constituted the main component. Complex **37** originates from the metal promoted rearrangement of **35** and is comparable to the previously observed [Rh($PPh_3$)$_2$($Ph_2POPPh_2$)][Cl] (**17**)[24] as well as the literature example [Rh($PPh_3$)$_2$($Ph_2POPPh_2$)][$PF_6$].[2] Despite the formation of these by-products, compound **35** is significantly more stable than the related [RhCl($PPh_3$)$_2$($Ph_2PO_2CCH_2CH_3$)] (**15**) which could never be isolated, marking the increase in stability achieved by changing from $PPh_3$ to the bidentate dppe as auxiliary ligand. In contrast, however, the analogous reaction of 2 equivalents of **1** with [{RhCl(dppb)}$_2$] in thf for 40 min did not produce the desired complex [RhCl(dppb)($Ph_2PO_2CCH_2CH_3$)] (**36**), but rather a mixture of rearrangement and other by-products of which the cationic complex [Rh(dppb)($Ph_2POPPh_2$)][Cl] together with $Ph_2P(O)PPh_2$ once again constituted the major components [Scheme 4.1]. Although the nature of this difference in behaviour is not fully understood, it is possible that owing to its less rigid backbone, dppb is more disposed to adopting a monodentate conformation which is perhaps in turn necessary for the formation of dimeric rearrangement intermediates.

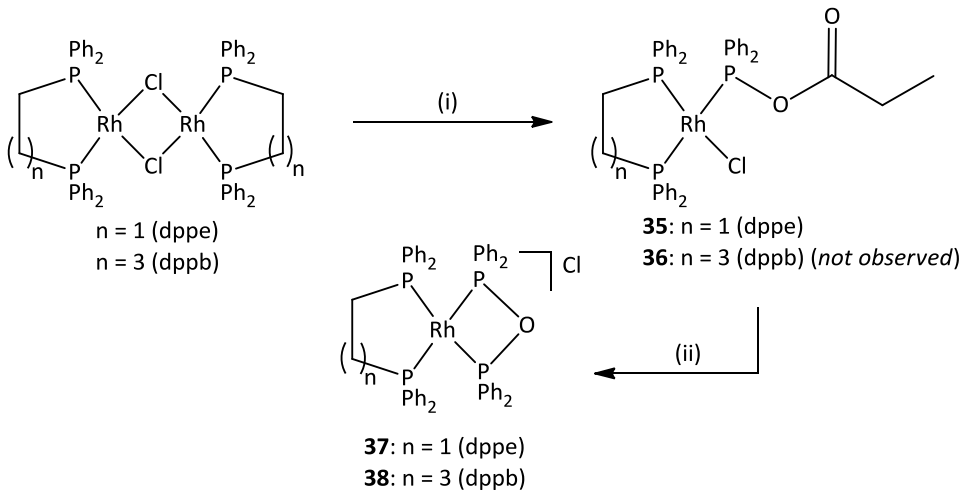


**Scheme 4.1** Rearrangement products **37–38** obtained during attempts to prepare Rh(I) diphosphine complexes of **35–36**. Conditions: (i) **1** (2 equivalents), R.T., thf, 40 min., 2 h; (ii) spontaneous conversion that proceeds over time in solution.

Curiously, for complexes of propionylphosphite ligand **8**, the incorporation of a dppe ligand did not bring about enhanced stability of the resultant complexes and treatment of **8** with [{RhCl(dppe)}$_2$] in thf at room temperature did not furnish the desired complex [RhCl(dppe)(**8**)] (**39**). Instead, a mixture composed of the starting dppe dimer, the rearrangement product **8$_{BP}$** and two new complexes was obtained. These new complexes could be identified tentatively as two isomeric forms of the POP bridged dimer [{RhCl(dppe)}$_2$(POP)] (**40a** and **40b**, where POP refers to 4,4'-oxydidinaphtho[2,1-*d*:1',2'-*f*][1,3,2]dioxaphosphepine) [Scheme 4.2]. A similar by-product, [{RhCl(PPh$_3$)$_2$}$_2$(POP)] (**28**),[25] was also observed for reactions of **8** with [RhCl(PPh$_3$)$_3$]. In the latter case, however, the desired complex [RhCl(PPh$_3$)$_2$(**8**)] (**27**) was stable enough to be isolated as the main constituent of the final product mixtures.

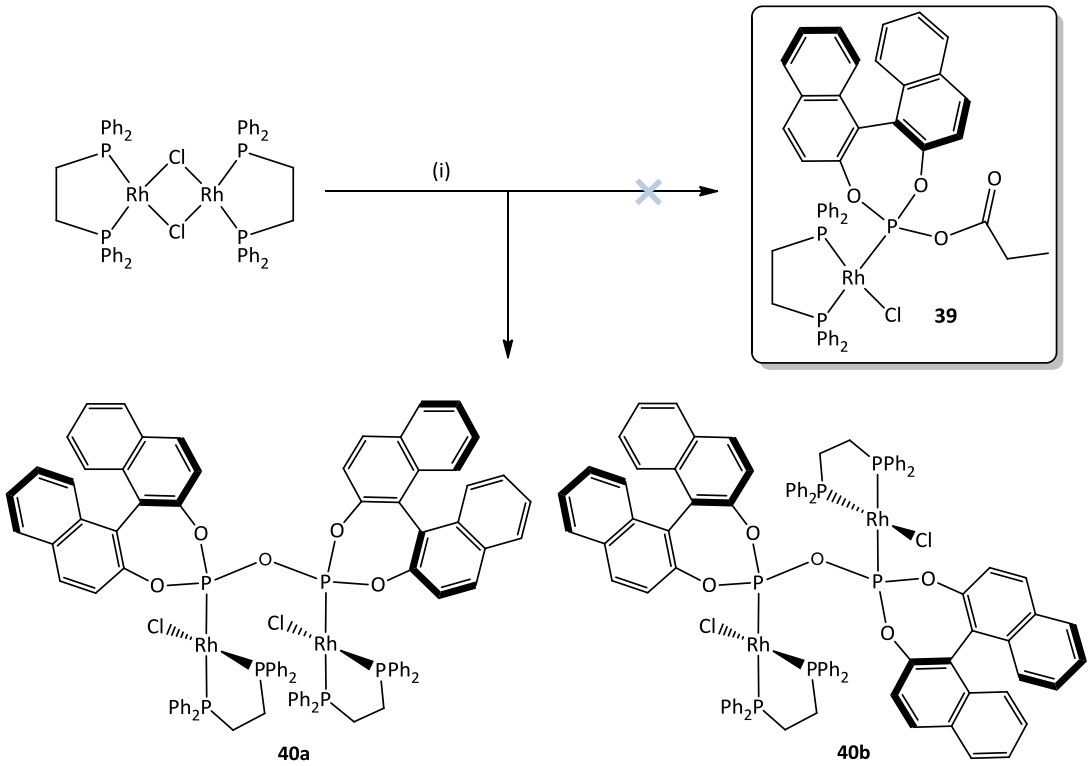


**Scheme 4.2** Rearrangement products **40a** and **40b** obtained during attempts to prepare complex **39**. Conditions: (i) **8** (2 equivalents), R.T., thf, 1 h.

As was the case for reactions of acylphosphite ligands **9** and **10** with [RhCl(PPh$_3$)$_3$], these ligands also react with [{RhCl(dppe)}$_2$] or [{RhCl(dppbz)}$_2$] to give complexes of the general form [RhCl(diphosphine)L] (where L = **9** or **10**) as the major products. Reactions of **9** and **10** with [{RhCl(dppe)}$_2$] in thf at room temperature for 2 h afforded complexes [RhCl(dppe)(**9**)]

(**41**) and [RhCl(dppe)(**10**)] (**42**) as yellow solids in fairly high yield and purity without the interference of unwanted rearrangement reactions. Similarly, reactions of **9** and **10** under the same conditions with [{RhCl(dppbz)}$_2$] furnished complexes [RhCl(dppbz)(**9**)] (**45**) and [RhCl(dppbz)(**10**)] (**46**). However, changing from Rh(I) precursors with a 5-membered chelated dppe or dppbz to [{RhCl(dppb)}$_2$] with a 7-membered chelate dppb, had a dramatic effect on the outcome of these reactions. Although reactions of ligands **9** and **10** with [{RhCl(dppb)}$_2$] under the same reaction conditions did lead to the formation of the desired complexes [RhCl(dppb)(**9**)] (**43**) and [RhCl(dppb)(**10**)] (**44**), these reactions did not proceed to completion and the final product mixtures were contaminated with significant amounts of the starting materials [Scheme 4.3]. It is not unreasonable to suggest that the larger bite angle of the dppb ligand forces the –PPh$_2$ moiety into closer proximity with the bulky *tert*-butyl group of **10**, with this steric interference resulting in the observed suppressed reaction.

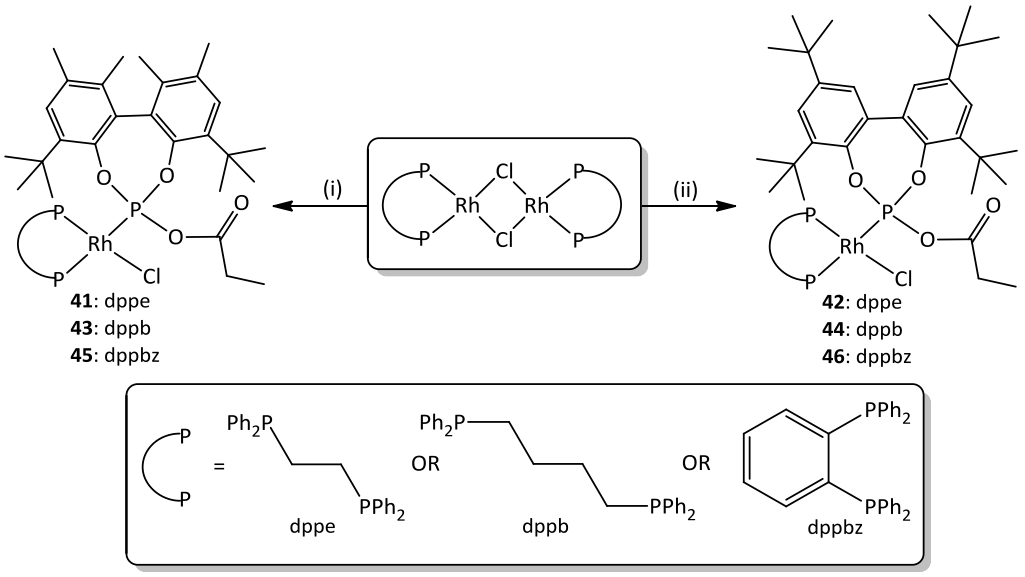


**Scheme 4.3** Reaction scheme for the preparation of Rh(I) diphosphine complexes **41**–**46**. Conditions: (i) **9** (2 equivalents), R.T., thf, 2 h; (ii) **10** (2 equivalents), R.T., thf, 2 h.

In addition to complex **44**, the reaction of **10** with [{RhCl(dppb)}$_2$] further afforded two closely related complexes which gave rise to resonances with very similar chemical shifts and multiplicities in the $^{31}P\{^1H\}$ NMR spectrum. The spectral profile of **44**, as well as the two additional complexes, indicated for each complex the presence of two dppb P-atoms coordinated to a Rh(I) centre in positions *cis* to one another with ligand **10** *trans* disposed to

one of these dppb P-atoms. Although the identity of the two additional complexes could not be assigned unambiguously, they are likely to represent two isomeric forms of the dimeric complex [{RhCl(dppb)(**10**)}$_2$] (**47**) [Figure 4.3], where the two dppe ligands are coordinated in a bridged rather than chelated manner between two Rh(I) centres. Similarly, the analogous dimer [{RhCl(dppb)(**9**)}$_2$] (**48**) is formed during the reaction of ligand **9** with [{RhCl(dppb)}$_2$]. In this case however, only one of the possible isomers is observed. Once again, the minimisation of repulsions between sterically demanding groups are proposed as the driving force for the formation of such less rigid, bridged complexes, given that the P–Rh–P angles in these complexes are not limited by ring constraints.

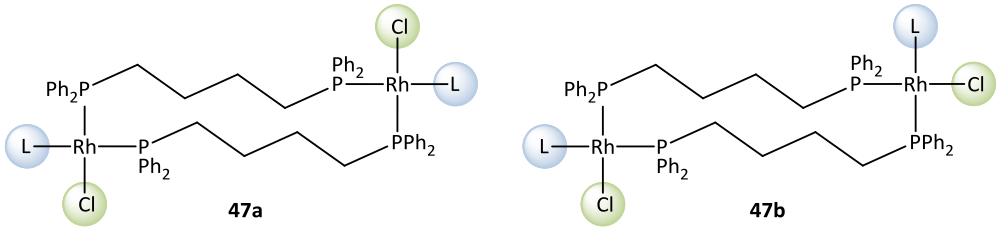


**Figure 4.3** Stereoisomers **47a** and **47b** (where L = **10**), in which mutually *cis* dppb ligands are coordinated in a bridged fashion between two Rh(I) centres, may represent the two closely related by-products observed in the final product mixtures obtained during the preparation of **44**.

Complexes **41–46** are yellow to light orange solids which are indefinitely stable in the solid state, provided that an inert atmosphere is maintained. When the complexes are left standing in solution, however, they decompose within days, with the specific products of decay dependent on the nature of the diphosphine auxiliary ligand employed. Specifically, complexes containing dppe as secondary ligands, **41** and **42**, quantitatively decomposed in solution over a period of 2-4 days *via* a decarbonylation pathway, similar to their [RhCl(PPh$_3$)$_2$(L)] analogues. This generated the dimeric CO complex [{RhCl(CO)dppe}$_2$] (**49**) together with phosphonates **52–53** as the main products of decomposition. In addition, trace amounts of what could be tentatively assigned as the oxygen coordinated metal salts **50** and **51** were also observed as part of the final mixtures [Scheme 4.4]. Based on these findings, it is evident that the incorporation of chelated diphosphine auxiliary ligands does not prevent the occurrence of such decarbonylation reactions as was first anticipated. Furthermore, it is possible that the observed decarbonylations proceed *via* a mechanism very similar to the one proposed in Scheme 3.14.[25] In this case, the formation of the initial dimer is, however, facilitated by the

dissociation of one of the dppe P-atoms, which is then coordinated in a monodentate rather than bidentate fashion. This may also explain why the [{RhCl(CO)(dppe)}$_2$] dimer is observed as the final product, as opposed to monomeric [RhCl(CO)(dppe)]. It needs to be said, however, that since no formal mechanistic studies were conducted, this reasoning is only speculative and it is therefore possible that decarbonylation proceeds *via* an entirely different mechanism.

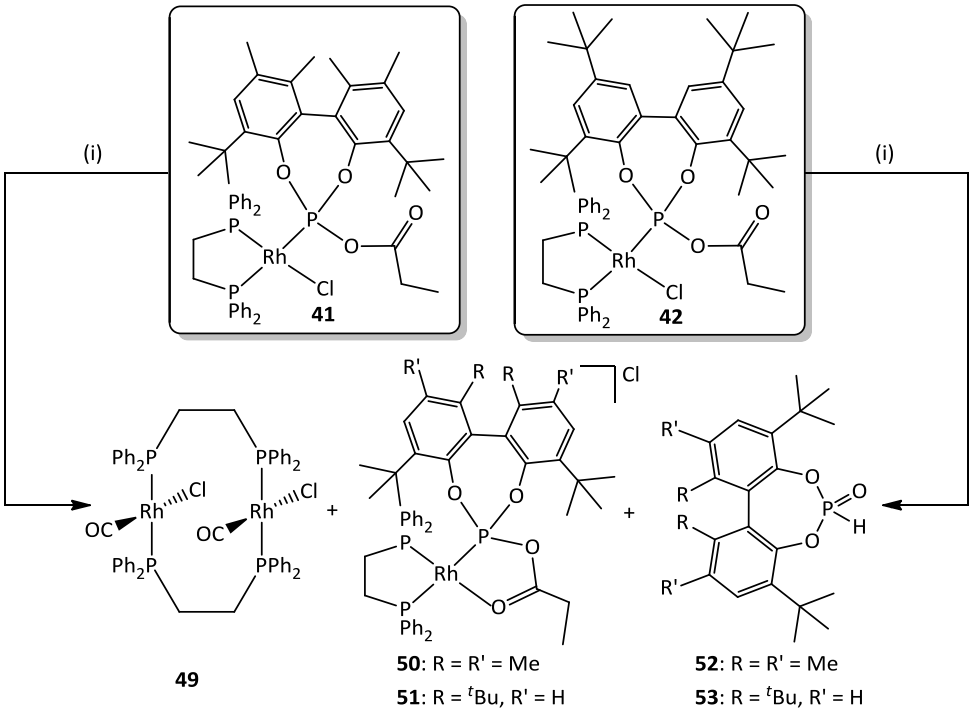


**Scheme 4.4** Rearrangement products **49**–**53** observed for Rh(I) dppe complexes **41** and **42** after (i) standing in solution for 4 days.

Although the dppbz complexes **45** and **46** also underwent quantitative decay over a period of 4 days in solution, the final reaction products differed significantly from those observed for their dppe counterparts, suggesting that a different mechanism of decay exist for these complexes. While the final product mixtures still contained large amounts of the phosphonates **52**–**53**, the analogous CO dimer [{RhCl(CO)dppbz}$_2$] was completely absent. As a substitute, a number of other dppbz containing complexes were observed which could not be assigned unambiguously. None of these were, however, consistent with the expected products of decarbonylation, i.e. [RhCl(CO)(dppbz)] or [{RhCl(CO)dppbz}$_2$]. This difference in behaviour noted between dppe and dppbz mixed anhydride complexes, may originate from the greater

rigidity of the dppbz phenyl backbone when compared to that of the dppe ligand. This increased rigidity would result in a strong preference for chelated rather than bridged coordination, which would translate to higher dissociation energies for the chelated dppbz P-atoms when compared to those of dppe. Since the dissociation of one end of the diphosphine plays an essential role in the proposed decarbonylation mechanism, this higher energy of dissociation may prevent the occurrence of such reactions and as a result, decomposition proceeds *via* other, more accessible, pathways.

#### *4.2.1.2 Spectroscopic characterisation of Rh(I) diphosphine complexes 35–53*

Routine spectroscopic data were collected for complexes **35–51** and are listed in more detail under the experimental section. $^{31}P\{^{1}H\}$ NMR data collected for complexes **35–51** are, however, given in Table 4.1 to simplify discussions regarding their in solution behaviour. In the FT-IR of complexes **35** and **41–46**, the presence of ligands **9** and **10** is confirmed by the characteristic $\nu$(C=O) bands observed in the region 1761–1772 $cm^{-1}$. These stretches vibrate, on average, at slightly lower frequencies than the C=O functionalities in the $PPh_3$ analogues, [RhCl($PPh_3$)$_2$(**9**)] (**29**; 1780 $cm^{-1}$) and [RhCl($PPh_3$)$_2$(**10**)] (**29**; 1775 $cm^{-1}$).

The $^{31}P\{^{1}H\}$ NMR spectrum of [RhCl(dppe)($Ph_2PO_2CCH_2CH_3$)] (**35**) contains two sets of doublets of doublets attributable to the chelated dppe at $\delta$ 55.4 and $\delta$ 71.8, respectively, while another doublet of doublets of doublets at $\delta$ 125.6 corresponds to coordinated **1**. In addition, the $^{31}P\{^{1}H\}$ NMR spectrum determined for **35** also contains resonances corresponding to the rearrangement product [Rh(dppe)($Ph_2POPPh_2$)][Cl] (**37**). In the latter, the POP phosphorus atoms are chemically equivalent but magnetically inequivalent. Also, the same holds true for the two dppe P-atoms and **37** therefore represents an AA'MXX' spin system that gives rise to a complex second order spectrum for which the coupling constants and chemical shifts could only be determined by simulation. Similarly, the rearrangement complex [Rh(dppe)($Ph_2POPPh_2$)][Cl] (**38**), obtained as the major product for reactions of **1** with [{RhCl(dppe)}$_2$], also represent an AA'MXX' spin system with a spectral profile very similar to that of **37** as well as the previously observed $PPh_3$ analogue [Rh($PPh_3$)$_2$($Ph_2POPPh_2$)][X] (**17**) (where X = unknown anion).[26] Figure 4.4 displays the $^{31}P\{^{1}H\}$ NMR spectrum recorded for **38** as an example of the typical spectral profile observed for such complexes.

**Table 4.1** $^{31}P\{^{1}H\}$ NMR spectral data for rhodium complexes **35–51**.

| Compound* | Chemical shifts δ (ppm)† | | | Coupling constants *J* (Hz) | | | | | | |
|---|---|---|---|---|---|---|---|---|---|---|
| | $P_A$ | $P_B$ | $P_C$ / $P_D$ | Rh-$P_A$ | Rh-$P_B$ | Rh-$P_C$ | $P_A$-$P_B$ | $P_A$-$P_C$ | $P_B$-$P_C$ | $P_C$-$P_D$ |
| **35** [RhCl{$Ph_2P_A(CH_2)_2P_BPh_2$}($Ph_2P_CO_2CCH_2CH_3$)] | 55.4 (ddd) | 71.8 (ddd) | 125.6 (ddd) | 134.6 | 183.6 | 161.5 | 34.3 | 408.8 | 36.7 | — |
| **37** [Rh{$Ph_2P_A(CH_2)_2P_BPh_2$}($Ph_2P_COP_DPh_2$)][Cl] ¤ | 57.9 (m) | 57.9 (m) | 106.9 (m) | 130.0 | 130.0 | 120.0 | 122.0 | -28.0 | 287.4 | 32.0 |
| **38** [Rh{$Ph_2P_A(CH_2)_4P_BPh_2$}($Ph_2P_COP_DPh_2$)][Cl] ¤ | 22.4 (m) | 22.4 (m) | 101.1 (m) | 131.0 | 131.0 | 121.0 | 115.0 | -33.0 | 283.0 | 39.0 |
| **40a** [{RhCl{$Ph_2P_A(CH_2)_2P_BPh_2$}}$_2$($P_COP_C$)] § | 46.1 (ddd) | 66.0 (ddd) | 101.0 (ddd) | 91.5 | 162.8 | 170.1 | 12.8 | 546.9 | 29.3 | — |
| **40b** [{RhCl{$Ph_2P_A(CH_2)_2P_BPh_2$}}$_2$($P_COP_C$)] § (isomer) | 44.6 (ddd) | 62.9 (ddd) | 96.7 (ddd) | 87.8 | 155.5 | 173.8 | 11.0 | 550.6 | 32.9 | — |
| **41** [RhCl{$Ph_2P_A(CH_2)_2P_BPh_2$}(**9**)] ‡ | 54.0 (ddd) | 70.4 (ddd) | 134.4 (ddd) | 133.2 | 178.2 | 322.5 | 33.8 | 548.4 | 46.1 | — |
| **42** [RhCl{$Ph_2P_A(CH_2)_2P_BPh_2$}(**10**)] ‡ | 54.5 (ddd) | 70.4 (ddd) | 138.5 (ddd) | 137.2 | 174.5 | 241.6 | 34.3 | 557.9 | 46.2 | — |
| **43** [RhCl{$Ph_2P_A(CH_2)_4P_BPh_2$}(**9**)] ‡ | 6.1 (ddd) | 52.1 (ddd) | 131.0 (ddd) | 127.8 | 177.7 | 246.3 | 46.8 | 536.3 | 46.8 | — |
| **44** [RhCl{$Ph_2P_A(CH_2)_4P_BPh_2$}(**10**)] ‡ | 5.7 (ddd) | 52.4 (ddd) | 133.7 (ddd) | 124.6 | 181.2 | 249.2 | 49.1 | 547.4 | 49.1 | — |
| **45** [RhCl{$Ph_2P_A$(1,2-bz)$P_BPh_2$}(**9**)] ‡ | 59.3 (ddd) | 70.1 (ddd) | 135.2 (ddd) | 134.1 | 179.8 | 236.7 | 34.1 | 552.3 | 44.7 | — |
| **46** [RhCl{$Ph_2P_A$(1,2-bz)$P_BPh_2$}(**10**)] ‡ | 59.4 (ddd) | 70.1 (ddd) | 139.3 (ddd) | 131.7 | 176.4 | 239.9 | 35.2 | 559.8 | 44.7 | — |
| **47a** [{RhCl{$Ph_2P_A(CH_2)_4P_BPh_2$}(**10**)}$_2$] ‡ | 9.6 (ddd) | 53.1 (ddd) | 140.5 (ddd) | 128.4 | 185.5 | 226.5 | 49.1 | 498.4 | 49.1 | — |
| **47b** [{RhCl{$Ph_2P_A(CH_2)_4P_BPh_2$}(**10**)}$_2$] ‡ (isomer) | 8.3 (ddd) | 52.4 (ddd) | 126.3 (ddd) | 120.8 | 177.9 | 260.5 | 49.1 | 570.1 | 49.1 | — |
| **48** [{RhCl{$Ph_2P_A(CH_2)_4P_BPh_2$}(**9**)}$_2$] ‡ | 8.0 (ddd) | 53.5 (ddd) | 136.4 (ddd) | 123.3 | 187.8 | 227.5 | 42.7 | 497.7 | 52.1 | — |
| **49** [{RhCl(CO){$Ph_2P_A(CH_2)_2P_APh_2$}}$_2$] | 67.8 (d) | — | — | 146.1 | — | — | — | — | — | — |
| **51** [Rh{$Ph_2P_A(CH_2)_2P_BPh_2$}(**10**)][Cl] ‡ | 58.9 (ddd) | 72.7 (ddd) | 172.4 (ddd) | 127.4 | 203.9 | 211.5 | 33.1 | 502.0 | 45.9 | — |

* Note: Identical labels given to different phosphorus atoms present within the same complex indicate magnetic equivalence.

† Chemical shifts relative to 85 % $H_3PO_4$ ($CD_2Cl_2$, 25 °C) with mulitiplicity given in parenthesis.

¤ Please note: Values based on a rough simulation. Modelled an AA'MXX' spin system, therefore $\delta P_A = \delta P_B$; $\delta P_C = \delta P_D$; $J_{PA\text{-}Rh} = J_{PB\text{-}Rh}$; $J_{PC\text{-}Rh} = J_{PD\text{-}Rh}$; $J_{PB\text{-}PC} = J_{PA\text{-}PD}$ and $J_{PA\text{-}PC} = J_{PB\text{-}PD}$.

‡ Phosphorus present in coordinated (propionyl)phosphinites listed as $P_C$.

§ POP refers to 4,4'-oxydidinaphtho[2,1-d:1',2'-f][1,3,2]dioxaphosphepine.

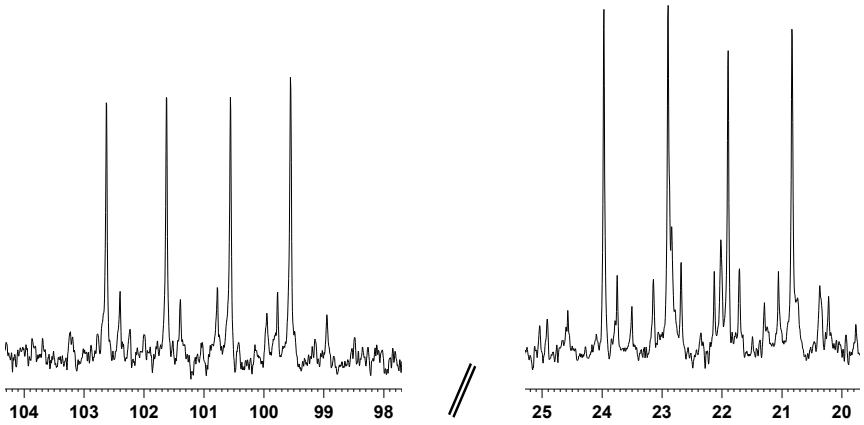


**Figure 4.4** Experimental $^{31}P\{^{1}H\}$ NMR spectrum (low resolution) recorded for complex **38**. Additional signals observed in the region δ 20–25 correspond to unassignable by-products.

Owing to the low resolution of the spectrum obtained for **38**, weaker signals that form part of the complex multiplets are not always observed. The chemical shifts and coupling constants for the $^{31}P\{^{1}H\}$ resonances of complexes **37** and **38** could be determined by simulation and are listed in Table 4.1. Note, however, that the low resolution of the collected NMR spectra together with the presence of overlap in the regions where dppe and dppb resonate, only allowed for a rough simulation. Figure 4.5 depicts the experimental (top) and simulated (reverse) POP regions in the $^{31}P\{^{1}H\}$ NMR spectra of complexes **37** [Figure 4.5 (a)] and **38** [Figure 4.5 (a)]. For these simulations, **37** and **38** were interpreted as $C_2$ symmetrical AA'MXX' spin systems. Although the dppe and dppb resonances were simulated successfully, they are not easily interpreted in the experimental spectra owing to overlap with other resonances in this region. For the sake of clarity, these resonances are therefore omitted from Figure 4.5.

As was mentioned, the reaction of **8** with $[\{RhCl(dppe)\}_2]$ resulted in two rearrangement products which could be tentatively assigned as isomers of the POP bridged dimer $[\{RhCl(dppe)\}_2(POP)]$ (**40a** and **40b**). Although the assignment of the observed resonances to specific isomers could only be done at random, **40a** and **40b** display very similar spectral profiles in the $^{13}P\{^{1}H\}$ NMR spectrum and are present in a 3:1 ratio based on NMR integrals. For each of these complexes, the two P-atoms of the bridging POP ligands are magnetically equivalent, giving rise to a doublet of doublets of doublets at δ 101.0 (assigned to **40a**) and δ 96 (assigned to **40b**). Similarly, the dppe P-atoms *cis* disposed to the POP ligands give rise to two distinct doublets of doublets of doublets in the region δ 62–66, while the two sets of doublets of doublets of doublets observed in the region δ 41–49 could be assigned to the dppe P-atoms *trans* to POP.

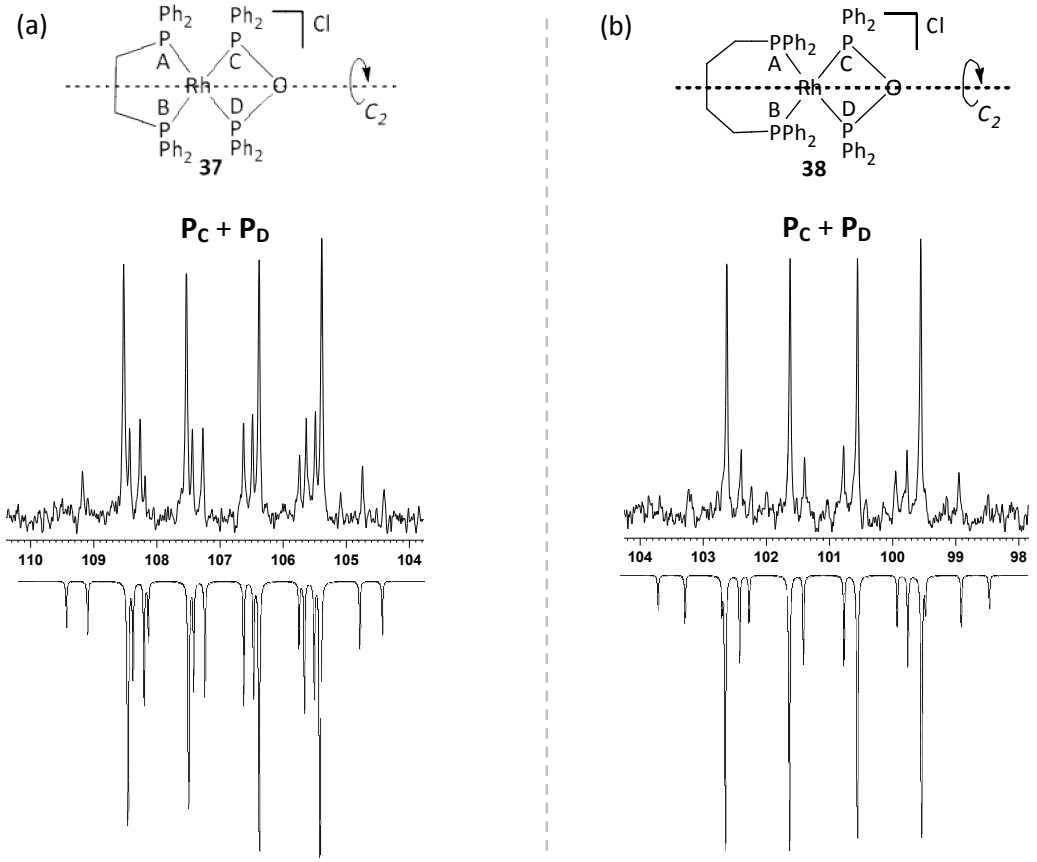


**Figure 4.5** Experimental (top) and simulated (reverse) spectra for the POP ligand resonances of (a) complex **37** and (b) complex **38**, modelled as $C_2$ symmetrical AA'MXX' spin systems.

Complexes **41**–**46** all display very similar coupling behaviour in the measured $^{31}P\{^{1}H\}$ NMR spectra. Figure 4.6 depicts the $^{31}P\{^{1}H\}$ NMR spectrum of [RhCl(dppe)(**9**)] as an example of the typical spectral profile observed for complexes of the general form [RhCl(diphosphine)(L)] (where L = **9** or **10**). For all complexes, the coordinated mixed anhydride ligand gives rise to a high field resonance (ddd) at δ 134–139, with large P–$P_{trans}$ couplings ranging from 536.3 Hz (for **43**) to 559.8 Hz (for **46**), intermediate P–Rh couplings ranging from 236.7 Hz (for **45**) to 322.5 Hz (for **41**) and small P–$P_{cis}$ couplings ranging between 44–49 Hz. These mixed anhydride resonances are all shifted downfield with respect to those of their [RhCl($PPh_3$)(L)] counterparts, **29** (δ 129.3) and **30** (δ 124.9). Similarly, the diphosphine P-atoms *trans* to Cl resonates as doublet of doublets of doublets at ~δ 70 (for dppe or dppbz) and ~δ 52 (for dppb) with P-Rh couplings ranging from 174.5 Hz (for **42**) to 181.2 Hz (for **44**). These atoms show mutual *cis* couplings of 33–47 Hz to the diphosphine P-atoms *cis* to Cl, which resonate as doublets of doublets of doublets at ~δ 54 (for dppe), ~δ 59 (for dppbz) or ~δ 6 (for dppb) and typically display P–Rh couplings falling within the range 124–137 Hz.

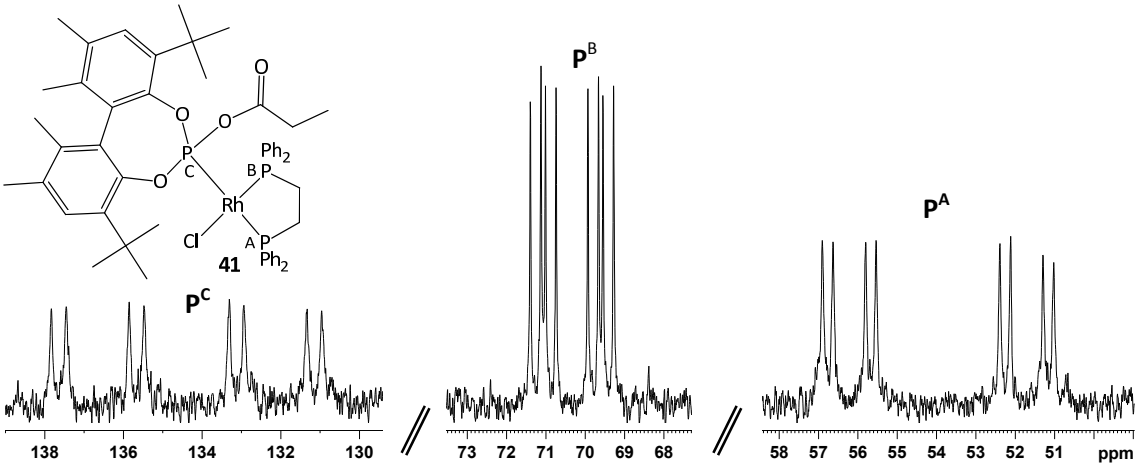


**Figure 4.6** $^{31}P\{^{1}H\}$ NMR spectrum of complex **41**, representing an example of the typical spectral profile observed for complexes of the form [RhCl(diphosphine)(L)] where diphosphine refers to dppe, dppb or dppbz and L denotes ligands **9** or **10**.

In the $^{31}P\{^{1}H\}$ NMR spectrum of **44** (Figure 4.7) the two observed by-products could be tentatively identified as isomeric forms of the complex [{RhCl(dppb)(**10**)}$_2$] (**47a** and **47b**), where the dppb ligands are coordinated in a bridged manner between two Rh(I) centres. Based on $^{31}P\{^{1}H\}$ NMR integrals, these complexes are present in a 1 (**47a**) : 22 (**44**) : 9 (**47b**) ratio. Resonances corresponding to the P-atoms of the dppb ligands in **44**, **47a** and **47b** have very similar chemical shifts and are therefore greatly overlapped in the relevant regions. In contrast, resonances corresponding to coordinated **10** in the various complexes show more distinct chemical shifts leading to three discrete sets of doublets of doublets of doublets in the region δ 124–150.

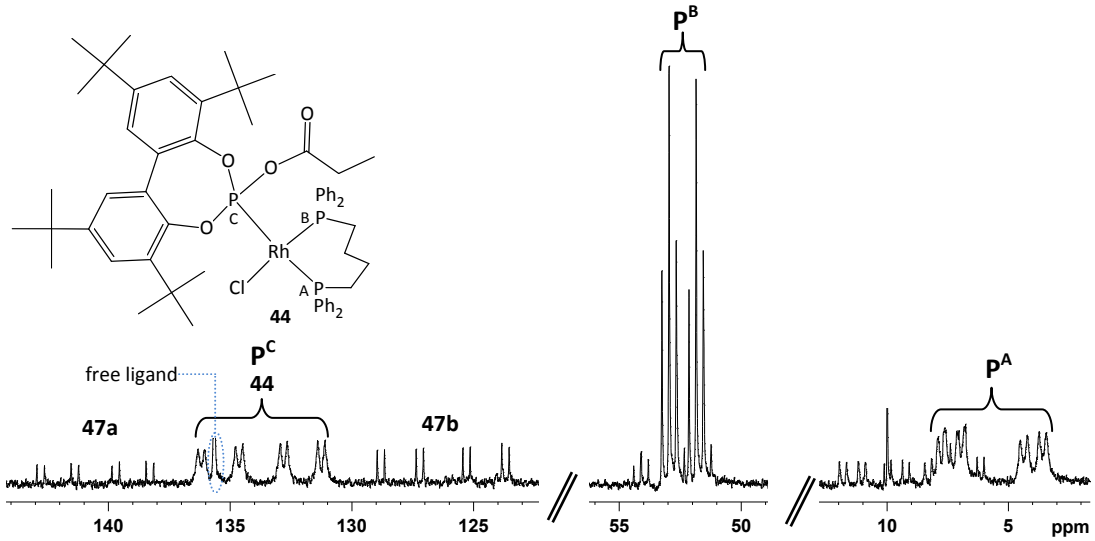


**Figure 4.7** $^{31}P\{^{1}H\}$ NMR spectrum for the product mixture obtained from the reaction of [{RhCl(dppb)}$_2$] with ligand **10**, showing resonance signals corresponding to the desired complex **44** and additional signals corresponding to the two observed by-products **47a** and **47b**.

As mentioned previously, dppe complexes **41** and **42**, when left standing in solution for a period of 2–4 days, decompose quantitatively to afford the decarbonylation product [{RhCl(CO)dppe}$_2$] (**49**) together with phosphonates **52**–**53** as the main products of decomposition. Figure 4.8 depicts the $^{31}P\{^1H\}$ NMR spectra collected for a sample of **41** in $CD_2Cl_2$ (a) prior to rearrangement and (b) after a period of 4 days in solution. In the latter, a doublet detected at δ 67.8 ($^1J_{P\text{-}Rh}$ = 146.1 Hz) could be tentatively assigned to the CO dimer **49**, while the phosphonate **52** resonates as a sharp singlet at δ 9.4. Although complex **49** have not been reported before, the observed values are in between those reported for the related literature compounds [{RhCl(CO)(dppm)}$_2$] [dppm = bis(diphenylphosphino)methane; δ 96.8 (d)] and [{RhCl(CO)(dppp)}$_2$] [dppp = 1,3-bis(diphenylphosphino)propane; δ 87.1(d)].[27,28] The $^{31}P\{^1H\}$ NMR spectrum of rearranged **42** is almost identical to spectrum (b) in Figure 4.8 and once again indicates the presence of **49** as an intense doublet at δ 67.8 together with the known phosphonate **53** as a singlet at δ 10.1.[29-31]

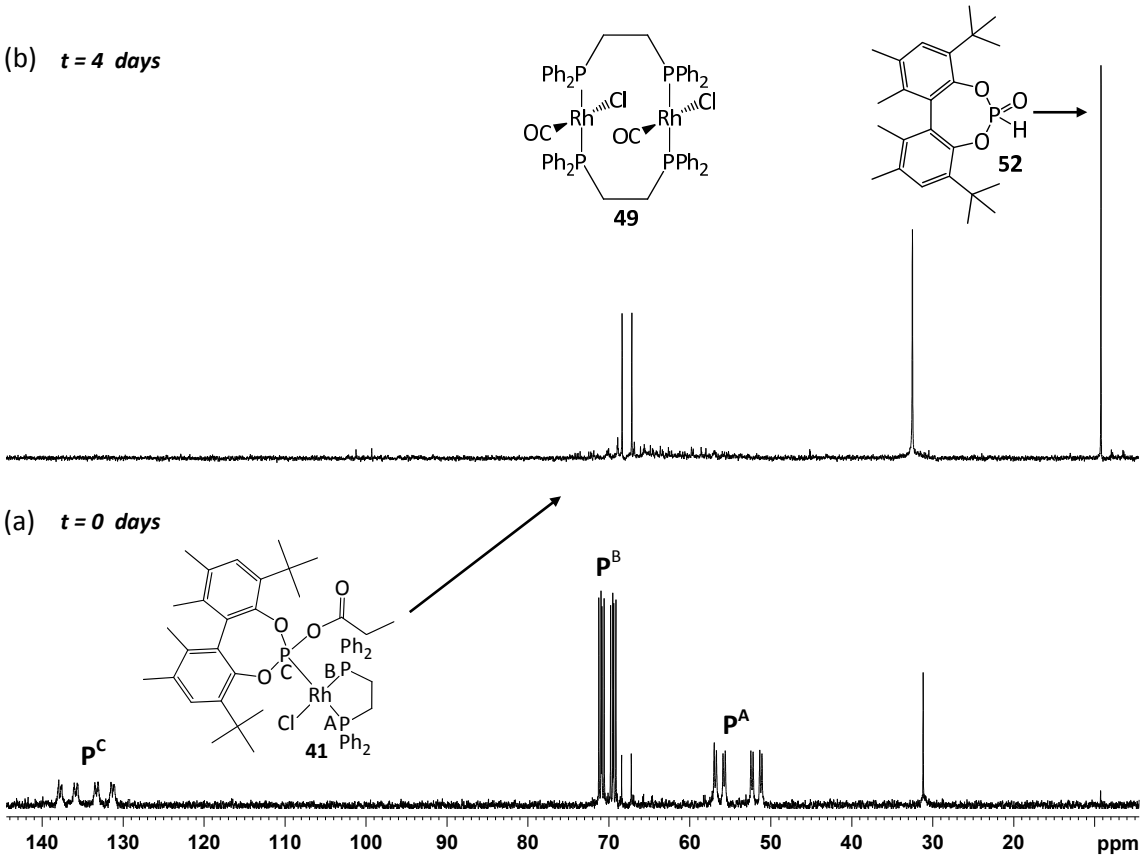


**Figure 4.8** $^{31}P\{^1H\}$ NMR spectrum of complex **41** (a) after preparation and (b) after standing in solution for 4 days.

In addition to the CO dimer **49** and phosphonates **52** and **53**, $^{31}$P NMR spectra of rearranged **41** and **42** also revealed the presence of minor amounts of the oxygen coordinated rearrangement products [Rh(dppe)(**9**)][Cl] (**50**) and [Rh(dppe)(**10**)][Cl] (**51**), respectively. For complex **50**, however, the weak intensities and poor resolution of the observed resonances did not allow for the accurate determination of coupling constants, and for this reason compound **50** is not listed in Table 4.1. Figure 4.9 displays the resonances corresponding to [Rh(dppe)(**10**)][Cl] (**51**) in the $^{31}$P{$^{1}$H} NMR spectrum collected for rearranged **42**. The very highfield chemical shift of δ 172.4 noted for coordinated **9**, is consistent with coordination *via* both oxygen and phosphorus, since the formation of a 5-membered ring is known to bring about a significantly downfield shift in the P-atom resonance.[32] Moreover, a downfield shift of Δδ 2.3 and Δδ 4.4 is observed for the two distinct dppe resonances. These observations are also in good agreement with the proposed structure, since the more electron poor Rh(I) centre of the cationic complex **42** would require an increased electronic contribution from the dppe ligands, resulting in more electron deficient, deshielded dppe P-atoms.

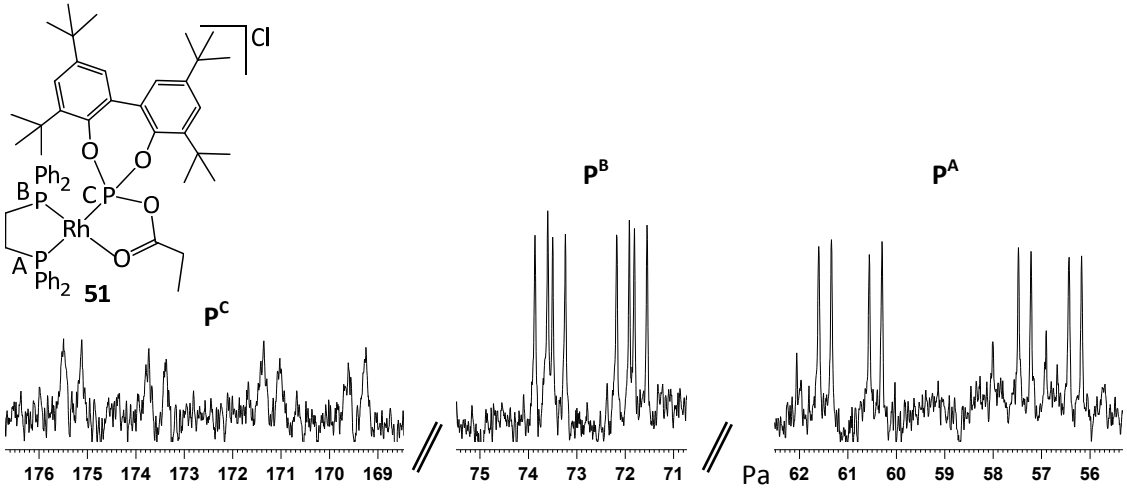


**Figure 4.9** Resonances corresponding the the O-coordinated rearrangement product **51** observed in the $^{31}$P{$^{1}$H} NMR spectrum of complex **42** after a period of 4 days in solution.

### *4.2.2 Rh(I) complexes with 1,2-bis(di-tert-butylphosphinomethyl)benzene*

As mentioned in the introductory section, potential C–H activation catalysts should ideally possess low valent transition metal centres coordinated to electron rich ligands. For this reason the electron rich diphosphine 1,2-bis(di-*tert*-butylphosphinomethyl)benzene (DTBPMB) was also considered as a possible secondary ligand in the stabilisation of mixed anhydride

complexes. For this purpose, we attempted to synthesise the complex [RhCl($PPh_3$)(DTBPMB)] (**54**) where the bidentate DTBPMB ligand is coordinated in a chelated manner. The aim was to employ this complex as a precursor in the preparation of electron rich Rh(I) mixed anhydride complexes similar to the earlier complexes **41**–**46**, by displacement of $PPh_3$ with ligands **9** or **10**. All attempts to prepare **54**, starting from either [RhCl($PPh_3$)$_3$] or [RhCl($PPh_3$)(COD)] under different conditions, however resulted in no reaction (Scheme 4.5) rendering subsequent conversion to mixed anhydride complexes unfeasible.

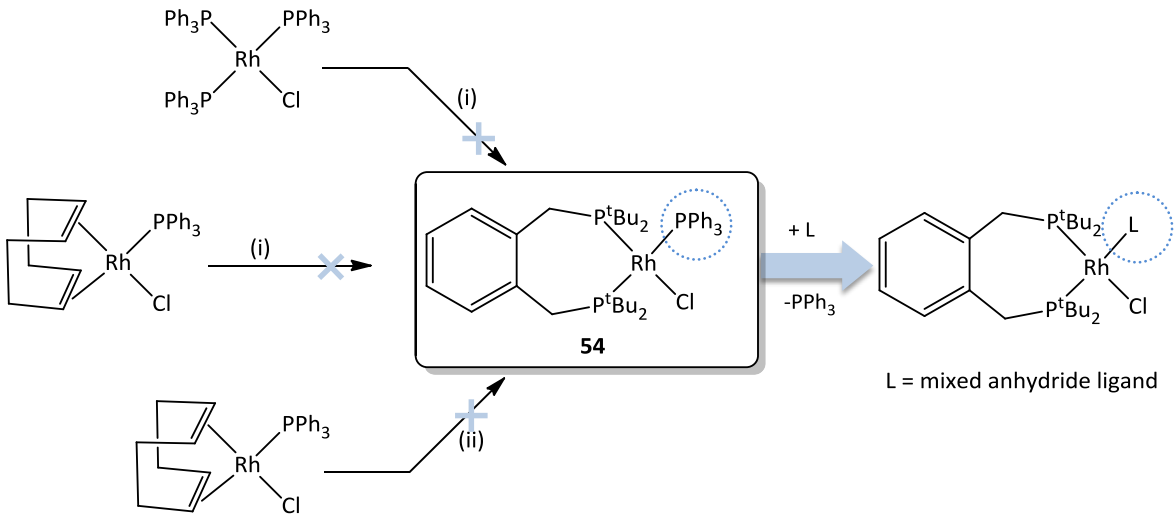


**Scheme 4.5** Failed attempts to prepare [RhCl($PPh_3$)(DTBPMB)] from [RhCl($PPh_3$)$_3$] or [RhCl($PPh_3$)(COD)]. [RhCl($PPh_3$)(DTBPMB)] was meant to serve as precursor for the preparation of more electron rich Rh(I) mixed anhydride complexes. Conditions: (i) DTBPMB, (1:1), R.T., dichloromethane, 1 h; (ii) DTBPMB, (1:1), R.T., toluene, 1 h.

In addition, attempts were made to prepare the dimer [{RhCl(DTBPMB)}$_2$] (**55**), for the same purpose as **54**, from the reaction of [{RhCl($CH_2$=$CH_2$)$_2$}$_2$] with 2 equivalents of DTBPMB in toluene at room temperature for 21 h [Scheme 4.6 (a)]. This reaction, however, did not proceed as expected and upon addition of the DTBPMB, the reaction mixture immediately turned dark green. Analysis of the isolated product, indicated the complete absence of the desired dimer **55**, with the complex [$Rh_2Cl_2$($CH_2$=$CH_2$)$_4$($\mu^1$–DTBPMB)], containing the DTBPMB ligand bridging between two [RhCl($CH_2$=$CH_2$)$_2$] entities, obtained as the final product almost exclusively. An analogous complex, [$Rh_2Cl_2$(COD)$_2$($\mu^1$–DTBPMB)], was also isolated by Jimenez-Rodriguez and co-workers[4] during attempts to prepare **55** from the reaction of [{RhCl(COD)}$_2$]

with DTBPMB in methanol under reflux conditions [Scheme 4.6 (b)]. Surprisingly, treatment of **56** with mixed anhydride **12** in dichloromethane at room temperature did not bring about any reaction with the starting material being recovered unaltered after work-up. Likewise, reactions in toluene under reflux conditions also failed to deliver any useful reaction products.

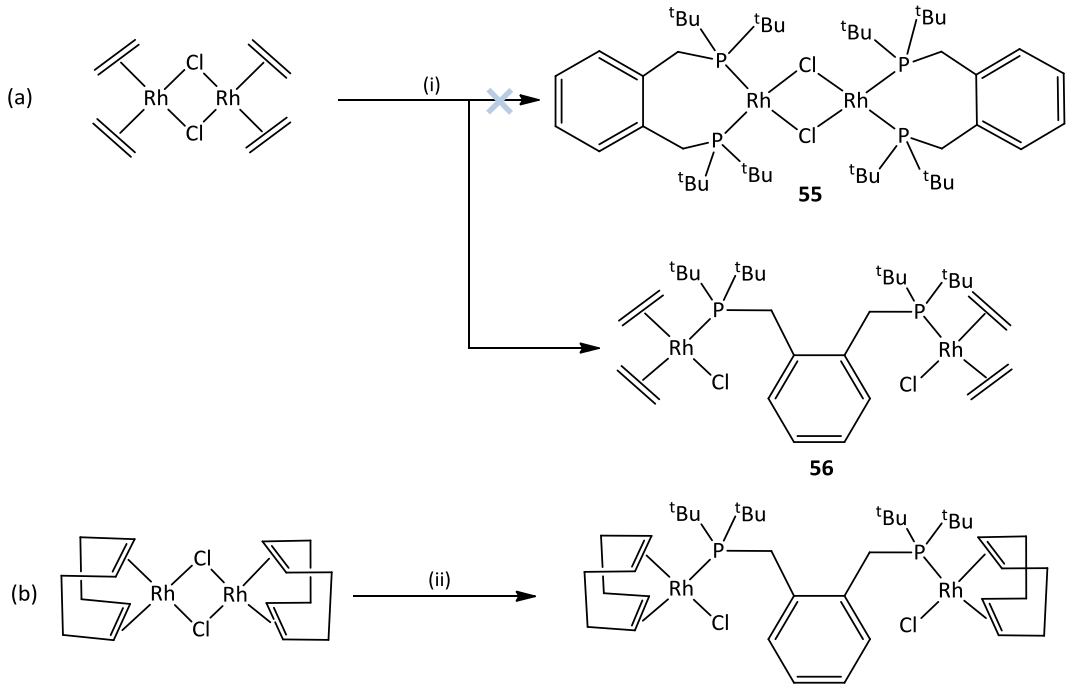


**Scheme 4.6** (a) Formation of **56** during attempts to prepare [{RhCl(DTBPMB)}$_2$] from [{RhCl($CH_2$=$CH_2$)$_2$}$_2$]. Conditions: (i) DTBPMB, (2 equivalents), R.T., toluene, 21 h. (b) Reaction of [{RhCl(COD)}$_2$] with DTBPMB reported in literature (ii) DTBPMB, (2 equivalents), methanol, reflux, 2 h.[4]

### *4.2.3 Rh(I) complexes with N,N-bis(diphenylphosphanyl)-tert-butylamine*

Finally, the *N*-substituted phosphinoamine ligand, $(Ph_2P)_2N^tBu$, was explored as possible auxiliary ligand in Rh(I) mixed anhydride complexes. Given that the previously explored diphosphines did not lead to an increased stability in the final Rh(I) mixed anhydride complexes, $(Ph_2P)_2N^tBu$ was considered as alternative since the heteroatomic backbone makes this ligand more closely related to the stable POP systems. Furthermore, since the nature of the *N*-substituent influences the overall electron richness of the ligand, $(Ph_2P)_2N^tBu$ prepared from the more basic tertiary butylamine was chosen as preliminary PNP ligand.[10] Employing this ligand, the new precursor complex [RhCl($PPh_3$){$(Ph_2P)_2N^tBu$}] (**57**) could be prepared successfully in high yield and purity by treatment of [RhCl($PPh_3$)$_3$] with 1 equivalent of

$(Ph_2P)_2N^tBu$ in thf at room temperature for 2 h [Scheme 4.7 (i)]. Attempts to convert this compound into the mixed anhydride complex $[RhCl\{(Ph_2P)_2N^tBu\}(Ph_2PO_2CCH_2CH_3)]$ (**58**) by treatment with a solution of **1** in thf at room temperature for 2 h, however, failed [Scheme 4.7 (ii)]. Final product mixtures comprised of **57,** mostly unaltered, contaminated with the free ligand rearrangement product $Ph_2P(O)PPh_2$ and only trace amounts of what may correspond to the desired complex **58**. Similarly, reactions of **57** with ligands **9** and **10** in dichloromethane at room temperature failed to deliver mixed anhydride complexes **59**–**60**, with final reaction mixtures only comprising of the unaltered starting materials [Scheme 4.7 (iii)].

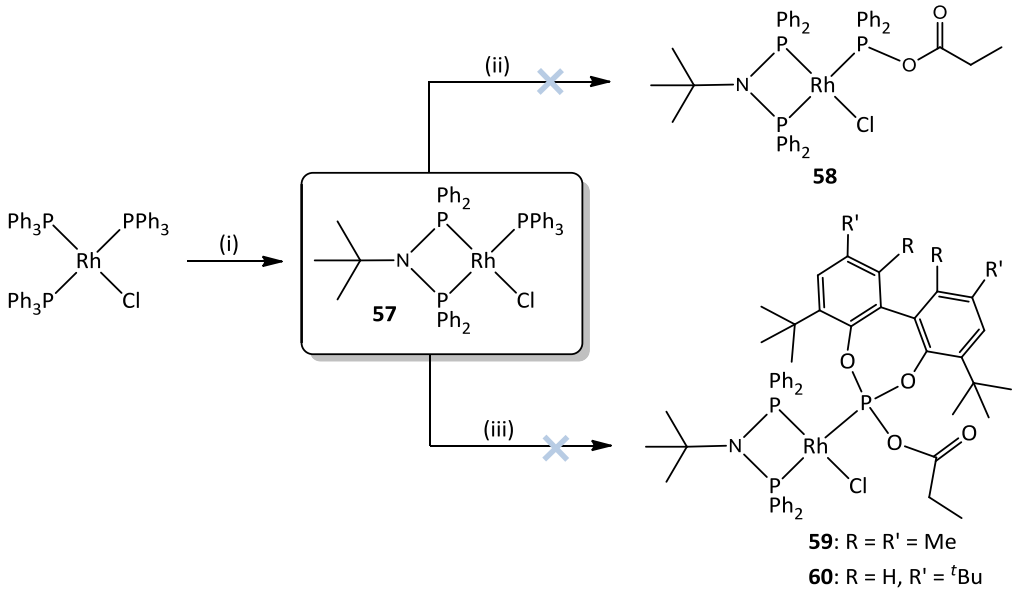


**Scheme 4.7** Preparation of the PNP Rh(I) complex **57** from $[RhCl(PPh_3)_3]$ and subsequent failed attempts to convert **57** to mixed anhydride complexes **58**–**60**. Conditions: (i) $(PPh_2)_2N^tBu$, (1:1), R.T., thf, 2 h; (ii) **1**, (1:1), R.T.,thf, 2 h, (iii) **9** (for **59**) or **10** (for **60**), R.T., dichloromethane, 2 h.

Compound **57** gives rise to three distinct sets of doublets of doublet of doublets in the $^{31}P\{^1H\}$ NMR spectrum (Figure 4.10) at δ 26.3, δ 52.7 and δ 67.4, corresponding to $PPh_3$ and the PNP P-atoms *cis* and *trans* to Cl, in the mentioned order. The PNP P-atoms display mutual *cis* coupling of 97.7 Hz, while the $PPh_3$ ligand couples to the PNP ligand with a small *cis* coupling of 25.0 Hz and a large *trans* coupling of 363.4 Hz. Observed P–Rh couplings vary from 121.3 Hz (for $P_B$) to 163.3 Hz (for $P_C$).

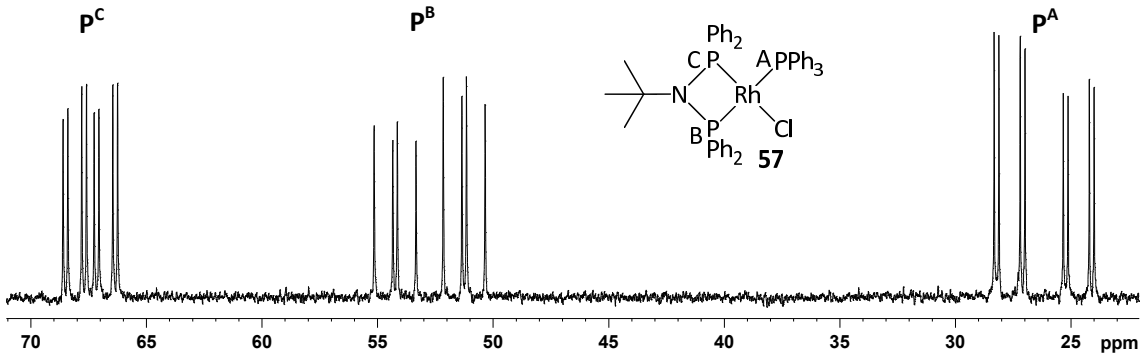


**Figure 4.10** $^{31}P\{^{1}H\}$ NMR spectrum showing the spectral profile of the Rh(I) PNP complex **57**.

Having had little success with the monomeric precursor **57**, we turned our attention to the related dimeric precursor $[RhCl\{(Ph_2P)_2N^tBu\}_2]$ (**61**). Complex **61** could be prepared in high yield and purity by the reaction of $[RhCl(CH_2{=}CH_2)_2\}_2]$ with 2 equivalents of the PNP ligand in toluene at room temperature for 21 h. Although **61** has never been reported before, related compounds $[RhCl(R_2NPh)\}_2]$ (where R = OPh, $OC_6H_4Br$-*p* or $OC_6H_4OMe$-*o*) have been prepared by Balakrishna and co-workers.[11,33] Attempts to split the chloride bridge with mixed anhydride **10**, however, once again only led to the formation of trace amounts of **62** with the starting materials largely recovered unaltered upon work-up.

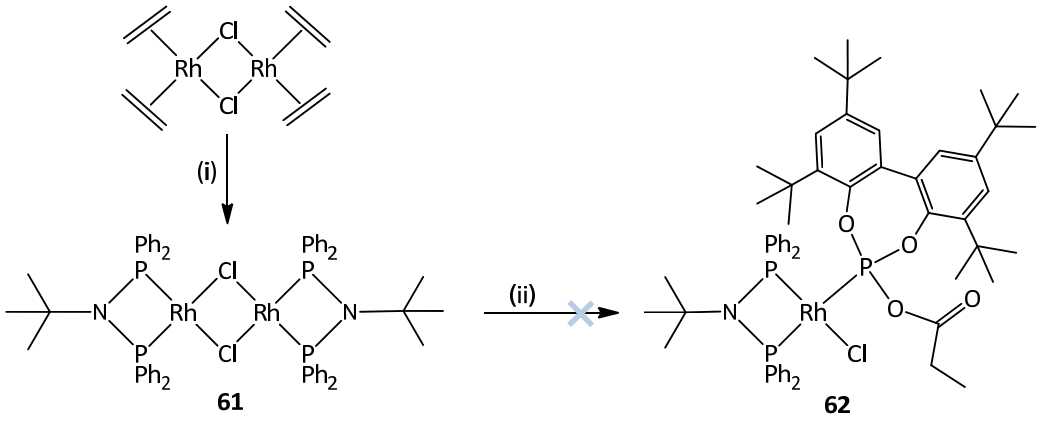


**Scheme 4.8** Preparation of the PNP Rh(I) dimer **61** from $[\{RhCl(CH_2{=}CH_2)_2\}_2]$ and the subsequent failed attempt to convert **61** to the mixed anhydride complex **62**. Conditions: (i) $^tBuN(PPh_2)_2$, (2 equivalents), R.T., toluene, 21 h; (ii) **10**, (2 equivalents), R.T., dichloromethane, 2 h.

### *4.2.4 Crystal and molecular structure determination*

The crystal and molecular structure of [RhCl(dppbz)(**9**)] (**45**) could be determined by single crystal X-ray diffraction. Complex **45** crystallises as yellow needles from a concentrated dichloromethane solution of **45** cooled to -22 °C in the monoclinic space group $P2_1/c$ with one molecule of **45** and three molecules of dichloromethane included in the asymmetric unit. Figure 4.11 depicts the molecular structure of **45**, while selected bond lengths and angles are given in Table 4.2. The molecular structure contains ligand **9** coordinated in a position *cis* to chloride to a Rh(I) centre confined to a distorted square planar environment. While the phosphorus atoms of the dppbz ligand lie within the plane, the phenyl ring that forms the backbone protrudes from the plane at an angle of 21.54°. Owing to ring constraints, the measured P(2)–Rh(1)–P(3) bite angle of 84.55(8)° are significantly smaller than the ideal 90° associated with square planar complexes. Furthermore, the steric demands of ligand **9** necessitates widening of the P(1)–Rh(1)–P(2) angle to 99.20(2)° with a consequential contraction of the P(1)–Rh(1)–Cl(1) angle [86.17(8)°].

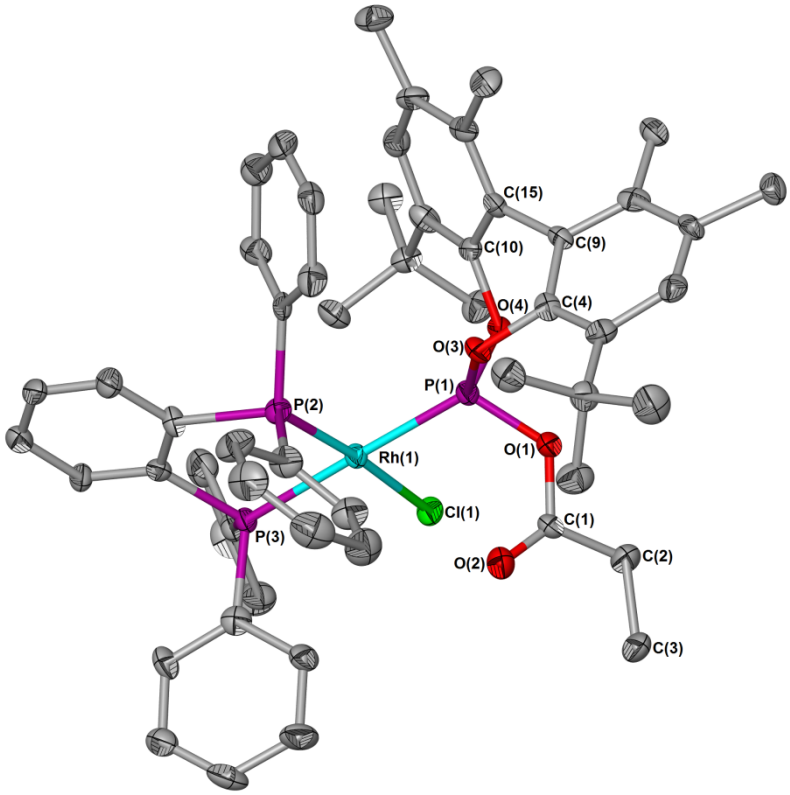


**Figure 4.11** Molecular structure of **45** showing the numbering scheme. Thermal ellipsoids set at 50 % probability and hydrogen atoms and solvent molecules are omitted for clarity.

Measured dihedral angles between the biphenyl rings of ligand **9** are larger than those observed for the related complex [RhCl($PPh_3$)$_2$(**12**)] (**31**)[34] and the structure of free **12**.[35] The Rh(1)–P(1) bond length of 2.236(2) Å is slightly longer than the corresponding bonds in [RhCl($PPh_3$)$_2$(**9**)] (complex **29**) [2.115(6) Å] and [RhCl($PPh_3$)$_2$(**10**)] (complex **30**) [2.140(2) Å],[34] owing to the greater *trans*-influence of the dppbz than that of the chloride ligands in **29** and **30**. Similarly, the Rh(I)–Cl(1) separation is longer than in **29** and **30**, once again indicative of a stronger *trans* influence by the dppbz ligand compared to that of the acylphosphites *trans* to Cl in complexes **29**–**30**.

**Table 4.2** Selected bond lengths (Å) and angles (°) of **45** with estimated standard deviations in parenthesis.

| | | | |
|---|---|---|---|
| *Bond lengths (Å)* | | | |
| Rh(1)–P(1) | 2.236(2) | O(1)–C(1) | 1.383(10) |
| Rh(1)–P(2) | 2.204(2) | C(1)–O(2) | 1.192(10) |
| Rh(1)–P(3) | 2.281(2) | C(1)–C(2) | 1.500(13) |
| Rh(1)–Cl(1) | 2.399(2) | C(2)–C(3) | 1.548(13) |
| P(1)–O(1) | 1.640(6) | O(3)–C(4) | 1.411(10) |
| P(1)–O(3) | 1.631(6) | O(4)–C(10) | 1.422(10) |
| P(1)–O(4) | 1.626(6) | | |
| *Bond angles (°)* | | | |
| P(1)–Rh(1)–P(2) | 99.20(9) | O(1)–P(1)–O(3) | 102.2(3) |
| P(1)–Rh(1)–P(3) | 175.78(8) | O(1)–P(1)–O(4) | 92.2(3) |
| P(1)–Rh(1)–Cl(1) | 86.17(8) | O(3)–P(1)–O(4) | 104.1(3) |
| P(2)–Rh(1)–Cl(1) | 174.62(8) | P(1)–O(1)–C(1) | 122.9(5) |
| P(3)–Rh(1)–Cl(1) | 90.07(8) | O(3)–C(4)–C(9) | 117.5(7) |
| P(2)–Rh(1)–P(3) | 84.55(8) | O(4)–C(10)–C(15) | 115.4(7) |
| Rh(1)–P(1)–O(1) | 115.8(2) | O(1)–C(1)–O(2) | 123.6(8) |
| Rh(1)–P(1)–O(3) | 121.4(2) | O(2)–C(1)–C(2) | 126.1(8) |
| Rh(1)–P(1)–O(4) | 116.5(2) | O(1)–C(1)–C(2) | 110.2(7) |

## 4.3 Conclusions

Herein the already existing collection of mixed anhydride Rh(I) complexes described in Chapter 3 were extended to include complexes with chelated dppe, dppb and dppbz auxiliary ligands. This study has shown that the substitution of $PPh_3$ for chelated diphosphine ligands does not lead to enhanced stability in the resultant mixed anhydride complexes with spontaneous rearrangement persisting to occur over a period of 2-4 days in solution. In the case of dppe, in particular, complexes were found to decompose *via* a decarbonylation pathway similar to those observed for the $PPh_3$ analogues to give the CO dimer [{RhCl(CO)(dppe)}$_2$] as major

product together with the relevant phosphonates. In contrast, for complexes with dppbz as secondary ligands, decomposition proceeded *via* alternative routes and the decarbonylation product, [{RhCl(CO)(dppbz)}$_2$], was not observed. This discrepancy in behaviour could be rationalised by the greater tendency of dppe, owing to its less rigid backbone, to participate in the formation of dimeric reaction intermediates by coordination in a bridged rather than chelated fashion.

Although the more electron rich 1,2-bis(di-*tert*-butylphosphinomethyl)benzene (DTBPMB) ligand seemed like a promising alternative to diphosphines such as dppe, dppb and dppbz, all attempts to prepare the precursor complex [RhCl(PPh$_3$)(DTBPMB)] failed. Similarly, attempts to prepare the dimeric precursor [{RhCl(DTBPMB)}$_2$] resulted in the isolation of the DTBPMB bridged dimer, [{Rh$_2$Cl$_2$(CH$_2$=CH$_2$)$_4$(μ-DTBPMB)], instead.

By employing the PNP ligand (Ph$_2$P)$_2$N$^t$Bu, which is more closely related to the POP systems, the Rh(I) PNP precursor complexes [RhCl(PPh$_3$){(Ph$_2$P)$_2$N$^t$Bu}] and [{RhCl{(Ph$_2$P)$_2$N$^t$Bu}}$_2$] could be prepared successfully. These incredibly stable complexes, however, proved resistant to ligand substitution reactions and treatment with mixed anhydride ligands failed to deliver any useful products.

## 4.4 Experimental

### *4.4.1 General materials, methods and instruments*

Reactions were carried out under dinitrogen gas ($N_2$, passed through a column of dichromate adsorbed on silica) using standard Schlenk, vacuum-line and cannula techniques. All glassware was flame-dried under vacuum. Triethylamine ($NEt_3$) and chlorodiphenylphosphine ($Ph_2Cl$) were purchased from Aldrich and distilled under $N_2$ prior to use. Before distilling, the $NEt_3$ was dried over potassium hydroxide (KOH) pellets. Triphenylphosphine, paraformaldehyde, 1,2-Bis(diphenylphosphino)ethane (dppe), 1,2-Bis(diphenylphosphino)benzene (dppbz) and 1,4-Bis(diphenylphosphino)butane (dppb) were purchased from Aldrich and used as received. Propanoic acid, purchased from BDH laboratories, was dried over anhydrous $Na_2CO_3$ and distilled under $N_2$ prior to use. Bis(di-*tert*-butylphosphinomethyl)benzene (DTBPMB) was supplied by Lucite International. All gases were purchased from BOC gases. [RhCl(PPh$_3$)$_3$] was

prepared from [$RhCl_3 \cdot 3H_2O$] and $PPh_3$ using a standard literature procedure.[36] [$RhCl_3 \cdot 3H_2O$] was purchased from either Engelhard or Alfa Aesar, while [{RhCl(ethylene)$_2$}$_2$], [{RhCl(COD)}$_2$], [RhCl($PPh_3$)(COD)] and *tert*-butylamine were purchased from Alfa Aesar. [{RhCl(dppe)}$_2$], [{RhCl(dppb)}$_2$] and [{RhCl(dppbz)}$_2$] were prepared from [{RhCl(ethylene)$_2$}$_2$] and the relevant diphosphines using a modified literature procedure.[22] *N*,*N*-Bis(diphenylphosphanyl)-*tert*-butylamine was prepared from $Ph_2PCl$ and *tert*-butylamine according to a literature procedure.[37]

Toluene, thf, diethyl ether and hexane were dried using a Braun Solvent Purification System and degassed by additional freeze-pump-thaw cycles when deemed necessary. Methanol and ethanol were distilled under nitrogen from magnesium. Deuterated dichloromethane and chloroform were purchased from Aldrich and dried over phosphorus pentoxide ($P_2O_5$), degassed via three freeze-pump-thaw cycles and trap-to-trap distilled prior to use.

NMR spectra were recorded on a Bruker Avance 300 FT or Bruker Avance II 400 MHz spectrometer ($^1$H NMR at 300/400 MHz, $^{13}$C{$^1$H} NMR at 75/100 MHz and $^{31}$P{$^1$H} NMR at 121/162 MHz) with chemical shifts δ reported relative to tetramethylsilane (TMS)($^1$H, $^{13}$C{$^1$H}) or 85 % $H_3PO_4$ ($^{31}$P{$^1$H}) as external reference. $^1$H and $^{13}$C{$^1$H} NMR spectra were referenced internally to deuterated solvent resonances which were referenced relative to TMS. NMR simulations were performed using DAISY software within a Bruker TOPSPIN environment.

Solid state IR spectra were recorded using pressed KBr pellets on a Perkin Elmer Spectrum GX IR spectrometer. Mass spectra were recorded either by the EPSRC National Mass Spectrometry Service Centre, Swansea on a Thermofisher LTQ Orbitrap XL high resolution instrument coupled to and Advion TriVersa NanoMate electrospray infusion system or by the Mass Spectrometry Service Centre at the University of St. Andrews using either of a Micromass GCT EI/CI or a Micromass LCT ES instrument.

GC-MS chromatograms were recorded on a Hewlett Packard 6890 series GC system equipped with an Agilent J&W HP-1 general purpose column (fused silica capillary) and an HP 5973 Mass selective detector for both qualitative and quantitative analysis. Method: flow rate 1 ml min$^{-1}$ (He carrier gas), split ratio 100 : 1, starting temperature 50 $^{\circ}$C (4 min) ramp rate 20 $^{\circ}$C min$^{-1}$ to 130 $^{\circ}$C (2 min), ramp rate 20 $^{\circ}$C min$^{-1}$ to 220 $^{\circ}$C (15.5 min).

### *2.4.2 Single crystal X-ray structure determinations*

A table containing a summary of the crystal data collection and refinement parameters of compound **45** can be found in Appendix 1. The data set was collected on a Rigaku Mo MM007 (dual port) high brilliance diffractometer with graphite monochromated MoKα radiation (λ = 0.71075 Å). The diffractometer is fitted with Saturn 70 and Mercury CCD detectors and two XStream LT accessories. Data reduction was carried out with standard methods using the software package Bruker SAINT,[38] SMART,[39] SHELXTL[40] and and Rigaku CrystalClear, CrystalStructure, HKL2000. All the structures were solved using direct methods and conventional difference Fourier methods. All non-hydrogen atoms were refined anisotropically by full-matrix least squares calculations on $F^2$ using SHELX-97[41] within an X-seed[42;43] environment. The hydrogen atoms were fixed in calculated positions. Figures were generated with X-seed and POV Ray for Windows, with the displacement ellipsoids at 50% probability level. Further information is available on request from Prof. Alexandra Slawin at the School of Chemistry, University of St. Andrews.

### *4.4.3 Synthetic procedures*

***[RhCl(dppe)(propionyloxydiphenylphosphine)], 35***

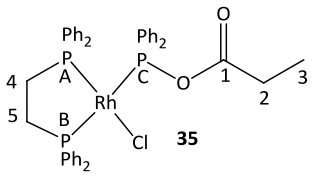

**35**

A solution of **1** (0.14 g, 0.54 mmol) in thf (10 ml) was added to a suspension of [{RhCl(dppe)}$_2$] (0.29 g, 0.27 mmol) in thf (10 ml) at room temperature. The reaction mixture was stirred at this temperature for 2 h during which the orange suspension cleared and a new yellow to pale orange suspension formed. All volatiles were subsequently removed under reduced pressure and the resulting residue dried *in vacuo* to yield the crude product as a pale orange solid, contaminated with **37**, $Ph_2P(O)PPh_2$ and other unassignable by-products. For compound **35**: $^1$H NMR (300 MHz, $CDCl_3$): $\delta_H$ = 0.79 (t, 3H, $^3J$ = 7.5 Hz; $H^2$), 1.99 (q, 2H, $^3J$ = 7.5 Hz; $H^3$), 2.00 (m, 2H; $H^4$), 2.26 (m, 2H; $H^5$), 7.01–7.86 (m, 30H; Ph). $^{13}C\{^1H\}$ NMR (75 MHz, $CDCl_3$): $\delta_C$ = 8.9 (s; $C^3$), 28.8 (s; $C^2$), 34.1 (d, $^1J_{C\text{-}P}$ = 23.5 Hz; $C^4$), 34.6 (d, $^1J_{C\text{-}P}$ = 23.5 Hz; $C^5$), 127.3 (d, $^3J_{C\text{-}P}$ = 10.9 Hz; PPh-$C^{meta}$), 127.8 (d, $^3J_{C\text{-}P}$ = 10.9 Hz; PPh-$C^{meta}$), 128.2(d, $^3J_{C\text{-}P}$ = 10.9 Hz; PPh-$C^{meta}$), 129.6 (s; PPh-$C^{para}$), 129.7 (s; PPh-$C^{para}$), 129.8 (s; PPh-$C^{para}$), 133.3 (d, $^2J_{C\text{-}P}$ = 14.5 Hz; PPh-$C^{ortho}$), 133.6 (d, $^2J_{C\text{-}P}$ = 12.3 Hz; PPh-$C^{ortho}$), 133.9 (d, $^2J_{C\text{-}P}$ = 12.3 Hz; PPh-$C^{ortho}$), 134.2 (d, $^1J_{C\text{-}P}$ = 37.0 Hz; PPh-$C^{ipso}$), 134.3 (d, $^1J_{C\text{-}P}$ = 37.0 Hz; PPh-$C^{ipso}$), 136.2 (d, $^1J_{C\text{-}P}$ = 37.9 Hz; PPh-$C^{ipso}$), 172.3

(d, $^2J_{C\text{-}P}$ = 5.8 Hz; C[1]). $^{31}P\{^1H\}$ NMR (121 MHz, $CDCl_3$): $\delta_P$ = 55.4 (ddd, $^1J_{PA\text{-}Rh}$ = 134.6 Hz, $^2J_{PA\text{-}PB}$ = 34.3 Hz, $^2J_{PA\text{-}PC}$ = 408.8 Hz; $P_A$), 71.8 (ddd, $^1J_{PB\text{-}Rh}$ = 183.6 Hz, $^2J_{PB\text{-}PA}$ = 34.3 Hz, $^2J_{PB\text{-}PC}$ = 36.7 Hz; $P_B$), 125.6 (ddd, $^1J_{PC\text{-}Rh}$ = 161.5 Hz, $^2J_{PC\text{-}PA}$ = 408.8 Hz, $^2J_{PC\text{-}PB}$ = 36.7 Hz; $P_C$). For compound **37**: $^{31}P\{^1H\}$ NMR (121 MHz, $CDCl_3$): This compound gives rise to second order $^{31}P\{^1H\}$ NMR spectrum. Chemical shifts and coupling constants were determined by means of simulation. For this, compound **37** was modelled as an AA'MXX' spin system with $C_2$ symmetry. $\delta_P$ = 57.9 (m, $^1J_{PA\text{-}Rh}$ = $^1J_{PB\text{-}Rh}$ 130.0 Hz, $^2J_{PA\text{-}PB}$ = 122 Hz, $^2J_{PA\text{-}PC}$ = $^2J_{PB\text{-}PD}$ = -28 Hz, $^2J_{PA\text{-}PD}$ = $^2J_{PB\text{-}PC}$ = 287.4 Hz; $P_A + P_B$), $\delta_P$ = 106.93 (m, $^1J_{PC\text{-}Rh}$ = $^1J_{PD\text{-}Rh}$ 120 Hz, $^2J_{PC\text{-}PD}$ = 32 Hz, $^2J_{PC\text{-}PA}$ = $^2J_{PD\text{-}PB}$ = -28 Hz, $^2J_{PD\text{-}PA}$ = $^2J_{PC\text{-}P\boldsymbol{B}}$ = 287.4 Hz; $P_C + P_D$).

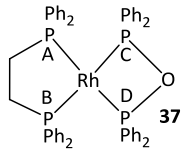

**37**

### *Attempt to prepare [RhCl(dppb)(propionyloxydiphenylphosphine)], 36*

A solution of **1** (0.13 g, 0.52 mmol) in thf (10 ml) was added to a solution of $[\{RhCl(dppb)\}_2]$ (0.29 g, 0.26 mmol) in thf (10 ml) at room temperature. The reaction mixture was stirred at this temperature for 40 min during which the dark orange solution changed colour to light orange. All volatiles were subsequently removed under reduced pressure and the resulting orange foamy residue was subjected to NMR analysis. Analysis of the solid revealed no traces of the desired complex. Instead, the rearrangement product **38** constituted the major product, together with various other unassignable by-products. For compound **37**: $^{31}P\{^1H\}$ NMR (121 MHz, $CDCl_3$): This compound gives rise to second order spectra. Chemical shifts and coupling constants were determined by means of simulation. For this, compound **37** was modelled as an AA'MXX' spin system with $C_2$ symmetry. $\delta_P$ = 22.4 (m, $^1J_{PA\text{-}Rh}$ = $^1J_{PB\text{-}Rh}$ 131 Hz, $^2J_{PA\text{-}PB}$ = 115 Hz, $^2J_{PA\text{-}PC}$ = $^2J_{PB\text{-}PD}$ = -33 Hz, $^2J_{PA\text{-}PD}$ = $^2J_{PB\text{-}PC}$ = 283 Hz; $P_A + P_B$), $\delta_P$ = 101.1 (m, $^1J_{PC\text{-}Rh}$ = $^1J_{PD\text{-}Rh}$ 121 Hz, $^2J_{PC\text{-}PD}$ = 39 Hz, $^2J_{PC\text{-}PA}$ = $^2J_{PD\text{-}PB}$ = -33 Hz, $^2J_{PD\text{-}PA}$ = $^2J_{PC\text{-}P\boldsymbol{B}}$ = 283 Hz; $P_C + P_D$).

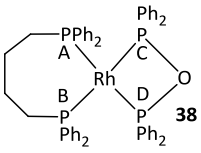

**38**

### *[RhCl(dppe){propionyl(5,5',6,6'-tetramethyl-3,3'-di-tert-butyl-1,1'-biphenyl-2,2'-diyl)--phosphite}], 41*

A solution of **9** (0.08 g, 0.18 mmol) in thf (15 ml) was added to a suspension of $[\{RhCl(dppe)\}_2]$ (0.91 g, 0.09 mmol) in thf (15 ml) at room temperature. The reaction mixture was stirred at this temperature for 2 h during which time the solution colour changed from orange to light yellow. The mixture was subsequently stripped of all volatiles under reduced pressure and the resulting yellow residue washed with hexane (2 × 25 ml), and dried *in vacuo* to yield the product as a light yellow solid (0.14 g, 78%). For compound **41**: $^1H$ NMR (300 MHz, $CD_2Cl_2$): $\delta_H$ =

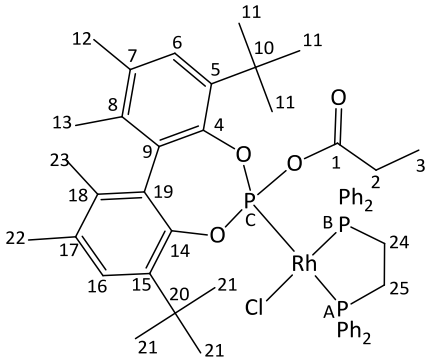

0.86 (q, 2H, $^{3}J$ = 7.4 Hz; $H^{2}$), 1.07 (t, 3H, $^{3}J$ = 7.4 Hz; $H^{3}$), 1.12 (s, 9H; $H^{11}$), 1.40 (s, 3H; $H^{12}$), 1.50 (s, 9H; $H^{21}$), 1.60 (s, 3H; $H^{22}$), 2.00 (dt, 2H, $^{3}J_{H\text{-}H}$ = 6.4 Hz, $^{2}J_{H\text{-}P}$ = 19.7 Hz; $H^{24}$), 2.14 (s, 3H; $H^{13}$), 2.18 (s, 3H; $H^{23}$), 2.41 (dt, 2H, $^{3}J_{H\text{-}H}$ = 6.4 Hz, $^{2}J_{H\text{-}P}$ = 19.7 Hz; $H^{25}$), 6.83–8.30 (m, 22H; Ph). $^{13}C\{^{1}H\}$ NMR (75 MHz, $CD_2Cl_2$): $\delta_C$ = 9.1 (s; $C^{3}$), 16.5 (s; $C^{13}$), 16.6 (s; $C^{23}$), 20.3 (s; $C^{12}$), 20.4 (s; $C^{22}$), 29.8 (s; $C^{2}$), 31.8 (s; $C^{11}$), 32.8 (s; $C^{21}$), 35.0 (s; $C^{10}$), 35.3 (s; $C^{20}$), 127.5 (s; $C^{6}$), 127.6 (s; $C^{16}$), 128.3 (d, $^{3}J_{C\text{-}P}$ = 9.9 Hz; PPh-$C^{meta}$), 128.5 (d, $^{3}J_{C\text{-}P}$ = 9.7 Hz; PPh-$C^{meta}$), 130.3 (s; PPh-$C^{para}$), 130.8 (s; PPh-$C^{para}$), 132.3 (s; $C^{7}$), 132.7 (s; $C^{17}$), 129.7 (s; $C^{9}$), 129.9 (s; $C^{19}$), 133.3 (m; PPh-$C^{ortho}$), 136.4 (m; PPh-$C^{ortho}$), 134.8 (s; $C^{8}$), 135.4 (s; $C^{18}$), 137.5 (s; $C^{5}$ / $C^{15}$), not observed - signal too weak (PPh-$C^{ipso}$, and $C^{4}$ / $C^{4'}$), 177.6 (s, $C^{1}$). $^{31}P\{^{1}H\}$ NMR (121 MHz, $CD_2Cl_2$): $\delta_P$ = 54.0 (ddd, $^{1}J_{PA\text{-}Rh}$ = 133.2 Hz, $^{2}J_{PA\text{-}PB}$ = 33.8 Hz, $^{2}J_{PA\text{-}PC}$ = 548.4 Hz; $P_A$), 70.4 (ddd, $^{1}J_{PB\text{-}Rh}$ = 178.2 Hz, $^{2}J_{PB\text{-}PA}$ = 33.8 Hz, $^{2}J_{PB\text{-}PC}$ = 46.1 Hz; $P_B$), 134.4 (ddd, $^{1}J_{PC\text{-}Rh}$ = 239.7 Hz, $^{2}J_{PC\text{-}PA}$ = 548.4 Hz, $^{2}J_{PC\text{-}PB}$ = 46.1 Hz; $P_C$). IR (KBr): $\tilde{\nu}$ = 3052 [m, $sp^2$ $\nu$(C–H)], 2957–2867 [m, $sp^3$ $\nu$(C–H)], 1761 [m, $\nu$(C=O)], 1483–1361 [st, Ar $\nu$(C=C)], 695 [m, $\nu$(P–O)]. ES-MS: *m/z* (%) = 957 (100) $[M - Cl]^+$, 500 (60) $[Rh(dppe)]^+$. For phosphonate **52** (formed during the decarbonylation of **41**): $^{1}H$ NMR (300 MHz, $CD_2Cl_2$): $\delta_H$ = 1.46 (s, 9H; $H^{11}$), 1.52, (s, 9H; $H^{21}$), 1.87 (s, 3H; $H^{12}$ ), 1.88 (s, 3H; $H^{22}$), 2.30 (s, 6H; $H^{13}$ / $H^{23}$), 7.0 (d, 1H, $^{1}J_{H\text{-}P}$ = 725.4 Hz; $H^{1}$), 7.26 (s, 1H; $H^{6}$), 7.30 (s, 1H; $H^{16}$). $^{31}P\{^{1}H\}$ NMR (121 MHz, $CD_2Cl_2$): $\delta_P$ = 9.4 (s).

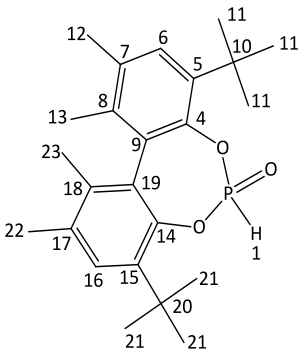

### *[RhCl(dppe){propionyl(3,3',5,5'-tetra-tert-butyl-1,1'-biphenyl-2,2'-diyl)phosphite}], 42*

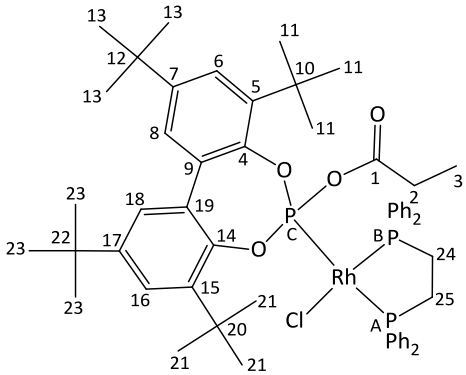

A solution of **10** (0.13 g, 0.26 mmol) in thf (20 ml) was added to a suspension of $[\{RhCl(dppe)\}_2]$ (0.14 g, 0.13 mmol) in thf (5 ml) at room temperature. The reaction mixture was stirred at room temperature for 3 h during which the solution colour changed from orange to yellow. The mixture was subsequently reduced to dryness and the resulting yellow residue washed with pentane (3 × 20 ml), and dried *in vacuo* to yield the product as a yellow solid (0.24 g, 87%).$^{1}H$ NMR (300 MHz, $CD_2Cl_2$): $\delta_H$ = 0.87 (q, 2H, $^{3}J$ = 7.5 Hz;

$H^2$), 1.02 (t, 3H, $^3J$ = 7.5 Hz; $H^3$), 1.32 (s, 36H; $H^{11}$ / $H^{21}$ / $H^{13}$ / $H^{23}$), 2.20 (dt, 2H, $^2J_{H\text{-}P}$ = 20.0 Hz, $^3J_{H\text{-}H}$ = 6.7 Hz; $H^{24}$), 2.30 (dt, 2H, $^2J_{H\text{-}P}$ = 20.0 Hz, $^3J_{H\text{-}H}$ = 6.7 Hz; $H^{25}$), 6.78–7.89 (m, 24H; Ph). $^{13}C\{^1H\}$ NMR (75 MHz, $CD_2Cl_2$): $\delta_C$ = 7.5 (s; $C^3$), 27.7 (d, $^2J_{C\text{-}P}$ = 2.5 Hz; $C^2$), 31.6 (s; $C^{11}$ / $C^{21}$), 31.8 (s; $C^{13}$ / $C^{23}$), 34.8 (s; $C^{10}$ / $C^{20}$), 35.9 (s; $C^{12}$ / $C^{22}$), 124.7 (s; $C^6$ / $C^{16}$), 127.6 (s; $C^8$ / $C^{18}$), 128.5 (d, $^3J_{C\text{-}P}$ = 9.6 Hz; PPh-$C^{meta}$), 130.2 (d, $^4J_{C\text{-}P}$ = 11.0 Hz; PPh-$C^{para}$), 134.0 (d, $^2J_{C\text{-}P}$ = 10.9 Hz; PPh-$C^{ortho}$), not observed - underneath Ph-$C^{ortho}$ resonance ($C^9$ / $C^{9'}$), 134.9 (d, $^1J_{C\text{-}P}$ = 43.9 Hz; PPh-$C^{ipso}$), 140.4 (s; $C^5$ / $C^{15}$), 145.3 (s; $C^4$ / $C^{14}$), 146.7 (s; $C^7$ / $C^{17}$), 169.6 (s; $C^1$). $^{31}P\{^1H\}$ NMR (121 MHz, $CD_2Cl_2$): $\delta_P$ = 54.5 (ddd, $^1J_{PA\text{-}Rh}$ = 137.2 Hz, $^2J_{PA\text{-}PB}$ = 34.3 Hz, $^2J_{PA\text{-}PC}$ = 557.9 Hz; $P_A$), 70.4 (ddd, $^1J_{PB\text{-}Rh}$ = 174.5 Hz, $^2J_{PB\text{-}PA}$ = 34.3 Hz, $^2J_{PB\text{-}PC}$ = 46.2 Hz; $P_B$), 138.5 (ddd, $^1J_{PC\text{-}Rh}$ = 241.6 Hz, $^2J_{PC\text{-}PA}$ = 557.9 Hz, $^2J_{PC\text{-}PB}$ = 46.2 Hz; $P_C$). IR (KBr): $\tilde{\nu}$ = 3054 [m, $sp^2$ $\nu$(C–H)], 2961–2867 [m, $sp^3$ $\nu$(C–H)], 1769 [m, $\nu$(C=O)], 1481–1398 [st, Ar $\nu$(C=C)], 694 [m, $\nu$(P–O)].

### *[RhCl(dppb){propionyl-(5,5',6,6'-tetramethyl-3,3'-di-tert-butyl-1,1'-biphenyl-2,2'-diyl)phosphite}], 43*

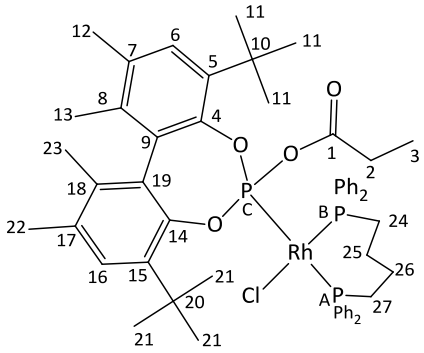


A solution of **9** (0.11 g, 0.24 mmol) in thf (20 ml) was added to a solution of [{RhCl(dppb)}$_2$] (0.14 g, 0.12 mmol) in thf (5 ml) at room temperature. The reaction mixture was stirred at this temperature for 3 h during which the solution colour changed from orange to dark yellow. All volatiles were subsequently removed under reduced pressure and the resulting yellow residue washed with pentane (3 × 20 ml), and dried *in vacuo* to yield the crude product as a yellow solid (0.20 g, 80 %). $^1H$ NMR (300 MHz, $CD_2Cl_2$): $\delta_H$ = 0.88 (q, 2H, $^3J$ = 7.2 Hz; $H^2$), 0.97 (t, 3H, $^3J$ = 7.2 Hz; $H^3$), 1.18 (s, 18H; $H^{11}$ / $H^{21}$), 1.28 (m, 2H; $H^{24}$), 1.53 (s, 2H; $H^{27}$), 1.70 (s, 4H; $H^{25}$ / $H^{26}$), 1.94 (s, 6H; $H^{12}$ / $H^{22}$), 2.15 (s, 3H; $H^{13}$), 2.33 (s, 3H; $H^{23}$), 6.61–7.74 (m, 22H; Ph). $^{13}C\{^1H\}$ NMR (75 MHz, $CD_2Cl_2$): $\delta_C$ = 8.9 (s; $C^3$), 16.6 (s; $C^{13}$), 16.8 (s; $C^{23}$), 20.3 (s; $C^{12}$), 20.5 (s; $C^{22}$), 23.1 (s; $C^{25}$ / $C^{26}$), 26.5 (d, $J_{C\text{-}P}$ = 4.7 Hz; $C^{24}$), 26.6 (d, $J_{C\text{-}P}$ = 4.7 Hz; $C^{27}$), 29.8 (s; $C^2$), 32.8 (s; $C^{11}$ / $C^{21}$), 35.4 (s; $C^{10}$), 35.6 (s; $C^{20}$), 128.5 (s; $C^6$), 128.7 (s; $C^{16}$), 127.8 (m; PPh-$C^{meta}$), 129.4 (s; PPh-$C^{para}$), 129.8 (s; PPh-$C^{para}$), 132.3 (s; $C^7$ /$C^{17}$), 130.7 (s; $C^9$), 131.5 (s; $C^{19}$), 134.6 (m; PPh-$C^{ortho}$), 135.7 (s; $C^8$ / $C^{18}$), 137.8 (s; $C^5$ / $C^{15}$), not observed - signal too weak (PPh-$C^{ipso}$, $C^4$ / $C^{14}$ and $C^1$). $^{31}P\{^1H\}$ NMR (121 MHz, $CD_2Cl_2$): $\delta_P$ = 6.1 (ddd, $^1J_{PA\text{-}Rh}$ = 127.8 Hz, $^2J_{PA\text{-}PB}$ = 46.8 Hz, $^2J_{PA\text{-}PC}$ = 536.3 Hz; $P_A$), 52.1 (ddd observed as dt, $^1J_{PB\text{-}Rh}$ = 177.7 Hz, $^2J_{PB\text{-}PA}$ = $^2J_{PB\text{-}PC}$ = 46.8 Hz; $P_B$), 131.0 (ddd, $^1J_{PC\text{-}Rh}$ = 246.3 Hz, $^2J_{PC\text{-}PA}$ = 536.3 Hz, $^2J_{PC\text{-}PB}$

= 46.8 Hz; $P_C$). IR (KBr): $\tilde{\nu}$ = 3055 [m, $sp^2$ $\nu$(C–H)], 2957–2867 [m, $sp^3$ $\nu$(C–H)], 1766 [w, $\nu$(C=O)], 1483–1364 [st, Ar $\nu$(C=C)], 694 [m, $\nu$(P–O)].

### *[RhCl(dppb){propionyl(3,3',5,5'-tetra-tert-butyl-1,1'-biphenyl-2,2'-diyl)phosphite}], 44*

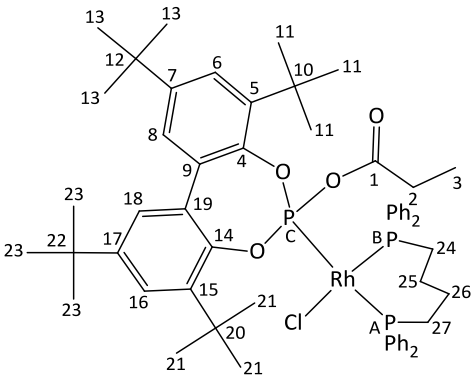

A solution of **10** (0.17 g, 0.33 mmol) in thf (15 ml) was added to a suspension of [{RhCl(dppb}$_2$] (0.19 g, 0.17 mmol) in thf (10 ml) at room temperature. The reaction mixture was stirred at room temperature for 2 h during which the solution colour changed from orange to yellow. The mixture was subsequently filtered (cannula filtration) into a separate flask and the filtrate reduced to dryness. The product was then extracted from the orange residue with hexane (2 × 20 ml) and the extract stripped of all volatiles under reduced pressure to obtain the product mixture as a bright yellow solid. In addition to some free ligand, the final product consisted of a mixture of the title product **44** and the two by-products **47a** and **47b**. These products could not be separated successfully by standard purification techniques. For compound **44**: $^1$H NMR (300 MHz, $CD_2Cl_2$): $\delta_H$ = 0.88 (q, 2H, $^3J$ = 7.4 Hz; $H^2$), 0.92 (t, 3H, $^3J$ = 7.4 Hz; $H^3$), 1.32 (s, 4H; $H^{25}$ / $H^{26}$), 1.38 (s, 18H; $H^{11}$ / $H^{21}$), 1.50 (s, 18H; $H^{13}$ / $H^{23}$), 1.64 (s, 4H; $H^{24}$ / $H^{27}$), 6.79–7.73 (m, 24H; Ph). $^{13}$C{$^1$H} NMR (75 MHz, $CD_2Cl_2$): $\delta_C$ = 8.9 (s; $C^3$), 23.4 (s; $C^{25}$ / $C^{26}$), 25.2 (d, $^1J_{C\text{-}P}$ = 20.5 Hz; $C^{24}$), 26.6 (d, $^1J_{C\text{-}P}$ = 11.7 Hz; $C^{27}$), 29.8 (bs; $C^2$), 31.6 (s; $C^{11}$ / $C^{21}$), 32.4 (s; $C^{13}$ / $C^{23}$), 34.9 (s; $C^{10}$ / $C^{20}$), 35.0 (s; $C^{12}$ / $C^{22}$), 125.2 (s; $C^6$ / $C^{16}$), 126.9 (s; $C^8$ / $C^{18}$), 127.9 (m; PPh-$C^{meta}$), 131.8 (s; $C^9$ / $C^{19}$), 132.6 (m; PPh-$C^{para}$), 134.8 (d, $^2J_{C\text{-}P}$ = 11.8 Hz; PPh-$C^{ortho}$), 140.6 (m; PPh-$C^{ipso}$), 140.1 (s; $C^5$ / $C^{15}$), 148.9 (s; $C^4$ / $C^{14}$), 146.8 (s; $C^7$ / $C^{17}$), 170.8 (s; $C^1$). $^{31}$P{$^1$H} NMR (121 MHz, $CD_2Cl_2$): $\delta_P$ = 5.7 (ddd, $^1J_{PA\text{-}Rh}$ = 124.6 Hz, $^2J_{PA\text{-}PB}$ = 49.1 Hz, $^2J_{PA\text{-}PC}$ = 547.4 Hz; $P_A$), 52.4 (ddd observed as dt, $^1J_{PB\text{-}Rh}$ = 181.2 Hz, $^2J_{PB\text{-}PA}$ = $^2J_{PB\text{-}PC}$ = 49.1 Hz; $P_B$), 133.7 (ddd, $^1J_{PC\text{-}Rh}$ = 249.2 Hz, $^2J_{PC\text{-}PA}$ = 547.4 Hz, $^2J_{PC\text{-}PB}$ = 49.1 Hz; $P_C$). IR (KBr): $\tilde{\nu}$ = 3056 [m, $sp^2$ $\nu$(C–H)], 2960–2869 [st, $sp^3$ $\nu$(C–H)], 1772 [w, $\nu$(C=O)], 1478–1398 [st, Ar $\nu$(C=C)], 694 [m, $\nu$(P–O)].

### *[RhCl(dppbz){propionyl(5,5',6,6'-tetramethyl-3,3'-di-tert-butyl-1,1'-biphenyl-2,2'-diyl)phosphite}], 45*

A solution of **9** (0.11 g, 0.24 mmol) in thf (20 ml) was added to a suspension of [{RhCl(dppbz)}$_2$] (0.15 g, 0.12 mmol) in thf (5 ml) at room temperature. The reaction mixture was stirred at this

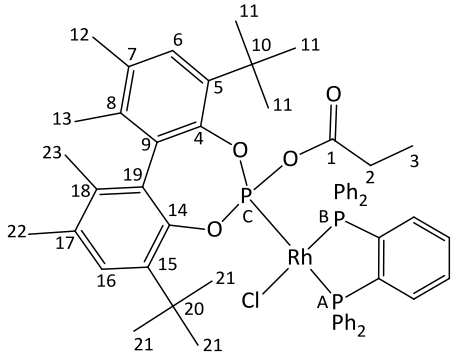

temperature for 2 h during which time the solution changed colour from orange to light yellow. All volatiles were subsequently removed under reduced pressure and the resulting yellow residue washed with hexane (3 × 20 ml), and dried *in vacuo* to yield the product as a light yellow solid (0.19 g, 74 %). Single crystals of **45** suitable for X-ray analysis were obtained as yellow needles by cooling a concentrated dichloromethane solution of **45** to -22 °C. $^{1}$H NMR (300 MHz, $CD_2Cl_2$): $\delta_H$ = 0.89 (q, 2H, $^{3}J$ = 7.0 Hz; $H^{2}$), 1.05 (underneath $H^{11}$ signal; $H^{3}$), 1.05 (s, 9H; $H^{11}$), 1.39 (s, 9H; $H^{21}$), 1.57 (s, 3H; $H^{12}$), 1.66 (s, 3H; $H^{22}$), 2.19 (s, 3H; $H^{13}$), 2.21 (s, 3H; $H^{23}$), 6.82–8.33 (m, 22H; Ph). $^{13}C\{^{1}H\}$ NMR (75 MHz, $CD_2Cl_2$): $\delta_C$ = 9.1 (s; $C^{3}$), 16.6 (s; $C^{13}$), 16.7 (s; $C^{23}$), 20.3 (s; $C^{12}$), 20.4 (s; $C^{22}$), 29.9 (s; $C^{2}$), 31.5 (s; $C^{11}$), 32.5 (s; $C^{21}$), 34.8 (s; $C^{10}$), 35.2 (s; $C^{20}$), 127.5 (s; $C^{6}$), 127.6 (s; $C^{16}$), 128.2 (PPh-$C^{meta}$), 128.4 (PPh-$C^{meta}$), 128.7 (PPh-$C^{meta}$), 129.9 (PPh-$C^{para}$), 130.5 (s; PPh-$C^{para}$), 130.9 (s; $C^{9}$), 132.4 (s; $C^{19}$), 132.8 (s; $C^{7}$), 133.8 (s; $C^{17}$), 134.0 (d, $^{2}J_{C\text{-}P}$ = 10.3 Hz; PPh-$C^{ortho}$), 135.2 (d, $^{2}J_{C\text{-}P}$ = 11.9 Hz; PPh-$C^{ortho}$), 135.9 (d, $^{2}J_{C\text{-}P}$ = 11.8 Hz; PPh-$C^{ortho}$), 134.8 (s; $C^{8}$), 135.5 (s; $C^{18}$), 136.4 (d, $^{1}J_{C\text{-}P}$ = 45.0 Hz; Ph-$C^{ipso}$), 137.9 (s; $C^{5}$), 138.4 (s; $C^{15}$), 145.9 (s;$C^{4}$), 146.0 (s; $C^{14}$), 170.3 (s, $C^{1}$). $^{31}P\{^{1}H\}$ NMR (121 MHz, $CD_2Cl_2$): $\delta_P$ = 59.3 (ddd, $^{1}J_{PA\text{-}Rh}$ = 134.1 Hz, $^{2}J_{PA\text{-}PB}$ = 34.1 Hz, $^{2}J_{PA\text{-}PC}$ = 552.3 Hz; $P_A$), 70.1 (ddd, $^{1}J_{PB\text{-}Rh}$ = 179.8 Hz, $^{2}J_{PB\text{-}PA}$ = 34.1 Hz, $^{2}J_{PB\text{-}PC}$ = 44.7 Hz; $P_B$), 135.2 (ddd, $^{1}J_{PC\text{-}Rh}$ = 236.7 Hz, $^{2}J_{PC\text{-}PA}$ = 552.3 Hz, $^{2}J_{PC\text{-}PB}$ = 44.7 Hz; $P_C$). IR (KBr): $\tilde{\nu}$ = 3054 [m, $sp^2$ $\nu$(C–H)], 2958–2867 [m, $sp^3$ $\nu$(C–H)], 1763 [m, $\nu$(C=O)], 1482–1361 [st, Ar $\nu$(C=C)], 693 [st, $\nu$(P–O)]. ES-MS: *m/z* (%) = 1005 (100) $[M - Cl]^+$.

***[RhCl(dppbz){propionyl(3,3',5,5'-tetra-tert-butyl-1,1'-biphenyl-2,2'-diyl)phosphite}], 46***

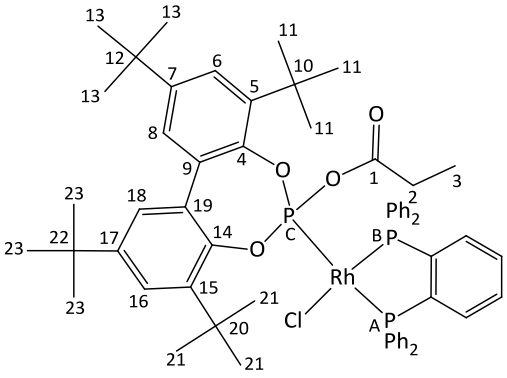

A solution of **10** (0.18 g, 0.36 mmol) in thf (10 ml) was added to a suspension of $[\{RhCl(dppbz)\}_2]$ (0.21 g, 0.18 mmol) in thf (10 ml) at room temperature. The reaction mixture was stirred at this temperature for 2 h during which the solution colour changed from orange to light yellow. The mixture was subsequently reduced to dryness and the product extracted from the yellow residue with hexane (3 × 20 ml). The resulting hexane extract was stripped of all volatiles under reduced pressure and the remaining solid dried *in vacuo* to yield the product as a light yellow solid

(0.30 g, 78%). $^{1}$H NMR (300 MHz, $CD_2Cl_2$): $\delta_H$ = 0.87 (qd, 2H, $^{3}J_{H\text{-}H}$ = 7.1 Hz, $^{4}J_{H\text{-}P}$ = 1.9; $H^2$), 1.11 (t, 3H, $^{3}J$ = 7.1 Hz; $H^3$), 1.19 (s, 18H; $H^{11}$ / $H^{21}$), 1.34 (s, 3H; $H^{13}$ / $H^{23}$), 7.20 (d, 2H, $^{4}J$ = Hz; $H^6$ / $H^{16}$), 7.49 (d, 2H, $^{4}J$ = 2.7 Hz; $H^8$ / $H^{18}$), 6.96–7.75 (m, 24H; Ph). $^{13}C\{^{1}H\}$ NMR (75 MHz, $CD_2Cl_2$): $\delta_C$ = 9.1 (s; $C^3$), 29.8 (s; $C^2$), 31.7 (s; $C^{11}$ / $C^{21}$ / $C^{13}$ / $C^{23}$), 34.9 (s; $C^{10}$ / $C^{20}$), 35.8 (s; $C^{12}$ / $C^{22}$), 124.8 (s; $C^6$ / $C^{16}$), 127.5 (s; $C^8$ / $C^{18}$), 128.4 (d, $^{3}J_{C\text{-}P}$ = 11.3 Hz; PPh-$C^{meta}$), 130.0 (s; PPh-$C^{para}$), 130.3 (s; PPh-$C^{para}$), 131.9 (s; $C^9$ / $C^{19}$), 135.7 (d, $^{1}J_{C\text{-}P}$ = 47.9 Hz; PPh-$C^{ipso}$), 140.6 (s; $C^5$ / $C^{15}$), 146.9 (s; $C^7$ / $C^{17}$), 147.8 (s; $C^4$ / $C^{14}$), 174.5 (s; $C^1$). $^{31}P\{^{1}H\}$ NMR (121 MHz, $CD_2Cl_2$): $\delta_P$ = 59.4 (ddd, $^{1}J_{PA\text{-}Rh}$ = 131.7 Hz, $^{2}J_{PA\text{-}PB}$ = 35.2 Hz, $^{2}J_{PA\text{-}PC}$ = 559.8 Hz; $P_A$), 70.1 (ddd, $^{1}J_{PB\text{-}Rh}$ = 176.4 Hz, $^{2}J_{PB\text{-}PA}$ = 35.2 Hz, $^{2}J_{PB\text{-}PC}$ = 44.7 Hz; $P_B$), 139.3 (ddd, $^{1}J_{PC\text{-}Rh}$ = 239.9 Hz, $^{2}J_{PC\text{-}PA}$ = 559.8 Hz, $^{2}J_{PC\text{-}PB}$ = 44.7 Hz; $P_C$). IR (KBr): $\tilde{\nu}$ = 3053 [w, $sp^2$ $\nu$(C–H)], 2961–2869 [m, $sp^3$ $\nu$(C–H)], 1772 [m, $\nu$(C=O)], 1478–1393 [st, Ar $\nu$(C=C)], 693 [m, $\nu$(P–O)]. ES-MS: *m/z* (%) = 1061 (100) $[M - Cl]^+$.

### *[{RhCl(CH$_2$=CH$_2$)$_2$}$_2$(DTBPMB)], 56*

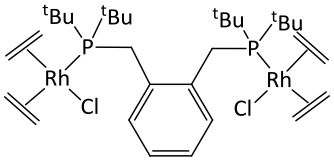


A solution of 1,2-bis((di-*tert*-butylphosphino)methyl)benzene (0.49 g, 1.23 mmol) in toluene (15 ml) was added slowly to a solution of [{RhCl($CH_2$=$CH_2$)$_2$}$_2$] (0.21 g, 0.18 mmol) in toluene (10 ml) at room temperature. Upon addition, the reaction mixture immediately changed colour from orange to dark green. Following a 21 h stirring period at room temperature, the reaction mixture was filtered (cannula filtration) and subsequently reduced to dryness. The crude products was washed with hexane (2 × 30 ml) and the remaining solid dried *in vacuo* to yield the product as a dark green solid (91 %). Complex **50** is extremely air sensitive and decomposes (changes colour from green to orange) within seconds in air. For this reason, no MS, IR or elemental analysis were performed for this compound. $^{1}$H NMR (300 MHz, $CD_2Cl_2$): $\delta_H$ = 1.16 (m, 8H; C*H$_2$*=C*H$_2$*), 1.46 (s, 18H; $^{t}$Bu), 1.50 (s, 18H; $^{t}$Bu), 3.23 (d, $^{2}J_{H\text{-}P}$ = 2.6 Hz; –C*H$_2$*–), 3.26 (d, $^{2}J_{H\text{-}P}$ = 2.3 Hz; –C*H$_2$*–), 7.13 (m, 2H; Ph), 7.24 (m, 2H; Ph). $^{31}P\{^{1}H\}$ NMR (121 MHz, $CD_2Cl_2$): $\delta_P$ = 76.2 (d, $^{1}J_{P\text{-}Rh}$ = 205.4 Hz; P). For comparative data see the values reported in literature for [{RhCl(COD)}$_2$(DTBPMB)].[4]

### *[RhCl(PPh$_3$){$^{t}$BuN(PPh$_2$)$_2$}], 57*

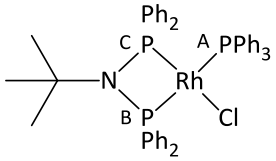


[RhCl($PPh_3$)$_3$] (0.45 g, 0.48 mmol) was suspended in thf (10 ml) at room temperature. To this suspension, a solution of *N,N*-bis(diphenylphosphanyl)-*tert*-butylamine (0.21 g, 0.48 mmol) in thf (10 ml) was added upon which the red reaction mixture became

clear. The resulting reaction mixture was allowed to stir for 2 h at room temperature. After the first 30 min of stirring, the title product precipitated from solution as a bright yellow microcrystalline solid. Upon completion of the 2 hour stirring period, the yellow solid was collected on a sinterglass frit (under inert conditions), washed with hexane (2 × 30 ml) and dried *in vacuo* to afford the pure product as a bright yellow solid (0.27 g, 67 %).$^{1}$H NMR (300 MHz, $CD_2Cl_2$): $\delta_H$ = 0.74 (s, 9H; $^{t}$Bu), 7.05 (m, 6H; Ph), 7.23 (m, 15H; Ph), 7.54 (m, 6H; Ph), 7.76 (m, 4H; Ph), 8.26 (m, 4H; Ph). $^{13}$C{$^{1}$H} NMR (75 MHz, $CD_2Cl_2$): $\delta_C$ = 31.3 (s; -*C*$H_3$), 62.1 [-*C*$(CH_3)_3$], 127.7 (d, $^{1}J_{C\text{-}P}$ = 39.9 Hz; Ph-C$^{meta}$), 128.1 (d, $^{3}J_{C\text{-}P}$ = 39.9 Hz; PPh-C$^{meta}$), 128.3 (d, $^{3}J_{C\text{-}P}$ = 39.9 Hz; PPh-C$^{meta}$), 129.2 (s; PPh-C$^{para}$), 130.4 (d, $^{4}J_{C\text{-}P}$ = 2.2 Hz; PPh-C$^{para}$), 130.7 (s; PPh-C$^{para}$), 133.8 (d, $^{2}J_{C\text{-}P}$ = 13.5 Hz; PPh-C$^{ortho}$), 134.8 (d, $^{2}J_{C\text{-}P}$ = 13.8 Hz; PPh-C$^{ortho}$), 135.1 (d, $^{2}J_{C\text{-}P}$ = 13.1 Hz; PPh-C$^{ortho}$), 135.4 (d, $^{1}J_{C\text{-}P}$ = 39.9; PPh-C$^{ipso}$), 135.5 (d, $^{1}J_{C\text{-}P}$ = 37.4; PPh-C$^{ipso}$), 135.6 (d, $^{1}J_{C\text{-}P}$ = 32.3; PPh-C$^{ipso}$). $^{31}$P{$^{1}$H} NMR (121 MHz, $CD_2Cl_2$): $\delta_P$ = 26.3 (ddd, $^{1}J_{PA\text{-}Rh}$ = 137.2 Hz, $^{2}J_{PA\text{-}PB}$ = 363.4 Hz, $^{2}J_{PA\text{-}PC}$ = 25.0 Hz; $P_A$), 52.7 (ddd, $^{1}J_{PB\text{-}Rh}$ = 121.3 Hz, $^{2}J_{PB\text{-}PA}$ = 363.4 Hz, $^{2}J_{PB\text{-}PC}$ = 97.7 Hz; $P_B$), 67.4 (ddd, $^{1}J_{PC\text{-}Rh}$ = 163.3 Hz, $^{2}J_{PC\text{-}PA}$ = 25.0 Hz, $^{2}J_{PC\text{-}PB}$ = 97.7 Hz; $P_C$). IR (KBr): $\tilde{\nu}$ = 3052 [w, sp$^2$ $\nu$(C–H)], 2983–2867 [w, sp$^3$ $\nu$(C–H), 1480–1367 [st, Ar $\nu$(C=C)], 1090 [st, $\nu$(C–N)]. ES-MS: *m/z* (%) = 579 (100) $[M - PPh_3]^+$.

### *[{RhCl($^{t}$BuN(PPh$_2$)$_2$)}$_2$], 61*

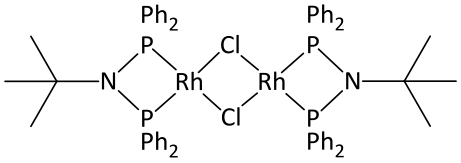


A solution of *N,N*-bis(diphenylphosphanyl)-*tert*-butylamine (0.38 g, 0.85 mmol) in toluene (7 ml) was added to a solution of [{RhCl($CH_2$=$CH_2$)$_2$}$_2$] (0.17 g, 0.48 mmol) in toluene (11 ml) at room temperature. Addition of the PNP ligand led to the immediate formation of a pale orange precipitate. The reaction mixture was stirred for 21 h at room temperature, after which the precipitate was collected on a sinterglass frit under inert conditions and dried *in vacuo* to afford the product as a pale yellow solid (0.46 g, 94 %).$^{1}$H NMR (300 MHz, $CD_2Cl_2$): $\delta_H$ = 0.78 (s, 18H; $^{t}$Bu), 7.22 (m, 24H; Ph), 7.39 (m, 16H; Ph). $^{31}$P{$^{1}$H} NMR (121 MHz, $CD_2Cl_2$): $\delta_P$ = 70.7 (d, $^{1}J_{P\text{-}Rh}$ = 117.9 Hz; P). IR (KBr): $\tilde{\nu}$ = 3054 [w, sp$^2$ $\nu$(C–H)], 2978–2866 [w, sp$^3$ $\nu$(C–H), 1480–1368 [st, Ar $\nu$(C=C)], 1093 [st, $\nu$(C–N)]. ES-MS: *m/z* (%) = 1158 (5) $[M]^+$, 579 (18) [RhCl{$(Ph_2P)_2N^{t}Bu$}].

## 4.5 Notes and References


(1) Irvine, D. J.; Preston, S. A.; Cole-Hamilton, D. J.; Barnes, J. C. *J. Chem. Soc., Dalton Trans.* **1991**, 2413-2418.

(2) Irvine, D. J.; Glidewell, C.; Cole-Hamilton, D. J.; Barnes, J. C.; Howie, A. *J. Chem. Soc., Dalton Trans.* **1991**, 1765-1772.

(3) *See* section 3.2.1, *C.*

(4) Jimenez-Rodriguez, C.; Porgorzelec, P. J.; Eastham, G. R.; Slawin, A. M. Z.; Cole-Hamilton, D. J. *Dalton Trans.* **2007**, 4160-4168.

(5) Gridnev, I. D.; Higashi, N.; Imamoto, T. *Organometallics* **2001**, *20*, 4542-4553.

(6) Fanjul, T.; Eastham, G.; Fey, N.; Hamilton, A.; Orpen, A. G.; Pringle, P. G.; Waugh, M. *Organometallics* **2010**, *29*, 2292–2305.

(7) Rucklidge, A. J.; Morris, G. E.; Slawin, A. M. Z.; Cole-Hamilton, D. J. *Helv. Chim. Acta* **2006**, *89*, 1783-1800.

(8) G. R. Eastham, G. R.; Tindale, N. (Lucite International UK Limited) *PCT Int. Appl.* **2007**, WO 2007/119079 A1.

(9) Clegg, W.; Eastham, G. R.; Elsegood, M. R. J.; Tooze, R. P.; Wang, X. L.; Whiston, K. *Chem. Commun.* **1999**, 1877–1878.

(10) Blann, K.; Bollmann, A.; de Bod, H.; Dixon, J. T.; Killian, E.; Nongodlwana, P.; Maumela, C. M.; Maumela, H.; McConnell, A. E.; Morgan, D. H.; Overett, M. J.; Prétorius, M.; Kuhlmann, S.; Wasserscheid, P. *J. Catal.* **2007**, *249*, 244-249.

(11) Ganesamoorthy, C.; Mague, J. T.; Balakrishna, M. S. *J. Organomet. Chem.* **2007**, *692*, 3400–3408.

(12) Majoumo-Mbe, F.; Lönnecke, P.; Novikova, E. V.; Belov, G. P.; Hey-Hawkins, E. *Dalton Trans.* **2005**, 3326-3330.

(13) du Toit, A; De Wet-Roos, D.; Joubert, D. W.; van Reenen, A. J. *J. Polymer Science: Part A: Polymer Chem.* **2007**, 1488-1501

(14) Schofer, S. J.; Day, M. W.; Henling, L. M.; Labinger, J. A.; Bercaw, J. E. *Organometallics* **2006**, *25*, 2743-2749.

(15) Agapie, T.; Schofer, S. J.; Labinger, J. A.; Bercaw, J. E. *J. Am. Chem. Soc.* **2004**, *126*, 1304-1305.

(16) Blann, K.; Bollmann, A.; Dixon, J. T.; Hess, F. M.; Killian, E.; Maumela, H.; Morgan, D. H.; Neveling, A.; Otto, S.; Overett, M. J. *Chem. Commun.* **2005**, 620-621.

(17) Kuhlmann, S.; Blann, K.; Bollmann, A.; Dixon, J. T.; Killian, E.; Maumela, M. C.; Maumela, H.; Morgan, D. H.; Prétorius, M.; Taccardi, N.; Wasserscheid, P. *Catal. Today* **2007**, *245*, 279-284.

(18) Overett, M. J.; Blann, K.; Bollmann, A.; Dixon, J. T.; Haasbroek, D.; Killian, E.; Maumela, H.; McGuinness, D. S.; Morgan, D. H. *J. Am. Chem. Soc.* **2005**, *127*, 10723-10730.

(19) Cooley, N. A.; Green, S. M.; Wass, D. F.; Heslop, K.; Orpen, A. G.; Pringle, P. G. **2001**, *20*, 4769-4771.

(20) Revés, M.; Ferrer, C.; León, T.; Doran, S.; Etayo, P.; Vidal-Ferran, A.; Riera, A.; Verdaguer, X. *Angew. Chem. Int. Ed.* **2010**, *49*, 9452-9455.

(21) Cao, P.; Wang, B.; Zhang, X. *J. Am. Chem. Soc.* **2000**, *122*, 6490–6491.

(22) Albano, P.; Aresta, M.; Manassero, M. *Inorg. Chem.* **1980**, *19*, 1069-1072.

(23) Ball, G. E.; Cullen, W. R.; Fryzuk, M. D.; James, B. R.; Rettig, S. J. *Organometallics* **1991**, *10*, 3767-3769.

(24) *See* section 3.2.1.1, *Chapter 3*.

(25) *See* section 3.2.3, *Chapter 3*.

(26) *See* section 3.2.1.4, *Chapter 3*.
(27) Sanger, A. R. *J. Chem. Soc., Chem. Commun.* **1975**, 893-894.
(28) Sanger, A. R. *J. Chem. Soc., Dalton Trans.* **1977**, 120-129.
(29) Spivack, J. D. *Ger. Offen.* **1979**, DE 2856801 A1 19790712.
(30) DeBellis, A. D.; Pastor, S. D.; Rihs, G.; Rodebaugh, R. K.; Smith, A. R. *Inorg. Chem.* **2001**, *40*, 2156-2160.
(31) Cobley, C. J.; Froese, R. D. J.; Klosin, J.; Qin, C.; Whiteker, G. T.; Abboud, K. A. *Organometallics* **2007**, *26*, 2986-2999.
(32) Garrou, P. E. *Chem. Rev.* **1981**, *81*, 229-266.
(33) Balakrishna, M. S.; Krishnamurthy, S. S. *Inorg. Chim. Acta* **1995**, *230*, 245-248
(34) *See* section 3.2.4, *Chapter 3*.
(35) *See* section 2.2.5, *Chapter 2*.
(36) Osborn, J. A.; Jardine, F. H.; Young, J. F.; Wilkinson, G. *Inorg. Phys. Theor. (J. Chem. Soc. A)* **1966**, 1711-1732.
(37) Maumela, M. C.; Blann, K.; Bod, H. d.; Dixon, J. T.; Gabrielli, W. F.; Williams, D. B. G. *Synthesis* **2007**, 3863-3867.
(38) *SAINT Data Reduction Software (version 6.45)*, Bruker AXS Inc. (Madison), WI, USA, **2003**.
(39) *SMART Data Collection Software (version 5.629)*, Bruker AXS Inc. (Madison), WI, USA, **2003**.
(40) *SHELXL program package (version 5.1)*, Bruker APX Inc. (Madison), WI, USA.
(41) Sheldrick, G. M. *SHELX-97 Program for Crystal Structure Analysis*, University of Göttingen (Göttingen), Germany, **1997**.
(42) Barbour, L. J. *J. Supramol. Chem.* **2003**, *1*, 189-191.
(43) Atwood, J. L.; Barbour, L. J. *Cryst. Growth Des.* **2003**, *3*, 3-8.

# Chapter 5

# Iridium PNP complexes in the C–H activation of methyl propanoate

– The factors governing the regioselectivity of such reactions –

*The utilisation of PNP iridium pincer complexes in the regioselective $sp^3$ C–H activation of methyl propanoate and other related esters was explored. In addition, these studies provided further insight into the factors that govern the regioselectivity of such reactions. These included factors such as the steric demands of the substrate, the formation of favourable ring systems as well as the electronic effects that may influence the $pK_a$ values of protons. In particular, the effects of water on the outcome of these reactions were of great interest, since earlier literature reports have shown the presence of water to promote selective C–H activation in the α-position of ketones. Finally, the catalytic functionalisation of methyl propanoate via C–H activation routes involving PNP iridium complexes were considered and are reported herein.*

## 5.1 Introduction

The catalytic activation and functionalisation of otherwise inert $sp^3$ C–H bonds has been the topic of extensive research for over 25 years, and progress in this field has been well reviewed.[1-6] Despite these efforts, the development of attractive homogenous routes to the selective functionalisation of hydrocarbons *via* catalytic C–H activation remains an unresolved challenge for synthetic chemists. $Sp^3$ C–H activation is generally regarded as a thermodynamically uphill transformation and therefore the thermally robust pincer-type complexes have been among the most attractive and widely studied systems for promoting both stoichiometric and catalytic C–H activations.[7-9] Iridium pincer variants, in particular, have been proven to be exceptionally active catalysts and have in recent years been at the forefront of many advances in this field.[7,10-12] Selective C–H activations typically involve a single cleavage event to form products with single M–$C_{sp3}$ bonds *via* an oxidative addition, electrophilic activation or σ-bond metathesis pathway.[13] In an initial contribution by Shaw[14] and other more recent reports, however, the direct formation of late transition metal carbene complexes by multiple C–H activations have been shown possible for selected substrates.[7,11-13] Given the rich reactivity associated with metal bound carbenes, generation of M=$C_{sp2}$ species by multiple activation routes are of great interest as they could offer viable routes to the catalytic functionalisation of $sp^3$ C–H bonds.[13]

Grubbs and co-workers,[7,12,13] in particular, have been important pioneers of such research. In a seminal study these authors have shown that *tert*-butyl ether undergoes *α*,*α*-dehydrogenation over a period of 16 h in the presence of [Ir(PNP)$(H)_2$] [PNP = bis{2-(diisopropylphosphino)-4-methylphenyl}amide] and norbornene to generate the Ir(I) Fisher carbene complex [Ir=CHO$^t$Bu(PNP)] [**I**; Scheme 5.1 (a)] upon loss of hydrogen. In the initial step the norbornene functions as a sacrificial hydrogen acceptor for the generation of the active [Ir(PNP)] species.[7] Subsequent carbene formation has been shown to proceed *via* a fast oxidative addition step to give the hydrido alkyl intermediate [Ir($CH_2$O$^t$Bu)(H)(PNP)], followed by slow *α*-hydrogen migration resulting in the liberation of dihydrogen.[13] The generated complex **I** is, however, thermally labile both in the solid state and in solution and undergoes gradual decarbonylation to afford the *trans*-dihydro carbonyl complex [Ir(CO)$(H)_2$(PNP)] and isobutene over a period of hours.[7] In a successive study aimed at elucidating the factors governing the regioselectivity of this activation process, the reaction scope was broadened to include the acyclic ethers *tert*-

amyl methyl ether, *sec*-butyl methyl ether and *n*-butyl methyl ether of which the latter two contain $\beta$-hydrogen atoms. In all cases, $\alpha$,$\alpha$-activation was favoured over $\alpha$,$\beta$-activation with exclusive formation of the metal carbene complexes **II–IV** [Scheme 5.1 (a)].[12]

Substantial backbonding by the electron rich Ir(I) centre decreases the electrophilicity of alkoxy carbenes **I–IV** to such an extent that these carbenes are impervious towards nucleophilic attack by Lewis bases. In contrast, these carbenes show remarkable reactivity towards electrophilic heterocumulenes representing attractive synthons for further functionalisation steps. Indeed, in reactions of carbene complex **I** with carbon dioxide, quantitative conversion to the carbonyl adduct [Ir(CO)(PNP)] proceed together with expulsion of *tert*-butyl formate. Similarly, transfer of a sulphur-atom or nitrene group occurs in reactions of **I** with carbonyl sulphide or phenyl isocyanate, respectively [Scheme 5.1 (b)].[13] This group transfer approach has already been successfully employed in a true catalytic cycle for the oxidation of methyl *tert*-butyl ether to *tert*-butyl *N*-adamantylformidate, making this an exciting prospect for future C–H activation chemistry.[13]

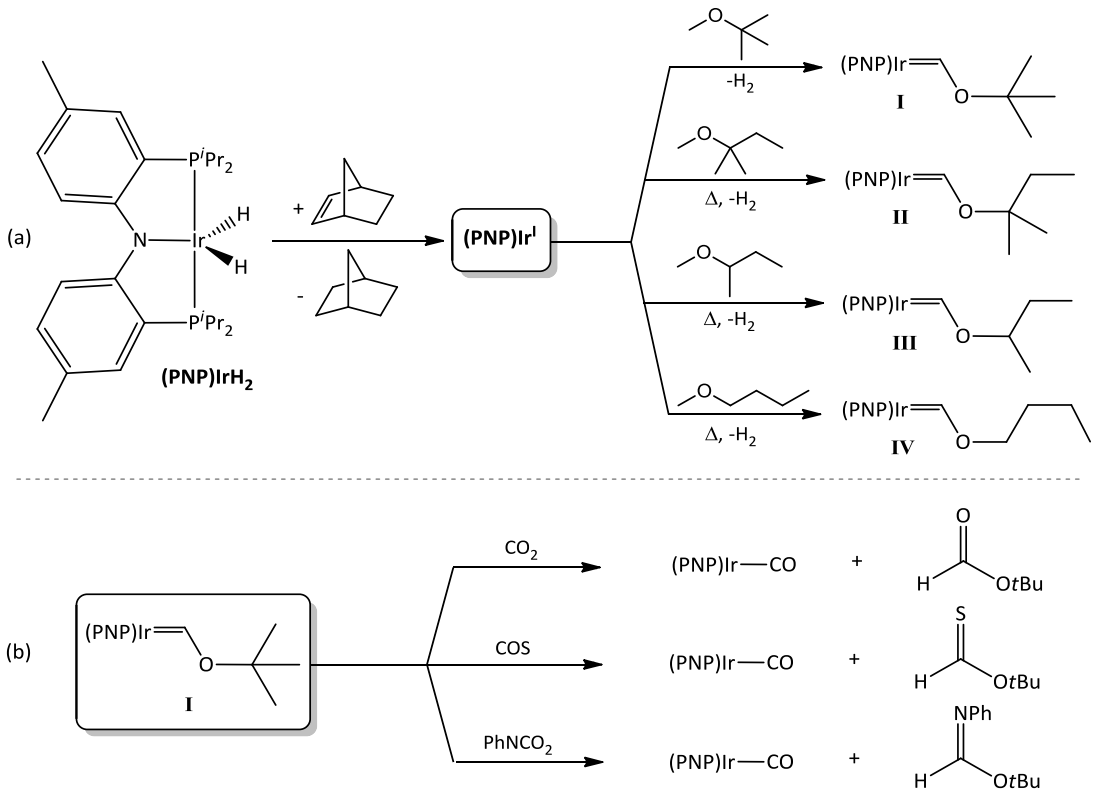


**Scheme 5.1** (a) Double C–H activation of acyclic methyl ethers by [(PNP)Ir] to form metal carbene complexes **I–IV** and (b) reaction of alkoxycarbene **I** with heterocumulene electrophiles. (*schemes adapted from literature*).[12,13]

Geminal double C–H activations by late transition metals to generate carbenes have also been shown possible for the $\alpha$-C–H bonds of cyclic ethers.[15-18] PNP-type iridium pincer complexes have been shown to facilitate such transformations, displaying high selectivity towards the formation of carbenes *via* $\alpha,\alpha$-C–H activation over vinyl ether formation, which would result from $\alpha,\beta$-hydrogen abstraction.[11,12] Whited and co-workers[12] have demonstrated that [Ir(PNP)$(H)_2$] converts cleanly to the cyclic carbene complex **V** [Scheme 5.2 (a)] over time, in the presence of norbornene and thf. This conversion, although very slow, proceeds *via* an initial dihydrido carbene complex [Ir$(C_4H_6O)$(PNP)$(H)_2$] with the final product, **V**, being remarkably stable towards thermolysis. Furthermore, this complex does not generate [IrCO$(H)_2$(PNP)] *via* decarbonylation pathways, as was the case for the analogous *tert*-butoxy- and *tert*-amyloxymethylidene complexes **I** and **II** [Scheme 5.1(a)].[12] Similar results have also been reported by Meiners and co-workers[11] for reactions of thf with iridium complexes derived from highly basic dialkylamido pincer ligands under mild conditions[Scheme 5.2 (b)].

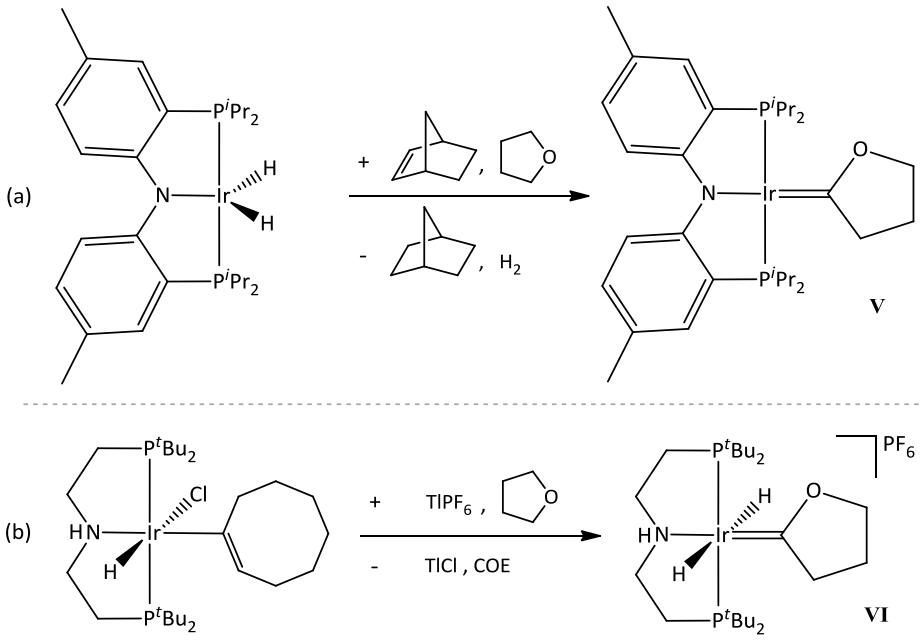


**Scheme 5.2** Literature examples of double geminal C–H activations of thf by iridium pincer complexes to form metal carbene complexes **V** and **VI** (*schemes adapted from the literature*).[11,12]

Although pincer ligands are often regarded merely as platforms to stable metal complexes, Milstein and co-workers[10] have recently shown that such ligands can cooperate in various reactions by adapting to changes at the metal centre. In iridium complexes derived from

deprotonated 2,6-bis{(di-*tert*-butylphosphino)methyl}pyridine (PNP*), in particular, metal-ligand cooperations of this nature have been shown to play a decisive role in their reactivity toward $sp^3$ C–H activations. The authors have shown that heated solutions of [Ir(PNP*)(COE)] in acetone afford the C-H activated Ir(I) acetonyl complex **VII** [Scheme 5.3 (i)] contaminated by trace amounts of the cyclooctanyl complex **VIII**. During this conversion, the deprotonated PNP* ligand cooperates by serving as a hydride acceptor to re-establish the aromaticity of the pyridine ring, without necessitating an overall change in the formal oxidation state of the Ir(I) centre. This addition is reversible and treatment of complex **VII** with CO leads to dearomatisation of the PNP ligands with concomitant expulsion of acetone to give the nonaromatic PNP complex **IX** [Scheme 5.3 (ii)]. In contrast, reactions with dihydrogen do not lead to dearomatisation of the PNP ligand and instead, the dihydrido acetonyl complex **X** is preferentially formed [Scheme 5.3 (iii)].[10]

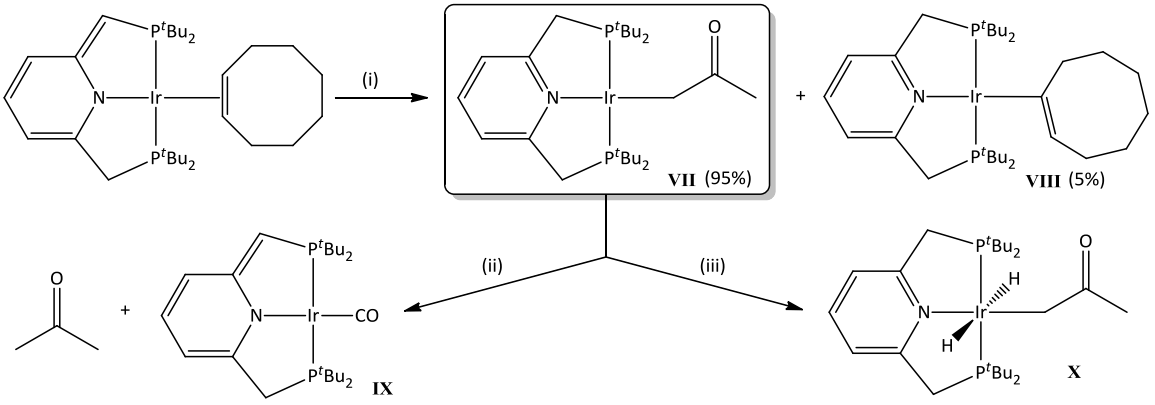


**Scheme 5.3** C–H activation of acetone by [Ir(PNP*)(COE)] and subsequent reactions with CO and $H_2$. Conditions: (i) acetone, 60 °C, 6 h; (ii) CO, benzene, R.T.; (iii) $H_2$, benzene, R.T.[10]

In an earlier report, Milstein and co-workers[19] showed that iridium pincer complexes can also be employed for the selective $sp^3$ activation in the $\beta$-position of other ketones despite the greater acidity of the $\alpha$-C–H bonds. In the presence of water, however, the regioselectivity of these reactions could be steered to favour activations in the $\alpha$-position instead. Reactions of the cationic complex [Ir(PNP)(COE)][$BF_4$] [PNP = 2,6-bis{(di-*tert*-butylphosphino)methyl}-pyridine] with either acetone or 2-butanone at 60 °C in the presence of water result in selective $\alpha$-C–H activation to give the complexes **XI** and **XII** [Scheme 5.4 (i)]. In these complexes, coordinated water assists in stabilising the activated ketonyl ligand *via* hydrogen

bonding to the carbonyl carbon to form a stable six membered ring structure. In the absence of water, [Ir(PNP)(COE)][$BF_4$] reacts with 2-butanone or 3-pentanone to quantitatively afford the $\beta$-activated hydrido complexes **XIV** and **XIII**, while acetone shows no reaction [Scheme 5.4 (ii)].[19] In these complexes, coordination through the carbonyl oxygen results in the formation of a highly favoured five membered ring structure which may explain the preference for activation in the $\beta$-position.

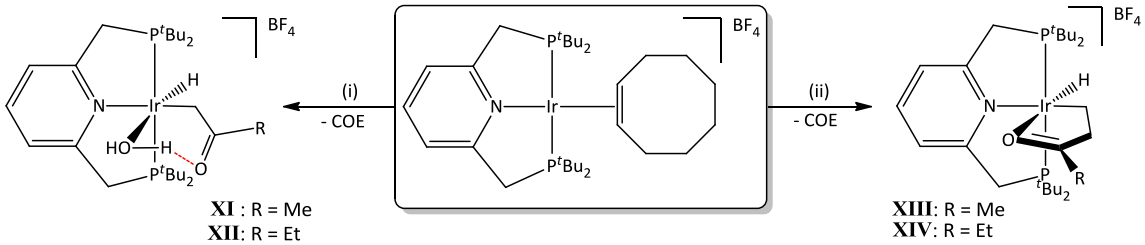


**Scheme 5.4** C–H activation of ketones by [Ir(PNP)(COE)][$BF_4$]. Conditions: (i) acetone (for **XI**) or 2-butanone (for **XII**), water, 60 °C, 3 h; (ii) 2-butanone (for **XIII**) or 3-pentanone (for **XIV**), 60 °C, 3 h.

Inspired by these findings we were interested to determine whether these methodologies could be further applied in the selective $sp^3$ C–H activation of saturated esters. More specifically, special focus was placed on methyl propanoate (MeP) as substrate in our ongoing efforts to explore new ways of converting MeP to the targeted methyl methacrylate (MMA) *via* C–H activation routes. In our attempts, which were strongly based on the reaction pathways and conditions originally delineated by Milstein and co-workers,[19] we further aimed to explore the effects of water on the regioselectivity of activations involving esters such as MeP. Although Milstein has shown that $\beta$-activation is favoured in longer chain ketones such as 2-butanone and 3-pentanone, we aimed to achieve selective C–H activation in the $\alpha$-position of esters, since conversion of MeP to MMA necessitates functionalisation in this position. In this account we present our experimental findings regarding the regioselectivity of C–H activation reactions involving the square planar Ir(I) pincer complex [Ir(PNP)(COE)][$BF_4$] and saturated esters in both the presence and absence of water. Furthermore, preliminary attempts to catalytically functionalise activated methyl propanoate were made and are briefly described herein.

## 5.2 Results and Discussion

In Section 5.2.1, reactions of esters with [Ir(PNP)(COE)][$BF_4$] in the presence of water are described, while section 5.2.2 is focussed on such reactions under anhydrous conditions. Spectroscopic techniques, and in particular two dimensional NMR experiments, were imperative for the successful execution of the study and the most important insights gathered from spectroscopic data are highlighted in section 5.2.2. Preliminary attempts to catalytically functionalise C–H activated MeP were made and are discussed in section 5.3.3. Crystal and molecular structures were determined for two of the observed complexes and are described in detail in section 5.3.4.

### *5.2.1 Reactions of [Ir(PNP)(COE)][$BF_4$] with esters in the presence of water*

As was mentioned in the introductory section, the work in this chapter was inspired by a seminal report by Milstein and co-workers[19] on the regioselective C–H activation of ketones. In this study, however, the reported methodologies were applied towards the activation of saturated esters. Scheme 5.5 illustrates the reaction products expected for reactions of MeP with [Ir(PNP)(COE)][$BF_4$], if these reactions were to follow the same pathways as were determined for reactions with ketones.

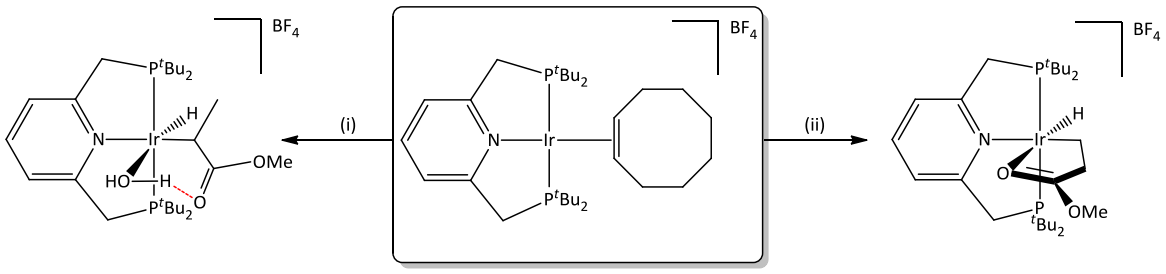


**Scheme 5.5** Expected reactions products for reactions of [Ir(PNP)(COE)][$BF_4$] with methyl propanoate following the Milstein approach. Conditions: (i) MeP, water, 60 °C; (ii) MeP, 60 °C.

A particular target of this study was to achieve selective activation in the $\alpha$-position of MeP [Scheme 5.5 (i)] by exploiting the reported water effect, since the resulting $\alpha$-activated product could represent a potential intermediate in the further functionalisation of MeP to MMA.

Employing MeP as both reagent and reaction solvent, [Ir(PNP)(COE)][$BF_4$] was dissolved in a MeP / water mixture (V : V ratio 50 : 1) and the resultant solution heated at 60 °C for 20 h. Not surprisingly, hydrolysis of the MeP ester bond occurred under these conditions to generate methanol and propanoic acid as products. As a result, analysis of the final reaction mixture indicated the formation of two unique complexes which could be identified as the *trans*-hydrido carbonyl complex **64** (derived from methanol) and the O–H activated propanoic acid complex **65** [Scheme 5.6]. Based on $^1$H NMR integrals, complexes **64** and **65** are formed in a 3 : 1 ratio, suggesting reactions of [Ir(PNP)(COE)][$BF_4$] with methanol, to give a stable CO complex, are favoured over reactions with propanoic acid.

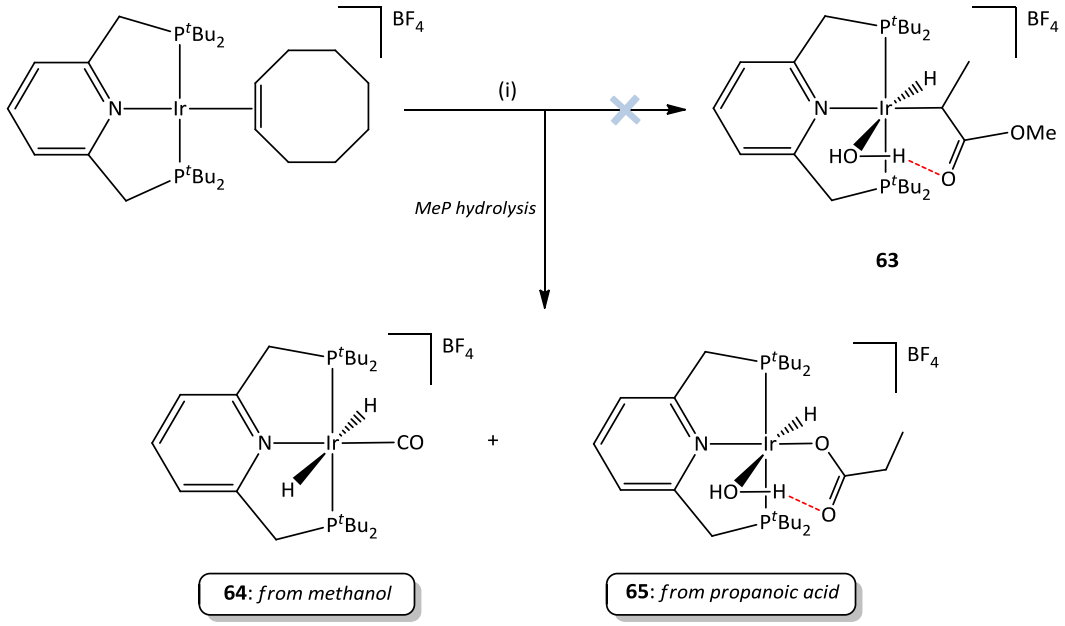


**Scheme 5.6** Reaction of [Ir(PNP)(COE)][$BF_4$] with MeP in the presence of water. Conditions: (i) MeP, water, 60 °C, 20 h.

The phosphorus atoms of complex **64** are magnetically equivalent resonating as a singlet at δ 68.8 in the $^{31}P\{^1H\}$ NMR spectrum. Furthermore, in the $^1$H NMR spectrum, complex **64** gives rise to a single virtual triplet at δ 1.42 ($J_{H\text{-}P}+J_{H\text{-}P'}$ = 14.6 Hz) corresponding to the *tert*-butyl groups and another at δ 1.42 ($J_{H\text{-}P}+J_{H\text{-}P'}$ = 8.0 Hz) for the methene groups, indicating a complex with $C_{2v}$ symmetry. Similarly, the mutually *trans* hydrides are observed as a triplet at δ -6.75 ($^2J_{H\text{-}P}$ = 12.6 Hz) which integrates as two protons. All these values are in good agreement with those reported for the analogous iridium complex, [Ir(CO)$(H)_2$(PNP)][$PF_6$].[20] Solid state infrared

data reveal a strong absorption in the carbonyl region at 2010 $cm^{-1}$ confirming the presence of the CO ligand. Furthermore, the high frequency of this vibration is consistent with limited metal to ligand π-back-donation, serving as further evidence for the presence of an Ir centre in the higher formal oxidation state of +3. The identity of **64** could also be verified by single crystal X-ray diffraction and the determined structure is described in more detail in section 5.2.4.

For the O–H activated propanoic acid complex **65** the magnetically equivalent phosphorus atoms are observed as a sharp singlet at δ 49.6 in the $^{31}P\{H\}$ NMR spectrum. In contrast, the *tert*-butyl groups on either side of the equatorial plane are chemically inequivalent giving rise to two distinct virtual triplets in the $^{1}H$ NMR spectrum. Similarly, the C$H_2$–P groups give rise to two doublets of virtual triplets at δ 1.31 and δ 1.36, respectively, displaying large geminal couplings of $^{2}J_{H-H}$ = 17.5 Hz and smaller couplings of $J_{H-P}$ + $J_{H-P'}$ = 8.0 Hz to phosphorus. A diagnostic hydride resonance is detected as a broad triplet, owing to coupling to phosphorus, at δ -29.0. In the $^{13}C\{^{1}H\}$ NMR spectrum, the relatively low field chemical shift of the carbonyl group resonance (δ 181) is consistent with no coordination through this functionality; an observation that supports the proposed structure in which water occupies the 6$^{th}$ coordination site. To confirm these assignments complex **65** was prepared independently by the facile reaction of damp propionic acid with [Ir(PNP)(COE)][$BF_4$] at 60 °C for 20 h (Scheme 5.7).

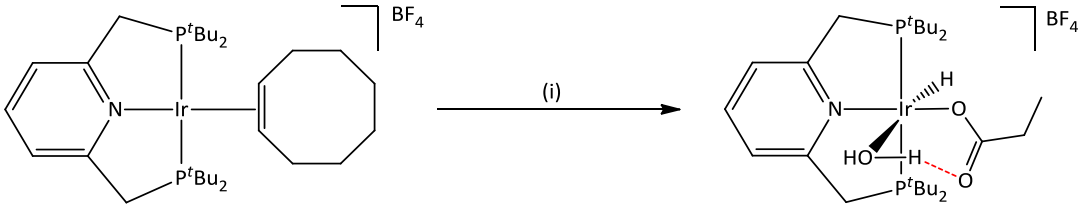


**65**

**Scheme 5.7** Formation of [Ir(PNP)(H){OC(O)$CH_2CH_3$}][$BF_4$] by the reaction of [Ir(PNP)(COE)][$BF_4$] with (i) propanoic acid, 60 °C, 20 h.

Spectroscopic data collected for the product of this reaction were in fairly good agreement with those obtained earlier. In must be noted, however, that minor differences between the characteristic chemical shifts exist and that these were ascribed to solvent effects. The structure of **65** could also be confirmed crystallographically and is described in section 5.2.4.

The formation of complex **64** from methanol and PNP iridium complexes is a well known conversion that proceeds *via* a stereoselective decarbonylation pathway.[20] The mechanism for this transformation is given in Scheme 5.8 and involves an initial O–H activation of methanol to give the methoxy hydrido complex [Ir(PNP)(H)(OMe)][$BF_4$] which can undergo further $\beta$-hydrogen abstraction to generate the dihydrido complex [Ir(PNP)$(H)_2$][$BF_4$] with concomitant expulsion of formaldehyde. In the final step, this dihydrido complex reacts with formaldehyde to reductively eliminate dihydrogen together with activation of the remaining aldehyde C–H bond to afford the *trans*–dihydrido carbonyl complex **64** stereoselectively. In this step, association of formaldehyde to the Ir(III) centre is thought to precede the reductive elimination of dihydrogen.[20]

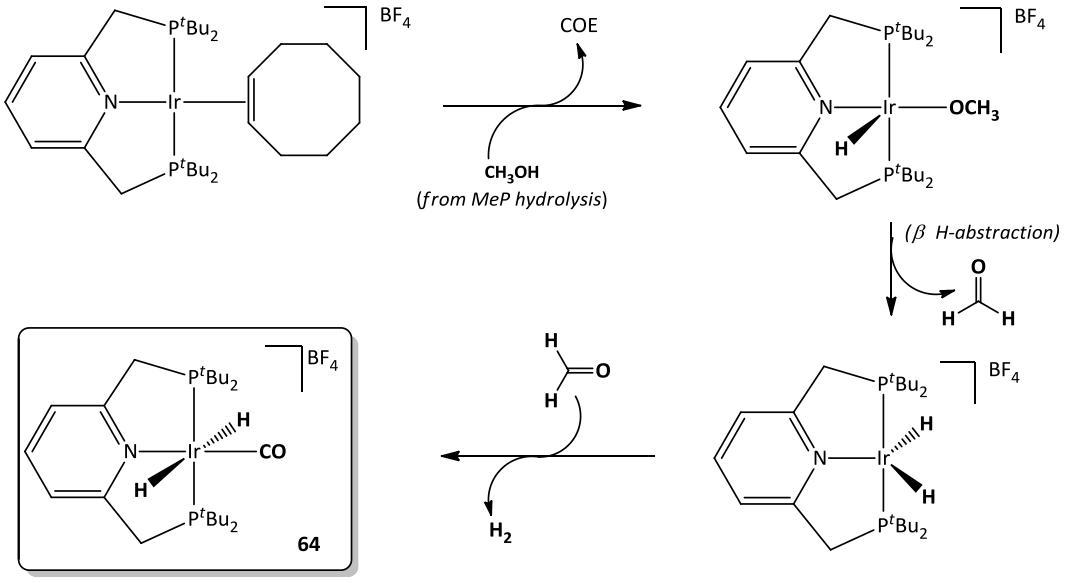


**Scheme 5.8** Mechanism for the formation of complex **64** from [Ir(PNP)(COE)][$BF_4$] and methanol.

To rule out the existence of other possible pathways of decarbonylation, the reactions of [Ir(PNP)(COE)][$BF_4$] with esters in the presence of water was also performed for *tert*-butyl propanoate and isopropyl propanoate. For these esters, hydrolysis would result in the formation of propanoic acid together with *tert*-butanol and isopropanol, respectively. Although these alcohols can undergo initial O–H activation to give hydrido alkoxy Ir(III) complexes, neither one of these complexes are able to participate in further decarbonylation reactions to afford CO complexes [Scheme 5.9]. For *tert*-butanol, further activation following the initial formation of the hydrido methoxy complex, is hampered by the absence of any $\beta$-

hydrogens. Similarly, although in the case of isopropanol the generated hydrido isopropoxy complex can undergo an additional $\beta$-hydrogen abstraction to afford the dihydrido acetone complex **67**, subsequent reductive elimination of dihydrogen is once again inhibited by the absence of a $\beta$-hydrogen atom, thus preventing the occurrence of further decarbonylations.

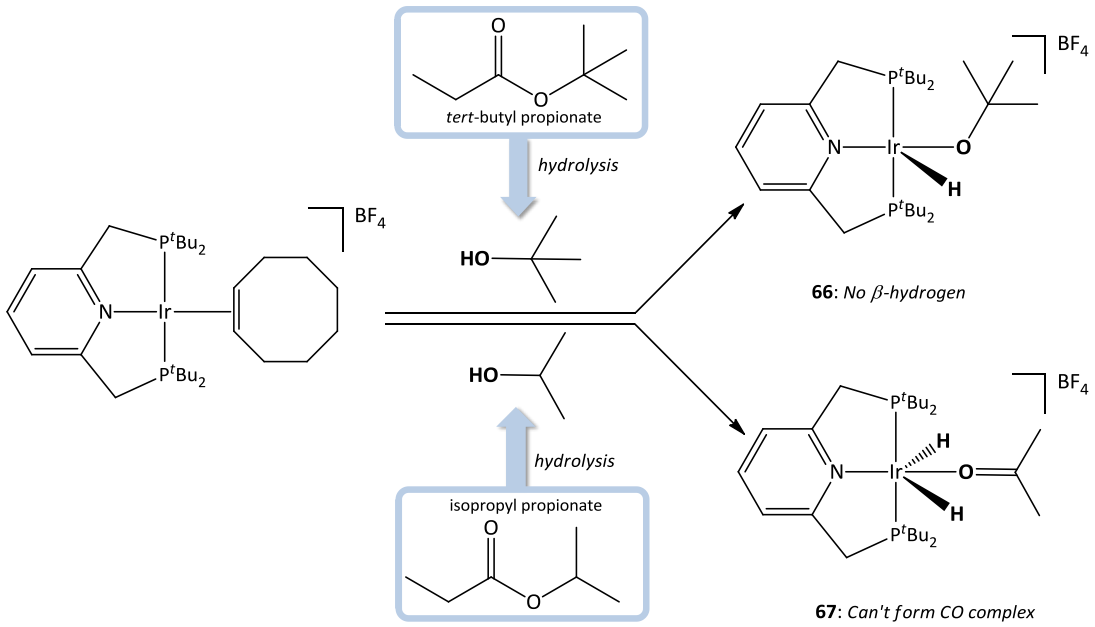


**Scheme 5.9** Reaction scheme to illustrate that reactions between [(PNP)(COE)][$BF_4$] and *tert*-butanol or isopropanol (hydrolysis products of *tert*-butyl propanoate and isopropyl propanoate, respectively) cannot afford the carbonyl complex, [Ir(PNP)(CO)$(H)_2$][$BF_4$].

As anticipated, reactions of [Ir(PNP)(COE)][$BF_4$] at 60 °C with either *tert*-butyl propanoate or isopropyl propanoate in the presence of water did not lead to the formation of [IrCO$(H)_2$(PNP)][$BF_4$] (**64**). Instead, spectroscopic characterisation of the isolated reaction products indicated quantitative conversion of [Ir(PNP)(COE)][$BF_4$] to the activated propanoic acid complex **65** for both substrates, with no evidence for the formation of either of complexes **64**, **66**, [Ir($O^iPr$)(H)(PNP)][$BF_4$] or **67**.

### *5.2.2 Reactions of [Ir(PNP)(COE)][$BF_4$] with esters in the absence of water*

In the absence of any added water, the reaction of [Ir(PNP)(COE)][$BF_4$] with MeP at 60 °C for 20 h resulted in the selective C–H activation of the methoxy protons in the $\beta$-position to give

the hydrido complex **68**, in which the 6th coordination site is filled by coordination of the carbonyl oxygen atom. Furthermore, precoordination of this functionality most likely preceded the activation event, fixing the substrate in close proximity to the metal centre. Although the $\alpha$–methene protons represent the most acidic protons in MeP ($pK_a \sim 25$),[21] C–H activation in this $\alpha$–position would lead to a structure where additional stabilisation *via* carbonyl coordination would necessitate the formation of a strained four membered ring system. Activation in the $\beta$–position is therefore driven by the formation of the highly favoured, more stable, five membered ring structure. The preference for activation of the methoxy over the methyl protons is not surprising, since the $pK_a$ value of the methoxy protons can be expected to be considerably lower than that of the methyl protons owing to the presence of a neighbouring, electron withdrawing oxygen atom. Complex **68** is remarkably stable both in solution and the solid state provided that an inert, anhydrous environment is maintained.

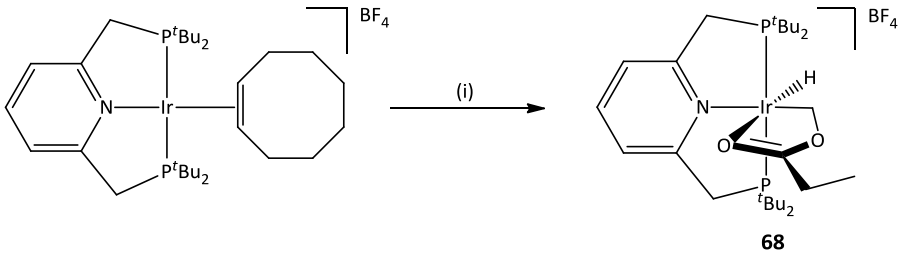


**68**

**Scheme 5.10** Formation of the methoxy activated complex **68** by the reaction of [Ir(PNP)(COE)][$BF_4$] with MeP under water free conditions; (i) MeP, 60 °C, 20 h.

Comparable to the literature example of the C–H activated ketone complex, [Ir(H)(PNP){$CH_2CH_3C(O)CH_2CH_3$}][$BF_4$],[19] the *tert*-butyl groups on either side of the equatorial plane are chemically inequivalent and are observed as two distinct virtual triplets at δ 1.21 and 1.24 in the $^1$H NMR spectrum of **68**. Similarly, the PNP methene protons on the same carbon are inequivalent giving rise to two distinct doublets of virtual triplets δ 3.58 and δ 3.73, respectively, owing to a large geminal coupling and a smaller coupling to the two phosphorus atoms. The activated methoxy group gives rise to a triplet that integrates to two protons at δ 6.47 ($^3J_{H\text{-}P}$ = 9.5 Hz), while the hydride is observed as a triplet at δ -23.74 ($^2J_{H\text{-}P}$ = 14.6 Hz). From a two dimensional HMQC $^1$H/$^{31}$P{$^1$H} NMR correlation, Figure 5.1), it is evident that both these resonances correlate with a singlet at δ 42.1 in the $^{31}$P{$^1$H} NMR spectrum. Despite rigorous drying of the MeP prior to use, contamination of complex **68** with minor amounts of

complexes **64** and **65** were always observed, as can be seen by the additional signals observed in the recorded 2D $^{1}H/^{31}P\{^{1}H\}$ NMR spectrum (Figure 5.1).

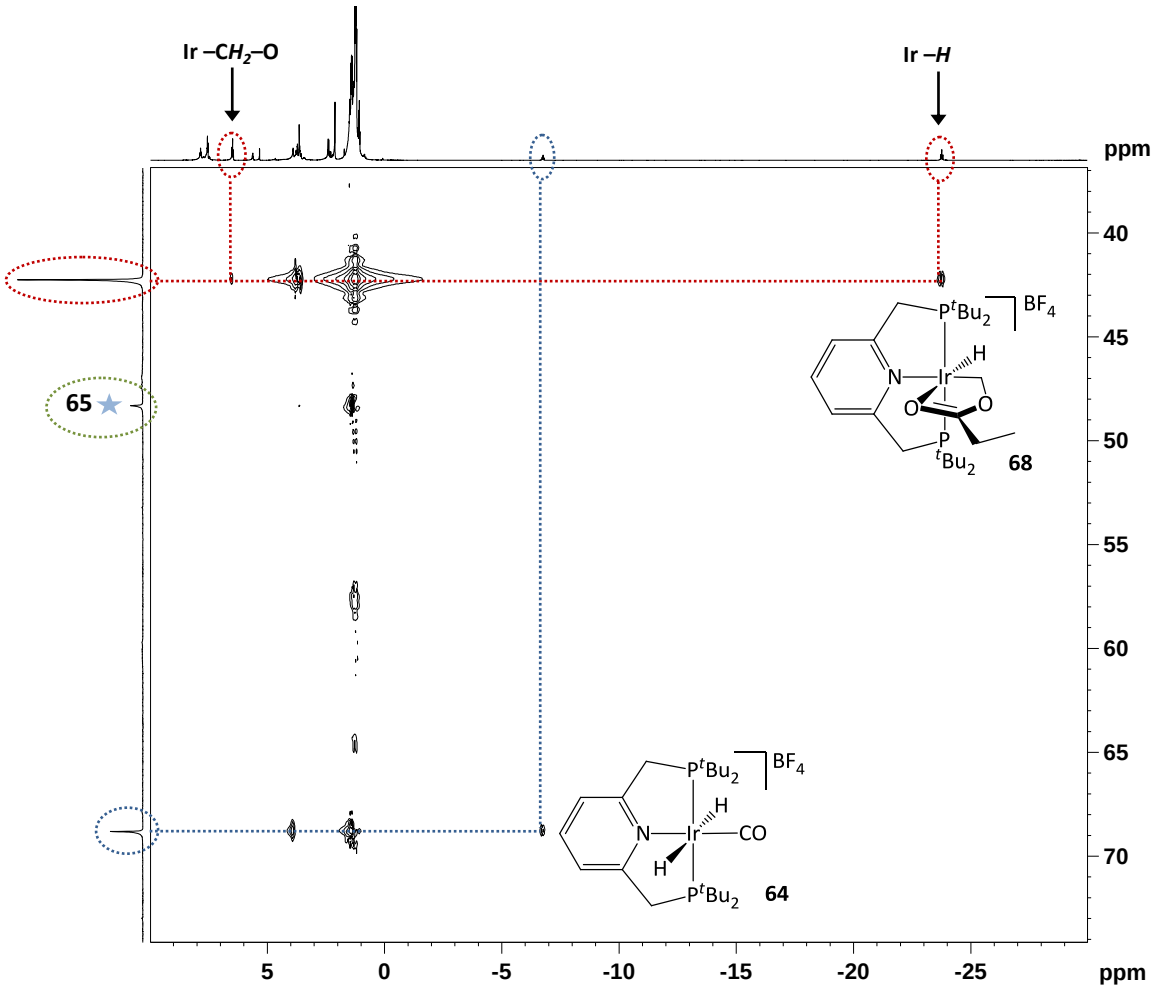


**Figure 5.1** 2D HMQC $^{1}H/^{31}P\{^{1}H\}$ spectrum recorded for the methoxy activated complex **68**, contaminated by small amounts of **64** and **65**, clearly showing the correlation of the triplets at δ 6.47 (Ir-C*H*$_2$-O) and δ -23.74 (Ir-*H*) in the $^{1}H$ NMR to the phosphorous resonance at δ 42.1.

Surprisingly, reactions of [Ir(PNP)(COE)][$BF_4$] with either isopropyl propanoate ($^{i}$PrP) or *tert*-butyl propanoate ($^{t}$BuP) under the same reactions conditions did not result in the formation of any *α*- or *β*-C–H activated products, with the final reaction mixture comprising solely of the unaltered starting materials (Scheme 5.11). It is possible that precoordination of the carbonyl moiety to the Ir centre is a prerequisite for successful C–H activation and that the increased steric requirements of the isopropyl and *tert*-butyl groups prevent such coordinations. Alternatively, the lack of reactivity may suggest that the *β*-protons in these esters are simply

not acidic enough to undergo C–H activation in the presence of [Ir(PNP)(COE)][$BF_4$]. Although this complex has been employed in the successful activation of C–H bonds in both the $\alpha$- and $\beta$-positions of 2-butanone and 3-pentanone, protons in the $\alpha$-position of ketones are known to have much lower $pK_a$ values when compared to those of esters [$CH_3C(O)CH_3$ → $pK_a$ 19 *vs.* $CH_3CH_2CO_2CH_3$→ $pK_a$ 25].[19,21]

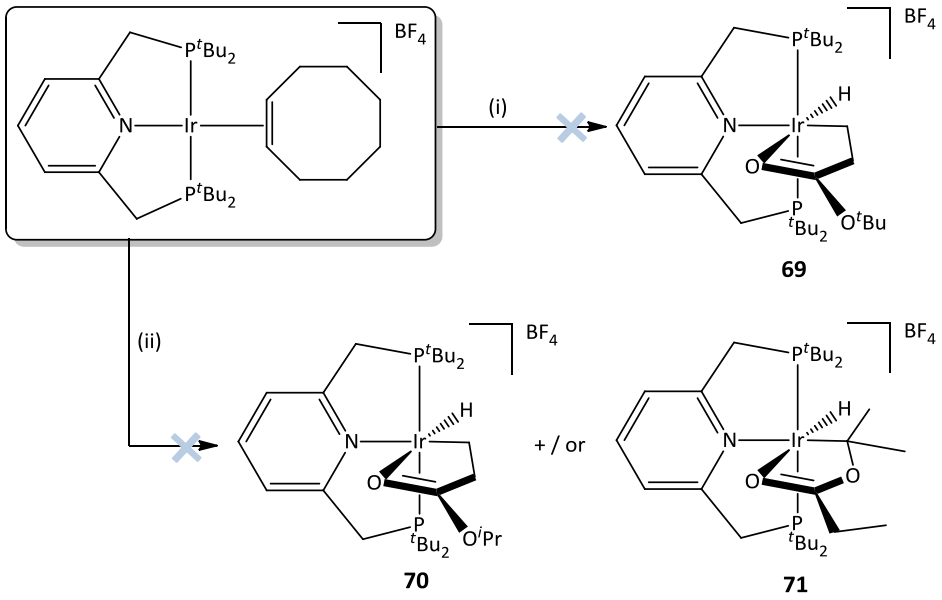


**Scheme 5.11** Reactions of [Ir(PNP)(COE)][$BF_4$] with $^t$BuP and $^i$PrP under water free conditions; (i) $^t$BuP, 60 °C, 20 h; (ii) $^i$PrP, 60 °C, 20 h.

### *5.2.3 Attempts to functionalise MeP via C–H activation*

Preliminary attempts to functionalise the activated methoxy group of complex **68** demonstrated no productive reactivity towards ethene. In initial reactions the methoxy activated complex was generated *in situ* by heating a solution of [Ir(PNP)(COE)][$BF_4$] in MeP to 60 °C in a stainless steel autoclave pressurised with ethene (30 bar) for 15 h (Scheme 5.12). Analysis of the isolated mixture, however, did not reveal the formation of any organic products. The reaction was subsequently also performed by reacting a solution of pre-formed **68** in MeP with ethene under the same conditions used for the *in situ* attempt. However, this reaction still did not result in the production of functionalised MeP or any other interesting products, with the final product mixture comparable to that isolated from the *in situ* experiment.

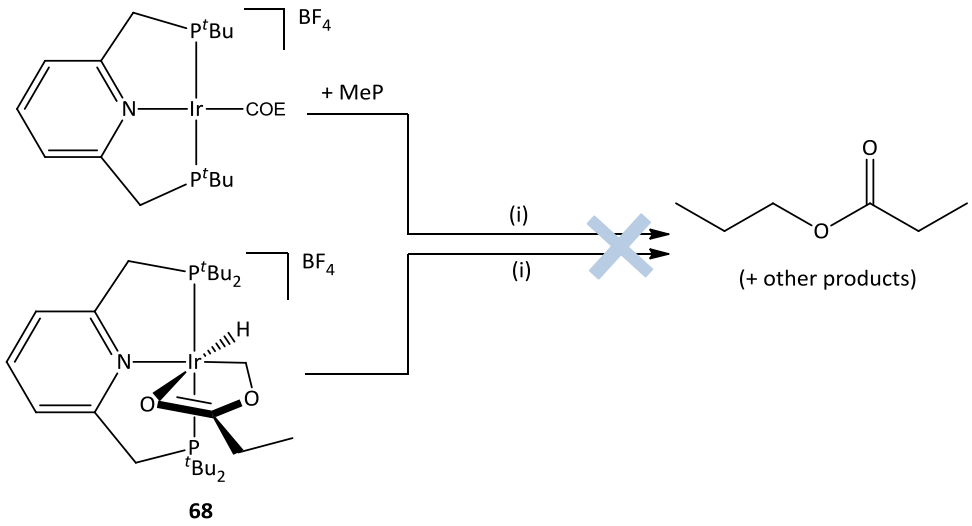


**68**

**Scheme 5.12** Unsuccessful attempts to alkylate the methoxy group of MeP *via* catalytic C–H activation; (i) ethene (30 bar), 60 °C, 20 h.

### *5.2.4 Crystal and molecular structure determination*

The structure of **64** could be confirmed by X-ray crystallography and crystals suitable for crystal and molecular structure determinations were grown by slow diffusion of pentane into a dichloromethane solution of **64**. An ellipsoid representation of the molecular structure of **64** is depicted in Figure 5.2, while selected bond lengths and angles are listed in Table 5.1. Complex **64** crystallises as orange plates in the monoclinic spacegroup $P2_1/n$ with Z = 1 molecule in the asymmetric unit. Although the relatively low electron density of the hydridic hydrogen atoms did not allow for their placement, the presence of these atoms could be confirmed by $^1$H NMR spectroscopic analysis of the isolated crystals. The carbonyl group is located in the plane of the PNP ligand ring, and the hydride ligands can therefore be assumed to occupy positions *trans* to one another with the molecule adopting an overall distorted octahedral geometry about the central Ir(III) atom. As a rule, such *trans*-dihydride complexes are not normally favoured over their *cis* counterparts, owing to the destabilising influence of having two strongly sigma donating ligands in mutually *trans* positions.[20] However, despite this destabilising influence, *trans* dihydrido iridium pincer complexes are not uncommon and a number of such complexes, including the analogous *trans*-[Ir(CO)(H)$_2$(PNP)][PF$_6$], have been reported in literature.[7,11,20,22-24] Moreover, the *trans* isomer has even be shown by Rybtchinski and co-workers[24] to be thermodynamically favoured over the *cis* isomer in the case of [Ir(CO)(H)$_2$(PCP)] [where PCP = 1,3-bis{(diisopropylphosphino)methyl}benzene]. While the CO ligand, Ir centre, pyridine ring

and methene groups of **64** all lie approximately within the same plane, the two phosphorus atoms are twisted with respect to the plane at torsion angles of 14.5(8)° [P(1)–Ir(1)–N(1)–C(4)] and 0.7(8)° [P(2)–Ir(1)–N(1)–C(8)] with one P-atom above and one below the plane [Figure 5.2 (b)]. All bond lengths and angles are in good agreements with the $PF_6$ analogue, *trans*–$[Ir(CO)(H)_2(PNP)][PF_6]$, reported in the literature.[20]

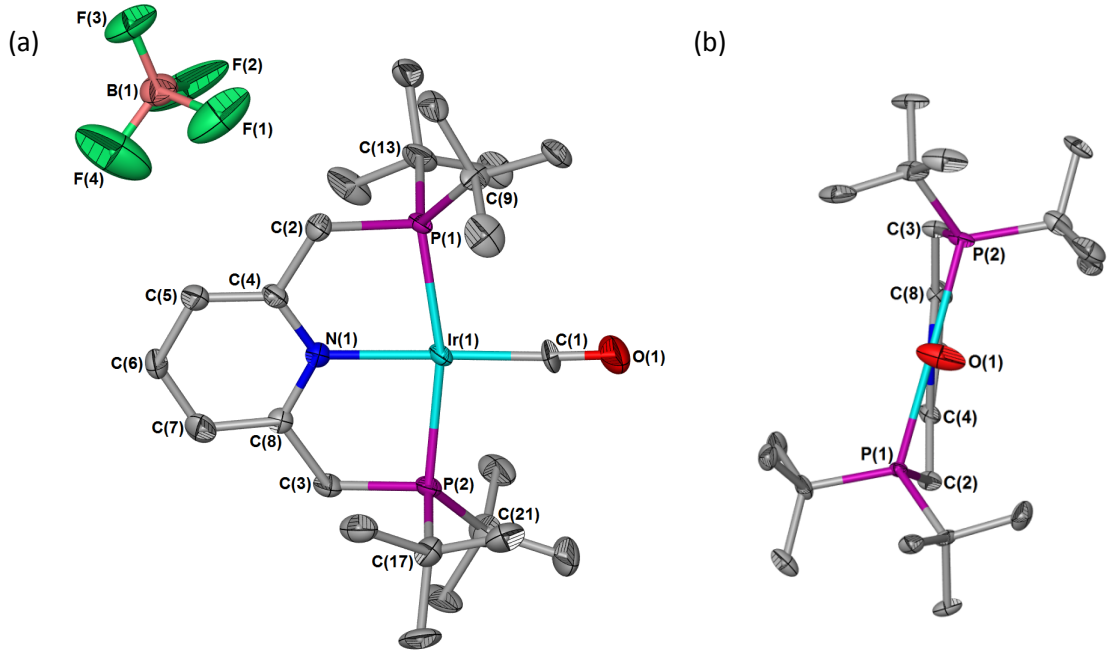


**Figure 5.2** (a) Molecular structure of the dihydrido CO complex **64** showing the numbering scheme. Thermal ellipsoids set at 50 % probability and hydrogen atoms are omitted for clarity. Hydride atoms are not observed owing to their low relative electron densities; (b) Side view of the molecular structure of **64** (ellipsoids set at 35 % probabilityand $BF_4$ omitted for clarity).

**Table 5.1** Selected bond lengths (Å) and angles (°) of **64** with estimated standard deviations in parenthesis.

| | | | |
|---|---|---|---|
| *Bond lengths (Å)* | | | |
| Ir(1)–P(1) | 2.329(3) | Ir(1)–C(1) | 1.886(12) |
| Ir(1)–P(2) | 2.326(3) | C(1)–O(1) | 1.114(17) |
| Ir(1)–N(1) | 2.109(9) | | |
| *Bond angles (°)* | | | |
| P(1)–Ir(1)–P(2) | 165.97(11) | P(2)–C(3)–C(8) | 114.1(9) |
| P(1)–Ir(1)–N(1) | 82.5(3) | C(2)–P(1)–Ir(1) | 98.8(4) |
| P(1)–Ir(1)–C(1) | 98.8(4) | C(3)–P(2)–Ir(1) | 98.2(4) |
| P(2)–Ir(1)–N(1) | 83.5(3) | C(2)–C(4)–N(1) | 118.3(10) |
| P(2)–Ir(1)–C(1) | 95.3(4) | C(3)–C(8)–N(1) | 118.3(10) |
| N(1)–Ir(1)–C(1) | 177.1(6) | Ir(1)–C(1)–O(1) | 176.1(16) |
| P(1)–C(2)–C(4) | 112.0(8) | | |

Single crystals of **65**, suitable for structure determination by X-ray diffraction, were grown by slow diffusion of hexane into a solution of **65** in dichloromethane at room temperature. Complex **65** crystallises as yellow prisms in the triclinic space group $P\bar{1}$ with the asymmetric unit consisting of one molecule of **65** together and one dichloromethane molecule. The collected data set was of sufficient quality to allow for the location of the hydride atom. An ellipsoid representation of the molecular structure is displayed in Figure 5.3 with selected bond lengths and angles summarised in Table 5.2. Analysis of the determined structure reveals a distorted octahedral geometry about the central Ir(III) atom with the propanoate coordinated in the equatorial plane *trans* to nitrogen with the hydride and water ligands occupying mutually *trans* axial positions. A hydrogen bond exists between the carbonyl oxygen and the coordinated water molecule, forming a six membered ring which aids in stabilising the structure. Similar to the structure of **64**, the pyridine ring, Ir(III) centre and coordinated propanoate oxygen atom all lie essentially within the same plane. In contrast to the structure of **64**, however, both P-atoms lie slightly above the plane at torsion angles of 1.4(5)$^{o}$ and 8.6(4)$^{o}$, pointing away from the coordinated propanoate ligand in order to minimise steric congestion [Figure 5.3 (b)].

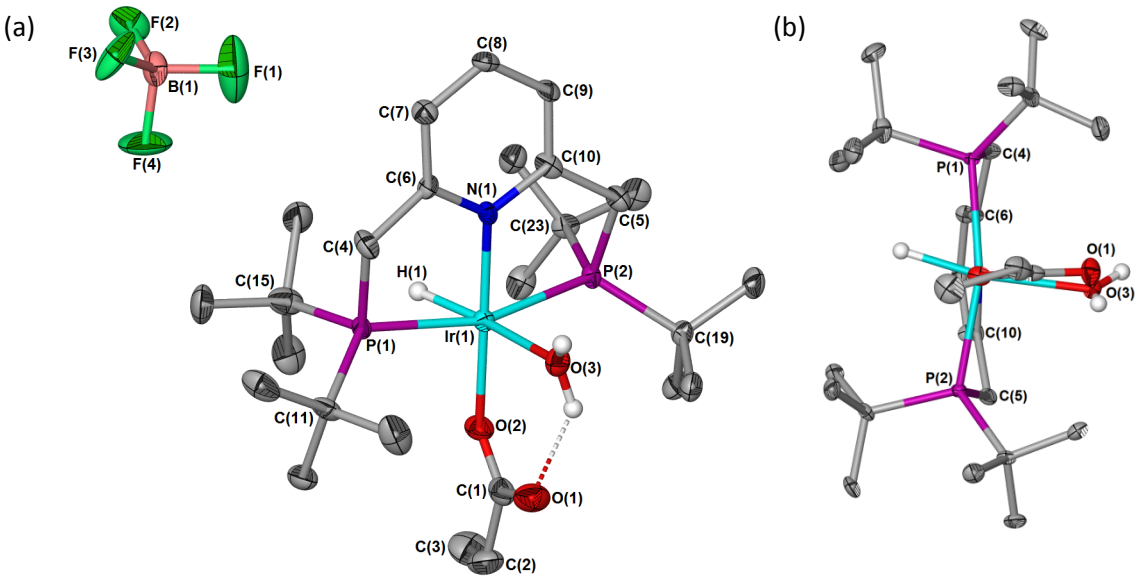


**Figure 5.3** (a) Molecular structure of **65** showing the numbering scheme. Thermal ellipsoids set at 50 % probability and hydrogen atoms (with the exception of the hydride and water protons) and solvent molecule are omitted for clarity; (b) side view of the structure (ellipsoids set at 35 % probability and $BF_4$ omitted).

As a consequence of this twisting, the P(1)–Ir(1)–P(2) angle deviates significantly from linearity, with the measured P(1)–Ir(1)–O(2) and P(2)–Ir(1)–O(2) angles widened to give angles greater than the ideal 90°. The measured Ir(1)–O(3) [2.271(5) Å] and Ir(1)–H(1) [1.64(6) Å] bond lengths are comparable to those of the C–H activated acetone complex [Ir(PNP)(H)($H_2O$){$CH_2C(O)CH_3$}][$BF_4$] reported in the literature [2.288(4) Å and 1.50(7) Å, respectively].[19] A significantly shorter Ir(1)–N(1) [2.066(5) Å] separation is, however, observed for **64** when compared to that of the mentioned literature example [2.136(4) Å], owing to the weaker *trans* influence of the propanoate O-atom compared to that of the methene group coordinated *trans* to nitrogen in [Ir(PNP)(H)($H_2O$){$CH_2C(O)CH_3$}][$BF_4$].[19]

**Table 5.2** Selected bond lengths (Å) and angles (°) of **65** with estimated standard deviations in parenthesis.

| | | | |
|---|---|---|---|
| *Bond lengths (Å)* | | | |
| Ir(1)–P(1) | 2.3228(16) | Ir(1)–H(1) | 1.64(6) |
| Ir(1)–P(2) | 2.3475(16) | O(1)–C(1) | 1.235(9) |
| Ir(1)–N(1) | 2.066(5) | C(1)–O(2) | 1.282(9) |
| Ir(1)–O(2) | 2.080(4) | C(1)–C(2) | 1.506(9) |
| Ir(1)–O(3) | 2.271(5) | C(2)–C(3) | 1.482(10) |
| *Bond angles (°)* | | | |
| P(1)–Ir(1)–P(2) | 161.93(6) | C(5)–P(2)–Ir(1) | 96.6(2) |
| P(1)–Ir(1)–N(1) | 84.35(14) | C(4)–C(6)–N(1) | 118.1(5) |
| P(1)–Ir(1)–O(2) | 95.38(13) | C(5)–C(10)–N(1) | 118.2(5) |
| P(1)–Ir (1)–O(3) | 100.74(13) | O(2)–Ir(1)–O(3) | 94.40(18) |
| P(1)–Ir(1)–H(1) | 69(2) | O(2)–Ir(1)–N(1) | 179.46(18) |
| P(2)–Ir(1)–N(1) | 84.39(14) | O(2)–Ir(1)–H(1) | 88.0(18) |
| P(2)–Ir(1)–O(2) | 95.76(13) | O(3)–Ir(1)–N(1) | 86.11(19) |
| P(2)–Ir(1)–O(3) | 92.56(12) | O(3)–Ir(1)–H(1) | 170(2) |
| P(2)–Ir(1)–H(1) | 97(2) | N(1)–Ir(1)–H(1) | 91.5(18) |
| P(1)–C(4)–C(6) | 112.4(4) | O(1)–C(1)–O(2) | 125.0(6) |
| P(2)–C(5)–C(10) | 111.7(4) | O(2)–C(1)–C(2) | 114.7(7) |
| C(4)–P(1)–Ir(1) | 99.2(2) | O(1)–C(1)–C(2) | 120.3(7) |

## 5.3 Conclusions

In this study the reactivity of the iridium pincer complex [Ir(PNP)(COE)][$BF_4$] towards the activation of C–H bonds in both the $\alpha$- and $\beta$-positions of the esters methyl propanoate, isopropyl propanoate and *tert*-butyl propanoate were explored. In addition, the potential of water to promote regioselective activation in the $\alpha$-position was assessed. In the presence of water, methyl propanoate did not undergo $\alpha$-C–H activation. Instead, hydrolysis of the ester

bond led to the formation of propanoic acid and methanol which participated in further reactions with [Ir(PNP)(COE)][$BF_4$] to generate the O–H activated propanoic acid complex [Ir(H)(PNP)($H_2O$){OC(O)$CH_2CH_3$}][$BF_4$] together with [Ir(CO)$(H)_2$(PNP)][$BF_4$]. The identity of these complexes could be confirmed by X-ray structure determinations. In addition, the formation of the carbonyl complex, [Ir(CO)$(H)_2$(PNP)][$BF_4$], could be shown to proceed *via* a methanol decarbonylation pathway, since similar reactions with isopropyl propanoate and *tert*-butyl propanoate failed to deliver this complex.

Reactions of MeP with [Ir(PNP)(COE)][$BF_4$] in the absence of added water led to selective C–H activation of the methoxy group in the $\beta$-position to give [$\overline{\text{Ir(H)(PNP)\{CH}_2\text{OC(O)}}$$CH_2CH_3$}][$BF_4$]. Unfortunately, all preliminary attempts to develop a catalytic protocol for the functionalisation of MeP *via* this methoxy C–H activated complex, were unsuccessful. Similar reactions with isopropyl propanoate and *tert*-butyl propanoate as substrates failed to deliver any C–H activated products. The lack of observed reactivity for these substrates was ascribed to ineffective coordination as a result of greater steric bulk, together with the higher $pK_a$ values associated with the $\alpha$- and $\beta$-protons of esters when compared to those of ketones.

## 5.4 Experimental

### *5.4.1 General materials, methods and instruments*

Reactions were carried out under dinitrogen gas ($N_2$, passed through a column of dichromate adsorbed on silica) using standard Schlenk, vacuum-line and cannula techniques. All glassware was flame-dried under vacuum. Triethylamine ($NEt_3$) was purchased from Aldrich and distilled under $N_2$ prior to use. Before distilling, the $NEt_3$ was dried over potassium hydroxide (KOH) pellets. Cyclooctene, silver tetrafluoroborate, 2,6-bis(chloromethyl)pyridine, *tert*-butanol, di-*tert*-butylphosphine and isopropanol were purchased from Aldrich and used as received. Propanoic acid, purchased from BDH laboratories, was dried over $Na_2CO_3$ and distilled under $N_2$ prior to use. All gases were purchased from BOC gases. $[NH_4]_3[IrCl_6]$ and isopropyl propanoate were purchased from Alfa Aesar, *tert*-butyl propanoate from Aldrich, phosphorus pentoxide from Fluka and pentane from Fischer Scientific. Methyl propanoate (supplied by Lucite International) and isopropyl propanoate were pretreated with $Na_2CO_3$, dried over $P_2O_5$,

degassed by three freeze-pump-thaw cycles and finally collected by trap-to-trap distillation prior to use. *Tert*-butyl propanoate was purified using the same methodology, but with omission of the $P_2O_5$ step. [{IrCl(COE)$_2$}$_2$] was either prepared from $[NH_4]_3[IrCl_6]$ and cyclooctene using a literature procedure[25] or purchased from Alfa Aesar. 2,6-Bis(di-*tert*-butylphosphinomethyl)pyridine (PNP),[26] $[IrCl(COE)_2(acetone)_2][BF_4]$[27] and $[Ir(PNP)(COE)][BF_4]$[22] were prepared using standard literature procedures. Drierite was purchased from Sigma-Aldrich, dried in a furnace at 400 to 500 $^oC$ for 2–4 h and cooled under vacuum prior to use. Water was distilled and degassed by nitrogen bubbling prior to use.

Toluene, tetrahydrofuran (thf), diethyl ether and hexane were dried using a Braun Solvent Purification System and degassed by additional freeze-pump-thaw cycles when deemed necessary. Methanol and ethanol were distilled under nitrogen from magnesium. Pentane and deuterated dichloromethane were purchased from Fisher Scientific and Aldrich, respectively, and were dried over phosphorus pentoxide ($P_2O_5$), degassed *via* three freeze-pump-thaw cycles and trap-to-trap distilled prior to use. Acetone, purchased from Fisher Scientific, was dried over Drierite (8 mesh, without indicator), degassed by three freeze-pump-thaw cycles and collected by trap-to-trap distillation prior to use.

NMR spectra were recorded on a Bruker Avance 300 FT or Bruker Avance II 400 MHz spectrometer ($^1$H NMR at 300/400 MHz, $^{13}C\{^1H\}$ NMR at 75/100 MHz and $^{31}P\{^1H\}$ NMR at 121/162 MHz) with chemical shifts δ reported relative to tetramethylsilane (TMS)($^1$H, $^{13}C\{^1H\}$) or 85 % $H_3PO_4$ ($^{31}P\{^1H\}$) as external reference. $^1$H and $^{13}C\{^1H\}$ NMR spectra were referenced internally to deuterated solvent resonances which were referenced relative to TMS.

Solid state IR spectra were recorded using pressed KBr pellets on a Perkin Elmer Spectrum GX IR spectrometer. Elemental analysis was performed by the University of St. Andrews microanalytical service using a Carlo Erba CHNS/O microanalyser. Melting points were determined on a Gallenkamp apparatus and are uncorrected. Mass spectra were recorded either by the EPSRC National Mass Spectrometry Service Centre, Swansea on a Thermofisher LTQ Orbitrap XL high resolution instrument coupled to an Advion TriVersa NanoMate electrospray infusion system or by the Mass Spectrometry Service Centre at the University of St. Andrews using either of a Micromass GCT EI/CI or a Micromass LCT ES instrument.

GC-MS chromatograms were recorded on a Hewlett Packard 6890 series GC system equipped with an Agilent J&W HP-1 general purpose column (fused silica capillary) and an HP 5973 Mass

selective detector for both qualitative and quantitative analysis. Method: flow rate 1 ml $min^{-1}$ (He carrier gas), split ratio 100:1, starting temperature 50 $^oC$ (4 min) ramp rate 20 $^oC$ $min^{-1}$ to 130 $^oC$ (2 min), ramp rate 20 $^oC$ $min^{-1}$ to 220 $^oC$ (15.5 min).

### *5.4.2 Single crystal X-ray structure determinations*

Tables containing a summary of the crystal data collection and refinement paramaters of compounds **64** and **65** can be found in Appendix 1. Data sets were collected on a Rigaku Mo MM007 (dual port) high brilliance diffractometer with graphite monochromated MoK$\alpha$ radiation ($\lambda$ = 0.71075 Å). The diffractometer is fitted with Saturn 70 and Mercury CCD detectors and two XStream LT accessories. Data reduction was carried out with standard methods using the software package Bruker SAINT,[28] SMART,[29] SHELXTL[30] and and Rigaku CrystalClear, CrystalStructure, HKL2000. All the structures were solved using direct methods and conventional difference Fourier methods. All non-hydrogen atoms were refined anisotropically by full-matrix least squares calculations on $F^2$ using SHELX-97[31] within an X-seed[32,33] environment. With the exception of hydride atoms, hydrogen atoms were fixed in calculated positions. Figures were generated with POV Ray for Windows in an X-seed environment, with the displacement ellipsoids at 50% probability level unless stated otherwise. Further information is available on request from Prof. Alexandra Slawin at the School of Chemistry, University of St. Andrews.

### *5.4.3 Synthetic procedures*

***Reaction of [Ir(PNP)(COE)][$BF_4$] with MeP in the presence of water: Formation of trans–[Ir(PNP)$(H)_2$(CO)][$BF_4$] (64) and Ir(PNP)(H)($H_2O$){OC(O)$CH_2CH_3$}][$BF_4$] (65)***

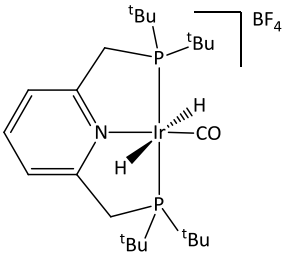


Water (0.60 ml) was added to a solution of [Ir(PNP)(COE)][$BF_4$] (0.14 g, 0.17 mmol) in methyl propanoate (2.75 g, 31.20 mmol, 3.00 ml). The mixture was then heated to 60 $^oC$ for 20 h during which time a biphasic mixture consisting of an orange organic phase and a colourless aqueous phase formed. The mixture was then cooled to room temperature and the two phases were allowed to separate. The organic phase was isolated and the product precipitated from this phase with the addition of hexane (20 ml). The

resultant precipitate was subsequently collected, washed with diethyl ether (2 × 30 ml) and dried *in vacuo* to furnish an orange solid (0.87 g) comprising of a mixture of **64** and **65** in a 4 : 1 ratio based on $^{31}$P NMR integrals. Single crystals of **64** suitable for structure determination by X-ray diffraction were obtained as orange plates by slow diffusion of pentane into a solution of the mixture of **64** and **65** in dichloromethane. Analytical data for compound **64**: $^{1}$H NMR (300 MHz, $CD_2Cl_2$): $\delta_H$ = -6.75 (t, 2H, $^{2}J_{H\text{-}P}$ = 12.6 Hz; Ir–*H*), 1.42 (vt, 36H, $^{3}J_{H\text{-}P}$ = 7.3 Hz; C(C*H*$_3$)$_3$), 3.87 (vt, 4H, $^{2}J_{H\text{-}P}$ = 4.0 Hz; C*H*$_2$–P), 7.52 (d, 2H, $^{3}J_{H\text{-}H}$ = 8.0 Hz; PNP-aryl), 7.83 (t, 1H, $^{3}J_{H\text{-}H}$ = 8.0 Hz; PNP-aryl). $^{31}$P{$^{1}$H} NMR (121 MHz, $CD_2Cl_2$): $\delta_P$ = 68.8 (s). IR (KBr): $\tilde{\nu}$ = 2954–2896 [m, sp$^3$ $\nu$(C–H)], 2010 [st, $\nu$(C=O)], 1804 [m, $\nu$(Ir–H)], 1465–1372 [st, Ar $\nu$(C=C)]. ES-MS: *m/z* (%) = 618 (100) [M – $BF_4$]$^+$. This data compare well with the literature values reported for the analogous complex $[Ir(CO)(H)_2(PNP)][PF_6]$.[20]

### *Reaction of [Ir(PNP)(COE)][BF$_4$] with Propanoic acid (PA): Formation of [Ir(PNP)(H)(H$_2$O){OC(O)CH$_2$CH$_3$}][BF$_4$], 65*

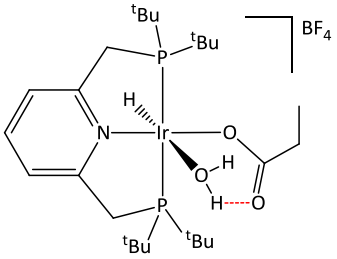


[Ir(PNP)(COE)][$BF_4$] (0.38 g, 0.49 mmol) was dissolved in propanoic acid (4.97 g, 67.02 mmol, 5.00 ml) to immediately give a yellow reaction solution. This solution was heated to 60 °C for 20 h with stirring. After this period, the mixture was cooled to room temperature and reduced to dryness under vacuum. The resulting residue was washed with hexane (3 × 10 ml) and dried *in vacuo* to afford the product as a pale orange solid (0.35g, 94 %). Yellow prisms suitable for structure determination by single crystal X-ray diffraction were obtained by slow diffusion of hexane at room temperature into a dichloromethane solution of **65**. $^{1}$H NMR (300 MHz, $CD_2Cl_2$): $\delta_H$ = -29.00 (t, 1H, $^{2}J_{H\text{-}P}$ = 11.6 Hz; Ir–*H*), 1.06 (t, 3H, $^{3}J_{H\text{-}H}$ = 7.4 Hz; propanoate-C*H*$_3$), 1.31 (vt, 18H, $^{3}J_{H\text{-}P}$ = 7.1 Hz; C(C*H*$_3$)$_3$), 1.36 (vt, 18H, $^{3}J_{H\text{-}P}$ = 7.1 Hz; C(C*H*$_3$)$_3$), 2.25 (q, 2H, $^{3}J_{H\text{-}H}$ = 7.4 Hz; propanoate-C*H*$_2$), 3.53 (dvt, 2H, $^{2}J_{H\text{-}H}$ = 17.5 Hz, $^{2}J_{H\text{-}P}$ = 4.0 Hz; C*H*$_2$–P), 3.80 (dvt, 2H, $^{2}J_{H\text{-}H}$ = 17.5 Hz, $^{2}J_{H\text{-}P}$ = 3.7 Hz; C*H*$_2$–P), 7.46 (d, 2H, $^{3}J_{H\text{-}H}$ = 8.1 Hz; PNP-aryl), 7.73 (t, 1H, $^{3}J_{H\text{-}H}$ = 8.1 Hz; PNP-aryl). $^{13}$C{$^{1}$H} NMR (75 MHz, $CD_2Cl_2$): $\delta_C$ = 9.2 (s; propanoate-*C*H$_3$), 27.9 (s; propanoate-*C*H$_2$), 29.3 (bs; C(*C*H$_3$)$_3$), 36.4 (vt, $^{1}J_{C\text{-}P}$ = 11.7 Hz; *C*(CH$_3$)$_3$), 37.6 (vt, $^{1}J_{C\text{-}P}$ = 10.0 Hz; *C*(CH$_3$)$_3$), 37.1 (vt, $^{1}J_{C\text{-}P}$ = 11.7 Hz; *C*H$_2$–P), 122.0 (vt, $^{3}J_{C\text{-}P}$ = 4.5 Hz; PNP-aryl), 139.3 (s; PNP-aryl), 166.5 (vt, $^{2}J_{C\text{-}P}$ = 3.1 Hz; PNP–aryl), 181.0 (s; propanoate-*C*=O). $^{31}$P{$^{1}$H} NMR (121 MHz, $CD_2Cl_2$): $\delta_P$ = 49.6 (s).

### *Reaction of [Ir(PNP)(COE)][BF$_4$] with tert-butyl propanoate ($^t$BuP) or isopropyl propanoate ($^i$PrP) in the presence of water: quantitative conversion to [Ir(PNP)(H)(H$_2$O){OC(O)CH$_2$CH$_3$}][BF$_4$] (65)*

Water (0.1 ml) was added to a suspension of [Ir(PNP)(COE)][$BF_4$] (0.04 g, 0.05 mmol) in *tert*-butyl propanoate (1.73 g, 13.29 mmol, 2.0 ml) or isopropyl propanoate (1.77 g, 15.20 mmol, 2.0 ml). The resulting mixture was heated to 60 °C for 15 h after which the orange mixture was cooled to room temperature and evaporated to dryness under vacuum. The obtained orange solid was analysed using standard NMR spectroscopic techniques without any further purification. Analysis of this solid indicated quantitative conversion of [Ir(PNP)(COE)][$BF_4$] to [Ir(PNP)(H)($H_2O$){OC(O)$CH_2CH_3$}][$BF_4$] (**65**) for both $^t$BuP and $^i$PrP with no trace of the CO complex [Ir(PNP)$(H)_2$(CO)][$BF_4$] (**64**).

### *Reaction of [Ir(PNP)(COE)][BF$_4$] with MeP in the absence of water: Formation of [Ir(PNP)(H){CH$_2$OC(O)CH$_2$CH$_3$}][BF$_4$], 68*

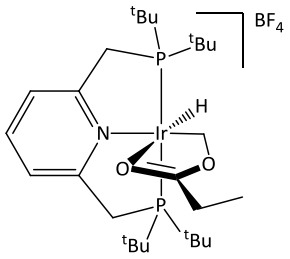


[Ir(PNP)(COE)][$BF_4$] (0.19 g, 0.24 mmol) was dissolved in methyl propanoate (3.66 g, 41.50 mmol, 4.00 ml) and the resulting red solution heated to 60 °C for 20 h with stirring. After this period, the orange mixture was cooled to room temperature and all volatiles removed under reduced pressure. The crude product was then washed with hexane (3 × 15 ml) and dried *in vacuo* to furnish the product as an orange solid (0.17 g, 94%). $^1$H NMR (300 MHz, $CD_2Cl_2$): $\delta_H$ = -23.74 (t, 1H, $^2J_{H\text{-}P}$ = 14.6 Hz; Ir–*H*), 1.08 (t, 3H, $^3J_{H\text{-}H}$ = 7.5 Hz; MeP-C*H*$_3$), 1.21 (vt, 18H, $^3J_{H\text{-}P}$ = 7.1 Hz; C(C*H*$_3$)$_3$), 1.24 (vt, 18H, $^3J_{H\text{-}P}$ = 7.1 Hz; C(C*H*$_3$)$_3$), 2.39 (q, 2H, $^3J_{H\text{-}H}$ = 7.5 Hz; MeP-C*H*$_2$), 3.58 (dvt, 2H, $^2J_{H\text{-}H}$ = 17.1 Hz, $^2J_{H\text{-}P}$ = 4.1 Hz; C*H*$_2$–P), 3.73 (dvt, 2H, $^2J_{H\text{-}H}$ = 17.1 Hz, $^2J_{H\text{-}P}$ = 3.5 Hz; C*H*$_2$–P), 6.47 (t, 2H, $^3J_{H\text{-}P}$ = 9.5 Hz; MeP-OC*H*$_2$-Ir), 7.53 (d, 2H, $^3J_{H\text{-}H}$ = 7.7 Hz; PNP-aryl), 7.53 (t, 1H, $^3J_{H\text{-}H}$ = 7.7 Hz; PNP-aryl). $^{13}$C{$^1$H} NMR (75 MHz, $CD_2Cl_2$): $\delta_C$ = 8.9 (s; MeP-*C*H$_3$), 27.2 (s; MeP-*C*H$_2$), 29.3 (bs; C(*C*H$_3$)$_3$), 29.7 (bs; C(*C*H$_3$)$_3$), 35.9 (vt, $^1J_{C\text{-}P}$ = 12.9 Hz; *C*(CH$_3$)$_3$), 37.1 (vt, $^1J_{C\text{-}P}$ = 9.7 Hz; *C*(CH$_3$)$_3$), 39.4 (vt, $^1J_{C\text{-}P}$ = 10 Hz; *C*H$_2$–P), 121.3 (vt, $^3J_{C\text{-}P}$ = 4.3 Hz; PNP-aryl), 51.8 (vt, $^2J_{C\text{-}P}$ = 6.3 Hz; MeP-*C*H$_2$-Ir), 137.1 (s; PNP-aryl), 163.0 (vt, $^2J_{C\text{-}P}$ = 2.7 Hz; PNP–aryl), 280.3 (m; MeP-*C*=O). $^{31}$P{$^1$H} NMR (121 MHz, $CD_2Cl_2$): $\delta_P$ = 42.1 (s). IR (KBr): $\tilde{\nu}$ = 2949–2871 [st, sp$^3$ $\nu$(C–H)], 1610 [st, $\nu$(C=O)], 1466–1371 [st, Ar $\nu$(C=C)], 1059 [st, $\nu$(C–O)]. ES-MS: *m/z* (%) = 676 (32) [M – $BF_4$]$^+$, 588 (44) [Ir(PNP)]$^+$, 532 (11) [Ir(H)(PNP) - $^t$Bu]$^+$.

***Attempt to catalytic functionalise C–H activated MeP by the "in situ" generation of [Ir(PNP)(H){$CH_2OC(O)CH_2CH_3$}][$BF_4$] (68)***

A solution of [Ir(PNP)(COE)][$BF_4$] (0.20 g, 0.25 mmol) in methyl propanoate (9.15 g, 103.85 mmol, 10 ml) was added to an autoclave under an inert atmosphere of dinitrogen. The autoclave was subsequently sealed tightly, pressurised with ethene (30 bar) and heated to 60 $^oC$ for 15 h with stirring. After this period, the autoclave was cooled to room temperature, vented to the atmosphere and opened to reveal the product mixture as a yellow solution containing a brown solid. Both phases were analysed making use of standard GC-MS and NMR spectroscopic techniques. The desired product methyl 2-methylbutanoate was, however, not detected. $^{31}P$ NMR revealed in addition to [Ir(PNP)$(H)_2$(CO)][$BF_4$] (**64**), the presence of two new complexes in the form of singlets at δ 73.1 and δ 50.7. These complexes, which do not have corresponding hydride resonances, could not be assigned unambiguously.

***Attempt to catalytic functionalise C–H activated MeP via preformed [Ir(PNP)(H){$CH_2OC(O)CH_2CH_3$}][$BF_4$] (68)***

A solution of [Ir(PNP)(H){$OC(O)CH_2CH_3$}][$BF_4$] (0.21 g, 0.29 mmol) in methyl propanoate (9.15 g, 103.85 mmol, 10 ml) was added to an autoclave under an inert atmosphere of dinitrogen. The autoclave was subsequently sealed tightly, pressurised with ethene (30 bar) and heated to 60 $^oC$ for 15 h with stirring. After this period, the autoclave was cooled to room temperature, vented to the atmosphere and the product mixture analysed using standard GC-MS and NMR spectroscopic techniques. As before, the desired product methyl 2-methylbutanoate was not observed and the measured $^{31}P$ NMR spectra were comparable to those previously obtained for the *in situ* attempt.

## 5.5 Notes and References


(1) Jazzar, R.; Hitce, J.; Renaudat, A.; Sofack-Kreutzer, J.; Baudoin, O. *Chem. Eur. J* **2010**, *16*, 2654-2672.
(2) Labinger, J. A.; Bercaw, J. E. *Nature* **2002**, *417*, 507-514.
(3) Crabtree, R. H. *J. Organomet. Chem.* **2004**, *689*, 4083-4091.
(4) Bergman, R. G. *Nature* **2007**, *446*, 391-393.
(5) Arndtsen, B. A.; Bergman, R. G.; Mobley, T. A.; Peterson, T. H. *Acc. Chem. Res.* **1995**, *28*, 154-162.
(6) Crabtree, R. H. *J. Chem. Soc., Dalton Trans.* **2001**, 2437-2450.

(7) Romero, P. E.; Whited, M. T.; Grubbs, R. H. *Organometallics* **2008**, *27*, 3422–3429.
(8) Bernskoetter, W. H.; Hanson, S. K.; Buzak, S. K.; Davis, Z.; White, P. S.; Swartz, R.; Goldberg, K. I.; Brookhart, M. *J. Am. Chem. Soc.* **2009**, *131*, 8603-8613.
(9) Bedford, R. B.; Betham, M.; Blake, M. E.; Coles, S. J.; Draper, S. M.; Hursthouse, M. B.; Scully, P. N. *Inorg. Chim. Acta* **2006**, *359*, 1870-1878.
(10) Schwartsburd, L.; Iron, M. A.; Konstantinovski, L.; Diskin-Posner, Y.; Leitus, G.; Shimon, L. J. W.; Milstein, D. *Organometallics* **2010**, *29*, 3817-3827.
(11) Meiners, J.; Friedrich, A.; Herdtweck, E.; Schneider, S. *Organometallics* **2009**, *28*, 6331-6338.
(12) Whited, M. T.; Zhu, Y.; Timpa, S. D.; Chen, C.-H.; Foxman, B. M.; Ozerov, O. V.; Grubbs, R. H. *Organometallics* **2009**, *28*, 4560-4570.
(13) Whited, M. T.; Grubbs, R. H. *Acc. Chem. Res.* **2009**, *42*, 1607-1616.
(14) Empsall, H. D.; Hyde, E. M.; Markham, R.; McDonald, W. S.; Norton, M. C.; Shaw, B. L.; Weeks, B. *J. Chem. Soc., Chem. Commun.* **1977**, 589-590.
(15) Boutry, O.; Gutiérrez, E.; Monge, A.; Nicasio, M. C.; Pérez, P. J.; Carmona, E. *J. Am. Chem. Soc.* **1992**, *114*, 1288-1290.
(16) Luecke, H. F.; Arndtsen, B. A.; Burger, P.; Bergman, R. G. *J. Am. Chem. Soc.* **1996**, *118*, 2517-2518.
(17) Slugovc, C.; Mereiter, K.; Trofimenko, S.; Carmona, E. *Angew. Chem. Int. Ed.* **2000**, *39*, 2158-2160.
(18) Carmona, E.; Paneque, M.; Santos, L. L.; Salazar, V. *Coord. Chem. Rev.* **2005**, *249*, 1729-1735.
(19) Feller, M.; Karton, A.; Leitus, G.; Martin, J. M. L.; Milstein, D. *J. Am. Chem. Soc.* **2006**, *128*, 12400-12401.
(20) Kloek, S. M.; Heinekey, D. M.; Goldberg, K. I. *Organometallics* **2006**, *25*, 3007-3011 *(and references therein)*.
(21) McMurry, J. (eds: Huber, J; Chelton, D; Henderson, M; Brooks, J. S.; Masson, C.) *in Organic Chemistry,* Brooks/Cole: Pacific Grove, USA, 2000, p913.
(22) Ben-Ari, E.; Cohen, R.; Gandelman, M.; Shimon, L. J. W.; Martin, J. M. L.; Milstein, D. *Organometallics* **2006**, *25*, 3190-3210.
(23) Tanaka, R.; Yamashita, M.; Nozaki, K. *J. Am. Chem. Soc.* **2009**, *131*, 14168-14169.
(24) Rybtchinski, B.; Ben-David, Y.; Milstein, D. *Organometallics* **1997**, *16*, 3786-3793.
(25) van der Ent, A.; Onderdelinden, A. L. *Inorg. Synth.* **1990**,*28*, 90-92.
(26) Hermann, D.; Gandelman, M.; Rozenberg, H.; Shimon, L. J. W.; Milstein, D. *Organometallics* **2002**, *21*, 812-818.
(27) Dorta, R.; Rozenberg, H.; Shimon, L. J. W.; Milstein, D. *J. Am. Chem. Soc.* **2002**, 188-189.
(28) *SAINT Data Reduction Software (version 6.45)*, Bruker AXS Inc. (Madison), WI, USA, **2003**.
(29) *SMART Data Collection Software (version 5.629)*, Bruker AXS Inc. (Madison), WI, USA, **2003**.
(30) *SHELXL program package (version 5.1)*, Bruker APX Inc. (Madison), WI, USA.
(31) Sheldrick, G. M. *SHELX-97 Program for Crystal Structure Analysis*, University of Göttingen (Göttingen), Germany, **1997**.
(32) Barbour, L. J. *J. Supramol. Chem.* **2003**, *1*, 189-191.
(33) Atwood, J. L.; Barbour, L. J. *Cryst. Growth Des.* **2003**, *3*, 3-8.

# Chapter 6

# Methanol dehydrogenation for the *in situ* production of anhydrous formaldehyde

– Preliminary study on the one-pot conversion of MeP to MMA –

*In this chapter, novel routes to the low cost, atom efficient production of methyl methacrylate (MMA) are explored. In particular, this study focuses on the possibility of producing anhydrous formaldehyde* in situ via *the catalytic dehydrogenation of methanol in the presence of carbonate salts and / or transition metal catalysts. Furthermore, in the hope of limiting the number of required steps in the large scale production of MMA, the use of a one-pot setup for the α-methylenation of methyl propanoate (MeP) with methanol is explored. In these reactions, formaldehyde is generated* in situ *from methanol by a suitable catalyst and then consumed in a one-pot, base catalysed condensation reaction with MeP to afford methyl 3-hydroxy-2-methylpropanoate, which undergoes spontaneous dehydration to furnish MMA as product.*

## 6.1 Introduction

Butlerov was the first to discover formaldehyde in 1859, and since then this compound has proceeded to become one of the most important chemicals in industrial processes.[1] The remarkable two-stage Alpha process developed by Lucite International for the large scale production of methyl methacrylate (MMA) from the simple, readily available chemicals ethene, methanol and carbon monoxide represent an example of such a process. As described before (Chapter 1), methyl propanoate (MeP) is generated in high yield and selectivity during the first stage of this process by the methoxycarbonylation of ethene in the presence of a proprietary Pd based catalyst. The produced MeP is then, in the second stage, converted to MMA (93 % selectivity) over a heterogeneous fixed bed catalytic system in which cesium oxide on silica represents the active component. During this second stage, the formation of coke (solid carbonaceous material) deposits on the catalyst causes decreased activity and selectivity over time. This problem is, however, partly mitigated by making use of two parallel MMA reactors which can be freed from coke, one at a time, *via* controlled *in situ* regeneration steps, whilst maintaining continuous production through the remaining reactor.[2]

The formaldehyde, required for condensation with MeP during the second stage, is initially produced as formalin in a separate process and then dehydrated to afford anhydrous formaldehyde, which can be introduced as reagent into the MMA feedstock. The use of anhydrous formaldehyde during this step is essential for ensuring high selectivity to MMA and for the prevention of excessive catalyst aging.*[2] Commercially available formalin processes generally involve the oxidation of methanol in the presence of iron-molybdenum oxides (formox process) or silver catalysts.[3] These processes, however, both require very harsh temperature conditions (300 °C to 700 °C) with the formalin produced typically having a maximum concentration of 55 % weight formaldehyde in water, contaminated by ~1 % of methanol.[1,2] Isolation of anhydrous formaldehyde from these mixtures is an expensive procedure, complicated by the formation of azeotropes.[3] Although Lucite International has patented a specially designed separation procedure that allows for the successful dehydration of formalin in the Alpha process, the development of a more atom efficient and cost effective route to the direct production of anhydrous formaldehyde would be of great economic benefit

* Catalyst aging refers to a situation where the selectivity and activity of a catalyst diminish over time.

† The temperatures quoted in this account reflect the external temperatures that the autoclave heating jacket was set to. We have recently discovered that the actual internal temperatures may be as much as 60 °C higher than

to the overall process. Furthermore, employing formaldehyde generated in a separate step is flawed by another drawback, namely the facile polymerisation of this compound both in the gas phase and in solution to form polyoxymethylenes. The latter are highly insoluble which leads to severe fouling of transfer lines over time, adding to the overall maintenance time and operational costs. The development of an alternative process for the *in situ* generation of anhydrous formaldehyde would therefore not only eliminate the need for an additional formaldehyde preparation and dehydration cycle, but would also overcome these issues with fouling.

The catalytic dehydrogenation of methanol represents an exciting alternative to the current commercial processes, since anhydrous formaldehyde is produced directly with valuable hydrogen gas as the only by-product. A vast array of silver, copper, zinc and transition metal based heterogeneous catalyst are known to be active and selective catalysts in methanol dehydrogenation. Most of these catalysts, however, are subject to fast deactivation as a result of oxide reduction and/or vaporization of some of the elements at the elevated temperatures required for successful dehydrogenation.[1] Furthermore, although heterogeneous fixed bed reactors with sodium carbonate as active catalyst have been shown to be stable, highly active and selective systems at the harsh reaction temperatures (527–727 $^{o}$C) required, these reactions tend to produce carbon monoxide, methane and trace amount of carbon dioxide, coke and water as by-products.[3,4]

A number of homogeneous transition metal catalysts are known to promote the dehydrogenation of methanol or other alcohols, including hydrogen transfer reactions, to furnish more reactive ketones and aldehydes.[5-9] Moreover, several reactions where the catalytic dehydrogenation of an alcohol to an aldehyde or ketone is followed by a one-pot bond construction step have been described.[9] In these reactions, the first dehydrogenation step is catalysed while the second bond forming step may or may not be catalysed. Furthermore, hydrogen is temporarily removed from the alcohol by the catalyst to generate a more electrophilic aldehyde or ketone which can participate in an *in situ* condensation reaction to furnish an alkene. This alkene is then catalytically reduced to the saturated product utilising the hydrogen initially removed from the alcohol. Given that no additional hydrogen is required for the alkene reduction step, this approach is often referred to as the "hydrogen borrowing strategy".[9] Furthermore, since water is formed as the only by-product, the indirect

functionalisation of alcohols *via* this method represents a highly attractive green alternative to more traditional C–C bond forming routes. Grigg *et al.*[10] were the first to report homogenous catalysts for these types of transformations in 1981 and since then Williams and co-workers, in particular, have been amongst the leading developers of such chemistry.[8,11-16] In more recent reports, these authors have shown the combination of $[RuCO(H)_2(PPh_3)_3]$ with certain biphosphines to be efficient catalytic systems for the alkylation of ketonitriles with alcohols.[11,15,16] Of the tested bisphosphines, xantphos together with $[RuCO(H)_2(PPh_3)_3]$, in particular, were found to be very efficient in catalysing the alkylation of ketonitriles with a wide range of alcohols (Scheme 6.1).[15] Furthermore, this methodology have also been applied successfully in indirect, $[\{IrCl(COD)\}_2]$ (COD = cyclooctadiene) catalysed Wittig,[17] aza-Wittig[12] and Horner-Wadsworth-Emmons type reactions.[11]

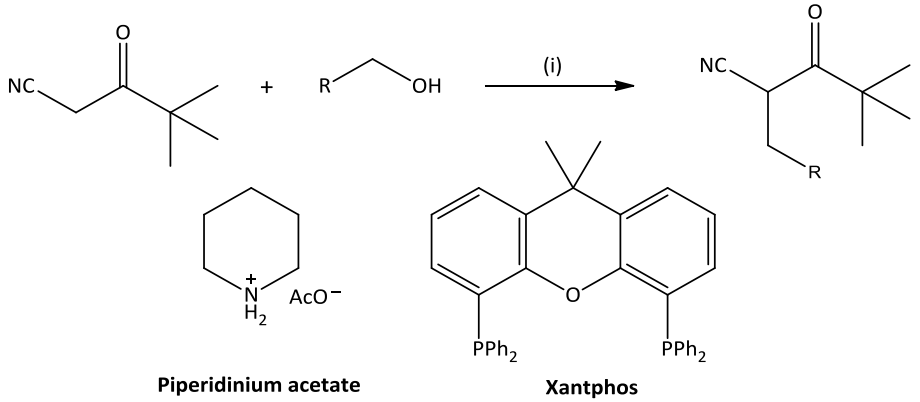


**Scheme 6.1** General reaction scheme for the catalytic alkylation of ketonitriles. Conditions: (i) 0.5 mol % $[RuCO(H)_2(PPh_3)_3]$, 0.5 mol % xantphos, 5 mol % piperidinium acetate, toluene, 110 °C, 3 h.[15]

Complementary to the work of Williams, Grigg *et al.*[18] have recently reported the iridium catalysed alkylation of *tert*-butyl cyanoesters with benzyl alcohols under solvent free conditions in the presence of a catalytic amount of potassium hydroxide (Scheme 6.2) at 100 °C. Under these conditions, the corresponding *α*-benzylated cyanoesters are obtained as final products in moderate yield. For some of the functionalised products, however, the liberated water results in ester bond hydrolysis, followed by thermal decarboxylation to give varied amounts of a by-product with the general formula $RCH_2CH_2CN$.[18] A similar decarboxylation product was also observed by Williams *et al.*[11] during related reactions aimed at the alkylation of dibenzyl malonate with benzyl alcohol. Curiously, when furfuryl alcohol is employed as alkylating alcohol, the reaction proceeds much more slowly compared to reactions with benzylic alcohols with only 52 % of the desired cyanoester produced over a 24 h period.

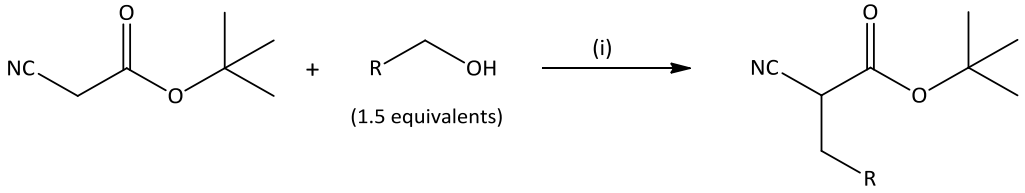


**Scheme 6.2** General reaction scheme for the alkylation of *tert*-butyl cyanoesters with benzyl alcohols (R = substituted Ph). Conditions: (i) 2.5 mol % [{Cp*$IrCl_2$}$_2$], 15–20 mol % KOH, 100 $^oC$, 4–24 h.[18]

Williams *et al.*[14] also explored the possibility of intercepting the final hydrogenation step in these types of reactions to access the unsaturated products prior to their reduction, by supplying a suitable sacrificial hydrogen acceptor. For this approach to be successful, the hydrogen acceptor must have a much greater affinity for hydrogen than the generated alkene. Furthermore, this acceptor should not possess the capacity to interfere with the hydrogen transfer catalysis or condensation step. Williams and co-workers[14] have shown that crotononitrile ($CH_3CH$=$CHCN$) satisfies all the criteria for a suitable hydrogen acceptor. In the presence of crotononitrile and [$RuCO(H)_2(PPh_3)$] / xanthphos as catalytic system, malonic half-esters successfully convert to unsaturated esters in moderate to high yields (71–95 %) according to the reaction given in Scheme 6.3 (a). When benzyl alcohols are employed as starting alcohols, $\alpha,\beta$-unsaturated esters are obtained selectively with these reactions displaying great tolerance for a wide variety of ring substituents. For aliphatic alcohols, however, mixtures of the $\alpha,\beta$ - and $\alpha,\gamma$-alkenes regioisomers are generated as can be expected.[14] This approach displays great potential over a wide range of transformations and has also been employed successfully in the preparation of nitroalkenes from nitroalkanes and alcohols *via* a tandem oxidation / nitroaldol condensation reaction [Scheme 6.3 (b)].[14]

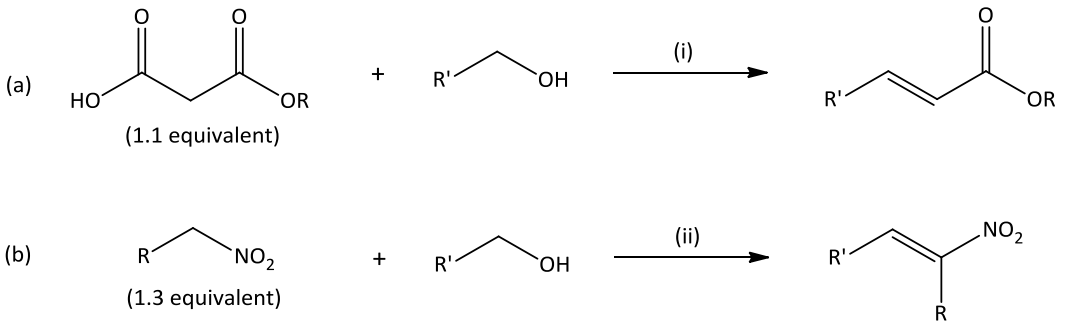


**Scheme 6.3** The catalytic formation of alkenes from alcohols in the presence of a hydrogen acceptor. Conditions: (i) 2.5 mol % [$RuCO(H)_2(PPh_3)_3$], 2.5 mol % xantphos, 30 mol % pyrollidine [for (a)] or 20 mol % piperidinium acetate [for (b)], 1.5 equiv. crotononitrile, toluene, reflux, 2 h.[14]

The direct synthesis of imines from alcohols and amines in the presence of a ruthenium PNP-type catalyst *via* a similar pathway has recently been shown possible by Milstein and co-workers (Scheme 6.4).[7] Remarkably, the generated imines are not reduced by the liberated hydrogen gas and for this reason, no sacrificial hydrogen acceptor is required. Furthermore, these reactions can be carried out in air, under neutral conditions with water and hydrogen gas as the only major by-products, rendering this a very environmentally benign route to the preparation of imines. In general, when substituted benzyl alcohols are employed, the desired imines are obtained in moderate to high yields. For reactions with aliphatic alcohols, however, reactions proceed less efficiently with the generated imines typically contaminated by varied amounts of the corresponding amides (10–18 %) and esters (4–7 %). The mechanism for this reaction (Scheme 6.4) has been proposed to involve an initial activation of the alcohol O–H bond together with rearomatisation of the pyridine ring system to generate intermediate **II**. Following $\beta$-hydrogen abstraction, the formed aldehyde is released from intermediate **III** and condensed with an amine in a separate step to generate an unstable hemiaminal which then undergoes spontaneous dehydration to afford the corresponding imine product. The catalyst **I** is regenerated by hydrogen abstraction from the PNP ligand in **IV**, resulting in dearomatisation of the pyridine ring system together with reductive elimination of molecular hydrogen.

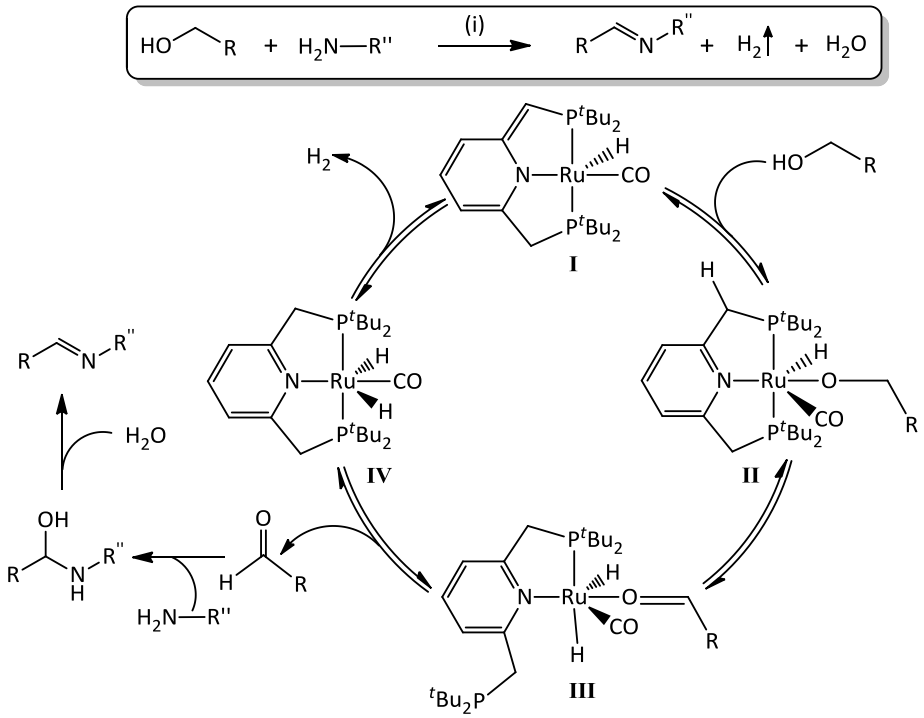


**Scheme 6.4** Overall reaction (block) and the mechanism proposed by Milstein and co-workers[7] for the preparation of imines from alcohols and amines. Conditions: (i) 0.2 mol % of **I**, toluene, reflux.

For this part of our study, the possibility of using a similar strategy for the one-pot conversion of methyl propanoate to methylmethacrylate was explored (Scheme 6.5). In an ideal system, anhydrous formaldehyde would be generated *in situ* by the catalytic dehydrogenation of methanol. The resultant formaldehyde can then undergo base catalysed condensation with MeP, in a one-pot set-up, to afford methyl 3-hydroxy-2-methylpropanoate as intermediate. Finally, spontaneous water elimination from this intermediate may proceed under the elevated reaction temperatures to afford MMA as the final product.

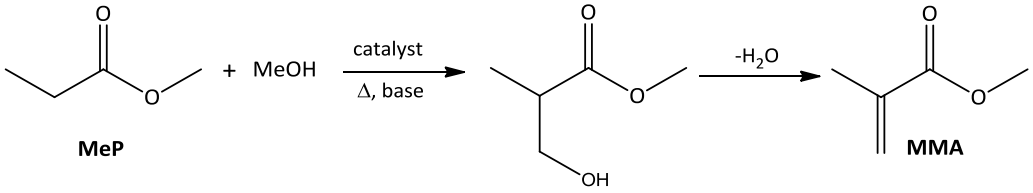


**Scheme 6.5** Proposed reaction scheme for the catalytic one-pot conversion of MeP to MMA in a basic medium.

If such an approach were to be successful, it would not only represent an environmentally benign process for the production of MMA, but would also eliminate many of the shortcomings still associated with the current Lucite Alpha process. Since anhydrous formaldehyde would be produced *in situ*, an additional cycle for the production and dehydration of formalin would no longer be required. Furthermore, the *in situ* generation of formaldehyde would also solve the fouling issues often associated with the passing of formaldehyde through transfer lines. Finally, since such a homogenous process would replace the current heterogeneous fixed bed system, the process would no longer require the use of two parallel MMA reactors to compensate for catalyst deactivation that results from coke deposits. All these alterations would not only dramatically simplify the process, but would also bring about a significant reduction in the overall production and maintenance costs. For this approach to succeed, however, the employed catalytic system needs to adhere to certain criteria: (1) the catalyst should be chemoselective for the dehydrogenation of alcohols to aldehydes and should not participate in the hydrogenation of alkenes or esters; (2) the catalytic system should not be affected by the presence of water and (3) finally, the catalyst should not promote the decarbonylation of formaldehyde to form inactive carbonyl complexes. Some of these limitations may, however, also be overcome with the aid of additives such as water scavengers and/or sacrificial hydrogen acceptors. In this very

preliminary study, a range of catalysts was screened for their performance in the one-pot conversion of MeP to MMA. Although a suitable catalyst that adheres to all the mentioned criteria could not yet be identified, the preliminary findings reported herein suggest that this reaction has the potential to succeed and therefore serves as an important proof of concept for future developments in this area.

## 6.2 Results and Discussion

### *6.2.1 Methanol dehydrogenation to formaldehyde in the presence of simple carbonates and subsequent condensation with MeP to form MMA*

The initial idea for this study came from the serendipitous discovery that minor amounts of MMA are produced in the absence of any added formaldehyde when MeP is heated together with $Na_2CO_3$ at 130 °C† for 21 h in a stainless steel batch reactor. In addition to MMA, the collected GC-MS chromatogram (Figure 6.1) for this reaction revealed the presence of the hydrogenated product, methyl isobutyrate (M$^i$Bu), along with 3-pentanone and significant amounts of methanol (Scheme 6.6). Furthermore, a white solid present at the bottom of the reactor after removal of the liquid phase analysed to contain significant amounts of sodium propanoate (NaP). When the same reaction was performed in the presence of $Cs_2CO_3$ instead of $Na_2CO_3$, the formation of an even greater amount of MMA was observed (Figure 6.2). Furthermore, this system displayed a somewhat greater selectivity towards MMA, with reduced amounts of the by-products M$^i$Bu and 3-pentanone detected. Similar to the reaction with $Na_2CO_3$, cesium propanoate (CsP) was generated during the course of this reaction and once again formed part of the solid phase.

Since metal carbonates are often contaminated with small quantities of water, hydrolysis of the ester bond may occur in the presence of these salts to afford methanol and propanoic acid. The latter would react with either $Na_2CO_3$ or $Cs_2CO_3$ to form the corresponding propanoate salts, while methanol would remain in the liquid phase, thus accounting for the detection of these compounds. Furthermore, additional water would be generated during the formation of MMA, which could further enhance the amount of MeP hydrolysis that occurs.

† The temperatures quoted in this account reflect the external temperatures that the autoclave heating jacket was set to. We have recently discovered that the actual internal temperatures may be as much as 60 °C higher than the external set temperatures.

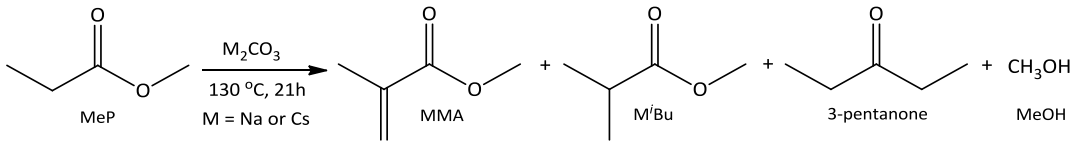


**Scheme 6.6** Products obtained when MeP is treated with either $Na_2CO_3$ or $Cs_2CO_3$ at 130 °C for 21 h.

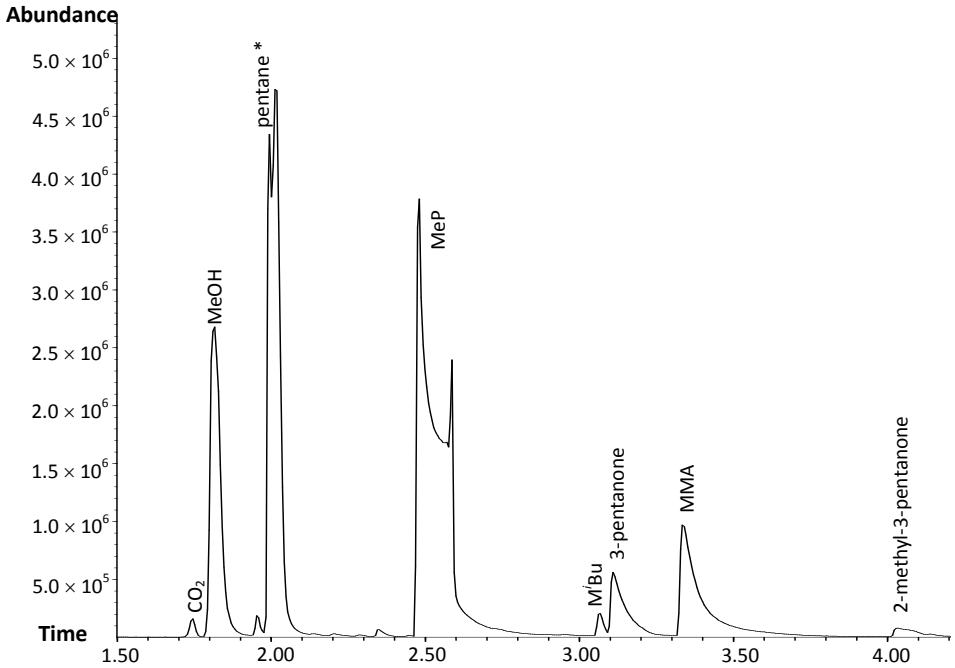


**Figure 6.1** GC-MS chromatogram collected for the reaction of MeP with $Na_2CO_3$ at 130 °C for 21 h in a stainless steel batch reactor.*Pentane is present as an impurity in the sample solvent (toluene).

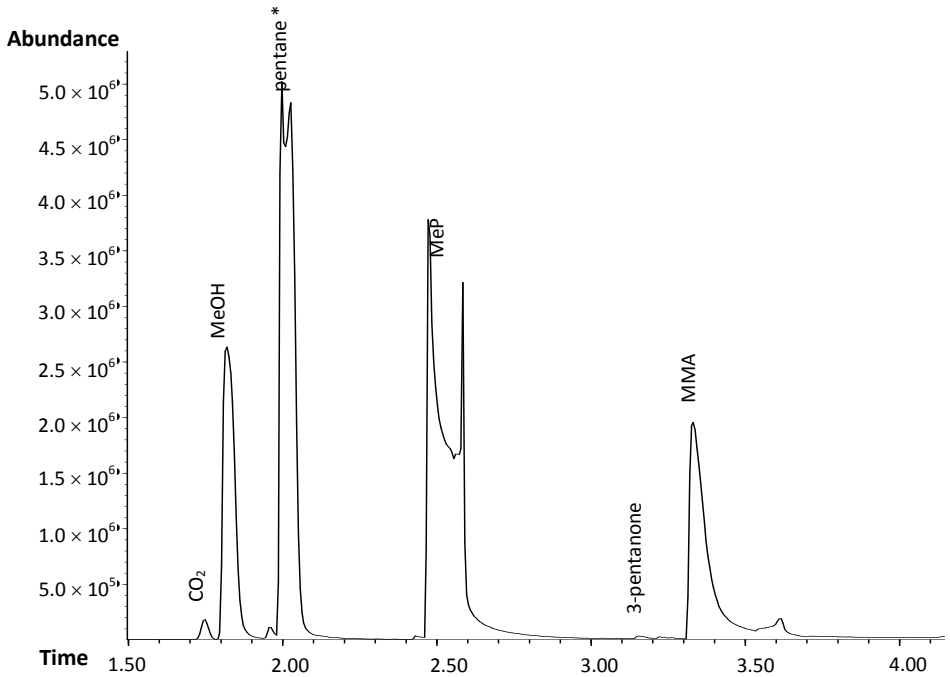


**Figure 6.2** GC-MS chromatogram collected for the reaction of MeP with $Cs_2CO_3$ at 130 °C for 21 h in a stainless steel batch reactor.*Pentane is present as an impurity in the sample solvent (toluene).

The presence of MMA and hydrogenated M$^{i}$Bu suggest that both a one carbon alkylating agent and hydrogen source must have been present at some stage during the course of the reaction. Based on this, methanol was considered to represent the most likely source of these reagents. This is a reasonable assumption, since earlier work by Renken and co-workers[3,4] has shown that selective dehydrogenation of methanol to anhydrous formaldehyde and hydrogen gas proceeds in the presence of $Na_2CO_3$ based fixed-bed flow reactors at temperatures of 530–730 $^{o}$C. Even though the reaction temperatures employed in our experiments were not nearly as high as the temperatures required for efficient $Na_2CO_3$ catalysed methanol dehydrogenation, it is still possible that very minor amounts of formaldehyde were generated at these lower temperatures.

As GC-MS data may only serve as a qualitative measure, GC-FID (Figure 6.3) and $^{1}$H NMR (Figure 6.4) data were collected for the $Cs_2CO_3$ experiment to allow for a rough quantification of the produced MMA. Even though no internal standards were employed, the final product mixture could be estimated to contain less than 1 % of MMA based on the relative quantities of unreacted MeP and MMA present. This figure, however, does not take into account the MeP removed from the system through hydrolysis, and the true MMA yield can therefore be expected to be even lower. Nevertheless, these results were of significance since they proved that in theory, under the appropriate catalytic conditions, such a one-pot conversion of MeP to MMA could indeed be possible.

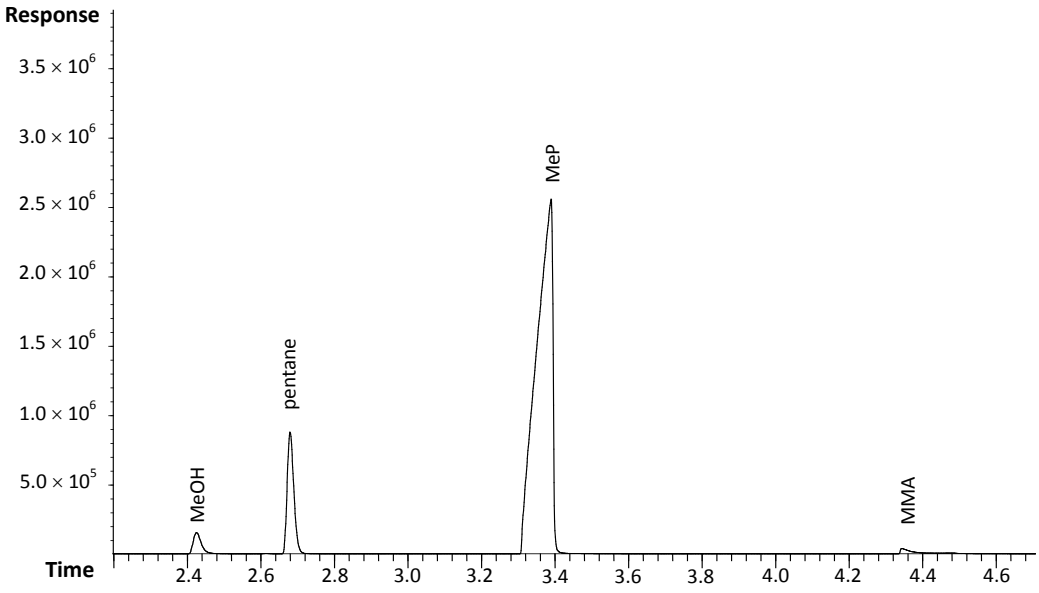


**Figure 6.3** GC-FID chromatogram collected for the reaction of MeP with $Cs_2CO_3$ at 130 $^{o}$C for 21 h.

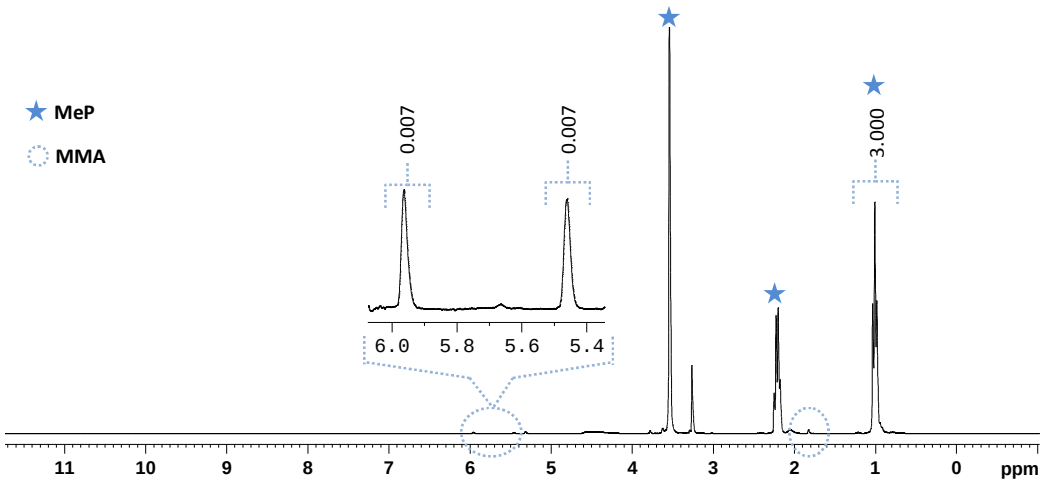


**Figure 6.4** $^{1}$H NMR spectrum for product mixture isolated for the reaction of MeP with $Cs_2CO_3$ at 130 $^{o}$C for 21 h, showing integrals for the MMA C=C*H*$_2$ protons versus that of the MeP C*H*$_3$ protons.

In order to confirm methanol as the alkylating agent in these reactions, a simple carbon labelling experiment was conducted and the final products analysed for labelling by means of GC-MS. For this experiment $^{13}$C labelled methanol was added to a mixture of MeP and $Cs_2CO_3$ in a stainless steel autoclave and heated to 130 $^{o}$C for 21 h. The addition of methanol to these reactions resulted in much more reactive system, which not only gave higher conversion of MeP to MMA, but also promoted the subsequent hydrogenation thereof to M$^{i}$Bu (Figure 6.5).

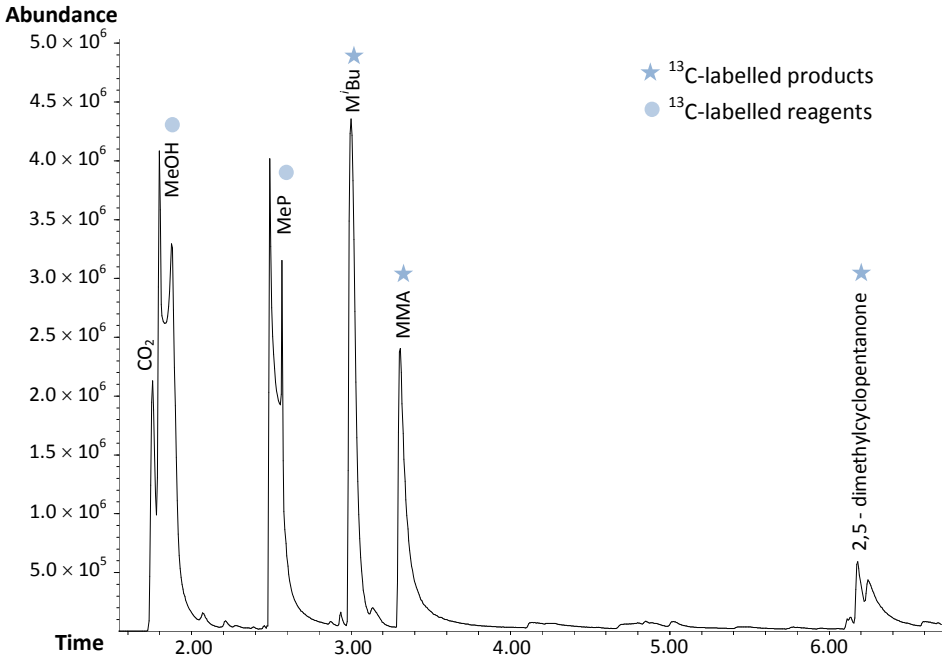


**Figure 6.5** GC-MS chromatogram for the deuterium labelling experiment with MeP, $Cs_2CO_3$ and methanol-$d_4$ at 130 $^{o}$C for 21 h in a stainless steel batch autoclave.

Furthermore, both MMA and M$^{i}$Bu were found to be $^{13}$C labelled, comprising of a mixture of non-labelled, mono-labelled and di-labelled compounds. The detection of di-labelled compounds is not surprising, since MeP, MMA and M$^{i}$Bu can all be expected to participate in transesterification reactions with labelled methanol to generate at least one label in these compounds, while for MMA and M$^{i}$Bu a second label is introduced by the incorporation of $^{13}$C-labelled methanol during the alkylation step. Furthermore, since such transesterification reactions would generate non-labelled methanol, which can be incorporated during indirect alkylation reactions, a certain fraction of the final products can be expected to contain either no labels or only one labelled carbon. Thus, taking all of these factors into consideration, the observed results are in full support of a system where methanol acts as the indirect alkylating agent and, it is therefore reasonable to conclude that methanol dehydrogenation represents the source of both formaldehyde and hydrogen in these systems.

Although $Na_2CO_3$ is known to catalyse methanol dehydrogenation, several transition metal complexes have been shown to possess similar potential.[1] Furthermore, Renken and co-workers[4] have shown that for fixed-bed $Na_2CO_3$ systems the rate of methanol dehydration can be enhanced by the addition of transition metals or activated carbon without modifying the formaldehyde selectivity. For this reason, the reaction of MeP with $Na_2CO_3$ in the absence of any added methanol was repeated in a Hastelloy™ reactor in order to determine whether the catalytic dehydrogenation of methanol in our systems was perhaps enhanced by the presence of transition metal impurities originating from stainless steel. Since Hastelloy™ is less susceptible to chemical corrosion, this material is less likely to generate such impurities. Interestingly, this reaction displayed very low productivity compared to the analogous reaction in a stainless steel reactor, with only trace amounts of MMA detected in the final reaction mixture, despite the presence of an ample amount of methanol. This finding then implies that the dehydrogenation of methanol is not promoted by $Na_2CO_3$ exclusively, but rather by a synergistic liaison between $Na_2CO_3$ and transition metal impurities. Although the nature of this relationship was not determined, it is most probable that the transition metal component in these systems enables methanol dehydrogenation to proceed at such low temperatures. Even though stainless steel represents a likely source of trace metal impurities, this reactor had also been employed in earlier work involving the transition metal complexes [Ir(PNP)(COE)][$BF_4$] (see Chapter 5) and [$RhCl(PPh_3)_3$] and contamination with these metal complexes can therefore not be excluded. Indeed, ICP-MS analyses of one of the product mixtures gave a

positive test for rhodium contamination. Hence, to determine what effects these complexes have on the one-pot conversion of MeP to MMA, two separate reactions were conducted in which catalytic amounts of these complexes were purposefully added to the reagent mixtures. Heating MeP and $Cs_2CO_3$ together in a Hastelloy™ autoclave at 130 °C in the presence of [Ir(PNP)(COE)][$BF_4$] resulted in an increased production of MMA, even though a large portion thereof had undergone subsequent hydrogenation to M$^i$Bu. In contrast to earlier samples, the final product mixture also contained additional, heavier condensation products (Figure 6.6).

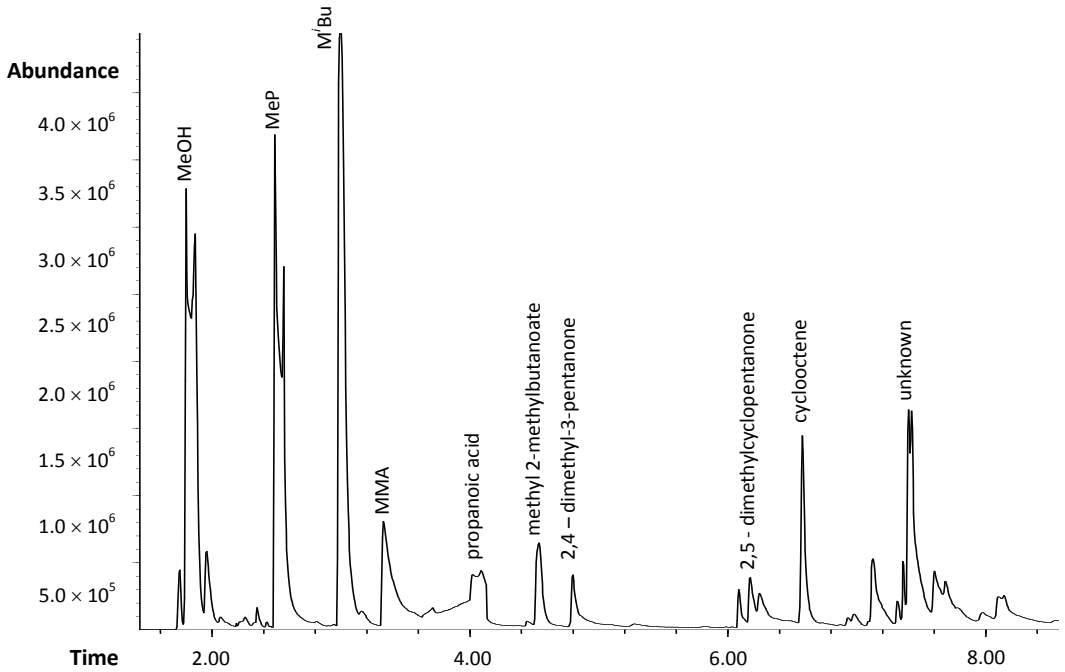


**Figure 6.6** GC-MS chromatogram for the reaction of MeP, with $Cs_2CO_3$ and MeOH in the presence of [Ir(PNP)(COE)][$BF_4$] at 130 °C for 21 h.

While fewer by-products were observed in the analogous reaction with [$RhCl(PPh_3)_3$], a significant amount of benzene was generated during this reaction by a mechanism not yet fully understood (Figure 6.7). Furthermore, MeP conversion was less productive for this reaction with the overall MMA and M$^i$Bu yields somewhat lower than those obtained for the iridium catalysed reaction. Despite the low yields and poor chemoselectivity of these reactions, it was very encouraging that the addition of transition metal additives could bring about such a significant increase in reactivity. Furthermore, having now gained a better understanding of the catalytic system through this collection of fundamental experiments, we turned our attention to finding a suitable transition metal catalyst capable of promoting the one-pot conversion of MeP to MMA both efficiently and chemoselectively *via* a more rational approach.

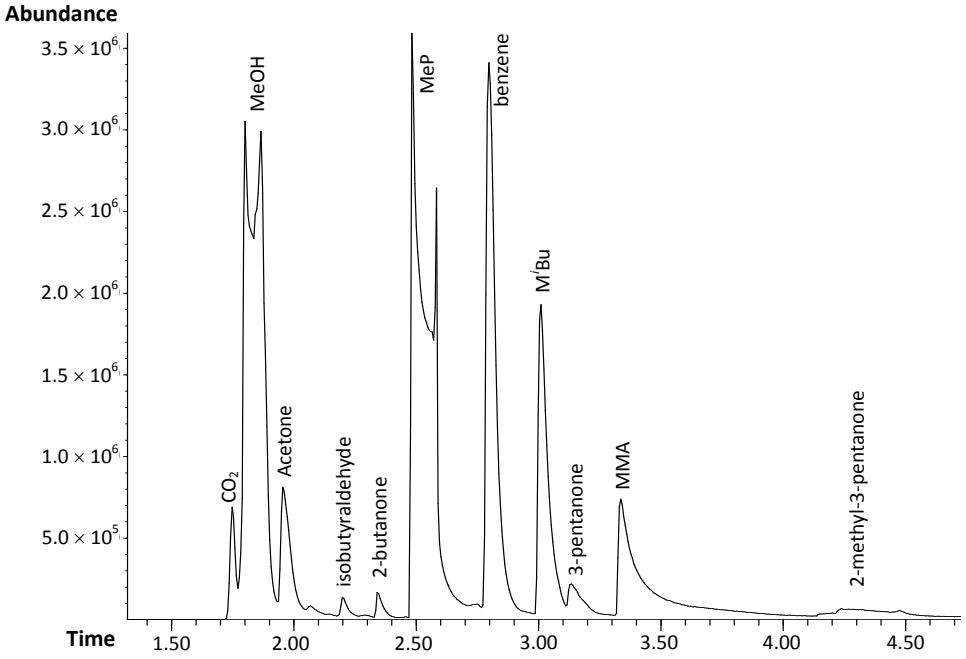


**Figure 6.7** GC-MS chromatogram for the reaction of MeP, with $Cs_2CO_3$ and MeOH in the presence of $[RhCl(PPh_3)_3]$ at 130 °C for 21 h.

### *6.2.2 Methanol dehydrogenation to formaldehyde in the presence of transition metal catalysts for the one-pot conversion of MeP to MMA.*

Cole-Hamilton and co-workers[19-21] have demonstrated that the catalytic production of hydrogen, together with aldehydes, can be achieved by the dehydrogenation of a range of alcoholic substrates using group 8 metal catalysts in the presence of added base. $[RhCl(PPh_3)_3]$, $[RhH(P^iPr_3)_3]$, $[Rh(bipy)_2]Cl$ (bipy = bipyridine), $[RuH_2(N_2)(PPh_3)_3]$, $[RuH_2(CO)(PPh_3)_3]$ and $[RuH_2(PPh_3)_4]$ were all shown to be active as catalysts for such dehydrogenation reactions, with $[RuH_2(N_2)(PPh_3)_3]$ proving particularly efficient. These metals, however, have a high affinity for CO and decarbonylation of the generated aldehydes therefore often proceeds to form inactive carbonyl complexes which poison these reactions over time.[20] Although $[RuH_2(N_2)(PPh_3)_3]$ also partakes in such decarbonylation reactions, the formed $[RuH_2(CO)(PPh_3)_3]$ and ultimately $[Ru(CO)_3(PPh_3)_2]$ are fortunately both active as alcohol dehydrogenation catalysts and hence do not inhibit the catalysis.[21] In fact, Cox and Cole-Hamilton[21] have shown $[RuH_2(CO)(PPh_3)_3]$ to be a viable catalyst for the catalytic production of hydrogen as fuel from the aqueous ethanol present in surplus wine supplies and waste streams. Scheme 6.7 depicts the mechanism of dehydrogenation proposed for such reactions. In the initial stages of the reaction an ethoxide

ion is generated by the deprotonation of ethanol in the presence of added NaOH. This species is then thought to enter the cycle by displacing $PPh_3$ from $[RuH_2CO(PPh_3)_3]$ (**V**) to form the anionic ethoxy intermediate **VI**. $\beta$-Hydrogen abstraction, followed by loss of acetaldehyde generates the anionic trihydrido carbonyl complex **VII** which can abstract a proton from a fresh molecule of ethanol to form molecular hydrogen by reductive elimination. The molecular hydrogen produced initially remains associated with metal complex **VIII**, but is then liberated in the final step to regenerate catalyst **V**.

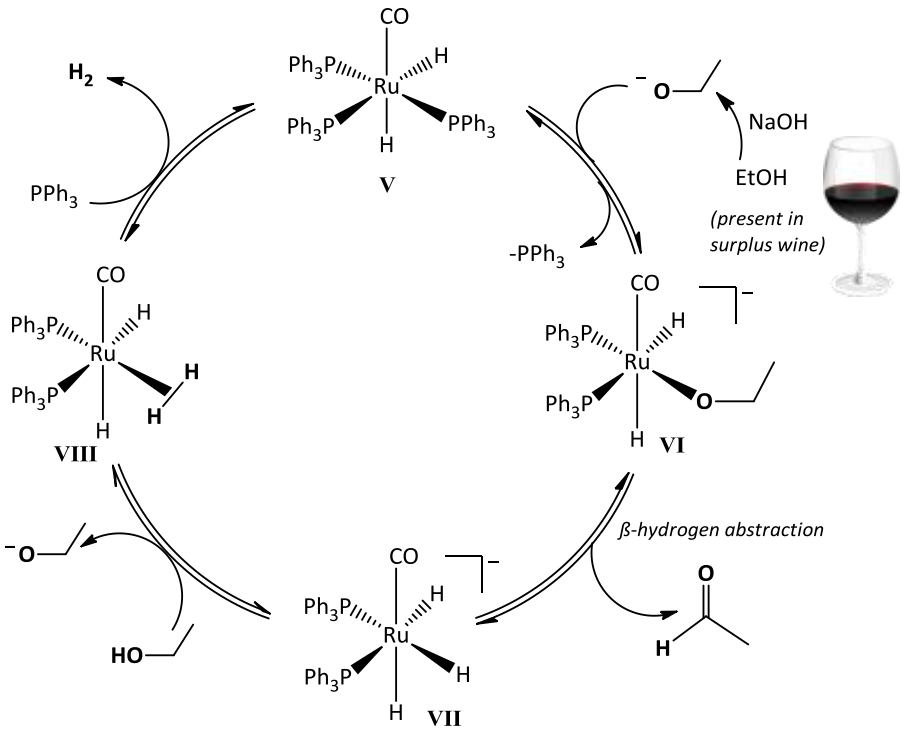


**Scheme 6.7** The production of dihydrogen by the dehydrogenation of the ethanol present in surplus wine in the presence of $[RhCO(H)_2(PPh_3)_3]$.[20,21]

Encouraged by these reports, $[RuH_2(CO)(PPh_3)_3]$ was also considered as a suitable dehydrogenation catalyst in our efforts aimed at the one-pot $\alpha$-methylenation of MeP with methanol. Scheme 6.8 depicts a plausible catalytic cycle for the conversion of MeP to MMA based on the cycle proposed for ethanol dehydrogenation. In the MMA cycle, however, the role of the added base is two-fold, participating in the deprotonation of both methanol and MeP. Furthermore, in this cycle methanol is dehydrogenated to anhydrous formaldehyde, with the liberation of hydrogen, in much the same way as was noted for ethanol. The generated

formaldehyde, however, is then consumed in a further condensation reaction with α-deprotonated MeP generated *in situ.* This gives rise to methyl 3-hydroxy-2-methylpropanoate as initial product, which undergoes spontaneously water elimination under the employed reaction conditions to afford MMA as final product. As mentioned previously, for this approach to succeed, the catalyst would need to be chemoselective for the dehydrogenation of methanol to formaldehyde and should not promote the hydrogenation of alkenes (to produce M$^{i}$Bu) or esters (to produce propanol).

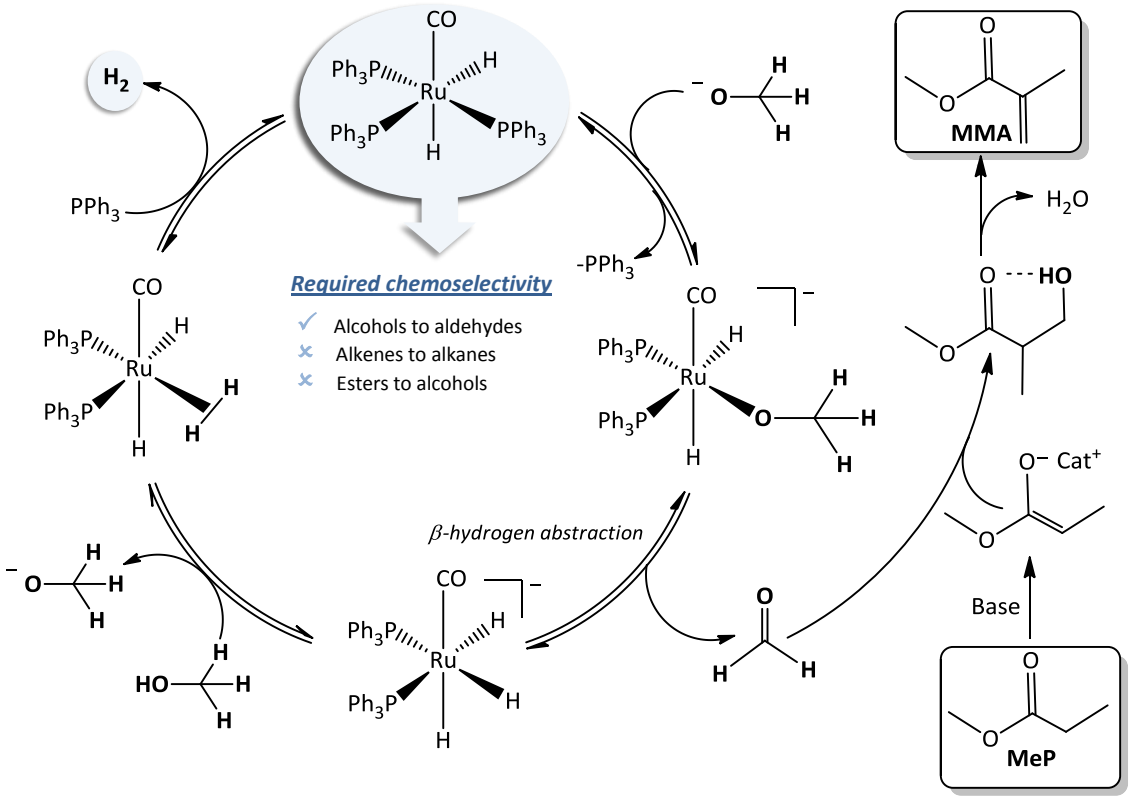


**Scheme 6.8** A proposed cycle for the ruthenium catalysed dehydrogenation of MeOH to formaldehyde and subsequent "one-pot" condensation with deprotonated MeP and dehydration to generate MMA. Also, the requirements for a chemoseletive successful catalyst is highlighted.

In order to minimise the formation of water and resultant ester bond hydrolysis, NaOMe was employed as base in all preliminary experiments performed. Using this one-pot approach MMA was produced, albeit in low yield, upon heating a solution of MeP, methanol, NaOMe and 0.13 mol% of $[RuH_2(CO)(PPh_3)_3]$ in toluene at 130 °C for 15 h. Under these conditions, however, the formed MMA largely underwent hydrogenation to afford M$^{i}$Bu (Figure 6.8) as product. Based on GC-FID data, the combined MMA + M$^{i}$Bu yield could be estimated as 9 %, of

which MMA represents 0.8 % and M$^{i}$Bu 8.2 %. As was observed before for the reaction of MeP with MeOH in the presence of $Cs_2CO_3$ and [$RhCl(PPh_3)_3$], benzene was generated as one of the by-products during this reaction.

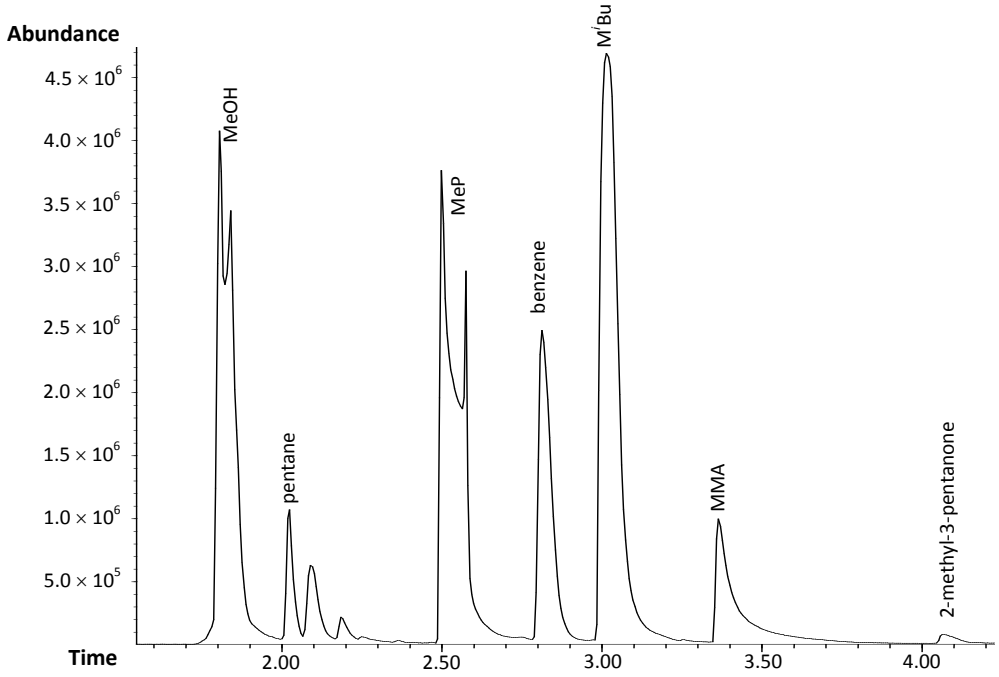


**Figure 6.8** GC-MS chromatogram of the product mixture obtained for the reaction: MeP, MeOH, NaOMe, toluene, [$RuH_2(CO)(PPh_3)_3$], 130 $^{o}$C, 15 h (entry 1, Table 6.1).

With a similar reaction, involving longer reaction times (63 h) at a lower temperature (100 $^{o}$C), greater selectivity towards MMA was observed (Figure 6.9), however this came at the expense of conversion with an estimated total conversion of only 5.8 % obtained (MMA 2.4 % + M$^{i}$Bu 3.4 %). Although the observed yields may seem insignificant at first glance, they are significant for preliminary experiments when viewed in the context of the low MMA yields (27 %) obtained per single pass in the second phase of the Lucite Alpha process. Furthermore, despite the occurrence of MMA hydrogenation under these conditions, the dramatic variations in production obtained by changes in the nature of the metal catalyst suggests that, in the presence of the appropriate catalytic system, this reaction may provide a viable route to atom efficient, low cost production of MMA.

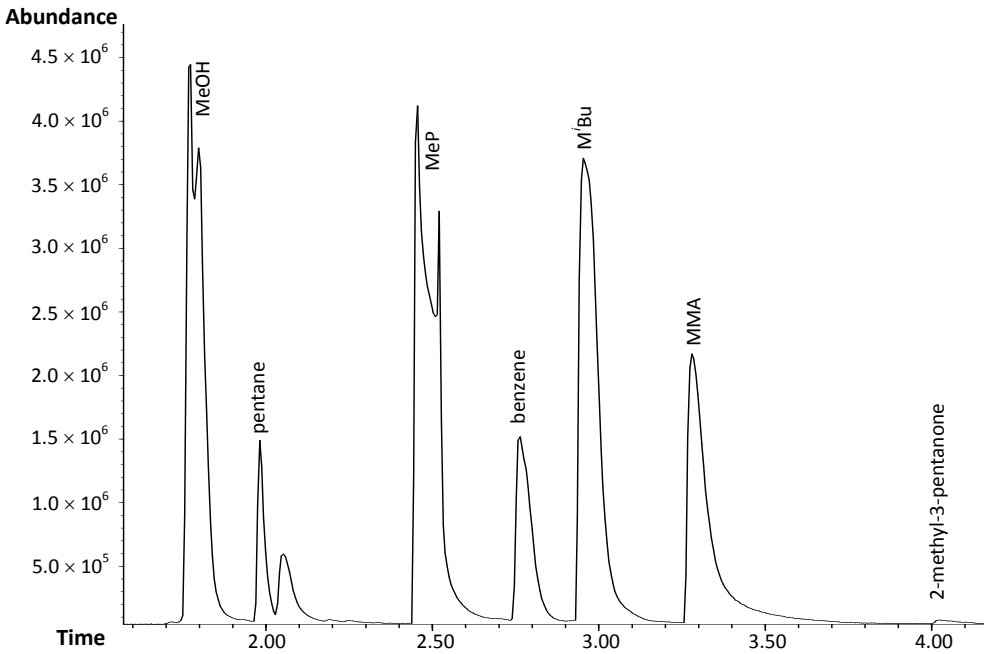


**Figure 6.9** GC-MS chromatogram of the product mixture obtained for the reaction: MeP, MeOH, NaOMe, toluene, $[RuH_2(CO)(PPh_3)_3]$, 100 °C, 63 h (entry 2, Table 6.1).

In an attempt to exclude the liberated $H_2$ from the reaction mixture and thereby minimising MMA hydrogenation, a similar reaction was performed in an open Schlenk system under reflux conditions while an inert dinitrogen atmosphere was maintained. For this experiment, a mixture of MeP, MeOH, NaOMe and $[RuH_2(CO)(PPh_3)_3]$ in toluene was heated under reflux for 8 h. No reaction, however, occurred under these conditions, most probably owing to the low reflux temperatures maintained in the presence of large volumes of methanol. Similarly, a repeat of this reaction with xylene as solvent still did not afford the desired condensation product. A summary of the described reactions is given in Table 6.1.

**Table 6.1** The conversion of MeP to MMA in the presence of different base and solvent systems.*

| No. | NaOMe (mmol) | MeOH (mmol) | MeP (mmol) | Solvent | Temp (°C) | Time (h) | Total conversion (%) | MMA (%) | M$^i$Bu (%) |
|---|---|---|---|---|---|---|---|---|---|
| 1 | 26.3 | 123.6 | 103.9 | toluene | 130 | 15 | 9 | 0.8 | 8.2 |
| 2 | 26.3 | 123.6 | 103.9 | toluene | 100 | 63 | 5.8 | 2.4 | 3.4 |
| 3 | 26.3 | 123.6 | 103.9 | toluene | reflux | 8 | 0 | 0 | 0 |
| 4 | 26.3 | 123.6 | 103.9 | xylene | reflux | 8 | 0 | 0 | 0 |

*Catalyst employed:$[RuH_2CO(PPh_3)_3]$ (0.12 g, 0.13 mmol, 0.13 mol %). Solvent (10 ml)

Based on the principle of microscopic reversibility, any complex that is active for the hydrogenation of aldehydes should, in theory, also be active for the dehydrogenation of alcohols. It would therefore be logical to consider metal complexes known to catalyse the hydrogenation of aldehydes chemoselectively in the presence of other reducible functionalities. Although several catalytic systems for the selective hydrogenation of ketones and aldehydes have been described in the literature,[22-25] diphosphine diamine ruthenium complexes of the general form shown in Figure 6.10 have been amongst the most successful catalysts known for such transformations.[26-29] Moreover, these catalysts have been shown to catalyse the chemo- and stereoselective hydrogenation of a range of ketones and aldehydes even in the presence of alkene or ester functionalities (Figure 6.10).[26,29] Based on the latter, these catalyst should, in theory, also perform well as alcohol dehydrogenation catalysts in the presence of these functionalities in the one-pot conversion of MeP to MMA .

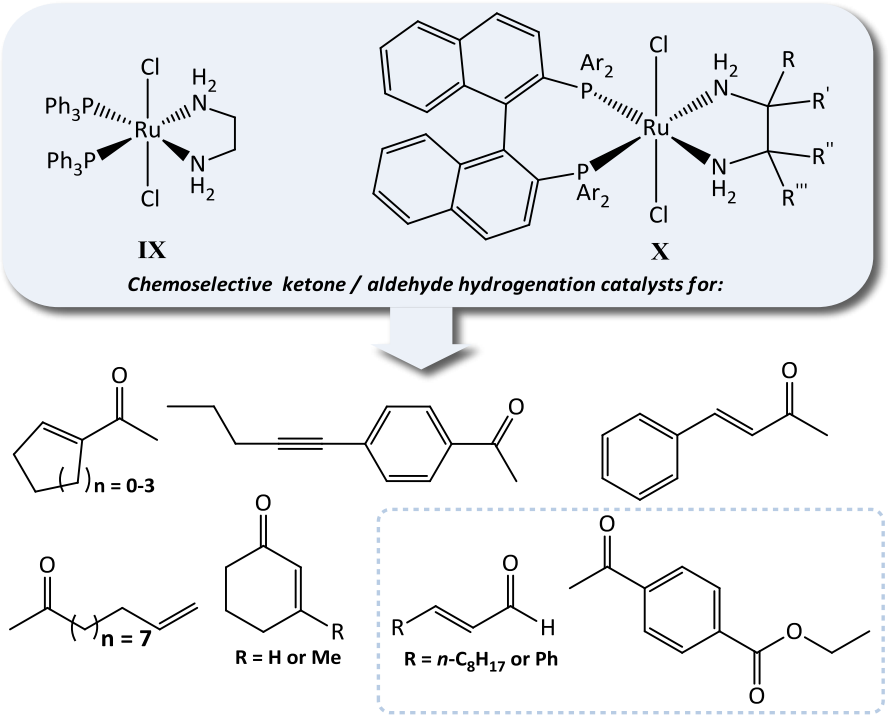


**Figure 6.10** Examples of diphosphine diamine ruthenium catalysts for the chemoselective hydrogenation of ketones and aldehydes in the presence of other reducible functionalities.[26,29]

In practice, however, all preliminary attempts to employ $[RuCl_2(NH_2CH_2CH_2NH_2)(PPh_3)_2]$ as catalyst in the $\alpha$-methylenation of MeP with methanol did not have the desired outcome.

Heating a solution of MeP, methanol and $Cs_2CO_3$ in toluene at 130 °C for 18 h in the presence of $[RuCl_2(NH_2CH_2CH_2NH_2)(PPh_3)_2]$ only brought about very insignificant conversions with the estimated MMA yield amounting to only 2 %. In addition, hydrogenation of the MMA, albeit minor, was still observed with the final mixtures containing approximately 0.3 % of M$^i$Bu. Furthermore, performing this reaction at a lower temperature (100 °C) for a longer period of time (48 h) resulted in almost no conversion with only trace amounts of MMA and M$^i$Bu detected in the final mixtures. Although the cause of this overall low productivity is not known, it is possible that slow or inefficient consumption of the generated formaldehyde by the condensation step results in the participation of this reagent in decarbonylation side reactions to generate inactive ruthenium carbonyl complexes, which ultimately poison the catalysis.

### *6.2.2 Future considerations for the one-pot production of MMA.*

Although a suitable catalyst for the one-pot conversion of MeP to MMA has not yet been identified during this preliminary study, the obtained results serve as a proof of concept that under the right conditions such transformation could indeed be possible. In addition to continuing the search for an efficient chemoselective dehydrogenation catalyst with a low affinity for CO, the use of additives such as water scavengers and sacrificial hydrogen acceptors are also worth investigating in future. As was mentioned in the introductory section the sacrificial hydrogen acceptor crotononitrile, has been found to successfully prevent alkene hydrogenation during the catalytic conversion of malonic halfesters to unsaturated esters (Scheme 6.3).[14] Similar approaches can be followed in future attempts to limit the hydrogenation of MMA to M$^i$Bu.

## 6.3 Conclusions

This study has shown that anhydrous formaldehyde can be produced *in situ* by the dehydrogenation of methanol in the presence of carbonate salts and trace transition metal cations. Furthermore, in the presence of MeP and a base, the generated formaldehyde participates in the one-pot condensation with MeP to furnish minor amounts of MMA, following dehydration of the initially generated methyl 3-hydroxy-2-methylpropanoate

intermediate. Owing to the presence of liberated $H_2$, hydrogenation of MMA to M$^i$Bu represents a major side-reaction during these reactions. In addition, the presence of transition metal impurities was found to enhance the rate of methanol dehydrogenation and consequently MMA production. The production of M$^i$Bu in these reactions is of considerable interest since it represents an unusual dehydrogenation-deprotonation-condensation-dehydration-hydrogenation cascade sequence.

Employing transition metal complexes such as [Ir(COE)(PNP)][$BF_4$], [RhCl($PPh_3$)$_3$] or [$RuH_2$(CO)($PPh_3$)$_3$], as methanol dehydrogenation catalyst in the one-pot conversion of MeP to MMA, resulted in increased productivity when compared to the carbonate salt systems. This increase in productivity was, however, accompanied by an increase in the hydrogenation of MMA. Although none of the tested catalyst displayed satisfactory activity or selectivity to make them viable catalysts for the large scale production of MMA, [$RuH_2$(CO)($PPh_3$)$_3$] gave the best overall conversion with an estimated MMA + M$^i$Bu yield of 9 %.

The diphosphine diamine ruthenium complex, [$RuCl_2$($NH_2CH_2CH_2NH_2$)($PPh_3$)$_2$], in principle appeared to be a suitable catalyst for these transformations, since it is reported to have low activity for alkene hydrogenations, but is very active for carbonyl hydrogenations.. However, in practice this catalyst only brought about very insignificant conversions of MeP to MMA with a total MMA + M$^i$Bu yield of only 2.3 % observed. Although an efficient catalytic system could not be identified during the course of this preliminary study, this account has served as a proof of concept for future studies.

## 6.4 Experimental

### *6.4.1 General materials, methods and instruments*

Reactions were carried out under dinitrogen gas ($N_2$, passed through a column of dichromate adsorbed on silica) using standard Schlenk, vacuum-line and cannula techniques or in a glovebox where necessary. [Ru(CO)$(H)_2$($PPh_3$)$_3$], triphenylphosphine, 1,2-diaminoethane, sodium metal and methanol-$d_4$ were all purchased from Aldrich and used as received. $Cs_2CO_3$ was purchased from Alfa Aesar, phosphorus pentoxide from Fluka and xylene, $Na_2CO_3$ and

NaOH from Fischer Scientific. Methyl propionate (supplied by Lucite International) was pretreated with $Na_2CO_3$, dried over $P_2O_5$, degassed by three freeze-pump-thaw cycles and finally collected by trap-to-trap distillation prior to use. Sodium methoxide was prepared by reacting sodium metal with dry, degassed methanol under an inert atmosphere. $[RhCl(PPh_3)_3]$ was prepared from $[RhCl_3{\cdot}3H_2O]$ and $PPh_3$, while $[RuCl_2(PPh_3)_4]$ and $[RuCl_2(PPh_3)_3]$ were prepared from $[RuCl_3{\cdot}3H_2O]$ and $PPh_3$, using standard literature procedures.[30;31] $[RhCl_3{\cdot}3H_2O]$ was purchased from either Engelhard or Alfa Aesar and $[RuCl_3{\cdot}3H_2O]$ from Strem Chemicals. $[Ir(PNP)(COE)][BF_4]$ was prepared according to a known literature procedure.[32]

Toluene was dried using a Braun Solvent Purification System and degassed by additional freeze-pump-thaw cycles when deemed necessary. Methanol was distilled under nitrogen from magnesium.

NMR spectra were recorded on a Bruker Avance 300 FT or Bruker Avance II 400 MHz spectrometer ($^1H$ NMR at 300/400 MHz, $^{13}C\{^1H\}$ NMR at 75/100 MHz and $^{31}P\{^1H\}$ NMR at 121/162 MHz) with chemical shifts δ reported relative to tetramethylsilane (TMS)($^1H$, $^{13}C\{^1H\}$) or 85 % $H_3PO_4$ ($^{31}P\{^1H\}$) as external reference. $^1H$ and $^{13}C\{^1H\}$ NMR spectra were referenced internally to deuterated solvent resonances which were referenced relative to TMS.

GC-MS chromatograms were recorded on a Hewlett Packard 6890 series GC system equipped with an Agilent J&W HP-1 general purpose column (fused silica capillary) and an HP 5973 Mass selective detector for both qualitative and quantitative analysis. Both quantitative analysis by a flame ionisation detector (GC-FID) and qualitative analysis by mass selective detector (GC-MS) were performed. A Hewlett-Packard Chemstation allowed for the computerised integration of peak areas. Method: flow rate 1 ml $min^{-1}$ (He carrier gas), split ratio 100 : 1, starting temperature 50 °C (4 min) ramp rate 20 °C $min^{-1}$ to 130 °C (2 min), ramp rate 20 °C $min^{-1}$ to 220 °C (15.5 min).

### *6.4.2 Synthetic procedures*

***General procedure for the conversion of MeP to MMA in the presence of MeOH (hydrolysis product) and $Na_2CO_3$ or $Cs_2CO_3$***

An autoclave (stainless steel or Hastelloy™), charged with methyl propanoate (9.15g, 103.85 mmol, 10 ml) and $Na_2CO_3$ (2.78 g, 26.27 mmol) or $Cs_2CO_3$ (8.56 g, 26.27 mmol) under aerobic

conditions, was sealed and heated to 130 °C for 21 h with stirring. The autoclave was subsequently cooled to room temperature, vented to the atmosphere and opened to reveal a white solid phase, consisting of a mixture of $Cs_2CO_3$ and cesium propanoate (CsP), and a light yellow liquid phase. The liquid phase was filtered and analysed qualitatively by GC-MS and quantitatively by GC-FID techniques together with $^1$H NMR.

### *Deuterium labelling experiment for the conversion of MeP to labelled MMA and M$^i$Bu in the presence of $^{13}$C-labelled methanol and $Cs_2CO_3$*

An autoclave (Hastelloy$^{TM}$) was charged with $Cs_2CO_3$ (8.56 g, 26.27 mmol) and pressure tested with $H_2$ gas. The autoclave was then vented and purged by three vacuum / $N_2$ cycles. Methyl propanoate (9.15g, 103.85 mmol, 10 ml) and $^{13}$C-labelled methanol (3 ml) were added to the autoclave under a flow of $N_2$. The autoclave was sealed and heated to 130 °C for 21 h with stirring. After this period of time, the autoclave was cooled to room temperature, vented to the atmosphere and opened. The liquid phase was separated from the solid phase, consisting of a mixture of $Cs_2CO_3$ and sodium propanoate (NaP), by filtration over a plug of celite and analysed by GC-MS.

### *Conversion of MeP to MMA and M$^i$Bu in the presence of MeOH (hydrolysis product), $Cs_2CO_3$ and [Ir(PNP)(COE)][$BF_4$]*

An autoclave (Hastelloy$^{TM}$) was charged with $Cs_2CO_3$ (8.56 g, 26.27 mmol) and [Ir(PNP)(COE)][$BF_4$] (0.20 g, 0.25 mmol) under an inert atmosphere. The autoclave was then sealed and pressure tested with dihydrogen gas. The autoclave was subsequently vented and purged with three vacuum / $N_2$ cycles. Methyl propanoate (9.15g, 103.85 mmol, 10 ml) was added to the autoclave under a flow of nitrogen *via* the injection port. The sealed autoclave was then heated to 130 °C for 21 h with stirring and subsequently cooled to room temperature, vented to the atmosphere and opened to reveal a brown solid phase, consisting largely of $Cs_2CO_3$ and CsP, and a yellow liquid phase. The liquid phase was filtered and analysed qualitatively by GC-MS and quantitatively by GC-FID techniques.

### *Conversion of MeP to MMA and M$^i$Bu in the presence of MeOH (hydrolysis product), [RhCl($PPh_3$)$_3$] and $Cs_2CO_3$*

The reaction was performed using the same method as was described for the reaction with [Ir(PNP)(COE)][$BF_4$]. However, [Ir(PNP)(COE)][$BF_4$] was replaced in the procedure by

$[RhCl(PPh_3)_3]$ (0.23 g, 0.25 mmol). A brown solid phase (mixture of $Cs_2CO_3$ and CsP) and brown liquid phase was obtained upon work-up. The liquid phase was filtered and analysed qualitatively by GC-MS and quantitatively by GC-FID techniques.

### *Conversion of MeP to MMA and M$^i$Bu in the presence of added MeOH, [RuCO(H)$_2$(PPh$_3$)$_3$] and NaOMe*

*This procedure was based on a combination of literature approaches*.[19-21] $[RuCO(H)_2(PPh_3)_3]$ was added to an autoclave (stainless steel or Hastelloy$^{TM}$) under an inert atmosphere. The autoclave was then sealed and pressure tested with dihydrogen. The autoclave was then vented and purged by three vacuum / $N_2$ cycles. Methyl propanoate (9.15g, 103.85 mmol, 10 ml), toluene (10 ml) and a solution of NaOMe (1.42 g, 26.27 mmol) in methanol (3.96 g, 123. 56 mmol, 5 ml) were added to the autoclave *via* the injection port. The autoclave was resealed and heated to 130 $^oC$ for 15 h with stirring. After this period, the autoclave was cooled to room temperature, vented to the atmosphere and opened to reveal a brown liquid phase together with a brown solid phase. The two phases were separated by filtration and the filtrate analysed by means of NMR spectroscopy and GC-MS, GC-FID chromatography to reveal the presence of MMA and M$^i$Bu. In addition, the solid phase was analysed by NMR spectroscopy and found to comprise of NaP. For NaP: $^1$H NMR (300 MHz, $CD_3OD$): $\delta_H$ = 1.10 (t, 3H, $^3J_{H\text{-}H}$ = 7.8 Hz; -C$H_3$), 2.17 (q, 2H, $^3J_{H\text{-}H}$ = 7.8 Hz; -C$H_2$-). $^{13}C\{^1H\}$ NMR (75 MHz, $CD_3OD$): $\delta_C$ = 11.5 (s, *C*$H_3$), 32.1 (s, -*C*$H_2$-), 148.0 (s, *C*=O).

### *Conversion of MeP to MMA and M$^i$Bu in the presence of added MeOH, [RuCO(H)$_2$(PPh$_3$)$_3$] and NaOMe at lower temperatures*

The procedure for this reaction is the same as was described for the reaction above, however, the reaction temperature was lowered to a 100 $^oC$ and the reaction time increased to 63 h. The final product mixture once again comprised of a brown solid phase (analysing as NaP) and a brown liquid phase. GC-MS and GC-FID analysis of the liquid phase indicated reduced hydrogenation of the formed MMA to M$^i$Bu.

### *Reaction of MeP , MeOH, [RuCO(H)$_2$(PPh$_3$)$_3$] and NaOMe under reflux conditions*

$[RuCO(H)_2(PPh_3)_3]$, methyl propanoate (9.15g, 103.85 mmol, 10 ml), toluene (10 ml) or xylene (10ml) and a solution of NaOMe (1.42 g, 26.27 mmol) in methanol (3.96 g, 123. 56 mmol, 5 ml) were added under inert conditions to a Schlenk flask fitted with a condenser and magnetic

stirrer bar. The mixture was subsequently heated under reflux conditions for 8 h in the dark (the outside of the flask was covered with aluminium foil to exclude light). After this period, the mixture was cooled to room temperature and subsequently analysed by means of GC-MS. However, from the analytical results it was evident that no appreciable reaction had occurred under these conditions.

### *Reactions of MeP , MeOH, $[RuCl_2(PPh_3)_2(NH_2CH_2CH_2NH_2)]$ and $Cs_2CO_3$*

**Method 1** *This procedure was adapted and customized from known literature procedures.*[28,29] Cesium carbonate (8.56 g, 26.3 mmol) was added to a Hastelloy™ autoclave. The autoclave was sealed and pressure tested with dihydrogen gas. After venting, the autoclave was purged by three vacuum / $N_2$ cycles. Ethylenediamine (0.40g, 6.55 mol, 0.44 ml) was dissolved in dry, degassed toluene (50 ml) in a Schlenk flask under inert conditions. Of this solution, 1ml (0.13 mmol ethylenediamine) was transferred to a separate flask containing dry degassed toluene (9 ml) under an inert atmosphere. This solution was further degassed by three additional freeze-pump-thaw cycles and then added to a separate Schlenk flask containing $[RuCl_2(PPh_3)_3]$ (0.13 g, 0.13 mmol). This mixture was allowed to stir for 30 min, during which time the brown mixture turned yellow. In another flask, dry degassed methanol (5ml) and MeP (5.49 g, 62.3 mmol, 6.0 ml) were added together and degassed by means of 3 freeze-pump-thaw cycles. This substrate solution, together with the catalyst solution, was subsequently transferred, under a stream of nitrogen, to the autoclave *via* the injection port. The sealed autoclave was then heated to 130 $^oC$ for 18 h with stirring. After this time, the mixture was cooled to room temperature and vented to the atmosphere. The obtained yellow product mixture was filtered and analysed by GC-MS.

**Method 2** Cesium carbonate (8.56 g, 26.3 mmol) was added to a Hastelloy™ autoclave. The autoclave was sealed and pressure tested with dihydrogen gas. After venting, the autoclave was purged by three vacuum / $N_2$ cycles. Ethylenediamine (0.40g, 6.55 mol, 0.44 ml) was dissolved in dry, degassed toluene (50 ml) in a Schlenk flask under inert conditions. Of this solution, 1ml (0.13 mmol ethylenediamine) was added to a separate Schlenk flask containing $[RuCl_2(PPh_3)_3]$ (0.13 g, 0.13 mmol). This mixture was allowed to stir for 30 min, during which time the brown mixture turned yellow. In another flask, dry degassed methanol (0.93ml) and MeP (9.15 g, 103.9 mmol, 10 ml) were added together and degassed by means of 3 freeze-pump-thaw cycles. This solution, together with the catalyst solution, was subsequently transferred, under a stream of nitrogen, to the autoclave *via* the injection port. The sealed

autoclave was then heated to 100 °C for 48 h with stirring. After this time, the mixture was cooled to room temperature and vented to the atmosphere. The obtained yellow product mixture was filtered and analysed by GC-MS.

## 6.5 Notes and References


(1) Su, S.; Zaza, P.; Renken, A. *Chem. Eng. Technol.* **1994**, *17*, 34-40.
(2) Harris, B. *Ingenia* **2010**, *issue 45*, 19-23.
(3) Su, S.; Prairie, M. R.; Renken, A. *Appl. Catal. A: Gen.* **1992**, *91*, 131-142.
(4) Su, S.; Prairie, M. R.; Renken, A. *Appl. Catal. A: Gen.* **1993**, *95*, 131-142.
(5) Field, L. D.; Li, H. L.; Messerle, B. A.; Smernik, R. J.; Turner, P. *Dalton Trans.* **2004**, 1418-1423.
(6) Zhang, J.; Gandelman, M.; Shimon, L. J. W.; Rozenberg, H.; Milstein, D. *Organometallics* **2004**, *23*, 4026-4033.
(7) Gnanaprakasam, B.; Zhang, J.; Milstein, D. *Angew. Chem. Int. Ed.* **2010**, *49*, 1468-1471.
(8) Owston, N. A.; Parker, A. J.; Williams, J. M. J. *Chem. Commun.* **2008**, 624-625.
(9) Dobereiner, G. E.; Crabtree, R. H. *Chem. Rev.* **2010**, *110*, 681-703.
(10) Grigg, R.; Mitchell, T. R. B.; Sutthivaiyakit, S.; Tongpenyai, N. *Tetrahedron Lett.* **1981**, *22*, 4107-4110.
(11) Black, P. J.; Cami-Kobeci, G.; Edwards, M. G.; Slatford, P. A.; Whittlesey, M. K.; Williams, J. M. J. *Org. Biomol. Chem.* **2006**, *4*, 116-125.
(12) Cami-Kobeci, G.; Williams, J. M. J. *Chem. Commun.* **2004**, 1072-1073.
(13) Edwards, M. G.; Jazzar, R. F. R.; Paine, B. M.; Shermer, D. J.; Whittlesey, M. K.; Williams, J. M. J.; Edney, D. D. *Chem. Commun.* **2004**, 90-91.
(14) Hall, M. I.; Pridmore, S. J.; Williams, J. M. J. *Adv. Synt. Catal.* **2008**, *350*, 1975-1978.
(15) Ledger, A. E. W.; Slatford, P. A.; Lowe, J. P.; Mahon, M. F.; Whittlesey, M. K.; Williams, J. M. J. *Dalton Trans.* **2009**, 716-722.
(16) Slatford, P. A.; Whittlesey, M. K.; Williams, J. M. J. *Tetrahedron Lett.* **2006**, *47*, 6787-6789.
(17) Edwards, M. G.; Williams, J. M. J. *Angew. Chem. Int. Ed.* **2002**, *41*, 4740-4743.
(18) Grigg, R.; Lofberg, C.; Whitney, S.; Sridharan, V.; Keep, A.; Derrick, A. *Tetrahedron* **2009**, *65*, 849-854.
(19) Morton, D.; Cole-Hamilton, D. J. *J. Chem. Soc., Chem. Commun.* **1988**, 1154-1156.
(20) Morton, D.; Cole-Hamilton, D. J. *J. Chem. Soc., Dalton Trans.* **1989**, 489-495.
(21) Cox, R. L.; Cole-Hamilton, D. J. *Unpublished results* **1988**.
(22) Joó, F.; Kovács, J.; Bényei, A. C.; Kathó, Á. *Catal. Today* **1998**, *42*, 441-448.
(23) Noyori, R.; Ohkuma, T. *Angew. Chem. Int. Ed.* **2001**, *40*, 40-73.
(24) Grosselin, J. M.; Mercier, C.; Allmang, G.; Grass, F. *Organometallics* **1990**, *10*, 2126-2133.
(25) Jiménez, S.; López, J. A.; Ciriano, M. A.; Tejel, C.; Martínez, A.; Sánchez-Delgado, R. A. *Organometallics* **2009**, *28*, 3193-3202.
(26) Ohkuma, T.; Koizumi, M.; Muñiz, K.; Hilt, G.; Kabuto, C.; Noyori, R. *J. Am. Chem. Soc.* **2002**, *124*, 6508-6509

(27) Sandoval, C. A.; Ohkuma, T.; Muñiz, K.; Noyori, R. *J. Am. Chem. Soc.* **2003**, *125*, 13490-13503.
(28) Ohkuma, T.; Koizumi, M.; Doucet, H.; Pham, T.; Kozawa, M.; Murata, K.; Katayama, E.; Yokozawa, T.; Ikariya, T.; Noyori, R. *J. Am. Chem. Soc.* **1998**, *120*, 13529-13530.
(29) Ohkuma, T.; Ooka, H.; Ikariya, T.; Noyori, R. *J. Am. Chem. Soc.* **1995**, *117*, 10417-10418.
(30) Osborn, J. A.; Jardine, F. H.; Young, J. F.; Wilkinson, G. *Inorg. Phys. Theor. (J. Chem. Soc. A)* **1966**, 1711-1732.
(31) Stephenson, T. A.; Wilkinson, G. *J. Inorg. Nucl. Chem.* **1966**, *28*, 945-956.
(32) Ben-Ari, E.; Cohen, R.; Gandelman, M.; Shimon, L. J. W.; Martin, J. M. L.; Milstein, D. *Organometallics* **2006**, *25*, 3190-3210.

# Chapter 7

# Simple base catalysed condensation of formaldehyde with propanoate derivatives

– The kinetics of deprotonation and the ideal source of formaldehyde –

*The capacity of a series of simple inorganic and organic bases to catalyse the condensation of methyl propanoate (MeP) with formaldehyde was investigated. In addition, deuterium labelling studies were performed to determine to what extent each base effect deprotonation in the α-position of MeP. Using sodium propanoate as model base, the kinetics of deprotonation were also explored. These studies collectively suggested deprotonation to occur readily for a whole range of bases, but that the generated carbanion possessed low reactivity towards formaldehyde. For this reason, attempts to increase the electrophilicity of formaldehyde in these reactions were made by the addition of secondary amine / carboxylic mixtures to facilitate formaldehyde activation through Mannich-type condensation reactions.*

## 7.1 Introduction

The production of methyl methacrylate (MMA) from a variety of substrates has been studied extensively over the past few decades.[1] However, despite the development and commercialisation of numerous processes, the most widely practised commercial route towards the synthesis of MMA still remains the original acetone cyanohydrin (ACH) process. As was mentioned in Chapter 1, this process suffers from several drawbacks such as the generation of large amounts of ammonium bisulfate waste, the necessity to make use of highly toxic hydrogen cyanide and the limited availability of large quantities of HCN.[1] The need for a more efficient and environmentally benign approach to the large scale production of MMA thus remains. Although virtually no waste is generated during the two stage Lucite Alpha Process, the base catalysed condensation of methyl propanoate (MeP) and formaldehyde in the second stage proceeds with such low efficiency that a maximum conversion of only 27 % is achieved per single pass. For this reason, multiple passes along with substrate recycling are required for the large scale production of MMA.

Mamoru Ai, has made several valuable contributions towards the development of more efficient catalytic routes to the vapour-phase condensation of formaldehyde with propanoate derivatives.[2-5] In one of these elegant studies, Ai demonstrated that by combining dioxopyrophosphatovanadium(IV) [$V_2O_2(P_2O_7)$] with silica gel in the presence of a small amount of phosphoric acid [$H_3PO_4$], a catalyst capable of promoting the vapour-phase aldol condensation of propanoic acid with formaldehyde to yield methacrylic acid (MAA) can be obtained. Likewise, this system was also shown to catalyse the formation of MMA from methyl propanoate (MeP) under the same conditions. The presence of water vapour, however, greatly retards these reactions and for this reason, formalin (~55 % wt formaldehyde in water) does not represent a practical source of formaldehyde. As an alternative, the related anhydrous forms trioxane and methylal [$CH_2(OCH_3)_2$] can be employed. Ai have found the vapour-phase condensation of MeP with formaldehyde to deliver a mixture of MMA, MAA, propanoic acid and formaldehyde as products when methylal is used as formaldehyde source.[3] In addition, these reactions are generally performed in the presence of a high concentration of methanol to prevent the occurrence of ester bond hydrolysis.[5] Addition of oxygen to these systems leads to an increase in the production of MAA, owing to the enhanced oxidation of methanol (formed during methylal decomposition) to formaldehyde. In the absence of high

concentrations of methanol, hydrolysis of the ester bond present in MeP and MMA is more likely, leading to the formation of propanoic acid and MAA, respectively.[3] V-Si-P catalysts with an atomic ratio of 1 : 8 : 2.2 were shown to give the best overall yield.[6] Similarly, the performance of the related tin phosphate catalyst possessing a P/Sn atomic ratio of 2.3 was reported to be comparable to that of the most effective V-Si-P catalyst. In general the optimum phosphorus/metal ratio in metal phosphate catalysts appears to be around 2.3.[5,7]

Bases such as KOH, CsOH and $Rb_2CO_3$, supported on silica gel, are known to catalyse the condensation of MeP or propanoic acid with formaldehyde to yield MMA or MAA.[8,9] Of all alkali- and alkaline earth metal hydroxides, silica supported CsOH has been reported to display the greatest selectivity for MMA formation from MeP and formaldehyde with the optimum Si:Cs atomic ratio in the range of 20:1000 or 25 : 1000.[10,11] With silica supported CsOH catalyst doped with Ag and Zr cations (Ag-Zr-Cs/$SiO_2$), it is possible to obtain MMA directly from MeP and methanol in the presence of a small amount of oxygen without any source of formaldehyde according to the reaction summarised in Scheme 7.1. This catalytic system not only promotes aldol condensation but also facilitates the conversion of methanol to formaldehyde.

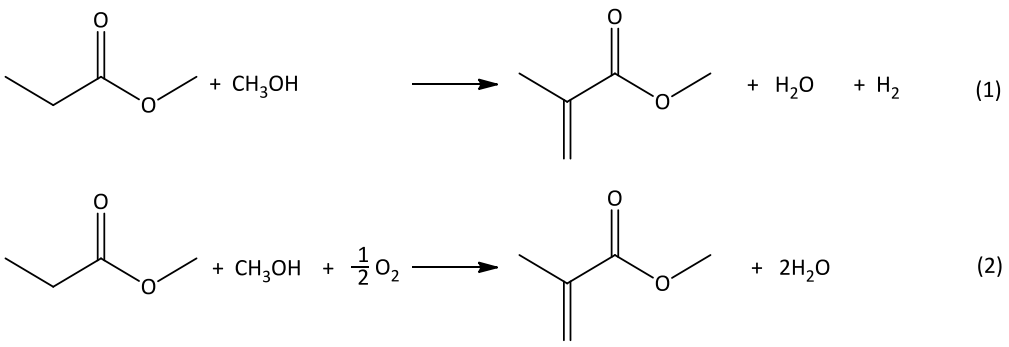


**Scheme 7.1** Reaction scheme for the preparation of MMA directly from MeP and methanol (1) with the involvement of oxygen (2).

In the early stages of Ag-Zr-Cs/$SiO_2$ catalysed condensation reactions between MeP and methanol, no MMA is obtained. Instead, the hydrogenated derivative methyl isobutyrate (M$^i$Bu) is produced almost exclusively together with minor amounts of carbon monoxide and hydrogen. However, as the reaction progresses the production of M$^i$Bu decreases sharply while the formation and of MMA increases. Furthermore, the selectivity of this reaction also increases with time. Ai proposed that this reaction commences with the initial

dehydrogenation of methanol to formaldehyde with liberation of hydrogen. Condensation of MeP with formaldehyde yields MMA which is hydrogenated directly after formation by free methanol to afford M$^{i}$Bu. This, in turn, generates more formaldehyde. Although both dehydrogenation reactions involving methanol are deactivated slowly with time-on-stream, deactivation of the latter occurs more rapidly and therefore results in a decreased production of M$^{i}$Bu over time. The activity of the condensation reaction between MeP and formaldehyde is very stable and hence MMA production rises sharply as the reaction progresses.[5]

Patented studies have disclosed the *α*-alkylated cyclic ester, *α*-methylene-*γ*-butyrolactone, to be accessible by the treatment of *γ*-butyrolactone with formaldehyde in the presence of a base (Scheme 7.2).[12] For this invention, paraformaldehyde, trioxane or (2-ethylhexyloxy)methanol represent suitable formaldehyde sources, while a variety of metal oxides, hydroxides, carbonates and phosphates may function as the catalytic base. These catalysts may either be unsupported or supported by a variety of suitable supports such as silica, titania, zirconia, alumina, carbon, zeolite derivatives or mixtures thereof. Potassium carbonate, cesium carbonate or potassium phosphate are the bases of choice for these reactions, and result in the best overall yield of the *α*-alkylated product.[12] Although this technology has only been applied to cyclic esters, it may be utilised in future to facilitate the preparation of MMA from MeP.

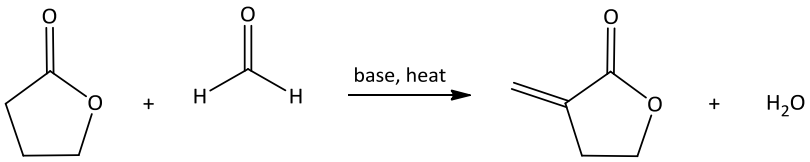


**Scheme 7.2** Preparation of *α*-methylene-γ-butyrolactone from γ-butyrolactone and formaldehyde.

The preparation of unsaturated aldehydes such as acrolein, methacrolein and ethacrolein *via* condensation reactions of aldehydes with formaldehyde has also been the subject of much discussion. Although paraformaldehyde and trioxane all represent acceptable sources of formaldehyde, the use of aqueous formalin is generally favoured. Furthermore, these reactions are frequently carried out in the presence of primary or secondary amines and a strong base catalyst such as sodium hydroxide. In these reactions, the amine reagent assists the transformation by participating in the activation of formaldehyde in a Mannich-type

condensation (Scheme 7.3).[13,14] Regeneration of the amine catalyst, however, becomes ineffective at higher temperatures (150 to 300 $^{o}$C) owing to the irreversible conversion thereof into the inactive tertiary amine analogue, $R_2NCH_3$. This represents a major disadvantage contributing to a significant decrease in the economics of such processes.[15] In a study directed towards the condensation of pentanal with formaldehyde, di-*n*-butylamine proved particularly suitable as the secondary amine reagent.[16,17]

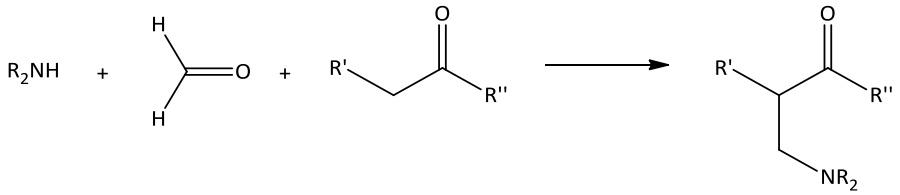


**Scheme 7.3** Ativation of formaldehyde by a secondary amine in a Mannich-type condensation.

The acid catalysed conversion of aldehydes into $\alpha$-methylenated derivatives can also be achieved by employing a mixture of a secondary amine and an organic carboxylic acid having up to five carbon atoms. Suitable organic acids include formic acid, acetic acid, isomers of butyric and valeric acid and propanoic acid, with the latter documented to be especially efficient. Once again, di-*n*-butylamine is regarded as the most effective secondary amine catalyst for these reactions.[13] In a recent study, acid base mixtures composed of either pyrrolidine and propanoic acid or the dipeptide L-proline-$\beta$-alanine (Figure 7.1), were shown to be a very mild, chemoselective and effective catalytic systems for the condensation of propanal with formaldehyde at room temperature. Even at short reaction times, these catalysts afford the functionalised products chemoselectively in yields as high as 99 %.[18]

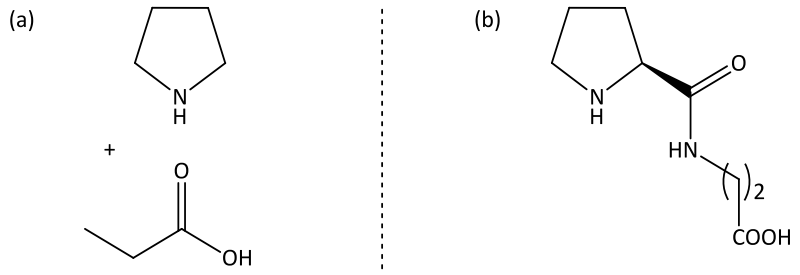


**Figure 7.1** Effective catalytic systems for the $\alpha$-methylenation of aldehydes: (a) pyrrolidine and propanoic acid; (b) L-proline-$\beta$-alanine

In this part of the study, the *α*-methylenation of MeP using formaldehyde was examined on a more fundamental level to gain a better understanding of the factors that limit the efficiency of this phase in the Alpha Process. Factors considered included the base to substrate ratio, the solvent system, the formaldehyde source and the reaction times and temperatures. With the use of deuterium labelling experiments, the extent to which a range of bases effect *α*-deprotonation of MeP as well as the kinetics of such deprotonations were explored. Furthermore, the possibility of generating of a more electrophilic formaldehyde source *in situ via* Mannich–type condensations between formaldehyde and secondary amines were considered.

## 7.2 Results and Discussion

The capacity of a range of soluble bases to catalyse the formylation of MeP was investigated and is discussed in section 7.2.1. In addition, deuterium labelling studies were carried out to determine to what extent deprotonation of the *α*-protons present in MeP proceeds for each base and are described in section 7.2.2. Finally, attempts to activate formaldehyde by Mannich-type condensation reactions were made and are described in section 7.2.3

### *7.2.1 Simple base catalysed condensation of formaldehyde with propionates*

A series of comparable reactions, all aimed at the base catalysed conversion of methyl propanoate to methyl methacrylate (MMA) were carried out. Within the series, the substrate to base ratios and reaction conditions were kept fairly constant while the choice of base and solvent system was varied. All reactions were carried out in a stainless steel autoclave with constant stirring. Scheme 7.4, outlines the general approach to these reactions, which was based on methodologies patented by Brandenburg and co-workers.[12]

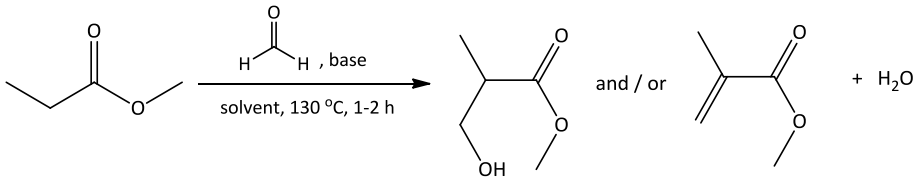


**Scheme 7.4** General approach for the based catalysed formylation of MeP to yield methyl 3-hydroxy-2-methylpropanoate and/or MMA.

The series of soluble bases considered during this investigation included $K_2CO_3$, 1,8-diazobicyclo[5.4.0]undec-7-ene (DBU), NaOH and $Cs_2CO_3$. In most of the performed reactions, paraformaldehyde was chosen as the formaldehyde source, owing to the anhydrous nature thereof. The ability of water not only to inhibit the reaction kinetics, but also to hydrolyse the MeP ester bond, makes the use of an anhydrous source of formaldehyde essential. On account of the water generated during the condensation reaction, a completely anhydrous environment could not be maintained during these reactions and a loss in both the ester feedstock and reaction kinetics was therefore inevitable.

Toluene, 2-ethylhexanol and methanol were considered as possible solvent systems in all preliminary experiments. The decision to include 2-ethylhexanol, was prompted by a literature report which suggested that (2-ethylhexyloxy)methanol, the hemiformal of 2-ethylhexanol, can be employed as an alternative source of formaldehyde.[12] According to the literature, this hemiformal can be prepared by the neat reaction of 2-ethylhexanol with paraformaldehyde at elevated temperatures.[19] In a trial experiment aimed at determining how readily this conversion proceeds, paraformaldehyde was reacted neat with 2-ethylhexanol (1:1 ratio) and heated at 80 $^{o}$C for 1 h (Scheme 7.5).

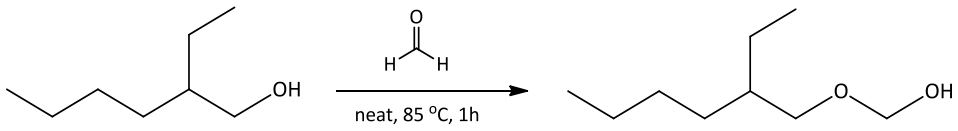


**Scheme 7.5** Preparation of (2-ethylhexyloxy)methanol by the neat reaction of 2-ethylhexanol with formaldehyde.

During the course of this period, the paraformaldehyde suspension dissolved to yield a homogeneous colourless solution. NMR spectroscopic analysis revealed this solution to contain a mixture of unreacted 2-ethylhexanol and (2-ethylhexyloxy)methanol. We aspired to exploit this reaction by using 2-ethylhexanol as solvent in condensation reactions involving paraformaldehyde. In these reactions, the 2-ethylhexanol would not only act as polar solvent but also participate in the *in situ* generation of (2-ethylhexyloxy)methanol. This hemiformal generated *in situ* may be more susceptible to thermal cracking than paraformaldehyde, and may therefore serve as a more effective formaldehyde source.

Table 7.1 summarises the reaction performed, the conditions employed and the quantities of MMA detected in the final product mixtures. In all initial attempts, $K_2CO_3$ was employed as base in condensation reactions between MeP and paraformaldehyde. A mixture of MeP (slight excess), paraformaldehyde and a catalytic amount of $K_2CO_3$ (4:1 ratio relative to MeP) was heated in toluene to 130 $^oC$ for 1 h. Upon cooling a biphasic product mixture consisting of a colourless liquid phase and a brown oily solid phase was obtained. Both phases were analysed by NMR spectroscopy for the presence of methyl 3-hydroxy-2-methyl-propanoate and / or the dehydration product, methylmethacrylate (MMA). Since MMA is known to polymerize readily to polymethyl methacrylate (PMMA) in the absence of a stabiliser, NMR spectra were also examined for traces of this compound. The $^1H$ NMR spectrum of the liquid phase only contained resonances corresponding to trace amounts (less than 1 %) of MMA. Furthermore, the water soluble solid phase did not contain MMA or any other alkylated derivatives of MeP. A repeat of this reaction with an increased amount of paraformaldehyde (1 : 1.5 ratio with respect to MeP) and 2-ethylhexanol as solvent resulted in no reaction. As before, the solid phase also tested negative for the presence of any desirable products.

**Table 7.1** The conversion of MeP to MMA in the presence of different base and solvent systems.

| No. | Base | Solvent | solvent (ml) | fomaldehyde source | formaldehyde (mmol) | MMA (%) |
|---|---|---|---|---|---|---|
| 1 | $K_2CO_3$ | toluene | 10.00 | paraformaldehyde | 9.7 | < 1 |
| 2 | $K_2CO_3$ | 2-ethylhexanol | 11.72 | paraformaldehyde | 15.0 | 0 |
| 3 | $K_2CO_3$ | 2-ethylhexanol | 4.69 | paraformaldehyde | 15.0 | 0 |
| 4 | DBU | toluene | 5.00 | paraformaldehyde | 15.0 | < 1 |
| 5 | DBU | 2-ethylhexanol | 4.69 | paraformaldehyde | 15.0 | < 1 |
| 6 | NaOH § | 2-ethylhexanol | 4.69 | paraformaldehyde | 15.0 | 0 |
| 7 | $Cs_2CO_3$ | 2-ethylhexanol | 4.69 | paraformaldehyde | 15.0 | < 1 |
| 8 | $Cs_2CO_3$ | methanol | 3.00 | paraformaldehyde | 15.0 | 0 |
| 9 | $Cs_2CO_3$ † | methanol | 2.00 | formalin (~37 % w/V) | 7.5 | 0 |
| 10 | $Cs_2CO_3$ | – | – | alcoform (~55 % w/w) | 15.0 | < 1 |
| 11 | $Cs_2CO_3$ ‡ | – | – | paraformaldehyde | 20.0 | < 1 |
| 12 | $Cs_2CO_3$ ¤ | – | – | alcoform (~55 % w/w) | 30.0 | ~ 5 |

*Reaction conditions: In an autoclave - MeP (10 mmol), base (2.53 mmol), 130 $^0C$, 1-2 h. § NaOH 3 mmol. † MeP (5 mmol) $Cs_2CO_3$ (6.27 mmol).‡ $Cs_2CO_3$ (2.67 mmol), ¤ $Cs_2CO_3$ (20.87 mmol), MeP (51.93 mmol), topanol A (0.17µl), 130 $^oC$, 6 h.

Given that none of the attempts with $K_2CO_3$ as base proved successful, we turned our attention to the strong non-nucleophilic organic base 1,8-diazobicyclo[5.4.0]undec-7-ene (DBU). Mixtures of MeP, paraformaldehyde and DBU in either toluene or 2-ethylhexanol as solvent, were heated to 130 $^oC$ for a 2 h period. In these reactions a MeP to base ratio of 4:1 was employed. In both cases, however, NMR spectroscopic analysis revealed the final mixtures to contain only trace amounts of MMA (less than 1 %).

Reacting MeP with paraformaldehyde (1 : 1.5 ratio) in the presence of 3 equivalents of NaOH and 2-ethylhexanol as solvent did not result in any significant MeP formylation and the final mixtures obtained were comparable to earlier experiments involving with DBU and $K_2CO_3$ as bases.

Finally, $Cs_2CO_3$ was explored as base in the catalysed condensation of MeP with paraformaldehyde. All reaction ratios and conditions used were identical to those previously described for reactions with $K_2CO_3$, DBU and NaOH. In the first of these attempts, 2-ethylhexanol was employed as solvent (in a 2 : 1 ratio with respect to paraformaldehyde). As with all other attempts, heating a mixture of MeP, paraformaldehyde and $Cs_2CO_3$ in 2-ethylhexanol resulted in a biphasic product mixture. Neither of these phases analysed to contain methyl 3-hydroxy-2-methyl-propanoate, MMA or PMMA. A small amount of MeP did, however, undergo transesterification with 2-ethylhexanol to yield 2-ethylhexyl propanoate.

The suitability of methanol as reaction solvent was assessed in all subsequent formylation experiments involving $Cs_2CO_3$ as base. Methanol was considered to be a suitable reaction solvent, since both MeP and $Cs_2CO_3$ are soluble in methanol. Furthermore, it has been suggested in the literature that the presence of an excess of methanol may, to some extent, suppress the hydrolysis of MMA and MeP caused by water liberation. Moreover, methanol may react with thermally cracked paraformaldehyde to form hemiformals of various chain lengths which may then serve as alternative, and possibly more accessible, sources of formaldehyde.

In contrast to the suggestion that methanol might inhibit the hydrolysis of MeP, heating a methanol solution of MeP, $Cs_2CO_3$ and paraformaldehyde together in our systems did lead to substantial ester bond hydrolysis, followed by the generation of large amounts of cesium propanoate (CsP). $^1H$ NMR and GS-MS did not provide evidence for the presence of any $\alpha$-

methylenated or formylated products. The $^{13}C\{^{1}H\}$ DEPT NMR spectrum did, however, reveal an array of new resonance signals in the region δ 60–80 ppm. Although these could not be assigned unambiguously, they are believed to correspond to hemiformals of various chain lengths that may have originated from the reaction of methanol with free formaldehyde.

The low MMA yields observed under these conditions were somewhat surprising, given that Brandenburg *et al.* reported *α*-methylene-γ-butyrolactone yields of up to 65 % for the $Cs_2CO_3$ catalysed condensation of formaldehyde and γ-butyrolactone under similar reaction conditions.[12] It was therefore a logical next step to repeat a selection of the earlier experiments using γ-butyrolactone as substrate, to validate the effectiveness of our catalytic system. Using paraformaldehyde as formaldehyde source, γ-butyrolactone was heated together with varied amounts of $Cs_2CO_3$ either neat or in the presence of 2-ethylhexanol or methanol (Scheme 7.6 and Table 7.2).

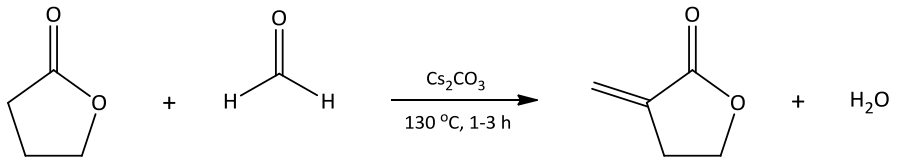


**Scheme 7.6** Preparation of *α*-methylene-γ-butyrolactone from γ-butyrolactone and formaldehyde.

**Table 7.2** The conversion of MeP to MMA in the presence of different base and solvent systems.*

| No. | 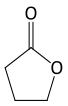 (mmol) | $Cs_2CO_3$ (mmol) | Solvent used | solvent (ml) | formaldehyde (mmol) | Time (h) | 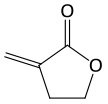 (%) |
|---|---|---|---|---|---|---|---|
| 1 | 10 | 2.67 | neat | – | 20.0 | 1.5 | 15 |
| 2 | 10 | 2.53 | 2-ethylhexanol | 4.69 | 15.0 | 2 | 30 |
| 3 | 2.5 | 7.96 | 2-ethylhexanol | 3.20 | 3.40 | 3 | 0 |
| 4 | 10 | 2.53 | methanol | 3.00 | 15.0 | 2 | < 1[§] |

*Reaction conditions: In a stainless steel autoclave at 130 $^{0}$C. § Also contains the ring opening product that underwent transesterification with methanol.

Interestingly, when a base : substrate : formaldehyde ratio of 1 : 4 : 6 was employed in the presence of 2-ethylhexanol as solvent, *α*-methylene-*γ*-butyrolactone was obtained in 30 %

yield (entry 2, Table 7.2). In contrast, the same reaction conditions with MeP as substrate only led to the formation of less than 1 % of MMA (entry 7, Table 7.1), suggesting that these seemingly similar substrates possess vastly different reactivities. Although the nature of this difference in behaviour is not fully understood, it is possible that the thermodynamic stability of the deprotonated intermediates differ for these compounds. For instance, both MeP and *γ*-butyrolactone can be deprotonated at the C atom *α* to the carbonyl group. This gives a carbon centred nucleophile, in which the negative charge can be delocalised into the carbonyl group to form an enolate. In the case of *γ* -butyrolactone, this enolate places a double bond into the ring inducing some ring strain as the angles required by the $sp^2$ hybridised carbons differ from the optimum ring angles. This disfavours the enolate form somewhat relative to that obtained from MeP so that the concentration of nucleophile is reduced for *γ*-butyrolactone. However, in the event of its formation, this disfavoured enolisation places more electron density on the carbon atom making it a better nucleophile and hence more able to react with formaldehyde (Scheme 7.7).

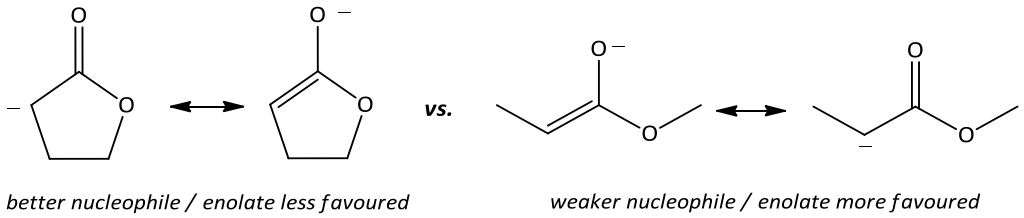


**Scheme 7.6** Stabilisation of *α*-deprotonated MeP and *γ*-butyrolactone through their enolate forms.

It may also be that several other factors contribute to the overall low productivity of the MeP systems. For instance, it could be that the rate of reprotonation in the MeP systems is much faster than nucleophilic attack on formaldehyde, resulting in limited product formation. Alternatively, limited formaldehyde availability and/or reactivity may also lead to restricted product formation. For example, it may be possible that a stronger electrophile is needed to drive these reactions. However, limitations relating to the formaldehyde source seem less likely to represent the bottleneck in these reactions, given that the same source of formaldehyde was employed in *α*-methylenation reactions of both MeP and γ-butyrolactone.

### 7.2.2 Deuterium labelling studies

To investigate the efficiency of a number of bases, three sets of deuterium labelling experiments were conducted with the single aim of determining to what degree $\alpha$-proton abstraction takes place under different reaction conditions. All reactions were performed in a manner similar to those previously described, but with omission of the formaldehyde source.

#### 7.2.2.1 Set 1: Reactions with $Cs_2CO_3$ as base, but different solvent systems

In the first set, the choice of base was kept constant whilst the solvent system and deuterating agent were varied. Cesium carbonate was chosen as the invariable base and Scheme 7.8 depicts the general approach followed for reactions contained within this set. To commence the study, MeP was reacted with $Cs_2CO_3$ in the presence of toluene as solvent and deuterium oxide as deuterating agent at 130 $^oC$ for 2 h. Not surprisingly, hydrolysis of the ester bond largely took place under these conditions to afford cesium propanoate (CsP) and methanol almost exclusively.

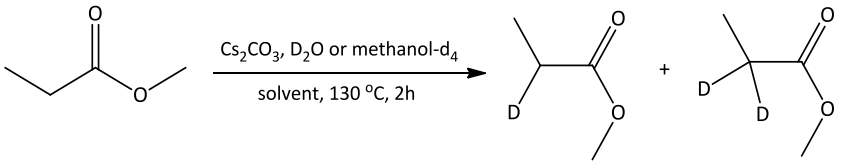


**Scheme 7.8** The general reaction procedure for the first set of deuterium labelling experiments, where "solvent" refers to either one of toluene, 2-ethylhexanol or methanol-$d_4$.

Similar results were also obtained when 2-ethylhexanol was employed as reaction solvent. In this case, however, deuterium labelling was observed for the generated CsP, with the methylene resonances of the non-, mono- and di-deuterated CsP species detected in the $^{13}C\{^1H\}$ DEPT NMR spectrum at δ 30.7 (singlet), δ 30.4 (triplet) and δ 29.3 (quintet), respectively, (Figure 7.2). Furthermore, the $CH_3$ group of the non-deuterated CsP gave rise to a singlet at δ 10.3, while the analogous resonances for the mono and di-deuterated CsP appeared at values $\beta$-shifted with respect to this singlet (δ 10.2 and δ 10.1). From the relative intensities of these resonances the ratio of $CH_3O_2CCH_2CH_3$ : $CH_3O_2CCHDCH_3$ : $CH_3O_2CCD_2CH_3$ could be estimated as 66 % : 28 % : 6 %.

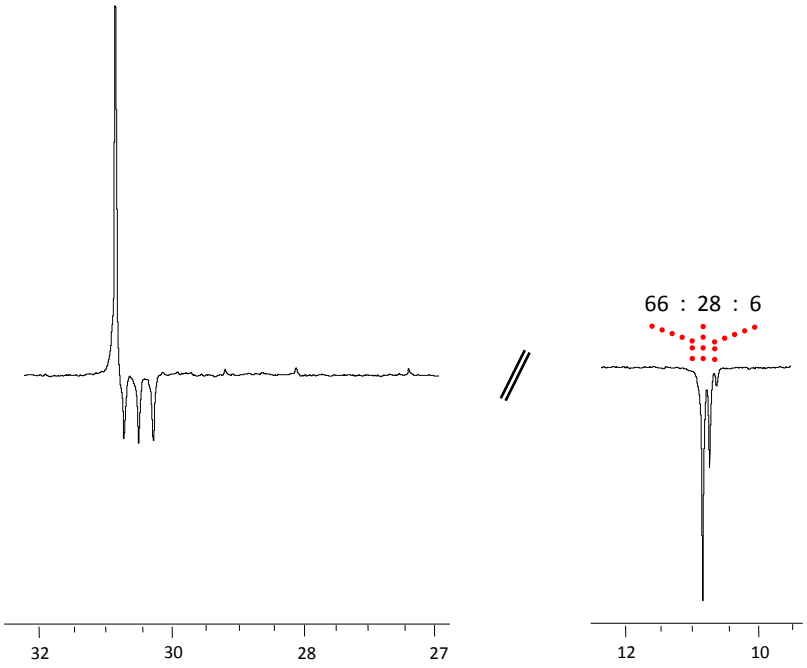


**Figure 7.2** Methylene and methyl resonances of CsP and deuterated derivatives thereof in the $^{13}C\{^{1}H\}$ DEPT NMR. The relative ratio of the non- to mono- to di-deuterated CsP (in %) is given above the methyl resonances.

When methanol-$d_4$ was employed as both reaction solvent and deuterating agent, a significant amount of ester bond hydrolysis was still observed despite numerous reports in the literature suggesting that this should be suppressed in the presence of excess methanol.[5] Recorded $^{1}H$ and $^{13}C\{^{1}H\}$ NMR data revealed the presence of both MeP and CsP. Since the carbanion generated by $\alpha$-deprotonation can be stabilised much better through delocalisation in MeP than in CsP, the MeP $\alpha$-protons can be expected to have somewhat lower $pK_a$ values than those of CsP. It is therefore not surprising that a greater extent of double deuteration is observed for MeP.

In the $^{13}C\{^{1}H\}$ DEPT NMR spectrum, methyl resonances attributable to MeP and its deuterated analogues appear at δ 9.6, δ 9.5 and δ 9.4, while the $–CH_2–$, –CHD– and $–CD_2–$ groups give rise to a doublet, triplet and quintet at δ 28.1, δ 27.9 and δ 27.6, respectively. Based on the relative intensities of the methyl signals, the three species $CH_3O_2CCH_2CH_3$, $CH_3O_2CCDHCH_3$ and $CH_3O_2CCD_2CH_3$ are present in a ratio of 8 % : 40 % : 52 %. Similarly, the methyl groups of the CsP derivatives $CsO_2CCH_2CH_3$, $CsO_2CCDHCH_3$ and $CsO_2CCD_2CH_3$ give rise to three singlets at δ 11.5, δ 11.4 and δ 11.3, with a relative intensity ratio of 36 % : 41 % : 23 %, while the methene resonances are detected in the region δ 30–δ 32 (Figure 7.3).

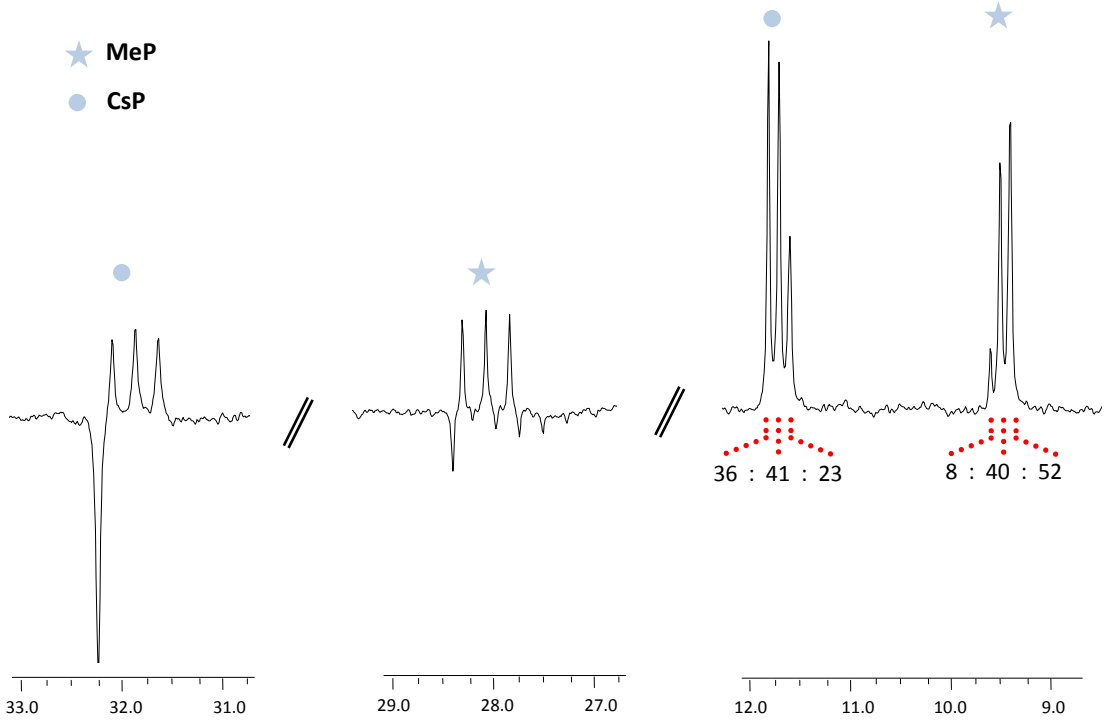


**Figure 7.3** Resonances detected in the $^{13}C\{^{1}H\}$ DEPT NMR spectrum corresponding to MeP, CsP and deuterated derivatives thereof with the relative ratio of the non- to mono- to di-deuterated CsP and MeP shown (in %) below the methyl resonances.

#### *7.2.2.2 Set 2: Reactions with different bases*

In the second set of labelling experiments, the extent to which a variety of bases affect $\alpha$-deprotonation in MeP under the same reaction conditions were explored. For these reactions the solvent system and deuterating agent were kept constant as methanol-$d_4$, while the choice of base was varied. Three parallel reaction mixtures each consisting of MeP, methanol-$d_4$ and one of the bases $K_2CO_3$, NaOH or $Cs_2CO_3$ were heated to 130 °C for a 2 h period. $^{13}C\{^{1}H\}$ DEPT NMR spectra collected for each of the final product mixtures were comparable in appearance, displaying resonances corresponding to non-, mono- and di- deuterated MeP. In all spectra the methyl group of non deuterated MeP gives rise to a singlet at δ 9.5, with related $\beta$-shifted singlets corresponding to the mono- and di-deuterated species detected at δ 9.4 and δ 9.3, respectively. Similarly, the corresponding methylene groups give rise to a singlet at δ 28.1 (–$CH_2$–), a triplet at δ 27.8 (–CDH–) and a quintet at δ 27.5 (–$CD_2$–). Although all spectra contained traces of $CH_3OH$ and $CD_3O_2CCH_3CH_2$ (formed *via* the transesterification of MeP with $CD_3OD$), no sodium, potassium or cesium propanoate derivatives were observed. Figure 7.4 depicts relevant regions in the $^{13}C\{^{1}H\}$ NMR spectra collected for these experiments.

From a comparison of the relative peak intensities of the methyl resonances, it is evident that $Cs_2CO_3$ is by far the most effective base for the $\alpha$-deprotonation of MeP, with a $CH_3O_2CCH_2CH_3$ : $CH_3O_2CCDHCH_3$ : $CH_3O_2CCD_2CH_3$ ratio of 10 %: 41 %: 49 %. $K_2CO_3$ proved to be the second most effective base with a corresponding ratio of 47 %: 42 %: 11 %, while NaOH was least effective, with 61 % of the MeP present in the non-deuterated form.

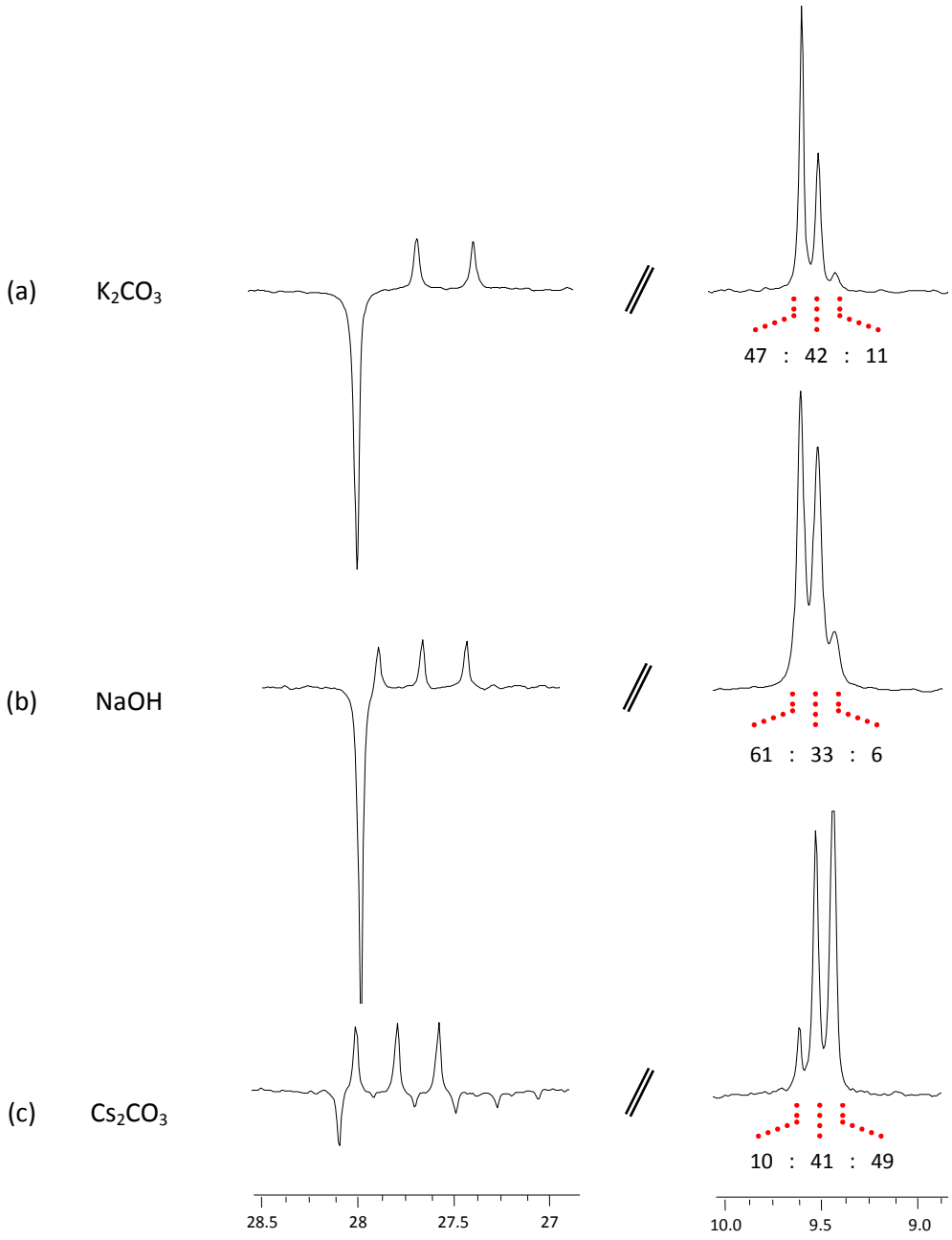


**Figure 7.4** Methylene and methyl resonances of MeP and deuterated derivatives thereof in the $^{13}C\{^1H\}$ DEPT NMR spectra of reactions with (a) $K_2CO_3$, (b) NaOH and (c) $Cs_2CO_3$ as base. The ratio of the non- to mono- to double deuterated MeP (in %) is given below each set of methyl signals.

For the sake of comparison, a deuterium labelling experiment using $Cs_2CO_3$ as base was also carried out for γ-butyrolactone. $^{13}C\{^1H\}$ DEPT NMR analysis of the final product mixture revealed a non- : mono- : di-deuterated γ-butyrolactone ratio of 8 % : 37 % : 55 % (Figure 7.5), which is comparable to that observed for MeP (Figure 7.4). Since the $\alpha$-protons in both of these substrates have $pK_a$ values in the order of 25,[20,21] the similar labelling patterns observed agree well with what can be expected. Furthermore, these observations are in support of the postulated hypothesis that the differences in reactivity of these substrates do not relate to the acidity of the $\alpha$-protons but rather to the nucleophilicity of the generated carbanions. For these intermediates, the carbanion is normally stabilised by resonance to form an enolate anion (Scheme 7.6), with more efficient stabilisation of this form resulting in weaker nucleophiles.

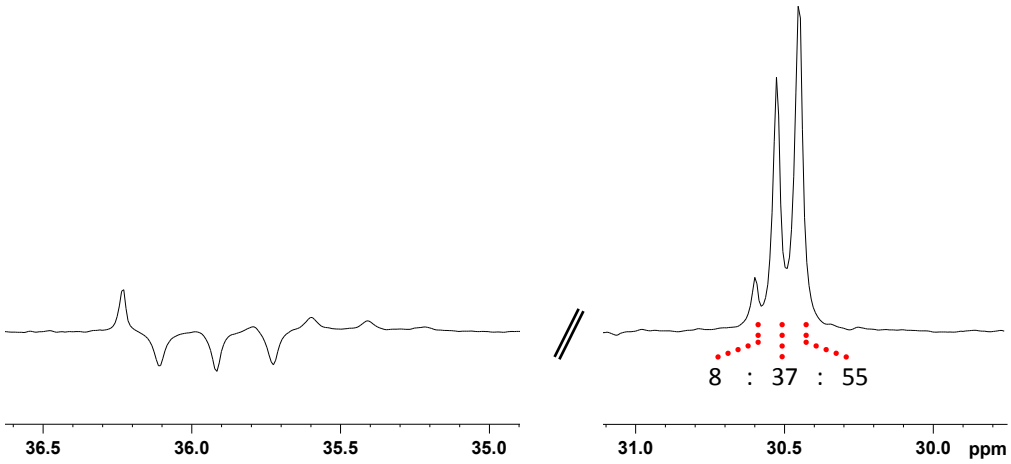


**Figure 7.5** $\alpha$- (left) and $\beta$-methylene (right) resonances of γ-butyrolactone and deuterated derivatives thereof in the $^{13}C\{^1H\}$ DEPT NMR spectrum. The ratio of non- to mono- to di-deuterated γ-butyrolactone is given below the $\beta$-methylene resonances (in %).

### *7.2.2.2 Set 2: The kinetics of deprotonation with sodium propanoate as base*

As mentioned before, the formation of significant amounts of cesium propanoate is often observed when $Cs_2CO_3$ is employed as base in condensation reactions between MeP and formaldehyde. For this reason, we were interested to determine whether such propanoate salts could perhaps be employed as alternatives to $Cs_2CO_3$ in these reactions. Furthermore, although earlier experiment have shown sufficient deprotonation to occur over a period of 1 h, we were interested in studying the kinetics of deprotonation to have a rough estimate of how fast equilibrium is reached. As before, deuterium incorporation in the $\alpha$-position of MeP was

used as a handle during these studies. Owing to availability, sodium propanoate was employed as the propanoate salt in our experiments. Using the set-up depicted in Figure 7.6, MeP was heated together with sodium propanoate to 220 °C in the presence of methanol-$d_4$ as deuterating agent in autoclave **2**. As the external temperature reading on the autoclave heater has been found to differ significantly from the temperature measured internally, the internal temperature was monitored using a temperature probe **1** that goes right down to the centre of the autoclaves for safety reasons. Using this reading, the internal temperature was manually maintained between 215 °C and 225 °C. Autoclave **2** was connected to a second empty autoclave **5** at room temperature. These autoclaves were sealed off from one another by taps **4**. The tap of autoclave **5** was kept open at all times, while the tap of **2** was only opened for brief intervals at the time of sampling. Samples of the reaction mixture were taken at time intervals 0 min (taken as the moment the internal temperature reached 220 °C), 5 min, 10 min and 60 min. To collect these datasets, the experiment had to be performed twice. During the first experiment a sample of the vapour phase was taken at time 0 min by opening tap **4** for a brief interval and allowing the inside pressure (65 bar) of autoclave **2** to drive a fraction of the MeP and methanol in the vapour phase across to autoclave **5** (at room temperature).

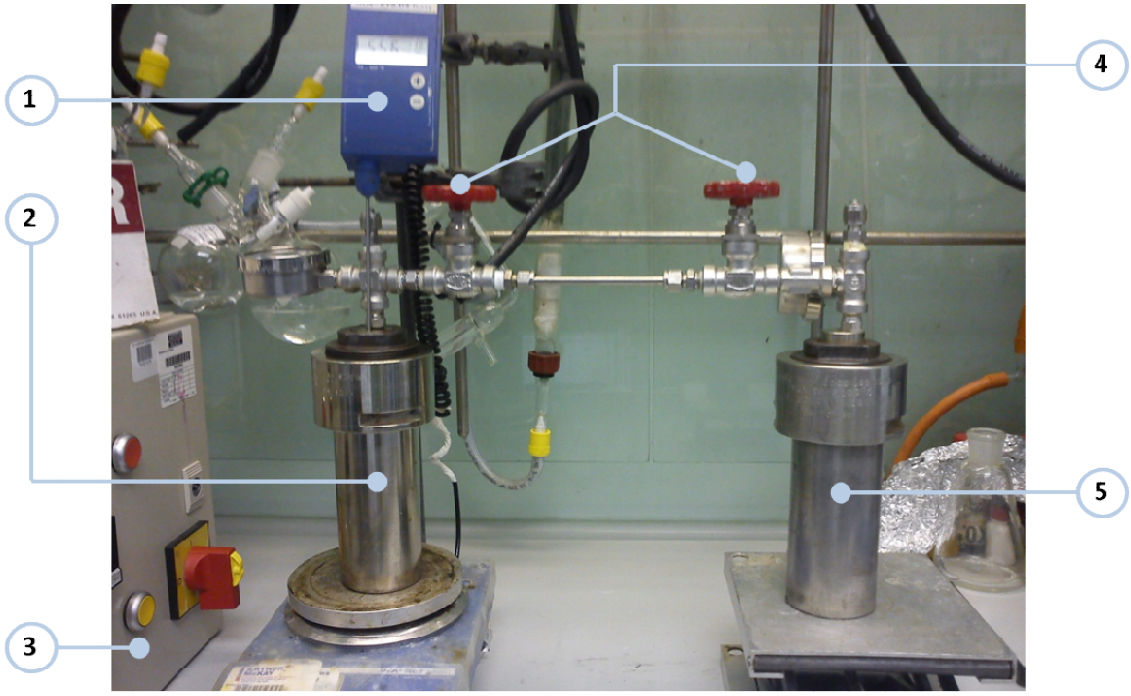


**Figure 7.6** Experimental setup for the time dependant deuterium labelling experiment with NaP as base. Components: (1) Internal temperature probe, (2) Autoclave containing reaction mixture (heating jacket and external temperature probe not shown), (3) Heater, (4) Valves to control sampling, (5) empty autoclave at room temperature for sample collection.

The reaction was then stopped after 10 min, cooled rapidly to room temperature by immersing the autoclave in cold water, and the final product mixture sampled. This reaction was repeated to collect samples at time intervals 5 min and 60 min, using the same method of sampling. It should be noted, however, that this means of sampling does not allow for very accurate measurements owing to temperature fluctuations and additional time delays caused by the initial heating and final cooling periods. These variations are not accounted for and the obtained data should therefore only be viewed as a very rough estimate of the kinetics of deprotonation.

Figure 7.7 depicts a comparison of the relevant regions in the $^{13}C\{^{1}H\}$ NMR DEPT spectra of samples collected at time (t) intervals 0, 5, 10 and 60 min. From the relative integral values measured for the methyl resonances (δ 9.0–9.5), it is evident that the initial ratio (t = 0 min) of non- : mono : di-deuterated MeP (19 % : 44 % : 37 %) increases during the first 5 min of the reaction to 14 % : 40 % : 46 %. After this period, however, the ratio remains relatively unchanged and it can therefore be concluded that the equilibrium position for this reaction had been reached within the first 5 min. Furthermore, based on the equilibrium ratio of non- : mono : di-deuterated MeP taken at t = 60 min (14 % : 40 % : 46 %), it is evident that both sodium propanoate and $Cs_2CO_3$, for which a non- : mono- : di-deuterated MeP ratio of 10 % : 42 % : 49 % was observed after 60 min, are capable of catalysing efficient deprotonation in the *α*-position of MeP. Based on these observations, it should be possible to employ propanoate salts in the base catalysed conversion of MeP to MMA as alternatives to $Cs_2CO_3$.

In addition to deuterated MeP, the final samples of the two experiments (t = 10 min and 60 min) also contained deuterium labelled sodium propanoate (NaP) as a result of self-deprotonation. The rate of this reaction is, however, significantly slower than the H/D exchange in MeP, with non- : mono- : di-deuterated NaP ratios of 50 % : 29 % : 21 % and 17 % : 40 % : 43 % recorded at times 10 min and 60 min, respectively. However, when a solution of NaP in methanol-$d_4$ is heated at 220 $^{o}$C for 60 min in the absence of MeP, a non- : mono- : di-deuterated NaP ratio of 5 % : 31 % : 64 % is observed for the final mixture. This then suggests that, in the absence of MeP, the equilibrium position for NaP deprotonation is shifted towards the right owing to the different H/D ratio. As a result a higher percentage of di-deuterated NaP is generated over a 60 min period.

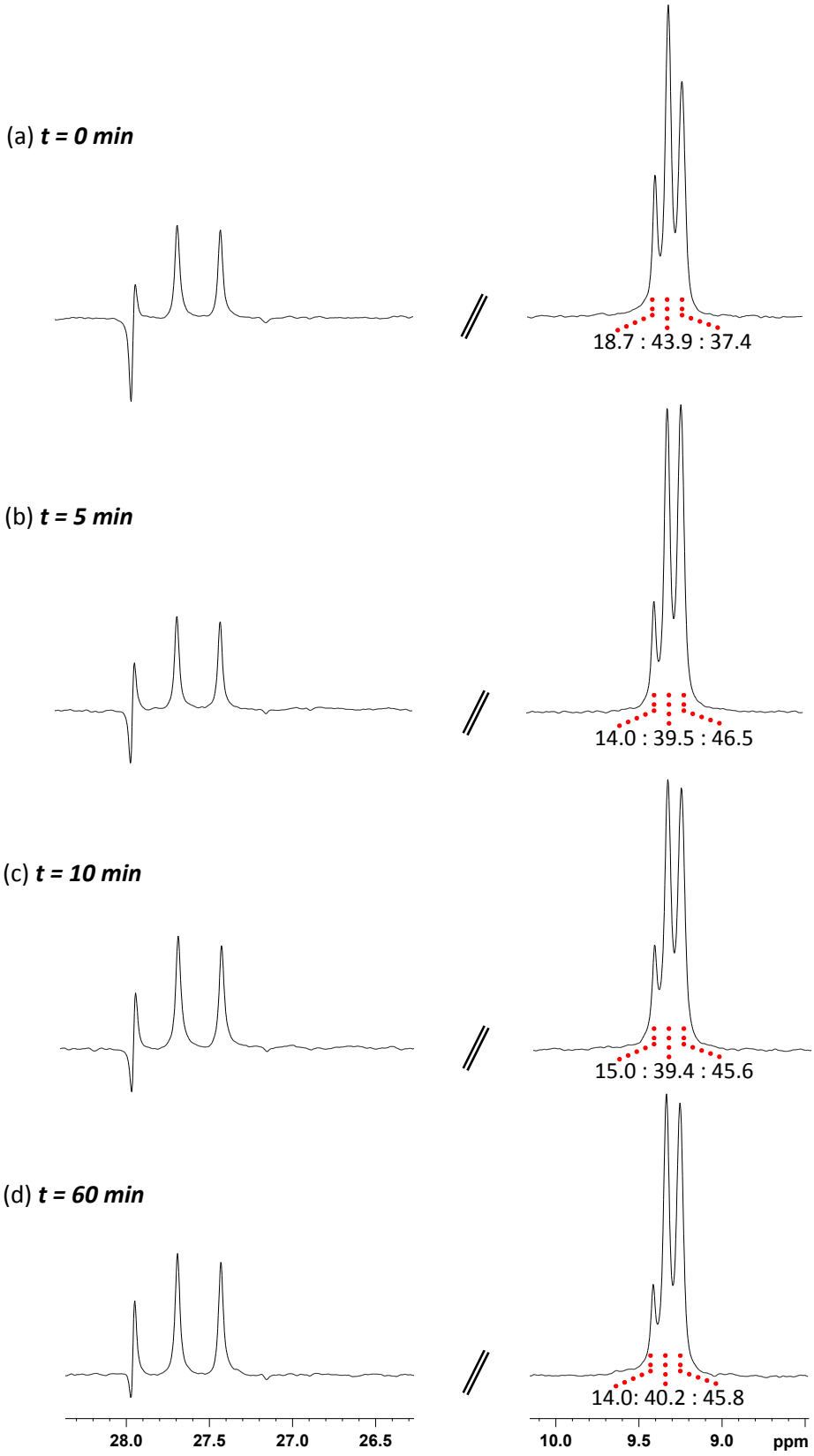


**Figure 7.7** $^{13}C\{^{1}H\}$ DEPT NMR spectra showing the extent of deuterium incorporation in MeP with NaP as base at time (a) 0 min, (b) 5 min, (c) 10 min and (d) 60 min. The ratio of the non- to mono- to double deuterated MeP (in %) is given below the methyl signals.

### 7.2.3 Activation of formaldehyde by Mannich-type condensations

From the range of deuterium labelling studies carried out, it would seem that the low conversion of MeP to MMA observed during base catalysed condensation reactions with formaldehyde does not result from insufficient deprotonation, but rather from the low reactivity of the generated nucleophile. Increasing the strength of the electrophile, i.e. formaldehyde, should, therefore, help in overcoming these limitations. One way of doing this is by the addition of a secondary amine / carboxylic acid mixture. In these reactions, the formaldehyde participates in a Mannich-type condensation reaction with the secondary amine to generate a more electrophilic and hence more reactive intermediate, which can then proceed to react with deprotonated MeP (Scheme7.9). Activation of formaldehyde in this way has been shown in the literature to be very effective in the simple, catalytic *α*-methylenation of aldehydes with aqueous formaldehyde.[13,18,22]

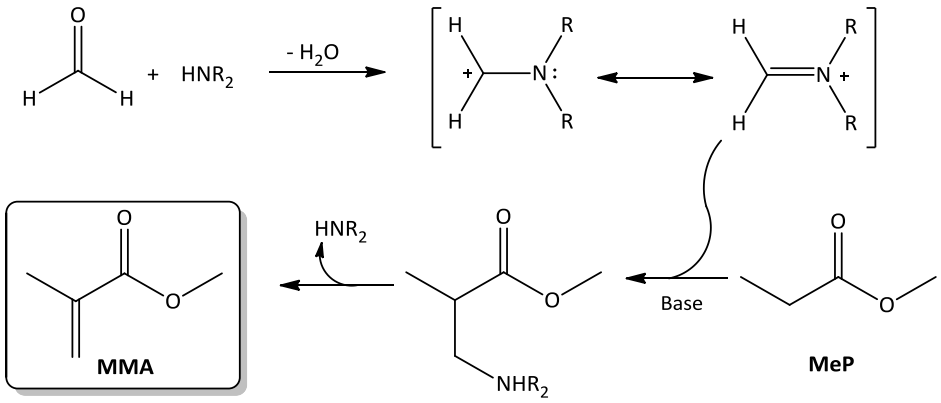


**Scheme 7.8** The activation of formaldehyde, prior to its reaction with MeP, *via* Mannich-type condensation reactions involving secondary amines.

Using this approach, a series of reactions was performed to which a variety of secondary amine / carboxylic acid combinations were added in an attempt to increase the reactivity of the formaldehyde. Owing to its structural similarity to MeP, propanoic acid (PA) was used as the carboxylic acid in all performed reactions, while diethylamine, *tert*-butylamine and pyrrolidine were screened as secondary amines. In a typical reaction, MeP was heated together with a secondary amine / propanoic acid mixture in the presence of a formaldehyde source for 1 h at 130 $^{o}$C. The final product mixtures were then analysed by means of GC- MS. Paraformaldehyde and alcoform (*ca.* 55 % wt. of formaldehyde in methanol) were employed

as the two sources of formaldehyde, while the secondary amines also served as the bases in these reactions. Table 7.3 summarises the different secondary amine / propanoic acid combinations screened as well as the % MMA obtained for each attempt. Unfortunately, none of the screened combinations resulted in an increased conversion of MeP to MMA, and the observed yields were similar to those observed previously for reactions with $Cs_2CO_3$ as base and paraformaldehyde as formaldehyde source.

**Table 7.3** The conversion of MeP to MMA in the presence of various *sec*-amines and propanoic acid.*

| No. | *Sec*-amine | amine (mmol) | PA (mmol) | MeP (mmol) | fomaldehyde source† | formaldehyde (mmol) | time | MMA (%) |
|---|---|---|---|---|---|---|---|---|
| 1 | $HNEt_2$ | 0.38 | 0.79 | 15.0 | PF | 15.0 | 30 min | < 1 |
| 2 | $HNEt_2$ | 0.38 | 0.79 | 15.0 | AF | 15.0 | 30 min | < 1 |
| 3 | $HNBu_2$ | 0.76 | 1.58 | 30.0 | PF | 30.6 | 1 h | < 1 |
| 4 | $HNBu_2$ | 0.76 | 1.58 | 30.0 | AF | 30.6 | 4 h | < 1 |
| 5 | pyrrolidine | 3.0 | 3.0 | 30.0 | PF | 30.6 | 4 h | 0 |
| 6 | pyrrolidine | 3.0 | 3.0 | 30.0 | AF | 30.6 | 4 h | 0 |

*Reaction conditions: In a stainless steel autoclave at 130 $^0$C for 1 h.
† PF = paraformaldehyde and AF = alcoform.

## 7.3 Conclusions

The ability of the series of bases $K_2CO_3$, DBU, NaOH and $Cs_3CO_3$ to catalyse the condensation of MeP with formaldehyde was investigated. None of the bases under consideration catalysed efficient condensation, with MMA yields of less than 1 % typically observed. Deuterium labelling studies, however, indicated that all of the considered bases were of sufficient strength to facilitate effective deprotonation in the $\alpha$-position of MeP. Furthermore, kinetic studies with NaP as base have revealed very fast rates of deprotonation with the equilibrium for this reaction reached within the first 5 min. From these observations it could be concluded that the low conversion of MeP to MMA by catalysed condensation with formaldehyde does not relate to ineffective deprotonation, but rather to low reactivity of the generated nucleophile. Attempts to overcome this problem were made by increasing the electrophilicity of formaldehyde through Mannich type condensations with secondary amines. These

attempts, however, had little success and other methods of formaldehyde activation would therefore need to be explored in future.

## 7.4 Experimental

### *7.4.1 General materials, methods and instruments*

All experiments were carried out in autoclaves under aerobic conditions. Paraformaldehyde, formalin, cesium carbonate, DBU, 2-ethylhexanol and methanol-$d_4$ were purchased from Aldrich. Sodium propanoate was purchased from Sigma, while methanol, sodium hydroxide (pellets) and potassium carbonate were obtained from Fisher Scientific. Methyl propanoate was supplied by Lucite International and used as received. $D_2O$ was purchased from Apollo Scientific Limited and toluene from Riedel-de-Haën. (2-Ethylhexyloxy)methanol was prepared using a literature procedure.[19]

NMR spectra were recorded on a Bruker Avance 300 FT or Bruker Avance II 400 MHz spectrometer ($^1$H NMR at 300/400 MHz and $^{13}$C{$^1$H} NMR at 75/100 MHz with chemical shifts δ reported relative to tetramethylsilane (TMS) as external reference. $^1$H and $^{13}$C{$^1$H} NMR spectra were measured internally relative to deuterated solvent resonances which were referenced relative to TMS. GC-MS chromatograms were recorded on a Hewlett Packard 6890 series GC system equipped with an Agilent J&W HP-1 general purpose column (fused silica capillary) and an HP 5973 Mass selective detector for both qualitative and quantitative analysis. Method: flow rate 1 ml min$^{-1}$ (He carrier gas), split ratio 100:1, starting temperature 50 $^o$C (4 min) ramp rate 20 $^o$C min$^{-1}$ to 130 $^o$C (2 min), ramp rate 20 $^o$C min$^{-1}$ to 220 $^o$C (15.5 min).

### *7.4.3 Experimental procedures*

***General procedure for the base catalysed condensation of MeP and formaldehyde***

*Please refer back to table 7.1 for the specific reagent ratio, solvent and formaldehyde source employed in each individual experiment.* An autoclave, charged with MeP, a base ($K_2CO_3$, DBU, NaOH or $Cs_2CO_3$), a formaldehyde source (paraformaldehyde, formalin or alcoform) and a solvent (toluene, 2-ethylhexanol or methanol) was heated to 130 $^o$C for 1–2 h with stirring. The

autoclave was then cooled to room temperature, vented to the atmosphere in a fumehood and the obtained product mixture analysed by means of GC-MS and NMR spectroscopy.

### *General procedure for the base catalysed condensation of γ-butyrolactone and formaldehyde*

*Please refer back to table 7.2 for the specific reagent ratio and solvent employed in each individual experiment.* An autoclave, charged with γ-butyrolactone (2.5–10 mmol), $Cs_2CO_3$ (2.53–7.96 mmol), paraformaldehyde (3.40–20 mmol) and a solvent (neat, 2-ethylhexanol or methanol), was heated to 130 $^oC$ for 1–3 h with stirring. The autoclave was then cooled to room temperature, vented to the atmosphere in a fumehood and the obtained product mixture analysed by means of GC-MS and NMR spectroscopy.

### *Deuterium labelling experiment with MeP, $Cs_2CO_3$, $D_2O$ and toluene.*

An autoclave, charged with MeP (0.88 g, 10.0 mmol, 0.96 ml), $Cs_2CO_3$ (0.82 g, 2.53 mmol), $D_2O$ (5 ml) and toluene (10 ml) was heated at 130 $^oC$ for 2 h with stirring. The autoclave was then cooled to room temperature, vented to the atmosphere and the obtained mixture analysed by means of NMR spectroscopy.

### *Deuterium labelling experiment with MeP, $Cs_2CO_3$, $D_2O$ and 2-ethylhexanol.*

An autoclave, charged with MeP (0.88 g, 10.0 mmol, 0.96 ml), $Cs_2CO_3$ (0.82 g, 2.53 mmol), $D_2O$ (0.50 ml) and 2-ethylhexanol (3.91 g, 30.0 mmol, 4.69 ml) was heated at 130 $^oC$ for 2 h with stirring. The autoclave was then cooled to room temperature, vented to the atmosphere and the obtained mixture analysed by means of NMR spectroscopy.

### *Deuterium labelling experiment with MeP, $Cs_2CO_3$ and methanol-$d_4$*

An autoclave, charged with MeP (0.88 g, 10.0 mmol, 0.96 ml), $Cs_2CO_3$ (0.82 g, 2.53 mmol) and methanol-$d_4$ (3 ml) was heated at 130 $^oC$ for 2 h with stirring. The autoclave was then cooled to room temperature, vented to the atmosphere and the obtained product mixture analysed by means of NMR spectroscopy.

### *Deuterium labelling experiment with MeP, $K_2CO_3$ and methanol-$d_4$*

This reaction was performed using the same procedure as was described for the analogous reaction with $Cs_2CO_3$, except that $K_2CO_3$ (0.35 g, 2.53 mmol) was employed as the base. The final product mixture was analysed by means of NMR spectroscopy.

### *Deuterium labelling experiment with MeP, NaOH and methanol-$d_4$*

This reaction was performed using the same procedure as was described for the analogous reaction with $Cs_2CO_3$, except that NaOH (0.12 g, 2.90 mmol) was employed as the base. The final product mixture was analysed by means of NMR spectroscopy.

### *Deuterium labelling experiment with γ-butyrolactone, $Cs_2CO_3$ and methanol-$d_4$*

An autoclave, charged with γ-butyrolactone (0.86 g, 10.0 mmol, 0.77 ml), $Cs_2CO_3$ (0.82 g, 2.53 mmol) and methanol-$d_4$ (3 ml) was heated at 130 $^{o}$C for 2 h with stirring. The autoclave was then cooled to room temperature, vented to the atmosphere and the obtained product mixture analysed by means of NMR spectroscopy.

### *Experiment for determining the time dependent deuterium labelling of MeP with NaP as base and methanol-$d_4$ as deuterium source*

Sodium propionate (5.48 g, 57.05 mmol) was added to a stainless steel autoclave fitted with a magnetic stirring bar. The autoclave was then sealed and pressure tested for leaks with hydrogen gas (30 bar) for 10 min, and subsequently purged. A seperate empty autoclave was sealed and pressure tested with hydrogen gas in the same way as before. The two autoclaves were then connected *via* their gas inlet ports using the set-up shown in Figure 7.6. Methyl propionate (10 ml, 103.85 mmol) and methanol-$d_4$ (28.97 ml, 713.26 mmol) were then added to the autoclave containing the sodium propionate by syringe *via* the injection port. The resulting mixture was then heated with stirring to 220 $^{o}$C and a sample of the vapour phase was taken at 0 min (taken as the time at which the autoclave reached 220 $^{o}$C) by opening tap **4** (see Figure 7.6) briefly and allowing a fraction of the vapour phase to collect in the connected empty autoclave. The remaining liquid in the heated autoclave was then heated for another 10min whereafter the autoclave was cooled rapidly to room temperature by immersing the autoclave set-up in cold water. The autoclaves were then disconnected, vented to the atmosphere and the two colourless solutions obtained were analysed for deuterium incorporation by means of $^{13}$C NMR spectroscopy. Simlarly, samples at 5min (vapour phase)

and 60 min were collected in a seperate identical experiment using the same method and once again analysed by means of $^{13}C$ NMR spectroscopy.

***Deuterium labelling experiment with NaP as both base and substrate, and methanol-$d_4$ as deuterium source***

Sodium propionate (5.48 g, 57.05 mmol) was added to a stainless steel autoclave fitted with a magnetic stirring bar. The autoclave was then sealed and pressure tested for leaks with hydrogen gas (30 bar) for 10 min, and subsequently purged. Methanol-$d_4$ (24 ml) was added to the autoclave by syringe via the injection port. The resulting mixture was then heated with stirring to 220 $^{o}C$ for 60 min, whereafer the autoclave was cooled to room temperature, vented to the atmosphere the isolated mixture analysed by means of $^{13}C$ NMR spectroscopy.

***General procedure for the base catalysed condensation of MeP and formaldehyde in the presence of secondary amine / propanoic acid mixtures***

*Please refer back to table 7.3 for the specific reagent ratio, amine and formaldehyde source employed in each individual experiment.* An autoclave, charged with MeP, a secondary amine ($HNEt_3$, $HNBu_2$ or pyrrolidine), propanoic acid and a formaldehyde source (paraformaldehyde or alcoform) was heated to 130 $^{o}C$ for 30 min–4 h with stirring. The autoclave was then cooled to room temperature, vented to the atmosphere in a fumehood and the obtained product mixture analysed by means of GC-MS.

## 7.5 Notes and References


(1) Nagai, K. *Appl. Catal. A: Gen.* **2001**, *221*, 367-377.
(2) Ai, M. *J. Catal.* **1987**, *107*, 201-208.
(3) Ai, M. *Bull. Chem. Soc. Jpn.* **1990**, *63*, 3722-3724.
(4) Ai, M. *Appl. Catal.* **1990**, *63*, 365-373.
(5) Ai, M. *Catal. Today* **2006**, *111*, 398-402.
(6) Ai, M. *Stud. Surf. Sci. Catal.* **1991**, *63*, 653-660.
(7) Ai, M.; Fujihashi, H.; Hosoi, S.; Yoshida, A. *Appl. Catal. A: Gen.* **2003**, *252*, 185-191.
(8) A. J. Pearson (Monsanto), *Ger. Offen.***1972**, 2,339,243.
(9) F. W. Schlaefer (Rhom and Haas), *Ger. Offen.* **1974**, 2,349,054.
(10) Ai, M. *Appl. Catal. A: Gen.* **2005**, *288*, 211-215.
(11) Ai, M. *Stud. Surf. Sci. Catal.* **2006**, *162*, 457-464.
(12) Brandenburg, C.; L. E. Manzer, L. E.; King, R. (Du Pont), *PCT* **2000**, WO 00/58298.

(13) Bach, H.; Brundin, E.; Gick, W. (Ruhrchemie AG), *U.S. Patent* **1982**, 4,346,239.
(14) Duembgen, G.; Fouquet, G; Krabetz, R.; Lucas, E.; Merger, F.; Nees, F (BASF), *U.S. Patent* **1985**, 4,496,770.
(15) Merger, F.; Foerster, H. J. (BASF), *U.S. Patent* **1983**, 4,408,097.
(16) Bernhagen, W.; Weber, J.; Bahrmann, H.; Springer, H. *U.S. Patent* **1982**, 4,317,945
(17) Hagemeyer, H. J. (Eastman Kodak) *U.S. Patent* **1953**, 2,639,295
(18) Erkkilä, A.; Pihko, P. M. *J. Org. Chem.* **2006**, *71*, 2538-2541.
(19) *Hemiformals* **1965**, 667360, 19pp.
(20) McMurry, J. (eds: Huber, J; Chelton, D; Henderson, M; Brooks, J. S.; Masson, C.) *in Organic Chemistry,* Brooks/Cole: Pacific Grove, USA, 2000, p913.
(21) http://www.chem.wisc.edu/areas/reich/pkatable/.
(22) MacLean, A. F; Frenz, B. G. (Celanese Corporation of America), *U.S. Pat. Office* **1958**, US 2 848 499, 2pp.

Chapter 8

# Conclusions and future work

*This chapter briefly summarises the main conclusions that could be drawn from each of the individual subtopics explored during the course of this study. Furthermore, taking these findings into consideration, this chapter also highlights some possible areas worth exploring in future endeavours. In particular, the* in situ *generation of formaldehyde and subsequent one-pot base catalysed condensation thereof with MeP showed great promise in preliminary studies and in this chapter some suggestions on how to improve the efficiency and selectivity of this system are made. Furthermore, a new and elegant formaldehyde free approach for the transition metal catalysed α-methylenation of either propanoic acid or methyl propanoate* via a *photochemically induced carbonylation pathway is proposed for future consideration.*

## 8.1 Conclusions

During this study, the functionalisation of either propanoic acid or MeP *via* C–H activation pathways was explored. Sadly, all initial attempts to employ simple mixed anhydride ligands derived from dialkyl phosphinous acid and propanoic acid in catalytic systems for the selective *α*-functionalisation of propanoic acid were complicated by the spontaneous rearrangement of these free ligands both in solution and in the solid state. Similarly, in the coordinated state these ligands underwent further rearrangement *via* a number of pathways to give a variety of rearrangement products. In particular, great preference for the formation of complexes containing $R_2POPR_2$ type ligands coordinated in a chelating manner was observed. The free mixed anhydride ligands could, however, be stabilised successfully by changing from chlorodialkylphosphines to chlorophosphites as precursors during their preparation and especially by increasing the steric bulk surrounding the central phosphorus atom. In particular, acylphosphites derived from (5,5',6,6'-tetramethyl-3,3'-di-*tert*-butyl-1,1'-biphenyl-2,2'-dioxy)chlorophosphine or (3,3',5,5'-tetra-*tert*-butyl-1,1'-biphenyl-2,2'-dioxy)chlorophosphine displayed remarkable stability and could be stored indefinitely under an inert atmosphere of $N_2$ either in solution or in the solid state.

Despite the enhanced stability of bulky acylphophites, complexes of the general formula $[RhCl(PPh_3)_2(L)]$ (L = bulky acylphosphite) still underwent metal promoted rearrangement in solution *via* a ligand decarbonylation pathway to give $[RhCl(CO)(PPh_3)_2]$, $[\{RhCl(PPh_3)_2\}_2]$ and $(RO)_2P(O)H$ as the major products of decay. The rate of this rearrangement was found to increase with temperature and as a result, complexes of this type did not show any catalytic potential. Unfortunately, attempts to prevent such rearrangements by replacing the $PPh_3$ ligands with chelating bisphosphine auxiliaries (dppe, dppb or dppbz) did not have the desired effect. These complexes too underwent spontaneous rearrangement in solution over a period of 2-4 days, with the specific pathway of decomposition dependent on the nature of the bisphosphine employed. In the case of dppe, complexes were found to decompose *via* a decarbonylation pathway similar to those observed for the analogous $PPh_3$ complexes, while dppbz complexes decomposed *via* alternative routes. This difference in behaviour was ascribed to the greater tendency of dppe to participate in the formation of dimeric reaction intermediates through coordination in a bridging rather than chelating manner. Similarly,

stabilisation attempts utilising 1,2-bis(di-*tert*-butylphosphinomethyl)benzene and $(Ph_2P)_2N^tBu$ as chelating auxiliary ligands did not have the desired outcome.

The reactivity and regioselectivity of the iridium pincer complex $[Ir(PNP)(COE)][BF_4]$, both in the presence and absence of water, towards the activation of C–H bonds in the $\alpha$- and $\beta$-positions of the esters methyl propanoate, isopropyl propanoate and *tert*-butyl propanoate was assessed. In the presence of water, methyl propanoate underwent ester bond hydrolysis to give propanoic acid and methanol which participated in further reactions with $[Ir(PNP)(COE)][BF_4]$ to generate the O–H activated propanoic acid complex $[Ir(H)(PNP)(OC(O)CH_2CH_3][BF_4]$ together with $[Ir(CO)(H)_2(PNP)][BF_4]$. The formation of the latter could be shown to proceed *via* a methanol decarbonylation pathway. In the absence of water, C–H activation of the methoxy group in the $\beta$-postion of MeP proceeded to furnish $[\overline{Ir(H)(PNP)(CH_2OC(O)}CH_2CH_3)][BF_4]$. Unfortunately, all preliminary attempts to utilise this strategy in the functionalisation of the methylene MeP were unsuccessful. Interestingly, similar reactions with isopropyl propanoate and *tert*-butyl propanoate as substrates did not furnish any C–H activated products.

In this study anhydrous formaldehyde could be generated *in situ* by the dehydrogenation of methanol in the presence of metal carbonates or transition metal catalysts such as $[RhCl(PPh_3)_3]$, $[Ir(PNP)(COE)][BF_4]$, $[RuH_2(CO)(PPh_3)_3]$ and $[Ru(NH_2CH_2CH_2NH_2)(PPh_3)_2]$. In the presence of a base such as NaOMe or $Cs_2CO_3$, the generated formaldehyde could be utilised in the conversion of MeP to MMA, albeit in low yield, using a one-pot setup. The evolution of hydrogen during these reactions, however, represented a major hurdle to its success and hydrogenation of the produced MMA largely proceeded to furnish $M^iBu$ as the final product. Although a suitable catalytic system for these reactions could not yet be identified, all preliminary findings suggested that this reaction has the potential to succeed and the studies therefore serve as an important proof of concept for future developments in this area.

Finally, the ability of the series of bases $K_2CO_3$, DBU, NaOH and $Cs_3CO_3$ to catalyse the condensation of MeP with formaldehyde was investigated. None of the considered bases resulted in an effective condensation reaction and MMA yields of less than 1 % were typically observed. Deuterium labelling studies, however, indicated these bases to catalyse sufficient deprotonation in the α-position of MeP. For NaP, in particular, kinetic studies revealed fast

deprotonation rates with the equilibrium for this reaction being reached within 5 min. From these observations it could be concluded that the low conversion of MeP to MMA does not relate to ineffective deprotonation, but rather to a low reactivity of the generated nucleophile. Attempts to overcome this problem by increasing the electrophilicity of formaldehyde through Mannich type condensations with secondary amines, however, had little success and other methods of formaldehyde activation would therefore need to be explored in future.

## 8.2 Future work

### *8.2.1 Future prospects for the one pot α-methylenation of MeP with methanol via transition metal catalysed methanol dehydrogenation*

The current study has suggested that the *in situ* generation of anhydrous formaldehyde and subsequent one-pot, base catalysed condensation thereof with MeP may be a viable route to the production of MMA, provided that a more selective and efficient catalytic system is developed. Based on these findings, it would certainly be worth continuing the search for a transition metal based catalyst that would selectively promote the dehydrogenation of methanol to formaldehyde without effecting alkene or ester hydrogenation. Alternatively, the use of sacrificial hydrogen acceptors such as crotononitrile or the removal of hydrogen by other methods can be explored in future.

In addition, it may be beneficial to explore the use of dehydrogenation catalysts for which the formaldehyde elimination step is slower than nucleophilic attack by the deprotonated MeP on formaldehyde. In this way, the transition metal catalysts could function both as dehydrogenation catalyst and Lewis acid for the activation of formaldehyde. Since the weak nucleophilicity of deprotonated MeP is suspected of representing the bottleneck in these condensation reactions, this approach may greatly aid in overcoming this limitation.

### *8.2.2 Carbonyl Rh(I) complexes in the functionalisation of propanoic acid by photochemical α-C–H activation*

As formaldehyde is a difficult substance to generate and handle, particularly on large scale, it would be of great advantage if the *α*-methylenation of MeP or propanoic acid can be achieved

by a strategy that does not necessitate the use of this reagent. An alternative pathway to explore in future could involve the photochemical carbonylation of MeP or propanoic acid and subsequent *in* or *ex situ* hydrogenation and dehydration to give either methacrylic acid of MMA as product. For propanoic acid selective α-functionalisation may be achieved by linking the substrate to phosphorus. Although similar complexes have shown low thermal stability in earlier studies, these complexes are not expected to decompose *via* ligand decarbonylation pathways since the precatalyst already contains coordinated CO. In fact, preliminary work in this area (not included in this account) has shown these complexes to possess great stability both in solution and in the solid state. The catalytic cycle proposed for the conversion under an atmosphere of CO is given in Scheme 8.1 and involves initial photochemical C–H activation of phosphorus linked propanoic acid selectively in the *α*-position since this would generate a favourable five-memeberd ring structure. This step is followed by migratory CO insertion and reductive elimination with simultaneous reoccupation of the generated vacant site by CO. Following reductive elimination, the functionalised product can be released by transesterification at phosphorus with introduction of a fresh molecule of propanoic acid. The released product can then be hydrogenated *in* or *ex situ* in the presence of a suitable hydrogenation catalyst and dehydrated at elevated temperatures to furnish methacrylic acid as the final product.

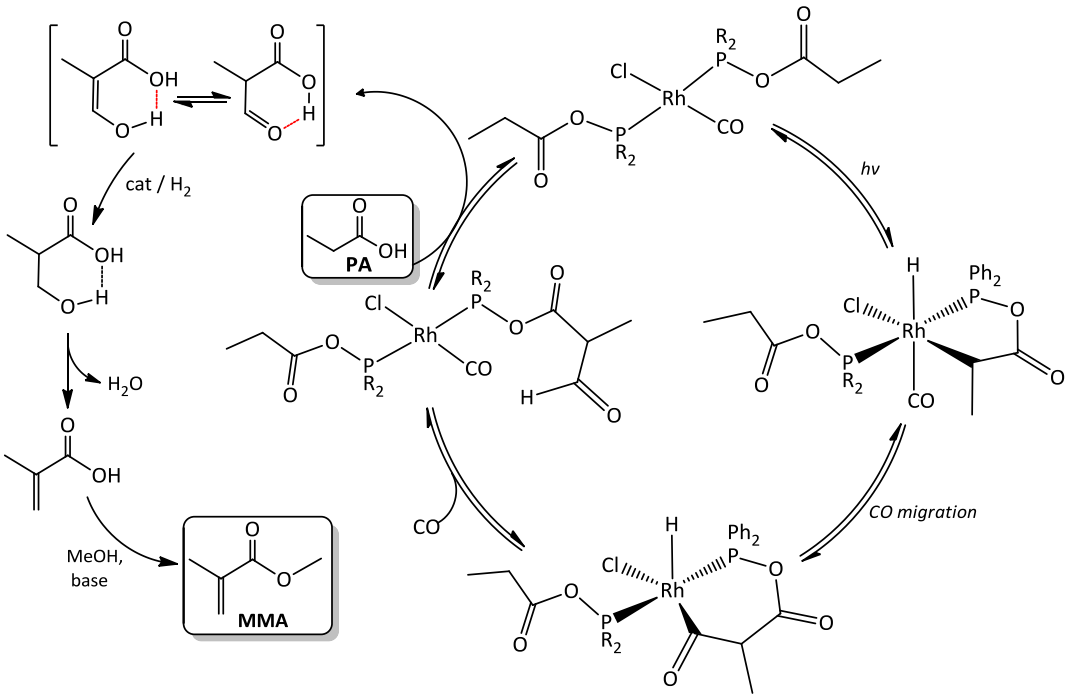


**Scheme 8.1** Proposed cycle for the *α*-methylenation of propanoic acid *via* photochemical carbonylation.

A similar approach can also potentially be followed for the photochemical carbonylation of MeP. Linking the substrate to phosphorus would, however, not apply for this substrate and other electron rich Rh(I) CO containing catalysts such as $[RhCl(CO)(PMe_3)_2]$ would have to be employed. Such reactions with $[RhCl(CO)(PMe_3)_2]$ is not unprecedented, and this complex has been employed before by Sakakura and Tanaka[1] as a catalyst in the photochemical carbonylation of pentane *via* a C–H activation route.

## 8.3 Notes and References

(1) Sakakura, T.; Tanaka, M. *J. Chem. Soc., Chem. Commun.* **1987**, 758-759.

# Appendix 1

## Crystallographic data tables

## A1.1 Appendix 1: Crystallographic data tables

**Table A1.1** Crystallographic data for compounds **9** and **12**.*

| **Compound reference** | **9** | **12** |
|---|---|---|
| Empirical formula | $C_{27}H_{37}O_4P$ | $C_{32}H_{39}O_4P$ |
| Formula weight (g/mol) | 456.54 | 518.60 |
| Temp. (K) | 93(2) | 93(2) |
| Wavelength (Å) | 0.71075 | 0.71075 |
| Crystal system | Orthorhombic | Monoclinic |
| Crystal dimensions ($mm^3$) | 0.28 × 0.15 × 0.06 | 0.15 × 0.15 × 0.03 |
| Crystal shape and colour | Prism, colourless | Prism, colourless |
| Space group | $Pna2_1$ (No. 33) | $P2_1/n$ (No. 14) |
| a (Å) | 15.562(6) | 10.820(7) |
| b (Å) | 10.686(4) | 16.178(10) |
| c (Å) | 15.625(6) | 15.982(10) |
| $\alpha$ (°) | 90.00 | 90.00 |
| $\beta$ (°) | 90.00 | 98.366(17) |
| $\gamma$ (°) | 90.00 | 90.00 |
| Unit cell volume ($Å^3$) | 2598.3(17) | 2768(3) |
| No. of formula units per unit cell, $Z$ | 4 | 4 |
| $d_{calcd}$ ($g/cm^3$) | 1.167 | 1.167 |
| Radiation type | MoK$\alpha$ | MoK$\alpha$ |
| Absorption coefficient, $\mu$ ($mm^{-1}$) | 0.134 | 0.135 |
| F(000) | 984 | 1112 |
| θ-range for data collection (°) | 2.31 to 25.32 | 1.80 to 25.46 |
| Index range | -18 ≤ h ≤ 18, -12 ≤ k ≤ 12, -18 ≤ l ≤ 14 | -13 ≤ h ≤ 10, -19 ≤ k ≤ 16, -18 ≤ l ≤ 19 |
| No. of reflections measured | 15727 | 18083 |
| No. of independent reflections | 4127 | 5075 |
| Refinement parameters / restraints | 301 / 1 | 344 / 0 |
| $R_{int}$ | 0.1675 | 0.2879 |
| Final $R_1$ values ($I > 2\sigma(I)$) | 0.0919 | 0.1477 |
| Final $wR(F^2)$ values ($I > 2\sigma(I)$) | 0.2168 | 0.3207 |
| Final $R_1$ values (all data) | 0.1454 | 0.2445 |
| Final $wR(F^2)$ values (all data) | 0.2491 | 0.3668 |
| Goodness of fit on $F^2$ | 0.992 | 1.002 |
| Largest diff. peak and hole ($e.A^{-3}$) | 0.957 and -0.536 | 1.189 and -1.314 |
| Weighing scheme † | a = 0.1260<br>b = 0 | a = 0.1809<br>b = 0 |

* The full Crystallographic Information Framework (CIF) files are available on the included compact disc.
† $wR2 = \{\Sigma[w(F_o^2-F_c^2)^2]/\Sigma[w(F_o^2)^2]\}^{1/2}$; $w = 1/[\sigma^2(F_o^2)+(aP)^2+bP+d+\text{esin}\theta]$; $P = [f(\text{Max}(0 \text{ or } F_o^2)] + (1\text{-}f)\ F_c^2$

**Table A1.2** Crystallographic data for compounds **13** and **22**.*

| **Compound reference** | **13** | **22** |
|---|---|---|
| Empirical formula | $C_{36}H_{47}O_4P$ | $0.5[C_{54}H_{52}Cl_2O_6P_4Rh_2]$ •0.5 $[C_7H_8]$ |
| Formula weight (g/mol) | 574.71 | 644.87 |
| Temp. (K) | 93(2) | 93(2) |
| Wavelength (Å) | 0.71075 | 0.71075 |
| Crystal system | Triclinic | Monoclinic |
| Crystal dimensions ($mm^3$) | $0.30 \times 0.30 \times 0.10$ | $0.10 \times 0.10 \times 0.10$ |
| Crystal shape and colour | Prism, colourless | Prism, yellow |
| Space group | $P\bar{1}$ (No. 2) | *C2/c* (No. 15) |
| a (Å) | 10.232(3) | 20.089(7) |
| b (Å) | 12.846(4) | 12.811(5) |
| c (Å) | 13.644(2) | 22.725(8) |
| $\alpha$ (°) | 78.15(2) | 90.00 |
| $\beta$ (°) | 68.93(2) | 101.120(5) |
| $\gamma$ (°) | 86.69(2) | 90.00 |
| Unit cell volume ($Å^3$) | 1637.6(8) | 5739(4) |
| No. of formula units per unit cell, *Z* | 2 | 4 |
| $d_{calcd}$ ($g/cm^3$) | 1.166 | 1.493 |
| Radiation type | MoK$\alpha$ | MoK$\alpha$ |
| Absorption coefficient, $\mu$ ($mm^{-1}$) | 0.120 | 0.830 |
| F(000) | 620 | 2632 |
| $\theta$-range for data collection (°) | 2.13 to 25.34 | 2.48 to 25.35 |
| Index range | -9 ≤ h ≤ 12, -14 ≤ k ≤ 15, -16 ≤ l ≤ 12 | -23 ≤ h ≤ 23, -15 ≤ k ≤ 15 -27 ≤ l ≤ 27 |
| No. of reflections measured | 10448 | 26636 |
| No. of independent reflections | 5799 | 5187 |
| Refinement parameters / restraints | 383 / 0 | 332 / 0 |
| $R_{int}$ | 0.0605 | 0.0522 |
| Final $R_1$ values ($I > 2\sigma(I)$) | 0.0789 | 0.0354 |
| Final $wR(F^2)$ values ($I > 2\sigma(I)$) | 0.2018 | 0.0910 |
| Final $R_1$ values (all data) | 0.1038 | 0.0372 |
| Final $wR(F^2)$ values (all data) | 0.2238 | 0.0932 |
| Goodness of fit on $F^2$ | 1.066 | 1.069 |
| Largest diff. peak and hole ($e.A^{-3}$) | 0.430 to -0.480 | 1.032 to -0.789 |
| Weighing scheme † | a = 0.1008 b = 0.7048 | a = 0.0511 b = 13.9419 |

* The full Crystallographic Information Framework (CIF) files are available on the included compact disc.

† $wR2 = \{\Sigma[w(F_o^2-F_c^2)^2]/\Sigma[w(F_o^2)^2]\}^{1/2}$; $w = 1/[\sigma^2(F_o^2)+(aP)^2+bP+d+\text{esin}\theta]$; $P = [f(\text{Max}(0 \text{ or } F_o^2)] + (1\text{-}f)\ F_c^2$

**Table A1.3** Crystallographic data for compounds **23** and **24**.*

| **Compound reference** | **23** | **24** |
|---|---|---|
| Empirical formula | $[C_{30}H_{30}Cl_2O_4P_2Ru]\bullet 2[C_7H_8]$ | $0.5[C_{54}H_{52}Cl_4O_6P_4Ru_2]\bullet CHCl_3$ |
| Formula weight (g/mol) | 872.76 | 751.80 |
| Temp. (K) | 93(2) | 93(2) |
| Wavelength (Å) | 0.71075 | 0.71075 |
| Crystal system | Monoclinic | Triclinic |
| Crystal dimensions ($mm^3$) | $0.12 \times 0.08 \times 0.02$ | $0.10 \times 0.10 \times 0.03$ |
| Crystal shape and colour | Platelet, orange | Platelet, orange |
| Space group | $P2_1/c$ (No. 14) | $P\bar{1}$ (No. 2) |
| a (Å) | 15.845(10) | 9.827(6) |
| b (Å) | 16.449(10) | 12.075(7) |
| c (Å) | 15.551(11) | 14.270(10) |
| $\alpha$ (°) | 90.00 | 107.82(4) |
| $\beta$ (°) | 100.535(10) | 99.41(4) |
| $\gamma$ (°) | 90.00 | 103.84(3) |
| Unit cell volume ($Å^3$) | 3985(4) | 1513.0(16) |
| No. of formula units per unit cell, $Z$ | 4 | 2 |
| $d_{calcd}$ ($g/cm^3$) | 1.441 | 1.521 |
| Radiation type | MoK$\alpha$ | MoK$\alpha$ |
| Absorption coefficient, $\mu$ ($mm^{-1}$) | 0.650 | 0.960 |
| F(000) | 1768 | 700 |
| $\theta$-range for data collection (°) | 1.31 to 25.37 | 4.99 to 28.13 |
| Index range | $-14 \le h \le 19$, $-19 \le k \le 19$, $-18 \le l \le 18$ | $-12 \le h \le 12$, $-10 \le k \le 15$, $-16 \le l \le 9$ |
| No. of reflections measured | 38943 | 8234 |
| No. of independent reflections | 7297 | 5506 |
| Refinement parameters / restraints | 447 / 0 | 355 / 0 |
| $R_{int}$ | 0.0843 | 0.1130 |
| Final $R_1$ values ($I > 2\sigma(I)$) | 0.0832 | 0.1921 |
| Final $wR(F^2)$ values ($I > 2\sigma(I)$) | 0.2114 | 0.4453 |
| Final $R_1$ values (all data) | 0.1184 | 0.2476 |
| Final $wR(F^2)$ values (all data) | 0.2443 | 0.4867 |
| Goodness of fit on $F^2$ | 1.097 | 1.702 |
| Largest diff. peak and hole ($e.A^{-3}$) | 1.770 to -1.312 | 4.930 to -1.663 |
| Weighing scheme † | a = 0.1330<br>b = 4.1111 | a = 0.2<br>b = 0 |

* The full Crystallographic Information Framework (CIF) files are available on the included compact disc.

† $wR2 = \{\Sigma[w(F_o^2-F_c^2)^2]/\Sigma[w(F_o^2)^2]\}^{1/2}$; $w = 1/[\sigma^2(F_o^2)+(aP)^2+bP+d+\text{esin}\theta]$; $P = [f(\text{Max}(0 \text{ or } F_o^2)] + (1\text{-}f)\ F_c^2$

**Table A1.4** Crystallographic data for compounds **29** and **30**.*

| **Compound reference** | **29**‡ | **30** |
|---|---|---|
| Empirical formula | | $C_{67}H_{75}ClO_4P_3Rh$ |
| Formula weight (g/mol) | | 1175.54 |
| Temp. (K) | 93(2) | 93(2) |
| Wavelength (Å) | 0.71075 | 0.71075 |
| Crystal system | Orthorhombic | Monoclinic |
| Crystal dimensions ($mm^3$) | $0.10 \times 0.10 \times 0.02$ | $0.30 \times 0.12 \times 0.02$ |
| Crystal shape and colour | Platelet, yellow | Needle, yellow |
| Space group | $Pna2_1$ | $P21/n$ (No. 14) |
| a (Å) | 40.9954(19) | 23.139(4) |
| b (Å) | 11.512(4) | 11.654(2) |
| c (Å) | 28.589(7) | 23.570(5) |
| $\alpha$ (°) | 90.00 | 90.00 |
| $\beta$ (°) | 90.00 | 109.147(4) |
| $\gamma$ (°) | 90.00 | 90.00 |
| Unit cell volume ($Å^3$) | 13492(6) | 6004(2) |
| No. of formula units per unit cell, $Z$ | | 4 |
| $d_{calcd}$ ($g/cm^3$) | | 1.300 |
| Radiation type | MoK$\alpha$ | MoK$\alpha$ |
| Absorption coefficient, $\mu$ ($mm^{-1}$) | | 0.456 |
| F(000) | | 2464 |
| $\theta$-range for data collection (°) | | 1.07 to 29.08 |
| Index range | | $-28 \le h \le 29$, $-15 \le k \le 14$, $-29 \le l \le 29$ |
| No. of reflections measured | 53786 | 51481 |
| No. of independent reflections | 21202 | 14097 |
| Refinement parameters / restraints | | 687 / 0 |
| $R_{int}$ | | 0.1740 |
| Final $R_1$ values ($I > 2\sigma(I)$) | | 0.1326 |
| Final $wR(F^2)$ values ($I > 2\sigma(I)$) | | 0.2890 |
| Final $R_1$ values (all data) | | 0.1818 |
| Final $wR(F^2)$ values (all data) | | 0.3340 |
| Goodness of fit on $F^2$ | | 1.274 |
| Largest diff. peak and hole ($e.A^{-3}$) | | 1.436 to -0.915 |
| Weighing scheme † | | a = 0.0994<br>b = 21.5783 |

* The full Crystallographic Information Framework (CIF) files are available on the included compact disc.

† $wR2 = \{\Sigma[w(F_o^2-F_c^2)^2]/\Sigma[w(F_o^2)^2]\}^{1/2}$; $w = 1/[\sigma^2(F_o^2)+(aP)^2+bP+d+\text{esin}\theta]$; $P = [f(\text{Max}(0 \text{ or } F_o^2)] + (1\text{-}f)\ F_c^2$

‡ The asymmetric unit of this structure contains at least 8 included, disordered dichloromethane molecules. Owing to this, the quality of this dataset is of too poor quality to allow for a more accurate refinement.

**Table A1.5** Crystallographic data for compounds **31** and **33**.*

| **Compound reference** | **31** | **33** |
|---|---|---|
| Empirical formula | $[C_{72}H_{77}ClO_4P_3Rh]\bullet 4[CH_2Cl_2]$ | $C_{37}H_{30}ClOP_2Rh$ |
| Formula weight (g/mol) | 1577.38 | 690.91 |
| Temp. (K) | 273(2) | 93(2) |
| Wavelength (Å) | 0.71075 | 0.71075 |
| Crystal system | Triclinic | Monoclinic |
| Crystal dimensions ($mm^3$) | $0.20 \times 0.20 \times 0.10$ | $0.10 \times 0.10 \times 0.10$ |
| Crystal shape and colour | Prism, yellow | Prism, yellow |
| Space group | $P\bar{1}$ (No. 2) | $P2_1/n$ (No. 14) |
| a (Å) | 12.273(3) | 11.746(4) |
| b (Å) | 14.005(3) | 23.734(6) |
| c (Å) | 20.777(5) | 12.177(4) |
| $\alpha$ (°) | 93.707(8) | 90.00 |
| $\beta$ (°) | 91.581(6) | 112.538(8) |
| $\gamma$ (°) | 93.876(10) | 90.00 |
| Unit cell volume ($Å^3$) | 3553.8(15) | 3135.4(16) |
| No. of formula units per unit cell, $Z$ | 2 | 4 |
| $d_{calcd}$ ($g/cm^3$) | 1.422 | 1.464 |
| Radiation type | MoK$\alpha$ | MoK$\alpha$ |
| Absorption coefficient, $\mu$ ($mm^{-1}$) | 0.694 | 0.761 |
| F(000) | 1568 | 1408 |
| $\theta$-range for data collection (°) | 2.29 to 25.36 | 2.50 to 25.31 |
| Index range | $-13 \le h \le 14$, $-15 \le k \le 16$, $-18 \le l \le 24$ | $-14 \le h \le 14$, $-28 \le k \le 21$, $-14 \le l \le 13$ |
| No. of reflections measured | 21963 | 18978 |
| No. of independent reflections | 12374 | 5631 |
| Refinement parameters / restraints | 812 / 0 | 380 / 0 |
| $R_{int}$ | 0.0304 | 0.0746 |
| Final $R_1$ values ($I > 2\sigma(I)$) | 0.0828 | 0.0514 |
| Final $wR(F^2)$ values ($I > 2\sigma(I)$) | 0.2157 | 0.0859 |
| Final $R_1$ values (all data) | 0.0926 | 0.0814 |
| Final $wR(F^2)$ values (all data) | 0.2253 | 0.0949 |
| Goodness of fit on $F^2$ | 1.044 | 1.084 |
| Largest diff. peak and hole ($e.A^{-3}$) | 2.681 to -2.177 | 0.585 to -0.762 |
| Weighing scheme † | a = 0.1088<br>b = 22.5791 | a = 0.0210<br>b = 0 |

* The full Crystallographic Information Framework (CIF) files are available on the included compact disc.

† $wR2 = \{\Sigma[w(F_o^2-F_c^2)^2]/\Sigma[w(F_o^2)^2]\}^{1/2}$; $w = 1/[\sigma^2(F_o^2)+(aP)^2+bP+d+\sin\theta]$; $P = [f(\text{Max}(0 \text{ or } F_o^2)] + (1\text{-}f)\ F_c^2$

**Table A1.6** Crystallographic data for compounds 3**4** and **45**.*

| **Compound reference** | **34** | **45** |
|---|---|---|
| Empirical formula | $0.5[C_{72}H_{60}Cl_2P_4Rh_2]\bullet CH_2Cl_2$ | $[C_{57}H_{61}ClO_4P_3Rh]\bullet 3[CH_2Cl_2]$ |
| Formula weight (g/mol) | 747.86 | 1296.17 |
| Temp. (K) | 173(2) | 93(2) |
| Wavelength (Å) | 0.71075 | 0.71075 |
| Crystal system | Triclinic | Monoclinic |
| Crystal dimensions ($mm^3$) | $0.03 \times 0.03 \times 0.03$ | $0.12 \times 0.05 \times 0.03$ |
| Crystal shape and colour | Prism, burgundy | Prism, yellow |
| Space group | $P\bar{1}$ (No. 2) | $P2_1/c$ (No. 14) |
| a (Å) | 9.6867(19) | 18.180(4) |
| b (Å) | 12.650(3) | 11.434(3) |
| c (Å) | 13.761(3) | 28.809(8) |
| $\alpha$ (°) | 85.460(15) | 90.00 |
| $\beta$ (°) | 81.765(14) | 90.505(6) |
| $\gamma$ (°) | 78.414(14) | 90.00 |
| Unit cell volume ($Å^3$) | 1632.6(6) | 5988(3) |
| No. of formula units per unit cell, $Z$ | 1 | 4 |
| $d_{calcd}$ ($g/cm^3$) | 1.517 | 1.438 |
| Radiation type | MoK$\alpha$ | MoK$\alpha$ |
| Absorption coefficient, $\mu$ ($mm^{-1}$) | 0.893 | 0.723 |
| F(000) | 756 | 2672 |
| $\theta$-range for data collection (°) | 1.50 to 27.37 | 2.27 to 25.36 |
| Index range | $-12 \le h \le 12$, $-14 \le k \le 16$, $-16 \le l \le 17$ | $-20 \le h \le 21$, $-13 \le k \le 13$, $-24 \le l \le 34$ |
| No. of reflections measured | 15896 | 31570 |
| No. of independent reflections | 6335 | 10662 |
| Refinement parameters / restraints | 364 / 0 | 697 / 0 |
| $R_{int}$ | 0.1649 | 0.1001 |
| Final $R_1$ values ($I > 2\sigma(I)$) | 0.1626 | 0.1025 |
| Final $wR(F^2)$ values ($I > 2\sigma(I)$) | 0.3589 | 0.2607 |
| Final $R_1$ values (all data) | 0.2033 | 0.1269 |
| Final $wR(F^2)$ values (all data) | 0.3871 | 0.2781 |
| Goodness of fit on $F^2$ | 1.173 | 1.112 |
| Largest diff. peak and hole ($e.A^{-3}$) | 1.923 to -1.844 | 3.146 to -1.042 |
| Weighing scheme † | a = 0.0717<br>b = 89.7872 | a = 0.1068<br>b = 53.1690 |

* The full Crystallographic Information Framework (CIF) files are available on the included compact disc.
† $wR2 = \{\Sigma[w(F_o^2-F_c^2)^2]/\Sigma[w(F_o^2)^2]\}^{1/2}$; $w = 1/[\sigma^2(F_o^2)+(aP)^2+bP+d+\text{esin}\theta]$; $P = [f(\text{Max}(0 \text{ or } F_o^2)] + (1\text{-}f)\ F_c^2$

**Table A1.7** Crystallographic data for compounds **64** and **65**.*

| **Compound reference** | **64** | **65** |
|---|---|---|
| Empirical formula | $C_{24}H_{43}BF_4IrNOP_2$ | $[C_{26}H_{51}BF_4IrNO_3P_2]\bullet CH_2Cl_2$ |
| Formula weight (g/mol) | 702.54 | 851.55 |
| Temp. (K) | 93(2) | 273(2) |
| Wavelength (Å) | 0.71075 | 0.71075 |
| Crystal system | Monoclinic | Triclinic |
| Crystal dimensions ($mm^3$) | $0.38 \times 0.34 \times 0.04$ | $0.15 \times 0.15 \times 0.10$ |
| Crystal shape and colour | Prism, yellow | Prism, yellow |
| Space group | $P2_1/n$ (No. 14) | $P\bar{1}$ (No. 2) |
| a (Å) | 12.3502(15) | 9.2649(15) |
| b (Å) | 8.3296(11) | 10.9156(19) |
| c (Å) | 28.499(4) | 17.297(3) |
| $\alpha$ (°) | 90.00 | 85.604(11) |
| $\beta$ (°) | 92.083(3) | 84.512(11) |
| $\gamma$ (°) | 90.00 | 79.863(9) |
| Unit cell volume ($Å^3$) | 2929.8(6) | 1710.9(5) |
| No. of formula units per unit cell, $Z$ | 4 | 2 |
| $d_{calcd}$ ($g/cm^3$) | 1.593 | 1.653 |
| Radiation type | Mo$K\alpha$ | Mo$K\alpha$ |
| Absorption coefficient, $\mu$ ($mm^{-1}$) | 4.708 | 4.202 |
| F(000) | 1400 | 856 |
| $\theta$-range for data collection (°) | 2.55 to 30.08 | 2.18 to 25.35 |
| Index range | $0 \le h \le 17$, $-11 \le k \le 11$, $-40 \le l \le 40$ | $-10 \le h \le 11$, $-8 \le k \le 13$, $-18 \le l \le 20$ |
| No. of reflections measured | 14701 | 10856 |
| No. of independent reflections | 8289 | 6026 |
| Refinement parameters / restraints | 310 / 0 | 413 / 2 |
| $R_{int}$ | 0.0705 | 0.0544 |
| Final $R_1$ values ($I > 2\sigma(I)$) | 0.1034 | 0.0468 |
| Final $wR(F^2)$ values ($I > 2\sigma(I)$) | 0.2106 | 0.0886 |
| Final $R_1$ values (all data) | 0.1244 | 0.0564 |
| Final $wR(F^2)$ values (all data) | 0.2212 | 0.0935 |
| Goodness of fit on $F^2$ | 1.149 | 1.024 |
| Largest diff. peak and hole ($e.A^{-3}$) | 8.669 to -4.493 | 1.737 to -1.806 |
| Weighing scheme † | a = 0.0491<br>b = 104.8285 | a = 0.0303<br>b = 0 |

* The full Crystallographic Information Framework (CIF) files are available on the included compact disc.

† $wR2 = \{\Sigma[w(F_o^2-F_c^2)^2]/\Sigma[w(F_o^2)^2]\}^{1/2}$; $w = 1/[\sigma^2(F_o^2)+(aP)^2+bP+d+\text{esin}\theta]$; $P = [f(\text{Max}(0 \text{ or } F_o^2)] + (1\text{-}f)\ F_c^2$